This is to certify that the

dissertation entitled

THE INTRINSIC ORGANIZATION AND CONNECTIVITY OF TRIGEMINAL NUCLEUS INTERPOLARIS AND THE INTERSTITIAL SYSTEM OF THE SPINAL TRIGEMINAL TRACT IN THE RAT

presented by

Kevin Dean Phelan

has been accepted towards fulfillment
of the requirements for

Ph.D. degree in Anatomy

William M. Falls
Major professor

Date 2-24-88

THE INTRINSIC ORGANIZATION AND CONNECTIVITY OF TRIGEMINAL NUCLEUS INTERPOLARIS AND THE INTERSTITIAL SYSTEM OF THE SPINAL TRIGEMINAL TRACT IN THE RAT

By

Kevin Dean Phelan

A DISSERTATION

Submitted to
Michigan State University
in partial fulfillment of the requirements
for the degree of

DOCTOR OF PHILOSOPHY

Department of Anatomy

1988

ABSTRACT

THE INTRINSIC ORGANIZATION AND CONNECTIVITY OF TRIGEMINAL NUCLEUS INTERPOLARIS AND THE INTERSTITIAL SYSTEM OF THE SPINAL TRIGEMINAL TRACT IN THE RAT

By

Kevin Dean Phelan

The intrinsic cyto- and myeloarchitectonic organization of trigeminal nucleus interpolaris (Vi) is examined using correlated Nissl and myelin stained preparations (CHAPTER ONE). Six distinct regions are defined in Vi. In addition, detailed descriptions of the rostral and caudal boundaries of Vi with the medullary dorsal horn (MDH) and trigeminal nucleus oralis (Vo) are provided.

The interstitial system of the spinal trigeminal tract (InSy-SVT) is demonstrated to consist of several morphologically and functionally heterogeneous regions based on differences in cytology (using Nissl, myelin and Golgi preparations), and efferent projections (revealed through the retrograde transport of horseradish peroxidase, HRP) (CHAPTER TWO). Two thalamic projecting components (the trigeminal extension of the parvocellular reticular formation and the dorsal paramarginal nucleus) and one cerebellar projecting nucleus (the insular trigeminal-cuneatus lateralis, iV-Cul) are defined. The paratrigeminal nucleus is also demonstrated to be morphologically distinct from the ramaining MDH derived components of InSy-SVT.

The regional distribution and morphology of thalamic, cerebellar and spinal projecting Vi neurons is compared (CHAPTER THREE). The two spinal recipient zones in Vi are revealed to contain either predominantly thalamic or cerebellar projecting neurons, while both

similarities and differences are reported for the organization of these projections in the remaining regions of Vi.

The origin, course, distribution and light microscopic morphology of spinotrigeminal afferents is revealed through the anterograde transport of HRP and tritiated amino acids (CHAPTER FOUR). Two regions of Vi, their extensions into caudal Vo, and similarly located regions in the trigeminal main sensory nucleus are identified as spinal recipient zones. In addition, a complex spatial relationship between the distribution of trigeminospinal projection neurons and spinal afferents is described.

An ultrastructural examination of neurons and neuropil within iV-Cul indicates that this component of InSy-SVT represents a unique medullary precerebellar nucleus (CHAPTER FIVE). Eight morphologically distinct types of presynaptic boutons and the striking absence of axo-axonic synapses characterize this nucleus. In addition, the ultrasructural morphology of HRP-labeled spinal afferent inputs to iV-Cul is described.

These combined results are discussed in terms of their impact on our present understanding of the structural and functional organization of Vi and InSy-SVT.

This dissertation is dedicated primarily to my mother who constantly instilled within her children the notion that they could achieve anything they desired in life, if only they put their minds to it and worked hard. Of course, she was right.

This dissertation is also dedicated to Dr. William R. Mehler who initially introduced me to the inner mysteries of the brain. His guidance and long exemplary devotion to experimental research have been central to the development of my own research career in the field of neuroscience. I will always be grateful to him for freely sharing with me his incredible wisdom of, and love for, neuroanatomy.

ACKNOWLEDGEMENTS

My sincerest thanks to my advisor, Dr. William M. Falls, who invited me into his laboratory as a second year graduate student, shared with me his breadth of knowledge of the organization of the trigeminal sensory system, and allowed me the freedom to experience and learn.

Special thanks are also extended to Drs. I. Grofova, J.I. Johnson, D. Tanaka, Jr., and J.E. Thornburg who all graciously offered their time as members of my Dissertation committee. Each provided invaluable support and criticisms during my graduate career at Michigan State University. I am indebted especially to Drs. Grofova, Johnson, and Tanaka for providing access to some of the equipment, supplies which were essential for some of the various phases of this research.

I also gratefully acknowledged the continued support and friendship of P.A. Patterson who was instrumental in my completion of the ultrastructural portions of this Dissertation.

Finally, I want to express my appreciation for the constant support and friendship that I received from several people, who are presently or will be, Doctors R.H. Bradley, E.F. Etter, F.R. Graziani, B.G. Heerdt, B.M. Spann, and especially P.A. Sissel. These close personal friends taught me the true nature of being a scientist. "Someday, when we are all famous, we'll look back upon our present anonymity and laugh."

TABLE OF CONTENTS

LIST OF FIGURES

CHAPTER ONE

CHAPTER TWO

CHAPTER THREE

CHAPTER FOUR

CHAPTER FIVE

LIST OF ABBREVIATIONS

a..... Astrocytic Glial Process
AchE..... Acetylcholinesterase
brVi..... Border Region of Vi
BZ..... Border Zone of Vo
CNS..... Central Nervous System
Cul..... Lateral Cuneate Nucleus
Cun..... Cuneate Nucleus
D..... Dendrite
DAB..... Deep Axon Bundle
DAO..... Dorsal Accessory Olive
DCF..... Dorsal Column Funiculi
DCN..... Dorsal Column Nuclei
dcVi..... Dorsal Cap Region of Vi
dlVi..... Dorsolateral Region of Vi
DM..... Dorsomedial Region of Vo
DPA..... Dental Pulp Afferents
G..... Golgi Apparatus
GABA..... Gamma-Aminobutyric Acid
GABA-T..... Gamma-Aminobutyric Acid Transaminase
GAD..... Glutamic Acid Decarboxylase
GER..... Granular Endoplasmic Reticulum
Gr..... Gracilis Nucleus
GSA..... General Somatic Afferent
HRP..... Horseradish Peroxidase
InSy-SVT..... Interstitial System of the SVT
irVi..... Intermediate Region of Vi
iV-Cul..... Insular Trigeminal-Cuneatus Lateralis Nucleus
LF..... Lateral Funiculus
LI..... Lamina I
LII..... Lamina II
Lin..... Nucleus Linearis
LR..... Lateral Reticular Nucleus
m..... Mitochondria
MDH..... Medullary Dorsal Horn
n..... Nucleus
NB..... Nissl body
PaMd..... Dorsal Paramarginal Nucleus
PaV..... Paratrigeminal Nucleus
pcRF..... Parvocellular Reticular Formation
POR..... Peri-Obex Region
PR..... Penetrating Ray
RB..... Restiform Body
S..... Somata
s..... Spine
SCT..... Spinal Cerebellar Tract
SER..... Smooth Endoplasmic Reticulum
SG..... Substantia Gelatinosa
SMJ..... Spinal Medullary Junction

SP ..... Substance P
SVC ..... Spinal Trigeminal Complex
SVN ..... Spinal Trigeminal Nucleus
SVT ..... Spinal Trigeminal Tract
TC ..... Trigeminocerebellar
TMB ..... Tetramethylbenzidine
TS ..... Trigeminospinal
TSC ..... Trigeminocollicular
TT ..... Trigeminothalamic
u ..... Unmyelinated Preterminal Axon
V ..... Trigeminal
V-Rpc ..... Trigeminal Extension of pcRF
Vi ..... Trigeminal Nucleus Interpolaris
VII ..... Facial Nerve
VLF ..... Ventrolateral Funiculus
vlVimc ..... Ventrolateral Magnocellular Region of Vi
vlVipc ..... Ventrolateral Parvocellular Region of Vi
Vms ..... Main Sensory Trigeminal Nucleus
Vo ..... Trigeminal Nucleus Oralis

INTRODUCTION

The series of investigations which form the body of this Dissertation were designed to provide more detailed information regarding the structural and functional organization of trigeminal nucleus interpolaris (Vi) and adjacent regions in the rat. In the last half century, somatosensory research has gradually focused more intently upon the trigeminal (V) sensory system. Early interest in this area was dominated by clinically oriented studies devoted specifically to identifying the neural mechanisms underlying orofacial pain, primarily in response to the need to define more effective treatments for the relief of pain associated with disorders of the V nerve (see, for example, Sjoqvist, '38; and others). With the advent of the modern armamentarium of hodological and neurobiological techniques came the realization that the V sensory system possesses many specialized features, the presence of which provide unique opportunities to investigate not only specific attributes of the system itself, but also more generalized somatosensory organization and function (Kruger, '71; and Kruger and Young, '81). Contemporary research of the V sensory system has, as a result, become far more diverse in nature and includes studies in every aspect of V sensory function. However, despite the vast amount of literature presently available in this area, our understanding of sensory processing within the V system is far from complete, as evidenced by the fact that the specific neural mechanisms underlying V somatic afferent sensations, including nociception (pain), still remain rather elusive.

Perhaps some of the foremost contemporary questions regarding the V sensory system concern the specific roles played by trigeminal nucleus oralis (Vo) and Vi in overall V sensory function. The relative importance of these two rostral subdivisions of the spinal V nucleus (SVN) is clearly reflected in the fact that they form the bulk of the SVN in mammals and give rise to a large proportion of the secondary V projections to diverse targets along the neuraxis. Although recent studies have begun to elucidate the functional nature of these nuclei, many aspects of their intrinsic organization still remain unknown. The anatomical information presented in this Dissertation, regarding the intrinsic organization of Vi and adjacent regions of the medulla in the rat, provide a foundation upon which future studies may build in order to eventually gain a fuller understanding of the overall function of these regions in medullary somatosensory mechanisms.

Background Review

The intent of this introduction is not to provide a complete review of the structural and functional organization of the V sensory system since more detailed background reviews are provided within the various chapters of this Dissertation as well as elsewhere in the literature (see, for example, the reviews by Matthews and Hill, '82; Brodal, '81; Kruger and Young, '81; Dubner, Sessle and Storey, '78; Anderson and Matthews, '77; Darian-Smith, '73; Dubner and Kawamura, '71; Kruger, '71; Kahn, Crosby, Schneider and Taren, '69; Darian-Smith, '66). The brief review which follows serves only as an introduction to the V sensory system in general, with particular emphasis on those aspects of its organization which are the focus of the various studies contained in this Dissertation.

The sensory V nuclear complex (SVC) consists of the main sensory V nucleus (Vms) and SVN. The latter nucleus has classically been divided into three cytoarchitectonically distinct nuclei which in rostrocaudal sequence of appearance are: Vo, Vi and the medullary dorsal horn (MDH). Each of the four components of

SVC receive the central processes of general somatic afferent (GSA) fibers of the V nerve. These fibers convey exteroceptive (cutaneous) impulses from nociceptive (pain), thermoceptive (temperature), and tactile receptors located in the skin of the face and head, mucous membranes of the nasal and oral cavities, the teeth and surrounding tissues, sinuses, cornea and conjunctiva, and much of the dura. These exteroceptive fibers arise from neurons located in the V (Gasserian or semilunar) ganglion and are peripherally distributed via the ophthalmic, maxillary and mandibular divisions of the V nerve to relatively non-overlapping territories organized in a dermatome-like fashion somewhat analogous to that established by spinal nerves, although some distinct differences exist (for further details see kruger, '71). An ascending branch of the V root, formed by the central processes of the primary V fibers, terminates in Vms while a descending branch courses caudally along the lateral aspect of the brainstem to form the spinal V tract (SVT) and terminates within SVN. The majority of the primary V sensory fibers dichotomize upon entering the brainstem into ascending and descending branches which terminate within Vms and the various subdivisions of SVN, respectively thereby supplying a dual input of primary V afferents to these nuclei. The remaining primary V fibers project exclusively to either Vms or SVN.

The peripheral somatotopy of the primary V afferent fibers is maintained throughout its central representations in SVC. The precise somatotopic organization of primary V afferents within SVT and SVC, however, is essentially an inverted representation of the ipsilateral head and face with ophthalmic division fibers situated ventrally, mandibular division fibers dorsally and maxillary division fibers lying in intermediate regions. The topographical organization of these fibers is arranged such that medial portions of the face are situated medially within the nucleus while lateral portions of the face and head are found in regions located near SVT. The somatotopic organization within MDH is far more complex, since primary

V afferents are differentially distributed to the various laminae of MDH. In addition, an "onion-skin" pattern in the organization of facial sensory regions within this nucleus, with midline structures (e.g., mouth and nose) represented rostrally within MDH and lateral regions of the face represented more caudally, is also present in MDH (Dejerine, '14).

In addition to the GSA fibers traveling within the V nerve, other exteroceptive GSA fibers traveling within the central processes of the facial (intermediate), glossopharyngeal and vagus cranial nerves terminate within SVC. The central processes of these non-trigeminal primary afferents, which are peripherally distributed to regions of the external ear and palate, conform to the general somatotopy of V afferents and are spatially located within the dorsal and lateral aspects of SVT and SVC (Yokota and Nishikawa, '77; and others).

The SVC along with the dorsal column nuclei (DCN) and adjacent related structures have collectively been considered to represent a functional somatosensory unit within the brainstem. In essence, these nuclei form a separate, but continuous, entire body surface representation of the peripheral distributions of the V, spinal and other cranial nerves.

Historically, it was assumed, mainly on the basis of clinical and pathological observations, that the specific sensory modalities conveyed in the V nerve were partially segregated centrally. The functional subdivision of SVC into a rostral "lemniscal" component, corresponding to Vms, and a caudal "spinothalamic" or "anterolateral" component, corresponding to MDH, was suggested on the basis of the fact that a dissociation of pain and temperature sensations could be selectively achieved through surgical interruption of SVT and SVN at the level of the obex with only minor tactile deficits (Sjoqvist, '38; Kunc, '70; and others). This separation of sensory modalities within SVC was a pleasing concept since it seemed to parallel the separation existing within spinal systems and supported the close similarities

between the V and spinal systems. However, it is now known that the situation is far more complex. In fact, there is no distinct separation of specific sensory modalities within SVC. Nociceptive and tactile impulses, for example, has been shown to distribute to all three subdivisions of SVN and Vms. However, although the different sensory nuclei of SVC share nociceptive and tactile related primary afferent inputs, there are distinct differences in the functional roles played by each nucleus within V sensory function. MDH, for example, is considered to contain the essential elements in the central transmission of nociceptive information originating in tooth pulp, while the nociceptive inputs to Vo may be more concerned with reflex activity (Hu and Sessle, '84). In addition, although V afferents form a topographically organized vibrissae afferent related pattern in Vms, Vi and MDH, it has recently been demonstrated that Vms plays the major role in vibrissae-related pattern formation in more central V structures (i.e.,thalamus and cortex), while the roles of Vi and MDH in this regard remain obscure.

The cytoarchitectonic distinctions of subdivisions within SVC is also supported by differences in their secondary projections within the neuraxis. It has long been known that the secondary projections of Vms mainly consist of a massive ascending projection to the thalamus. In addition, minor projections to other intramedullary sites including the cerebellum, inferior olive, cranial motor nuclei, parabrachial nucleus have been described. These latter projections exist primarily in the form of collaterals. On the other hand, the projections of SVN as a whole are rather widespread including ascending projections to the thalamus, the superior colliculus, the cerebellum, and the parabrachial nucleus; descending projections to the spinal cord; and intramedullary projections distributed to the medullary reticular formation, the inferior olive and several cranial motor nuclei. In addition, each of the different nuclei of SVN exhibit distinct patterns in their projections within the neuraxis. Thus, thalamic projections have been shown to arise from neurons situated

only in distinct lamina of MDH and numerous neurons throughout Vi, while the number of thalamic projecting neurons within Vo appears to vary according to species. In addition, distinct differences exist within the precise spatial termination pattern of the various trigeminothalamic efferent projections from MDH or Vi (Peschanski, '84). In contrast, cerebellar projecting neurons are absent within MDH while such neurons are present throughout Vi as well as restricted primarily within the dorsomedial subdivision of Vo (Falls, Rice and VanWagner, '85). The complexity of the V secondary projection system is increased by the presence of an expansive intranuclear projection system within the SVC which allows for extensive modulation amongst the various subnuclei and modulation at all levels of the SVC. Thus, for example, MDH has been demonstrated to exert a strong inhibitory modulatory influence over more rostral levels of the SVN, especially Vo. Certain homologies have been inferred between the various nuclei of SVC and components of the spinal somatosensory system based on similarities in their structural and functional organization. Anatomical and electrophysiological studies have firmly established the presence of morphological and functional similarities between the organization of MDH and the spinal dorsal horn. MDH is now widely accepted as the V homologue of the dorsal horn, hence its name. The SVT is in this case spatially continuous with and considered functionally analogous to the tract of Lissauer.

The relay of tactile impulses through Vp to the thalamus has resulted in the general consideration of Vp as the functional V homologue of the DCN (that is, nucleus gracilis and nucleus cuneatus) which belong to the "lemniscal system'. Although some questions still remain concerning its questions regarding strict homologies (see Kruger, '71, '81).

In contrast to MDh and Vms, the rostral subdivisions of SVN (i.e., Vi and Vo) remain rather enigmatic and have not generally been recognized as

homologous to any specific nucleus in the spinal somatosensory system. It has been suggested that the origin of a large, secondary V projection to the cerebellum within Vi indicates that Vi may represent the V homologue of the lateral cuneate nucleus (Cul). However, this relationship has been disputed in the literature. It has also been postulated that Vo and Vi may represent nuclei unique to the V sensory system and therefore do not represent simple homologues of components in the spinal somatosensory system. On the other hand, it has also been suggested that the rostral part of Vo along with Vms may together represent the V homologue of the DCN. However, this latter view is hard to reconcile with the distinct differences in the projections of these nuclei. The resolution of this question must await the results of future studies on the structural and functional organization of Vi and Vo.

Our present body of knowledge pertaining to the intrinsic structural and functional organization of SVC is limited. Although extensive studies have been conducted on the structural and functional organization of Vp and MDH, primarily with respect to their processing of tactile and nociceptive stimuli, respectively; relatively fewer studies have focused on the more rostral subdivisions of SVN. Particularly conspicuous is the lack of detailed anatomical investigations on the structural and functional organization of Vi especially considering the importance of Vi in the V sensory system.

This importance is clearly exemplified by the fact that Vi is unique among the various nuclei of SVC in that it contributes to secondary V projections directed towards diverse targets within the neuraxis including the thalamus, the superior colliculus, the cerebellum, the inferior olive, the reticular formation, and the spinal cord. However, despite this information, the precise role of Vi in the processing of orofacial somatosensory information remains unclear. Detailed anatomical studies on the cyotarchitectural organization of Vi are not available in any species. Questions concerning the homogeneity of Vi are debated. In addition, despite the

presence of several different populations of projection neurons in Vi, few detailed studies of the distribution and morphology of these neurons have been conducted. The answers to these questions are essential in order to analyze the extent of similarities between the various nuclei of the SVC and the proposed homologous regions in the spinal cord.

Overall Objectives and Specific Aims

The overall goal of this Dissertation is to address the presently inadequate level of understanding of the intrinsic structural and functional organization of Vi and adjacent regions in mammals. The intent of the combined experiments is to provide more specific anatomical information on the structural organization of rat Vi, the intrinsic organization of three of its major efferent projections (i.e., thalamic, cerebellar and spinal) and the organization of one of its non-trigeminal afferent inputs (i.e., spinal input). In addition, these studies are designed to provide anatomical information on the intrinsic organization and connectivity of the interstitial system of the SVT (InSy-SVT). It is hoped that the results of these studies in conjunction with previous investigations will enhance our understanding of the structural and functional organization of Vi and InSy-SVT, provide a clearer indication of the roles of these regions in overall V sensory function, and allow for more direct comparisons of the organization of these regions across species.

The selection of rat to investigate the structural and functional organization of Vi was based on several factors. First, the central sensory representation of the V nerve in the rat occupies a relatively large portion of lateral medullary, thalamic and cortical levels of the brain and clearly reflects the central importance of the V sensory system in this animal. Second, rats possess a highly specialized mystacial vibrissae system which accounts for a large part of the area occupied by medullary thalamic and cortical regions concerned with the processing of orofacial sensory information. Since this vibrissae system exhibits a precise somatotopic organization,

which is conserved throughout its central representation at various levels of the brain, it provides a unique opportunity to study the somatotopic organization of the sensory system in general. Furthermore, histochemical (Belford and Killackey, '79; and Durham and Woolsey, '84) and cytological (Ma and Woolsey, '84) markers for this system have been established. Third, the rat has been extensively used as a model for the development, organization, plasticity and function of sensory systems, primarily due to the presence of the large, highly unique V sensory system and the ease with which it can be manipulated. Finally, detailed information on the V sensory system in the rat is invaluable from a purely comparative standpoint in determining generalized patterns in the organization of this system throughout mammalian species.

This Dissertation consists of five main phases of research represented by the individual chapters which are presented in the form of separate papers. Each chapter addresses a specific set of particular aims concerning the structural and/or functional organization of rat Vi and InSy-SVT.

1) Chapter One is an investigation of the intrinsic organization of Vi using correlated Nissl and myelin stained preparations. The specific aims of this study are to provide detailed descriptions of the cyto- and myeloarchitecture throughout Vi in order to determine whether regional differences exist in this nucleus, as well as whether precise boundaries can be identified between Vi and MDH and Vi and Vo.

2) Chapter Two is an investigation of the intrinsic organization of InSy-SVT using correlated Nissl and myelin stained preparations, as well as Golgi and retrograde horseradish peroxidase (HRP) axonal transport techniques. The specific aims of this study are to provide detailed descriptions of the cytology and connectivity of neurons within InSy-SVT in order to determine whether morphological and functional heterogeneity exists within this system and to determine the extent of structural and functional similarities which this region may

share with adjacent somatosensory regions (e.g., Cul, SVC, and lateral reticular (LR) nuclei.

3) Chapter Three is an investigation of the organization of trigeminothalamic (TT), trigeminocerebellar (TC) and trigeminospinal (TS) projections originating from neurons within Vi using the retrograde transport of HRP. The specific aims of this study are to examine and compare the distribution and morphology of TT, TC and TS neurons throughout the rostrocaudal extent of Vi in order to determine whether morphological criteria can be used to identify either of these projection neuron populations in Vi, as well as to determine whether regional differences exist in the organization of these three major efferent projections.

4) Chapter Four is a light microscopic investigation of the spinal afferent input to the SVC using anterograde transport techniques (i.e., HRP and tritiated amino acids). This study also examines the relationship between this afferent input and trigeminospinal projection neurons within SVC by taking advantage of the simultaneous anterograde and retrograde transport of HRP. The specific aims of this study are to provide details concerning the origin, course, distribution and morphology of spinal afferents throughout each of the SVC nuclei and adjoining regions and to determine the spatial interrelationship of these afferents with the distribution of trigeminospinal neurons.

5) Chapter Five is an investigation of the ultrastructural organization of the insular trigeminal-cuneatus lateralis nucleus (iV-Cul) which represents one of several components of InSy-SVT defined in Chapter Two of this Dissertation. The first aim of this study is to provide an ultrastructural survey of the cytology and synaptic organization of iV-Cul in order to gain insights into its structural and functional organization, as well as to compare its structural organization to that of other adjacent sensory nuclei (i.e. Cul, LR and SVN). The second aim of this study

is to ultrastructurally identify and characterize the spinal afferent input to this nucleus which was revealed in Chapter Four of this Dissertation.

Significance

The overall significance of the studies presented in this dissertation is related to the contribution that it provides towards a greater understanding of the role of Vi in V sensory processing mechanisms. On a broader scale, it is hoped that the information will ultimately enhance our understanding of the organization of medullary somatosensory systems in general.

CHAPTER ONE

AN ANALYSIS OF THE CYTO- AND MYELOARCHITECTONIC ORGANIZATION OF TRIGEMINAL NUCLEUS INTERPOLARIS IN THE RAT

INTRODUCTION

The mammalian spinal trigeminal nucleus (SVN) has classically been divided into three cytoarchitecturally distinct nuclei: a rostrally situated trigeminal nucleus oralis (Vo), an intermediately positioned trigeminal nucleus interpolaris (Vi), and a caudally located trigeminal nucleus caudalis (Olszewski, '50). This latter nucleus has more recently been referred to as the medullary dorsal horn (MDH) to reflect structural and functional similarities it shares with the spinal dorsal horn (Gobel, Falls, and Hockfield, '77; Craig and Burton, '81; Hoffman, Dubner, Hayes, and Medlin, '81; Shigenaga, Chen, Suemune, Nishimori, Nasution, Yoshida, Sato, Okamoto, Sera, and Hosoi, '86). Although there have been a multitude of anatomical and electrophysiological studies focused upon MDH and Vo, primarily because of their early recognition as central components in trigeminal (V) pain pathways; Vi has, by contrast, received relatively little attention. Only recently has it become clear that Vi plays an important role in the reception, central processing and modification, and the relay of primary V afferent inputs, including nociceptive information (Biedenbach, '77; Mann, Oliveras, Sierralta, and Besson, '82; Hayashi, Sumino, and Sessle, '84; Hayashi, '85; Arvidsson and Gobel, '81; Westrum, Canfield, and Black, '76a,b; Westrum, Canfield, and O'Connor, '80, '81; and Jacquin, Mooney,

and Rhoades, '86). The recognition of these functions has sparked a renewed interest in the structural and functional organization of Vi.

A review of the literature indicates that knowledge regarding the cytoarchitectural organization of Vi is limited. Although Vi has been described in a variety of mammals including the rat (Torvik, '56; Wunscher et al., '65; Fukishima and Kerr, '79; and Altman and Bayer, '80), mouse (Astrom, '53; and Steindler, '85), opossum (Oswaldo-Cruz and Rocha-Miranda, '68), rabbit (Meessen and Olszewski, '49), goat (Karamanlidis, '74), pig (Breazile, '67), cat (Brodal, '56; Eisenmann et al., '63; Wold and Brodal, '72; and Ikeda, '79) and various primates including man (Olszewski and Baxter, '54; Brown, '56, '58a; Noback and Goss, '59; Kerr, '68; Gerhardt and Olszewski, '69). However, these descriptions are limited to cursory accounts of constituent cell types and their distribution throughout the nucleus. In addition, the myeloarchitecture of Vi has only been briefly examined (Gobel, '71; and Gobel and Purvis, '72), despite the fact that such analyses have proven useful in determining the intrinsic structural organization of MDH and Vo (Gobel et al., '77; Falls and King, '80; Falls, Rice and VanWagner, '86). The absence of a comprehensive and correlative analysis of the cyto- and myeloarchitectural organization of Vi, in any species, is especially surprising considering the fact that such an analysis would prove useful in settling disputes in the literature concerning the presence of distinct boundaries between Vi and MDH and Vi and Vo, as well as questions regarding the presence of regional cytoarchitectural heterogeneity within the nucleus.

The precise delineation of a boundary between Vi and MDH, in the peri-obex region (POR), would allow for more accurate descriptions of the organization of afferent and efferent systems within this region of SVN. This delineation gains particular importance since this portion of SVN has recently been implicated in the processing of nociceptive information (Hayashi et al., '84; Hayashi, '85b) including

that emanating from the tooth pulp (Westrum et al., '76a,b, '80, '81). There is presently considerable disagreement regarding the existence of a precise border between Vi and MDH, in spite of the fact that Vi does not exhibit the distinct laminar organization which characterizes MDH. It has generally been reported that there is a gradual change in the structural organization of SVN in this region with some investigators suggesting the presence of a rostral alaminar MDH within this transition zone in rat (Arvidsson, '82; Wunscher, Schober and Werner, '65), cat (Craig and Burton, '81; Marfurt, '81; and Eisenmann, Landgren and Novin, '63) and primate (Gerhardt and Olszewski, '69). Several studies provide brief cyto-, myelo- or chemoarchitectural evidence which support the view that a distinct spatial overlap exists between separate regions belonging to Vi and MDH within POR of man (Brown, '56), monkey (Kusama and Mubachi, '70), rabbit (Meessen and Olszewski, '49), pig (Breazile, '67), guinea pig (Friede, '59) and rat (Krieg, '42). More recently Steindler ('85) has reported the presence of a unique cytoarchitecturally distinct "septum" which forms a distinct border between Vi and MDH in the mouse; while Jacquin, Renehan, Mooney, and Rhoades ('86) and Shigenaga et al. ('86) schematically illustrate at least a partially distinct border between Vi and MDH in the rat and cat, respectively. It is clear from the above reports that the presence of a distinct boundary between MDH and Vi has not gained general acceptance. This is perhaps the result of not having the cyto- or myeloarchitectural changes which occur within this region fully characterized, therefore making it difficult to compare the structural organization of the MDH/Vi transition zone across species.

The presence of a cytoarchitecturally distinct border between Vi and Vo has also been disputed in the literature. Although several studies suggest the existence of a sharp Vi/Vo border in primates (Olszewski, '50; Gerhardt and Olszewski, '69), donkey (Karamanlidis, '75), and pig (Breazile, '67); other investigators have denied that such a boundary is readily distinguishable in monkey (Kerr, Kruger,

Schwassman and Stern, '68), goat (Karamanlidis, '68), and cat (Wold and Brodal, '73). None of these studies however, provide ample cytoarchitectural evidence to support either view. This controversy is further compounded by the fact that some investigators have reported the existence of a separate "dorsomedial" subdivision or nucleus which spans Vi and Vo, thereby providing some structural continuity between these two nuclei (Astrom, '53; Torvik, '56; Valverde, '61, '62). However, the presence of this "dorsomedial" nucleus within rostral SVN has not generally gained acceptance in the literature. In fact, some investigators have even questioned the significance of subdividing rostral SVN based on cytoarchitectural criteria alone (Kerr et al., '68; Bates and Killackey, '85). In response to these criticisms, recent studies in the rat redefined the Vi/Vo border based on correlative differences in cytoarchitecture and thalamic (Fukishima and Kerr, '79) and cerebellar (Falls et al., '86) connectivity of rostral SVN. These studies however, fail to provide adequate documentation of the cytoarchitectural changes which occur at the Vi/Vo transition zone to permit resolution of whether there is a sharp border between Vi and Vo in the rat. Although the conflicting reports cited above may simply reflect a species difference in the organization of the Vi/Vo transition zone, it is also possible that many of these inconsistencies might be resolved if detailed analyses of this region were conducted across species. Regardless, it is clear that a comprehensive analysis of this region would ensure more accurate descriptions of the distribution of afferent and efferent systems within rostral SVN, thereby contributing to a more complete understanding of the functional organization of Vi.

The intrinsic organization of Vi has long been the subject of controversy. While cytoarchitectural studies, in general, have indicated that Vi possesses a population of small, medium and large-sized neurons which are distributed rather uniformly throughout the nucleus without forming any apparent subdivisions (Olszewski, '50; Olszewski and Baxter, '54; Crosby and Yoss, '54; Brodal, Szabo, and

Torvik, '56; Brown, '58b, '62; Noback and Goss, '59; Taber, '61; Breazile, '67; Oswaldo-Cruz and Rocha-Miranda, '69; Gerhardt and Olszewski, '69; and Wold and Brodal, '73), other studies provide indications to the contrary. A conspicuous concentration of larger neurons has been reported within the ventrolateral aspect of rat Vi (Torvik, '56; Wunscher et al., '65; and Fukishima and Kerr, '79) and this region in mouse has recently been shown to contain discrete cytological patterns of organization which are similar, although complementary, to vibrissae afferent segmental zones revealed by succinic dehydrogenase histochemistry (Ma and Woolsey, '84). Moreover, the cytoarchitectural descriptions provided by Torvik ('56) and Krieg ('50) each suggest the presence of at least two or more morphologically distinct regions within Vi. The non-homogeneity of Vi suggested in these latter studies is generally supported by the Golgi study of Astrom ('53) in the mouse which identifies several morphologically distinct regions within the nucleus based primarily on differences in the morphology and distribution of afferent fibers. In addition, the results of axonal transport studies of the distribution of specific afferent inputs to Vi also suggest that there are regional differences in its functional organization (Phelan and Falls, '84b; and Hayashi, '85b; see also Chapter Four). In fact, it has become increasingly clear that Vi is a non-homogeneous nucleus containing a marked heterogeneity of morphologically and functionally distinct neurons which do exhibit some disparity in their distribution (Phelan and Falls, '83, '85; and Panneton and Burton, '85; see also Chapter Three). Despite the fact that there exists ample evidence to indicate that Vi is a rather heterogeneous nucleus, there have been no cytoarchitectural studies which specifically provide support for any of the proposed subdivisions. Considering the emerging complexity in the organization of Vi, it appears essential to conduct a comprehensive analysis of the intrinsic cyto- and myeloarchitectural organization of this nucleus to serve as a basis for future studies on its structural and functional organization.

This study provides detailed descriptions of the cyto- and myeloarchitectural organization of Vi in the rat. A combination of Nissl, Kluver-Barrera, cytochrome oxidase, and serial semithin myelin stained sections are utilized in order to more precisely define the borders of Vi, especially the MDH/Vi and Vi/Vo transitions, as well as the regional intrinsic organization of the nucleus.

METHODS

Adult, male Sprague-Dawley albino rats (200-300 gms.) were used in this investigation. The main cytoarchitectonic observations of Vi reported in this study were obtained through examination of three brains sectioned in the transverse, horizontal or parasagittal plane. Each animal was anesthetized and perfused transcardially, using a Masterflex pump delivery system, with an initial brief heparanized physiological saline wash followed by 500 ml of a fixative consisting of 1% formalin, 0.5% glacial acetic acid and 5.9% ethyl alcohol. The brains were left in situ and submerged in the same fixative for one week at 4° C. They were subsequently removed from the skull, blocked, stored for an additional two days in fixative and then successively placed into 10% and 30% sucrose solutions until they sank. Serial brainstem sections were cut on a freezing microtome at a thickness of 50 μm. One set of alternating serial sections from each animal was stained according to routine Nissl staining procedures with 0.5% cresyl-violet acetate. The remaining sets of serial sections from each animal were stained for the simultaneous demonstration of cells and myelinated fibers within the same section according to the Kluver-Barrera ('53) staining method using 1% Luxol Fast Blue and 1% Safranin.

The observations noted in the material prepared above were compared with those obtained in supplemental material from several additional animals which were perfused in a similar manner with a fixative consisting of 1% paraformaldehyde, 1%

glutaraldehyde and 0.5% $CaCl_2$ in a 0.12 M phosphate buffer (pH 7.4). The brains of these animals were removed from the skull immediately following perfusion and postfixed in the same fixative for an additional one to three hours at 4° C. The brains were then serially sectioned on an Oxford Vibratome, at a thickness of 50 μm, in one of the three standard planes. A single set of serial sections were mounted from each animal and stained using either 0.5% cresyl-violet acetate or 1% neutral red.

The myeloarchitectonic features reported in this study were determined through examination and comparison of Kluver-Barrera stained sections and serial plastic embedded semithin myelin stained sections. The semithin sections were included in this study since they allow for easy visualization of the smaller myelinated fibers which permeate Vi. Five animals were specifically prepared for serial semithin light microscopic analysis. These animals were perfused intracardially with a brief, heparanized physiological saline wash followed by 500 ml of a fixative consisting of 1% paraformaldehyde, 1% glutaraldehyde and 0.5% $CaCl_2$ in a 0.12M phosphate buffer (pH 7.4). The brains were removed from the skull and the brainstems were immediately blocked and serially sectioned on an Oxford Vibratome, at a thickness of 100 μm, in either the transverse or horizontal planes. Serial sections throughout the rostrocaudal extent of Vi were trimmed, osmicated, dehydrated and embedded in Epon-Araldite. Serial sections, 1-2 μm thick, were cut from the face of each block, heat mounted onto glass slides and subsequently stained with P-phenylenediamine (Hollander and Vaaland, '68).

The location and boundaries of Vi and adjacent structures, as well as the borders of each of the proposed regions within Vi (Figure 1), were determined on the basis of relative differences in the overall cyto- and myeloarchitectonic features present within each of the preparations described above. In particular, differences in the size, density, distribution and orientation of myelinated fiber systems, the overall

texture of the neuropil and the types, orientation and distribution of cell profiles were used as a basis for this differentiation. Careful attention was paid to the size, distribution and orientation of the bundles of myelinated fibers which permeate Vi neuropil (Gobel and Purvis, '72). The cytological characteristics of neurons within Vi were examined using a 50X objective. Neurons were classified into different types based on their overall Nissl staining characteristics, their orientation within the nucleus and their relative somatic and nuclear size and shape.

The pattern of cytochrome oxidase staining within the peri-obex region of the medulla was revealed in three animals using the histochemical modification of Wong-Riley ('79). The animals were anesthetized with an intraperitoneal injection of Nembutal (50 mg/kg) and perfused intraaortically with a brief heparanized 0.9% physiological saline wash followed by 500 ml of a fixative consisting of 1% paraformaldehyde and 1% glutaraldehyde in 0.15M phosphate buffer (pH 7.4). The brains were then removed from the skull and immediately placed in a 0.15M phosphate buffer overnite at 4° C. Transverse serial sections were cut on a Vibratome at a final thickness of 50 μm and collected in 0.15M phosphate buffer. Alternate serial sections throughout the medulla from all three animals were simultaneously incubated at 37° C in the dark for 1-2 hours in an incubation medium consisting of: 50 mg diaminobenzidine tetrahydrochloride (filtered), 90 ml 0.15M phosphate buffer (pH 7.4), 15-30 mg of cytochrome C, and 4 mg sucrose. The sections were then visually checked every 30 minutes for the presence of light to dark brown reaction product within the tissue and the incubation stopped when there was a clear differentiation between reactive and nonreactive areas of the brain. The sections were then washed in 0.15M phosphate buffer, mounted onto gelatinized glass slides and air dried. In one animal the sections were counterstained with 0.5% cresyl-violet, while the sections in the remaining animals were coverslipped unstained for purposes of comparison. Cytochrome oxidase positive

zones were identified as regions of relatively dark areas against a pale background. The staining was classified as either intense, moderate, or relatively low levels of cytochrome oxidase activity. Differences in the relative intensity of cytochrome oxidase staining throughout the peri-obex region were taken to indicate differences in the metabolic activity of the various regions.

The somatic cross-sectional areas of neurons within each of the proposed regions of Vi were determined from the transverse, Nissl stained sections with the aid of a Nikon Image Analyzer and a drawing tube attached to a Leitz Orthoplan microscope using a 40X objective. All of the neurons in a single field of view exhibiting a distinct nucleolus were included in the sampling. Measurements were pooled from randomly selected rostrocaudal and mediolateral areas within each cyto- and myeloarchitecturally defined region. These measurements were grouped into block intervals of 25 μm^2 and plotted as frequency histograms of somatic cross-sectional areas for each region (Figure 9B-G). The total somatic cross-sectional area histogram for Vi (Figure 9A) was compiled from the combined percentages calculated from each separate region. The mean and standard deviations were calculated for all pooled sets of measurements and appropriate statistical tests applied to these data as necessary.

RESULTS

Based on correlated light microscopic observations taken from Nissl, Kluver-Barrera and serial myelin stained semithin sections, rat Vi extends approximately 2.2 to 2.4 mm rostrocaudally in the lateral medulla. Its caudal pole is located in the POR and its rostral pole is situated at the level of the caudal end of the facial motor nucleus (Figure 1, levels 1 and 8, respectively). The caudal boundary of Vi is marked by a distinct spatial overlap with the rostral pole of MDH (Figure 1, levels 1 and 2), while the rostral boundary is characterized partly by a distinct overlap with Vo,

especially the caudal pole of its dorsomedial region (DM), and partly by a more gradual transition with Vo, especially in ventral and lateral regions of the nucleus (Figure 1, levels 7 and 8). The spinal V tract (SVT) forms the lateral and ventral borders of Vi throughout its entire length. The spinocerebellar tract (SCT) and the restiform body (RB) cover the lateral aspect of SVT.

The structures forming the medial border of Vi vary according to the particular rostrocaudal level within the medulla. At the extreme caudal pole of Vi, the medial border is formed by the rostral pole of MDH (Figure 1, levels 1 and 2; Figures 2, 10A-D, and 11A) which gradually gives way to the parvocellular reticular formation (pcRF) at intermediate and more rostral levels of the nucleus (Figure 1, levels 3-7). In addition to pcRF, the medial border of the extreme rostral pole of Vi is partly formed by the overlapping caudal pole of Vo (Figure 1, levels 7 and 8; Figures 2D and 11D). The dorsal border of Vi is formed by ventral regions of either the cuneate (Cun), lateral cuneate (Cul) or spinal vestibular nuclei. The medial border of Vi is difficult to distinguish in Nissl or myelin stained sections alone. However, a careful comparison of the appearance of these regions in Kluver-Barrera stained preparations reveals certain cell and myelinated fiber patterns which can be used as a guide in closely approximating the position of these borders in either Nissl or myelin stained sections alone. In particular, there is a sharp increase in the size and density of myelinated fiber bundles, as well as an equally sharp decrease in the size, staining intensity and density of cells as one progresses from Vi to neighboring regions of the medulla (Figures 2, 10F and 11).

The overall shape of Vi, as seen in transverse sections, varies with respect to its position within the lateral medulla. The extreme caudal pole of Vi is represented by a small crescent-shaped region which gradually expands within POR. At the level at which components of Vi have entirely replaced the rostral remnants of MDH (see Figure 1, level 3), the nucleus is ovoid in shape and measures approximately 2.2 mm

by 4.7 mm with its long axis directed dorsomedially within the lateral medulla. Rostrally, the nucleus gradually becomes smaller in size and undergoes a slight shift in its orientation. At a level just prior to the transition from Vi to Vo (see Figure 1, level 8) the area occupied by Vi measures approximately 1.9 mm by 4.2 mm with its long axis oriented in a more dorsoventral direction. Further rostrally, Vi gradually reduces in size as it is displaced by the medially enlarging caudal pole of Vo.

Six separate and distinct regions of rat Vi can be distinguished on the basis of differences in their overall cyto- and myeloarchitecture. The relationship between these various regions can best be appreciated in the transverse plane as schematically illustrated in Figure 1. Briefly, these six regions are: 1) A ventrolateral parvocellular region (vlVipc) which occupies the ventrolateral caudal half of Vi; 2) A ventrolateral magnocellular region (vlVimc) which occupies a similar region in the rostral half of the nucleus; 3) A border region (brVi) interposed between SVT and vlVipc and vlVimc; 4) A dorsolateral region (dlVi) which lies predominantly in the rostral half of Vi subjacent to the dorsal half of SVT; 5) A dorsal cap region (dcVi), occupying the dorsomedial aspect of the nucleus throughout its entire rostrocaudal extent; and 6) An intermediate region (irVi) which lies immediately ventral to dcVi within the concavity formed by the medial borders of vlVipc and vlVimc.

The cells in Vi could be separated into small (< 15 μm in diameter), medium (15-25 μm in diameter) and large (> 25 μm in diameter) neurons. The somatic cross sectional areas of these neurons range from approximately 25-800 μm^2. The vast majority of cells in Vi are small and medium-sized cells with somatic cross sectional areas less than 250 μm^2. The somatic cross sectional areas of neurons in each of the six regions of Vi generally parallels the distribution in the nucleus as a whole (Figure 9B-G). However, these regions can be reported into two groups. The first group consists of brVi, vlVipc and irVi which contain predominantly small to

medium-sized neurons measuring less than 250 μm^2. The second group consists of dlVi, vlVimc, and dcVi which contain a more evenly distributed population of medium and large-sized neurons. Although the regions in these two groups may exhibit extensive overlapping with regard to the distribution of somatic cross sectional areas, these regions can be distinguished by differences in the somatic shape and staining characteristics of its constituent cells (see below).

In order to facilitate descriptions of the progressive changes in the interrelationships among the various regions of Vi as well as the specific changes occurring at the rostral and caudal borders of the nucleus, the regional cyto- and myeloarchitecture of Vi will be described from caudal (levels 1 through 4) to rostral (levels 5 through 8) levels in reference to Figure 1.

The caudal half of Vi (Levels 1 through 4)

Level 1. The caudal pole of Vi first appears in the POR at a level which closely corresponds to the first simultaneous appearance of the three subgroups of the caudal medial accessory olive (Gwynn, Nicholson and Flumerfelt, '77). This level also corresponds to the point at which SCT has just begun to wrap laterally around SVT. The caudal pole of Vi is easily recognized as a thin crescent-shaped area situated in the ventrolateral aspect of SVN (Figures 2A, 10, and 11A). This area consists of the caudalmost extensions of vlVipc and brVi. Gradually, the crescent-shaped area enlarges rostrally and displaces the rostral pole of MDH dorsally and medially such that the ventral half of the substantia gelatinosa (SG, laminae I and II) is shifted to a position deeper within SVN. Typically, the medially displaced SG fractures into two or more small, round or irregular shaped pockets of neuropil which lie along the medial border of the crescent-shaped area (Figures 10, 11A, and 12A). In addition, small, irregular-shaped pockets of SG commonly remain wedged between SVT and the caudal pole of Vi, especially along its ventromedial edge. These latter pockets of SG usually invade SVT to form irregular-shaped islands of

neuropil which contribute to the interstitial system of SVT (InSy-SVT, Falls and Phelan, '84; see also Chapter Two). The dorsal half of SG remains subjacent to SVT (Figure 10C-E) and a few thin strands of neuropil can be seen extending laterally into SVT to become contiguous with the dorsal paramarginal nucleus (PaMd), one of several distinct components of rat InSy-SVT (see Chapter Two). Although a few intensely stained neurons morphologically similar to marginal (lamina I) neurons are present along the SG/vlVipc border, it is difficult to determine whether these cells belong to lamina I or vlVipc. In fact, it is not clear in Nissl stained sections whether a distinct marginal layer exists along the lateral margin of the displaced SG. No other observable changes in the structural organization of MDH are present at this level. The spatial dislocation of lamina II during the transition from MDH to Vi is most clearly evident in cytochrome oxidase stained preparations (Figure 10), where SG is relatively pale stained compared to the more intensely stained portions of neighboring MDH and Vi.

In myelin stained semithin sections the crescent-shaped area of caudal Vi is easily distinguishable from the medially displaced laminated MDH (Figure 11A), since the area is relatively devoid of large diameter deep axon bundles (DAB, Gobel and Purvis, '72). The few DAB's in this area differ from those in MDH in that they contain a conspicuous population of larger diameter myelinated axons similar in size to those in medial SVT. The SG/vlVipc border is marked by the presence of numerous small diameter DAB's which represents the DAB's which form the border between laminae I and II of MDH (Gobel, Falls, and Hockfield, '77)(Figure 11A).. A large number of penetrating rays (PR, Gobel and Purvis, '72) extend throughout the entire depth of the crescent-shaped area and diffuse abruptly upon entering MDH. Another prominent myeloarchitectural feature of this area is the presence of a dense system of fine, myelinated axons which course parallel to SVT as well as a large number of smaller groups of myelinated axons coursing perpendicular to SVT

(Figure 11A). These latter myelinated fiber groups are primarily responsible for the contrasting appearance of the neuropil of this area in comparison to the characteristic nonmyelinated appearance of the adjoining regions of SG. The crescent-shaped region of Vi is also evident in cytochrome oxidase stained preparations where it appears as a relatively intensely stained region compared to the unstained lamina II neuropil (Figure 10B-D).

In Nissl stained sections, a number of small and medium-sized neurons as well as a few larger cells are observed within the caudal pole of vlVipc (Figure 5). The smallest cells have oval to fusiform-shaped somata (measuring < 15 μm in diameter) and central or eccentrically placed nuclei which often display prominent nuclear indentations (Figures 5A-E). These neurons have a high nuclear to cytoplasmic ratio and many exhibit a deeply stained thin rim or cap of cytoplasm containing a fine, granular Nissl substance. Pale staining cells are also common. The small cells are distributed uniformly throughout the region and frequently are seen as closely apposed pairs.

The medium-sized neurons in caudal vlVipc have oval to fusiform-shaped somata (measuring 15-30 μm in diameter) with a prominent central or eccentrically placed smooth nucleus (Figure 5F and G). These cells exhibit a relatively low nuclear to cytoplasmic ratio compared to the small neurons. Their cytoplasm contains a fine to coarse, evenly dispersed intensely stained Nissl substance. However, some pale staining medium-sized neurons are also found. The majority of the neurons have their long axis oriented parallel to SVT. Medium-sized neurons are also distributed uniformly throughout this region.

The largest neurons in caudal vlVipc have multipolar or stellate shaped somata with a large centrally placed nucleus and an abundant amount of coarse, intensely stained Nissl substance forming distinct Nissl bodies. A few thick primary dendrites are usually seen in Nissl stained sections. The largest and most intensely

stained of these neurons, especially those with stellate-shaped somata, are situated in the dorsolateral aspect of vlVipc. The number of larger-sized cells is relatively few in comparison to the numbers of small to medium-sized neurons.

The most striking cytoarchitectural feature of vlVipc portions of the crescent-shaped area of caudal Vi is the increased density of compactly arranged small to medium sized, intensely stained neurons in comparison to adjoining portions of MDH. Many of the intensely stained neurons are organized into small aggregates of five or more cells. These aggregates of intensely stained neurons, along with less intensely stained cells, are typically organized into three large clusters which are evenly spaced from the dorsolateral tip ventrally along the arcing contour of the crescent-shaped area (Figure 2A). This unique clustering pattern is restricted to the caudal 150 μm of vlVipc and occupies the entire mediolateral width of this region. Rostrally, at levels corresponding to positions between levels 1 and 2, these large clusters are replaced by large aggregates. These latter aggregates are not always seen in serial sections indicating that they represent discrete groups of neurons rather than continuous rostrocaudally oriented columns of cells. However, they occupy similar spatial positions within Vi from section to section. Although the presence of DAB's may partially contribute to the appearance of the aggregates of cells in this region, the consistent size and position of these aggregates in the nucleus suggest that they are not artifactual in nature.

The crescent-shaped area also contains the caudal pole of brVi which is characterized at this level by three unique cell patterns. The ventromedial edge of brVi is represented by a band approximately 150 μm wide consisting of small to medium-sized cells subjacent to SVT. The majority of the cells have oval to fusiform-shaped somata with their long axes oriented parallel to SVT (Figure 3A and B; and Figure 12D). A few small, round cells are also present (Figure 3C). These cells were morphologically similar to those found in adjacent portions of

vlVipc, however their distinct organization into a band along the border of SVT is a pattern not evident within vlVipc. The dorsolateral part of brVi contains one to two distinct oval-shaped clusters of intensely stained neurons which directly abut SVT. These clusters measure approximately 130 μm by 230 μm and represent discrete rather than rostrocaudally oriented columns since they are not always observed in serial sections. The small and medium-sized cells within the clusters are morphologically similar to those found within vlVipc, however because of their organization into distinct clusters bordering SVT, they are considered to belong to caudal brVi. The rest of brVi lying in between these clusters is characterized by a decrease in the number, density and staining intensity of neurons in comparison to vlVipc. The small and medium-sized oval to fusiform-shaped neurons which inhabit this area are morphologically similar to those in vlVipc and have their long axis oriented parallel to SVT. The distinct band of generally fusiform-shaped cells and the relatively cell poor, less intensely stained areas bordering SVT are characteristics representative of brVi throughout its rostrocaudal extent. In cytochrome oxidase stained section through the POR, discrete clusters of intensely stained neuropil are located in similar locations adjacent to SVT (Figure 10B-E).

Level 2. The crescent-shaped area has expanded to occupy a greater portion of the ventral half of SVN at this level of the medulla. The fractured elements of SG are no longer present. However, differences in cyto- and myeloarchitecture still mark the border between vlVipc and MDH. The vlVipc portion of the crescent-shaped area now more closely resembles the more rostral levels of vlVipc. This region exhibits numerous DAB's which are organized into three to four parallel curvilinear arrays. Dorsolaterally these arrays are more tightly compacted while they gradually diverge in a ventromedial direction within vlVipc. This pattern of DAB organization is not found in other areas of Vi at this level. The numerous PR's in this region, which far outnumber those found more caudally, penetrate the entire

depth of vlVipc and disperse abruptly into the lateral portions of the remaining regions of MDH. The neuropil of vlVi at this level is still characterized by the presence of a dense system of finely myelinated axons. Small bundles of these axons are organized parallel to the arcing arrays of DAB's.

The neurons present within this level of vlVipc are morphologically similar to those described in the extreme caudal pole of vlVipc. However, a larger number of medium-sized multipolar-shaped neurons are seen. The large clusters of intensely stained cells which characterize the extreme caudal pole of vlVipc are no longer present. In their place, numerous small aggregates of intensely stained cells are distributed throughout vlVipc, although they are more prominent dorsolaterally. The largest of these cells are evenly distributed along the arcing arrays of DAB's.

The oval-shaped clusters of cells characterizing portions of caudal brVi are absent at this level of the nucleus. Cytoarchitecturally, brVi is represented by distinct bands of cells as well as relatively pale, cell poor regions. In myelin stained sections, numerous DAB's are seen breaking away from SVT and passing through brVi on their way to vlVipc (Figure 12D). In addition, bundles of myelinated fibers, partially representing the branches of PR's, course within brVi. These two fiber systems impart a general pale appearance to brVi in Nissl stained sections. The dorsolateral aspect of brVi at this level sometimes exhibits a strip of intensely stained small and medium-sized fusiform-shaped neurons. These cells are contiguous with cells that traverse SVT to join the insular trigeminal-cuneatus lateral nucleus (iV-Cul) a component of InSy-SVT (Falls and Phelan, '84; see also Chapter Two). The similarity in size, shape and staining characteristics of these cells as well as the continuity of this region with iV-Cul suggest that these cells may represent an extension of InSy-SVT into the territory of brVi.

The remnants of SG are no longer present in the extreme ventromedial corner of the nucleus. Instead, a wedge-shaped region at this point represents a

transitional area between Vi and pcRF. This area possesses longitudinally directed bundles of myelinated fibers which are organized into tightly compacted rows fanning out in a ventrolateral direction from the medially adjacent pcRF (Figure 10F). The small pale staining cells in this region have oval, multipolar and triangular-shaped somata which are primarily oriented parallel to SVT. However, a cytoarchitecturally distinct border between Vi and pcRF is difficult to determine. The density of cells in this area corresponds more closely to that found in Vi as opposed to pcRF. Occasionally, giant multipolar-shaped neurons exhibiting intensely stained coarse Nissl bodies and belonging to pcRF invades this region. In general though, this region is much more paler in appearance than brVi or vlVipc. In the present study, this region is considered a portion of SVN on the basis of the presence of its continuity with brVi and vlVipc and the fact that many of the cells appear similar to those throughout vlVipc.

A small wedge-shaped area lies along the dorsolateral border of vlVipc next to SVT. This area corresponds to the caudal ventralmost part of dlVi. Numerous thick PR's penetrate through this part of dlVi and extend to the deeper located areas of rostral MDH (Figure 12B and C). The few DAB's in this region are smaller in diameter compared to those in vlVipc and are organized into dorsomedially directed rows. The individual DAB's are also elongated in a dorsomedial direction. The majority of the cells in this region are medium-sized neurons with fusiform shaped somata and their long axis directed dorsomedially parallel to the rows of DAB's (Figure 4, and Figure 12B and C). These neurons have a large central nucleus with light to intensely stained granular Nissl substance evenly dispersed throughout the cytoplasm. Two or three thick primary dendrites are often prominently seen extending from many of these cells parallel to SVT. Small neurons with a high nuclear to cytoplasmic ratios are also present but in fewer numbers than in either vlVipc or brVi. Another group of cells corresponding to the caudal dorsal

part of dlVi is present in the dorsal aspect of Vi subjacent to SVT. This region is also characterized by tightly compacted elongated myelinated fiber bundles and predominantly medium-sized fusiform-shaped neurons oriented in parallel with these bundles. Separating these two regions of dlVi at this level is a thin band of neuropil representing the rostralmost part of dorsolateral SG. This portion of SG appears pale stained in comparison to adjoining parts of dlVi. Strands of neuropil connect this strip of SG with the caudal part of PaMd situated in the enlarged dorsolateral aspect of SVT. A second, larger and irregular-shaped region of SG neuropil often lies more medially within the nucleus as a result of the appearance of the caudal pole of dcVi dorsally. The spatial relationship of the latter structures is clearly evident in cytochrome oxidase stained sections (Figure 10C-F).

The dorsal border of dcVi is formed by a large number of tightly packed small diameter myelinated fiber bundles elongated in a mediolateral direction. Many PR's arising from the dorsal aspect of SVT course mediolaterally through this part of dcVi. The ventral border of dcVi is formed by a large number of thinner diameter PR's which also course mediolaterally on their way to deeper regions representing the rostral remnants of MDH. The dcVi contains a few small diameter DAB's which are also elongated in a mediolateral direction in the nucleus. The axons in these bundles are similar in size to those found in the bundles situated along the dorsal and medial margins of the nucleus. The irregular medial border of dcVi is formed by small, longitudinally oriented myelinated fiber bundles in pcRF.

The cells in the caudal pole of dcVi consist of compactly arranged groups of small to medium-sized neurons with staining characteristics similar to those in vlVipc. The intense staining in these cells contrasts sharply with the pale stained cells found in neighboring areas. The most prominent cells are medium-sized neurons with oval to fusiform-shaped somata which have their long axis directed mediolaterally within the nucleus (Figure 7). The mediolateral orientation of these

cells contrasts with the dorsomedially orientation of cells in adjoining parts of dlVi. Many of the oval-shaped neurons exhibit a distinctive amount of intensely stained Nissl substance distributed throughout the cytoplasm (Figure 7A and B), while other cells possess a moderate staining of Nissl substance which often extends into proximal portions of primary dendrites. The medium-sized neurons in dcVi exhibit a prominent central nucleus and a low nuclear to cytoplasmic ratio. The remaining cells in dcVi are morphologically similar to the lightly stained small and medium-sized neurons in vlVipc (Figure 7C).

The remaining portions of the section represent rostral remnants of the deeper layers of MDH which lie between dcVi and vlVipc. These portions of MDH gradually disappear, along with the rostral remnants of SG, and results in the two parts of dlVi becoming contiguous.

Levels 3 and 4. These two levels of caudal Vi will be described together since they do not exhibit significant differences in their structural organization. These levels of SVN are composed entirely of regions belonging to Vi. The majority of the ventrolateral half of Vi is now occupied by vlVipc. The most evident change in this latter region is the appearance of a medial and a lateral segment. These segments exhibit slight differences in their cyto- and myeloarchitecture, however there is no sharp border between them. The lateral segment of vlVipc represents the rostral continuation and expansion of the more caudal parts of vlVipc. The DAB's in this region have greatly increased in number, although they remain morphologically similar to those at caudal levels of the nucleus. However, the DAB's which are located in the lateral segment of vlVipc are organized into three to four distinct curvilinear arrays. The medial segment of vlVipc exhibits DAB's which contain smaller diameter fibers and are less clearly organized into parallel arrays. The individual axons in these bundles are more within the size range of those found in the bundles of myelinated fibers in the adjoining regions of pcRF. Numerous PR's

course through the lateral segment of vlVipc and some of them enter the medial segment of this region. The medial and lateral segments of vlVipc are further distinguished by the presence of a large number of small, single myelinated fibers which course predominantly in a mediolateral direction in the medial segment and primarily parallel to the PR's in the lateral segment. The texture of the neuropil in vlVipc is fairly coarse due to the many myelinated fibers which permeate the region (Figure 13A).

The neurons in the lateral segment of vlVipc remain organized into discrete aggregates of intensely stained cells. On the other hand, the cells in the medial segment of vlVipc are not as intensely stained and are generally not organized into aggregates, except in its dorsolateral tip. An occasional large multipolar-shaped cell belonging to pcRF invades the medial segment of vlVipc at these levels of the medulla. The density of cells in the medial segment is much less than that found in the lateral segment of vlVipc.

There is no change in the composition of brVi at these levels of the nucleus. However, there is a decrease in the number of myelinated fibers coursing parallel to SVT in this region.

The dorsolateral part of Vi at these levels is formed by one continuous wedge-shaped region representing dlVi. This region extends from the mid-dorsoventral extent of the nucleus to the dorsal tip of SVT, where it merges with the ventral part of Cun. The border between dlVi and Cun is not easily distinguished and these two regions appear to form a continuous band of cells in the dorsolateral medulla (Figure 2B). Numerous DAB's elongated parallel to SVT are distributed throughout dlVi (Figure 11B). These DAB's are smaller in diameter than those present in vlVipc. The individual axons in these bundles resemble those in the medial part of SVT. A large number of PR's penetrate through dlVi to reach the deeper regions of Vi. The neuropil of dlVi is also characterized by a prominent

system of dense myelinated fibers oriented along the long axis of dlVi parallel to SVT (Figure 12C). The region appears pale in Nissl stained sections due to the presence of these myelinated fibers. The cells in dlVi at these levels are morphologically similar to those present at more caudal levels of the nucleus. However, there are a greater number of the small-sized neurons exhibiting oval to fusiform-shaped somata. The most notable feature in dlVi is the presence of a small strip of neuropil arising from the paratrigeminal nucleus (PaV) which extends along the medial border of SVT at levels corresponding to level 4 (Figure 11B). This latter nucleus represents another distinct component of InSy-SVT which lies within the dorsal aspect of SVT (Falls and Phelan, '84; see also Chapter Two). This medial strip of PaV consists of dorsoventrally directed dendrites tightly bundled together (Figure 12C).

The area occupied by dcVi is greater in size at these two levels of the nucleus. The region exhibits a large round medial portion which curves to form a ventrolaterally directed tail which lies adjacent to dlVi (Figures 2 and 11B). This region is relatively devoid of myelinated fibers. A few DAB's are found within this region, but the PR's which penetrate Vi are primarily located along its ventral border with irVi. The region is still characterized by a large number of intensely stained medium-sized oval and multipolar-shaped cells with their long axis directed mediolaterally. Occasionally, a large multipolar-shaped cell belonging to pcRF invades the medial aspect of dcVi at these levels. The ventral part of dcVi contains predominantly small fusiform-shaped cells oriented mediolaterally. The most intensely stained neurons are located along the lateral border and in the center of this region. The cells within the lateral "tail" of dcVi are conspicuously elongated along with the curve of this region in a ventrolateral direction. These cells can be distinguished from those belonging to neighboring parts of dlVi by their intense staining and by their location in a region lacking the dense myelinated fibers

characterizing dlVi. There is no cell aggregation in dcVi comparable to that found in the medial and lateral parts of vlVipc. The medial border of dcVi is sharply demarcated in semithin preparations where the density of myelinated fiber bundles form a clear border with pcRF (Figure 11B). The neuropil in dcVi is more finely textured in comparison to that in vlVipc (Figure 13C).

The region immediately beneath dcVi at these levels of Vi represents the caudal pole of irVi which has replaced the rostral remnants of MDH (Figure 2B). This region resembles in many respects the medial segment of vlVipc. In fact, there is no sharp border between irVi and the medial segment of vlVipc. In myelin stained sections, a fewer number of PR's permeate this region, while the DAB's found in this region are morphologically similar to those found in the medial segment of vlVipc (Figure 11B). The neuropil in irVi is finely textured (Figure 13D). The cells in irVi at these levels are primarily small pale staining cells (Figure 8). A few of the intensely stained cells which characterize dcVi are sometimes found in irVi. The medial border of irVi is well demarcated in myelin stained sections by the large number of myelinated fiber bundles in pcRF (Figure 10B).

The rostral half of Vi (Levels 5 through 8)

Level 5. The most notable structural change at this level of Vi is the replacement of vlVipc by vlVimc. The overall size of vlVimc is smaller than that of vlVipc. The first evidence of the transition from vlVipc to vlVimc is a decrease in the density of cells in the lateral part of the nucleus. A number of medium-sized intensely stained round, oval and multipolar-shaped cells are scattered throughout the region. The medial segment of vlVimc is morphologically similar to the medial segment of rostral vlVipc. A few large intensely stained cells are occasionally distributed in the dorsolateral part of this medial segment. The lateral region of vlVimc contains widely spaced large multipolar-shaped cells (Figure 6C-F) distributed among smaller round to oval-shaped cells (Figures 6A and B). At the

level of Vi lying between levels 4 and 5, clusters of large multipolar-shaped cells form a distinct band in the lateral segment of vlVimc. This band gradually enlarges to fill the lateral part of vlVimc. The morphology and organization of the DAB's in vlVimc is largely similar to that found in the rostral part of vlVipc.

A few scattered intensely stained cells are found in brVi at this level of the medulla. These cells are morphologically similar to the cells in the lateral segment of vlVimc. However, the majority of the cells in brVi are pale stained in comparison to the intensely stained cell in the adjoining parts of vlVimc. The number of myelinated fibers in brVi is less than that found in the caudal half of the nucleus.

The density of cells in dlVi increases at this level, since the medial strip of PaV no longer occupies the lateralmost part of the region at this level of the medulla. In addition, the cells in this region are intensely stained in Nissl stained sections.

The number of intensely stained cells in dcVi increases at this level (Figure 2C). The size and shape of cells is similar to those found in more caudal levels of this region.

Level 6. The size of vlVimc decreases further at this level. The intensely stained cells in vlVimc are more evenly distributed throughout the region (Figure 2C). The lateral segment of vlVimc contains a number of fusiform-shaped cells while the medial segment contains some large multipolar-shaped cells. Smaller round, oval and multipolar-shaped cells are scattered throughout the medial and lateral segments of vlVimc. These latter cells are sometimes organized into small aggregates in the dorsolateral aspect of the medial segment. However, the overall texture of the neuropil in vlVimc is the coarsest of all regions in Vi due to the presence of many thick myelinated axons and dendritic processes which are randomly oriented within the neuropil (Figure 13B). This level of Vi is characterized by a number of myelinated fibers which exit vlVimc in a

dorsomedially arcing fashion and collect in pcRF to form a diffuse bundle of myelinated axons directed medially in the medulla (Figure 11C).

The most dramatic change in Vi at this level of the medulla is found in brVi. The cells in this region are organized into a distinct band extending throughout the dorsoventral extent of brVi. They primarily consist of small, pale staining fusiform-shaped cells oriented parallel to SVT. These cells contrast sharply with the large intensely stained cells in the adjoining parts of vlVimc. A few smaller round and oval-shaped cells and a few medium-sized fusiform-shaped cells are also present in brVi (Figure 12E). The latter cells are especially prominent in the dorsolateral aspect of the region.

The cells in dlVi are generally larger in size than those found at more caudal levels of Vi. However, they still have a similar shape and orientation. The appearance of dcVi is not any different from more caudal levels except that it is decreased in its overall size. The region occupied by irVi is very distinct at this level. The cells in this region are less intensely stained than cells in the adjacent portions of dcVi or vlVimc and are slightly smaller than those in dcVi (Figure 2C). In myelin stained sections, the neuropil is pale by comparison to that present in the latter two regions (Figure 11C).

Level 7. The size of vlVimc is decreased at this level in parallel to the decrease in the overall size of Vi. The decrease in size is accompanied by the loss of any distinguishable differences between the medial and lateral parts of this region.

The cells in this region consist primarily of fusiform and multipolar-shaped neurons distributed evenly throughout the neuropil. The distinct band of cells characteristic of brVi continues at this level of the medulla. There are no distinct changes in the composition of dlVi at this level. The overall size of dcVi and irVi decreases at this level of the medulla. A number of myelinated fibers exit dcVi in a ventromedially arcing fashion to enter pcRF where they join other myelinated fibers

arising from vlVimc. The medial border of these two regions is formed by a small collection of neurons belonging to the DM region of Vo (Astrom, '53; and Falls, Rice and VanWagner, '85). The cells in this latter region are primarily small pale stained neurons. However, a few intensely stained cells which morphologically resemble cells in the pcRF form small aggregates within DM. The cells in irVi are increased in size and intensity of staining compared to those at more caudal levels. The region more closely resembles dcVi than the ventrolateral part of Vi at this level. The similar appearance of dcVi and irVi at this and more rostral levels gives the impression that together they form a unit in the dorsomedial aspect of Vi.

Level 8. This level of Vi exhibits a more prominent overlap of regions belonging to Vi and Vo. In addition to the enlarging region of DM situated along the medial border of dcVi and irVi, a small area of neuropil lies along the medial margin of vlVimc. This latter area is characterized by the presence of a a few "giant" multipolar-shaped cells which represent a caudal extension of the ventrolateral (VL) region of Vo. The large multipolar neurons in vlvimc decreases at this level as the number of medium-sized neurons increases. The remaining regions of Vi are morphologically similar to the caudal levels of the nucleus, although they are smaller in size and generally contain fewer cells.

The transition from the rostral pole of Vi to the caudal pole of Vo gradually continues at more rostral levels. The dcVi and irVi regions disappear as DM increases in size. Finally, vlVimc disappears as VL enlarges. The regions occupied by brVi and dlVi are gradually replaced by the border zone (BZ) of Vo.

Figure 1

A schematic diagram illustrating the topographical relationship of the six cytoarchitecturally defined regions of Vi at eight representative levels of the nucleus. The inset shows the shading patterns used to identify these regions in the figure. The numbers on the upper left of each section refers to the distance from the obex in millimeters. The numbers to the lower right of each section represent the levels of Vi referred to in the text.

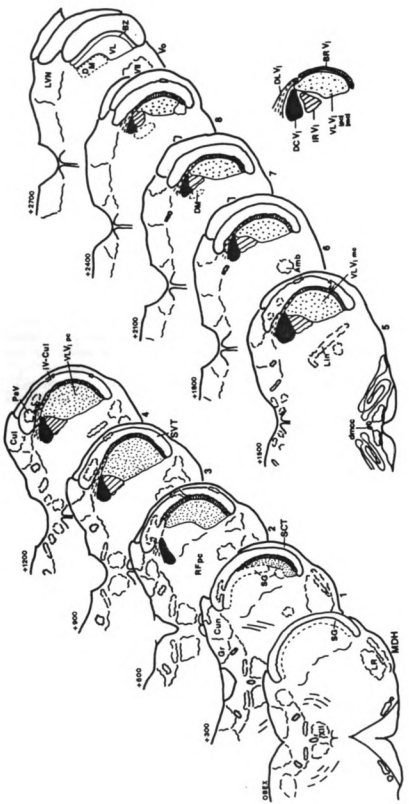
+2700
+2400
+2100
+1800
+1500
+1200
+900
+600
+300
0
LVM
DMV
Amb
Lim
Pyrc
RVT
RFpc
Cu
Gr
Sol
MDH
SBT
Cun
Gol
RVV
LV-Cul
LVVpc
DLVi
DCVi
IRVi
VLVi
SRVi
Vi
Vi,Vi mm
Vi,Vi pc

Figure 2

A series of low power photomicrographs comparing the cytoarchitectural appearance of Vi at four rostrocaudal levels corresponding to level 1 (A), level 3 (B), level 5 (C), and level 7 (D) from Figure 1. The dashed lines indicate the medial border of Vi. The dotted lines indicate the borders between the individual regions of Vi. X22. Nissl stain.

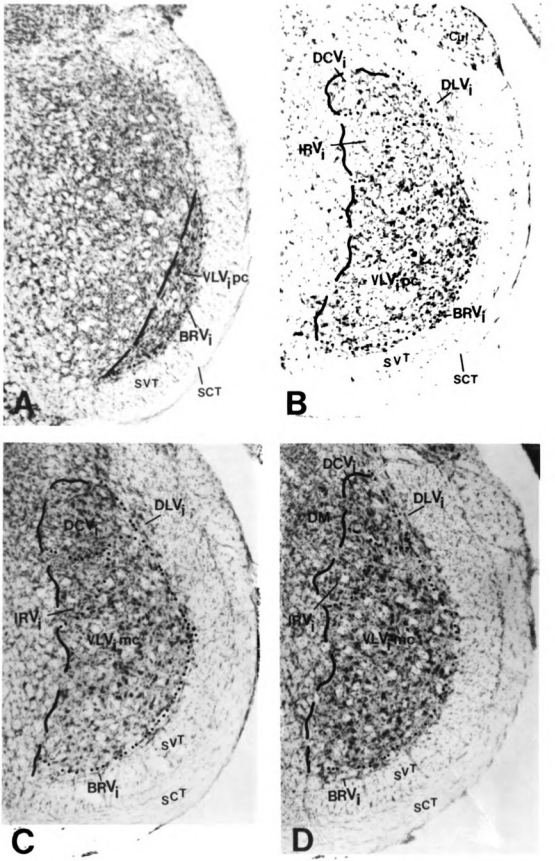
A
VLVi pc
BRVi
SVT
SCT
B
DCVi
DLVi
IRVi
VLVi pc
BRVi
SVT
SCT
C
DCVi
DLVi
IRVi
VLVi mc
SVT
BRVi
SCT
D
DCVi
DLVi
DM
IRVi
VLVi mc
SVT
BRVi
SCT

Figures 3-8

A series of low power photomicrographs comparing and comparing the cytology of representative neurons in brVi (3A-C), dlVi (4A-D), vlVipc (5A-G), vlVimc (6A-F), dcVi (7A-C)-, and irVi (8A-C). X800. Nissl stain.

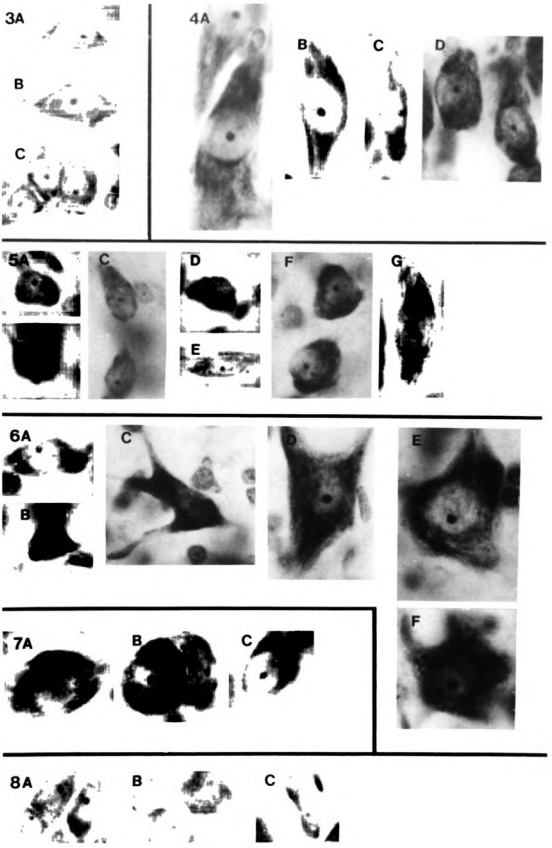
3A
B
C
4A
B
C
D
5A
C
D
E
F
G
6A
B
C
D
E
7A
B
C
F
8A
B
C

Figure 9

Frequency distribution histogram of the somatic cross sectional areas of neurons throughout the entire Vi nucleus (A) and in each of the six distinct regions of Vi (B-G).

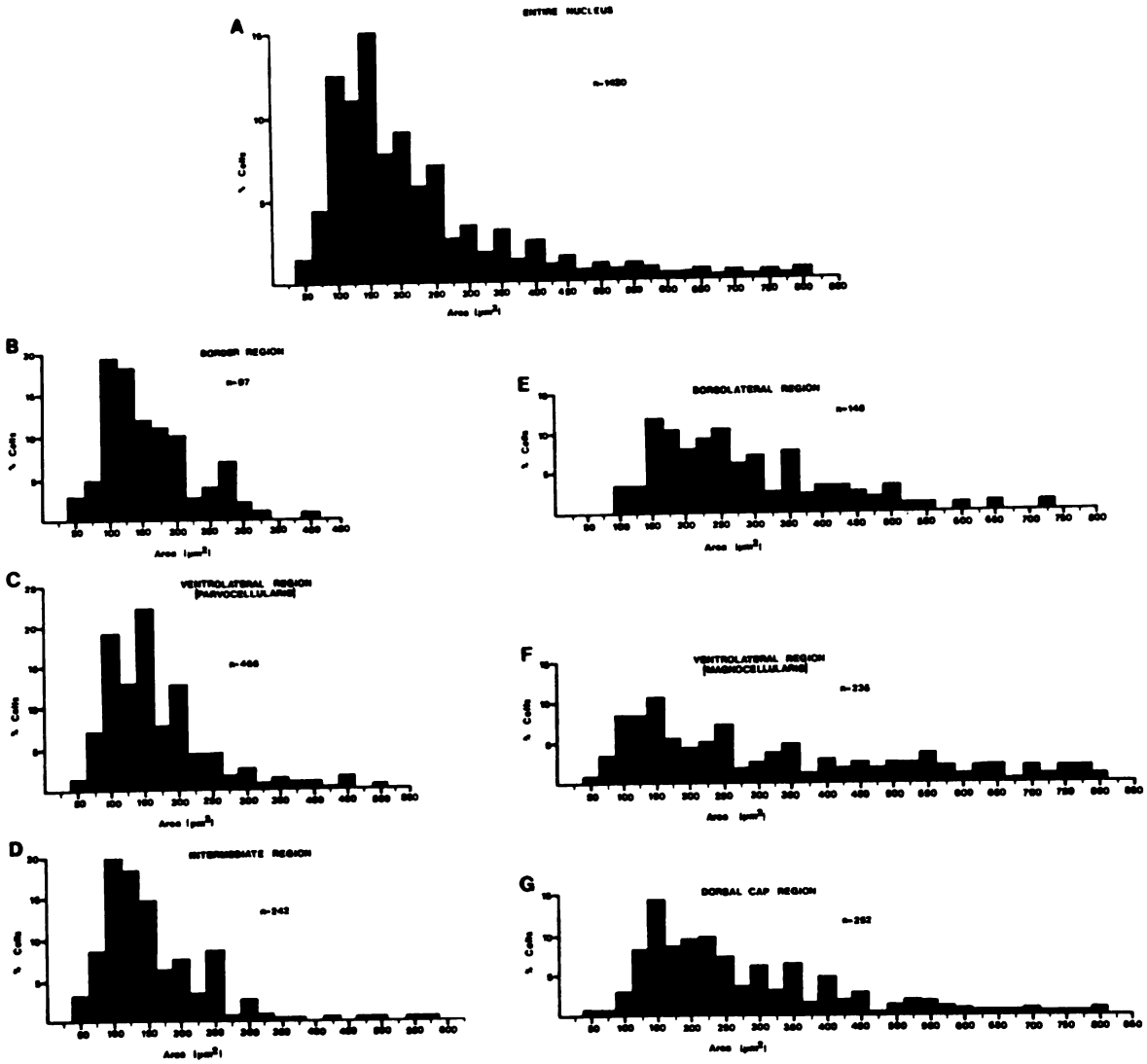
A
ENTIRE NUCLEUS
n=1480
% Cells
Area (μm²)
B
BORDER REGION
n=97
C
VENTROLATERAL REGION
(PARVOCELLULAR)
n=466
D
INTERMEDIATE REGION
n=343
E
DORSOLATERAL REGION
n=146
F
VENTROLATERAL REGION
(MAGNOCELLULAR)
n=236
G
DORSAL CAP REGION
n=252

Figure 10

A series of photomicrographs illustrating the spatial dislocation of lamina II neuropil during the MDH/Vi transition in the peri-obex region of the medulla from caudal (A) to rostral (F) levels in cytochrome oxidase stained sections. The dotted lines indicate the position of lamina II neuropil. Arrows in E point to columns of cytochrome oxidase staining in vlVipc. X17.

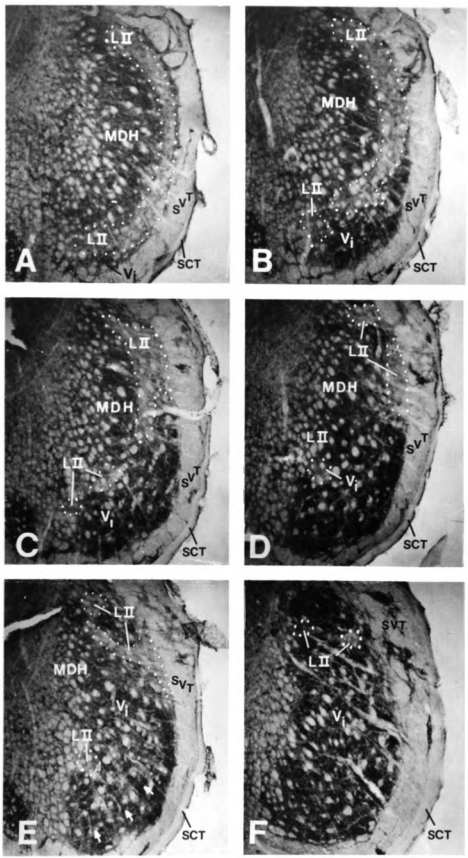
A
LII
MDH
SVT
LII
Vi
SCT
B
LII
MDH
LII
SVT
Vi
SCT
C
LII
MDH
LII
SVT
Vi
SCT
D
LII
MDH
LII
SVT
Vi
SCT
E
LII
MDH
SVT
Vi
LII
SCT
F
SVT
LII
Vi
SCT

Figure 11

A series of photomicrographs illustrating the myeloarchitectural features of Vi at four representative levels of the nucleus corresponding to level 1 (A), level 3 (B), level 5 (C), and level 7 (D) from Figure 1. Kluver-Barrera (A) and P-phenylenediamine (B-D) stained sections. The dashed lines indicate the medial border of Vi. The dotted lines indicate the borders between the individual regions of Vi. X22.

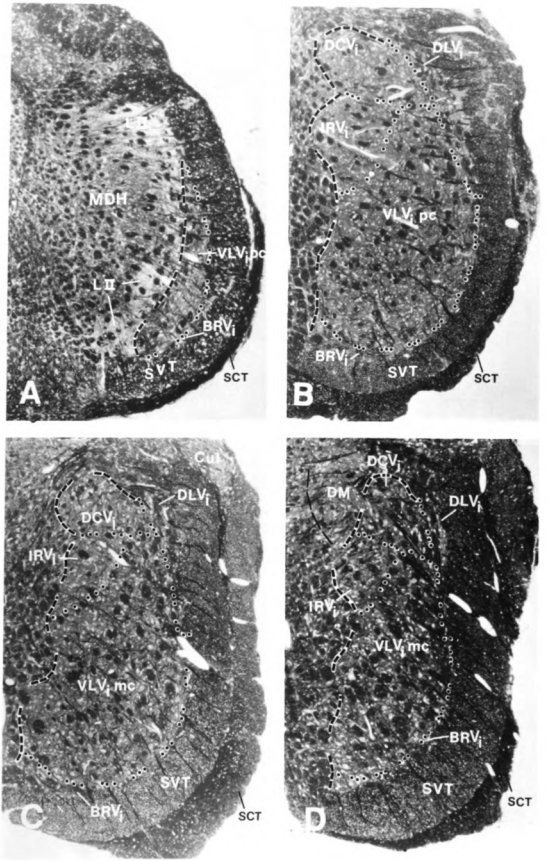
MDH
VLVi pc
LII
BRVi
SVT
SCT
A
DCVi
DLVi
IRVi
VLVi pc
BRVi
SVT
SCT
B
CuI
DLVi
DCVi
IRVi
VLVi mc
SVT
BRVi
SCT
C
DCVi
DM
DLVi
IRVi
VLVi mc
BRVi
SVT
SCT
D

Figure 12

A series of high power photomicrographs comparing the texture of the neuropil in the medially displaced portion of lamina II (A), dlVi (B and C) and brVi (D and E). The arrows in C mark the medial strip of PaV which encroaches into dlVi. X320. P-phenylenediamine stained semithin section.

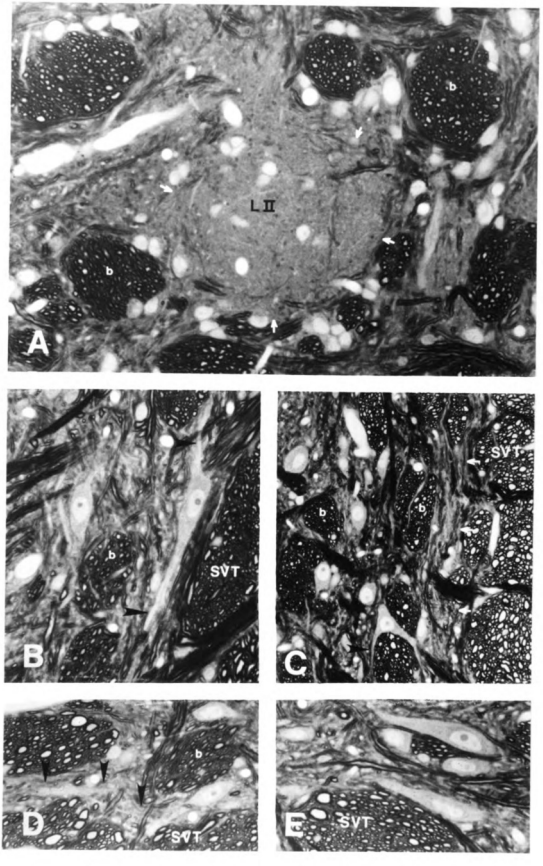
A
b
b
LII
B
b
SVT
C
b
SVT
D
b
SVT
E
SVT

Figure 13

A series of high power photomicrographs comparing the texture of the neuropil in vlVipc (A), vlVimc (B), dcVi (C) and irVi (D). Open block arrow in A points to bundle of fibers representing a penetrating ray (PR). Large arrow in B points to large myelinated fibers, while the small arrows point to small pale stained cells. Arrows in C point to dendritic processes. b = deep axon bundle (DAB). X600. P-phenylenediamine stained semithin section.

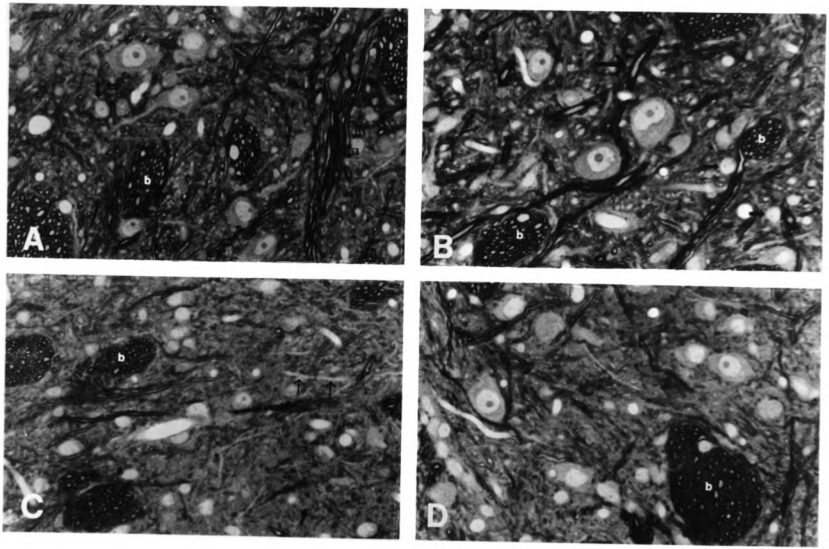
A
b
B
b
b
C
b
D
b

DISCUSSION

The present investigation represents the first comprehensive analysis of the overall cyto- and myeloarchitectural organization of Vi in any species. Two major findings concerning the structural organization of Vi are revealed. First, this study clarifies the rostral and caudal boundaries of Vi, in particular documenting that its caudal border is characterized by a distinct overlap with MDH, while its rostral border is characterized by a more gradual transition with Vo. Second, this study demonstrates the presence of six distinct regions within Vi which can be distinguished by differences in the morphology and distribution of their constituent neurons as well as by differences in their overall myeloarchitectural appearance.

Prior to discussing and comparing the specific results of the present investigation with previous studies, a brief introduction to the terminology used in these other studies in reference to SVN will be presented. This is provided in order to clarify the potentially confusing variations in nomenclature which will often be referred to during the course of the discussion.

Nomenclature

Olszewski ('50) was the first to demonstrate, in man and macaque monkey, that the mammalian SVN could be subdivided into three cytoarchitecturally distinct nuclei: nucleus oralis (Vo), nucleus interpolaris (Vi) and nucleus caudalis. The latter subdivision is now more commonly referred to as the medullary dorsal horn (MDH) to reflect the anatomical and functional similarities it shares with the spinal dorsal horn (Gobel, Falls, and Hockfield, '77). The phylogenetic (Crosby and Yoss, '54) and ontogenetic (Brown, '56, '58a, '62; and Altman and Bayer, '80a,b) development of each of these three nuclei has been well established. It is important to note however, that these developmental studies indicate that the three

subdivisions of SVN undergo different rates of differentiation and growth such that in lower vertebrate species and early stages of embryonic growth in primates, rostral SVN may not easily be differentiated into distinct Vi and Vo components. In subprimate forms, for instance, Crosby and Yoss ('54) reported that the rostral portion of SVN was represented by a single unit which they referred to as nucleus oralis. In those species where they were able to identify two distinct subdivisions within this nucleus, they referred to them as nucleus oralis pars rostralis and pars interpolaris to reflect their similarity to primate Vi and Vo, respectively.

Meessen and Olszewski ('49) introduced an entirely different terminology for the cytoarchitectural subdivision of rabbit SVN. They identified two main nuclei: a nucleus caudalis and a nucleus oralis (Vo). However, they further subdivided their "Vo" into three distinct subnuclei: Vo alpha, Vo beta and Vo gamma. This particular terminology was later adopted by Eisenmann, Landgren and Novin ('63) in the cat as well as Kusama and Mabuchi ('70) and Gerhardt and Olszewski ('69) in various primates. Moreover, Darian-Smith ('73) later provided preliminary Golgi impregnation data to support the distinction of a Vo alpha and Vo beta in the cat. Although none of these studies specifically distinguished a separate Vi, the "Vo alpha" in each of these studies has generally been considered to correspond to Olszewski's Vi; while "Vo beta" and "Vo gamma" have together been considered to correspond to Olszewski's Vo. However, some exceptions have been noted. Karamanlidis, Michaloudi, Mangana, and Saigal ('78) reported, for example, that they regard Meessen and Olszewski's "Vo alpha" and "Vo beta" to correspond to Olszewski's Vi, while their "Vo gamma" corresponds to his Vo. On the other hand, Ikeda ('79) considered Eisenmann et al.'s "Vo alpha" to correspond to what they identified as the caudal level of Olszewski's Vo in the cat, while Eisenmann et al.'s "Vo beta" and "Vo gamma" corresponded to the middle and rostral levels of their Vo, respectively.

In other studies, Friede ('59) recognized a nucleus caudalis and a nucleus oralis within guinea pig SVN but did not distinguish separate subdivisions within nucleus oralis. On the other hand, Brodal et al. ('56) recognized distinct Vi and Vo nuclei in cat SVN and further distinguished a nucleus "gamma" in the rostral part of Vo which they believed corresponded to Meessen and Olszewski's "Vo gamma". In his cytoarchitectonic atlas of cat brainstem, Berman ('68) provided still another separate terminology for subdividing SVN in which he describes caudal "laminar" (i.e., MDH) and rostral "alaminar" nuclei. He further reports that his "alaminar nucleus" consists of caudal, parvocellular and rostral, magnocellular portions. He specifically noted that his "parvocellular, alaminar nucleus" corresponded to Eisenmann et al.'s ('63) "Vo alpha" and "Vo beta" as well as the combined Vi and Vo nuclei of Brodal et al. ('56) minus their "nucleus gamma"; while his "magnocellular, alaminar nucleus" corresponded to Brodal et al.'s ('56) and Eisenmann et al.'s ('63) "nucleus gamma". In a more recent study, Bandler ('78) reported that the magnocellular and rostral parvocellular portions of Berman's "alaminar" nucleus corresponded to Olszewski's "Vo" while the caudal parvocellular portion of Berman's "alaminar" nucleus corresponded to Olszewski's "Vi".

The nomenclature of Olszewski ('50) was first applied to the rat by Torvik ('56). However, in a recent study Fukishima and Kerr ('79) redefined the position of the Vi/Vo border in the rat medulla based on differences in cytoarchitecture and thalamic connectivity as revealed through correlated Nissl and retrograde transport experiments. However, since some publications have not yet incorporated this change, the literature contains some references to rat Vo which are actually referring to a level now considered to correspond to Vi (See "Vi/Vo Transition" below for further details).

In addition to the main subdivisions of SVN cited above, some authors have proposed the presence of distinct regions within MDH, Vi, and Vo in a variety of

species. Some of these have been designated as separate nuclei. The most prominent of these nuclei is the reported existence of a separate "dorsomedial nucleus" (DM) situated within rostral SVN (Astrom, '53; Torvik, '56; Brown, '58b; Valverde, '61, '62; Falls et al., '86). However there is considerable disagreement concerning the rostrocaudal extent of this nucleus. Several authors have further distinguished a distinct "alaminar" portion to MDH at the level of the obex (Eisenmann et al., '63; Wunscher et al., '65; Gerhardt and Olszewski, '69; Marfurt, '81; Craig and Burton, '81; and Arvidsson, '82). (For a further discussion of the presence of subdivisions within SVN see below).

The Boundaries of Vi

Medial and Dorsomedial Borders

It has generally been recognized that the medial and dorsomedial borders of Vi are difficult to establish using cytoarchitectural criteria alone. The present study demonstrated that these borders are recognizable through careful correlated observations in Nissl and myelin stained preparations. In particular, these borders are characterized by differences in the size, staining intensity and density of cells within the Vi as well as by prominent changes in the size, distribution and density of the DAB's. It is worth noting that the relative position of myelinated fibers alone are useful in determining these borders. Since the position of myelinated fiber bundles is easily seen using darkfield or phase contrast illumination, an approximation of the medial and dorsomedial borders can easily be obtained even in unstained experimental preparations.

It has been well established that the pcRF medially bordering Vi receives a primary trigeminal input. However, anatomical studies clearly demonstrate that the density of termination of these primary V afferents is relatively sparse in comparison to that found in Vi. In fact, Kruger and Saporta ('77) suggest that the autoradiographic tracing of the V root distribution provides a good means of

defining the medial limits of SVN in the cat. It remains to be determined just how the medial borders of Vi, as determined in the present study, correspond to a medial border of Vi based on differences in the density of primary V afferents in rat SVN.

Retrograde transport studies providing detailed illustrations of the distribution of identified projection neuron populations within Vi, indicate that the distribution of specific neuronal populations within Vi conform to the limits of the nucleus as defined in the present study (see Chapter Three). The distribution of thalamic projection neurons, in particular, demarcate a sharp boundary between Vi and the pcRF which is relatively devoid of thalamic projecting neurons in the vicinity immediately bordering Vi in the rat.

In the rat atlas of Paxinos and Watson ('85), the medial border of Vi is delimited by differences in the distribution of acetylcholinesterase activity. The position of this histochemically defined border corresponds rather closely with that identified in the present study. A similarly positioned medial border of rat Vi is seen in the cytochrome oxidase stained sections provided in the present study. It appears, therefore, that the medial borders of Vi defined in the present study correspond with various histochemically defined borders in the rat.

The MDH/Vi Transition

The interface between MDH and Vi has long been regarded as a region of transition in which there is a gradual change in the structural organization of SVN from the laminated appearance of MDH to the non-laminated structure of Vi. This region has generally remained cytologically indistinct due to the lack of any detailed analysis of the cyto- and myeloarchitectural changes which occur during this transition. The results of the present study clearly document a distinct overlap of separate MDH and Vi components within this region in the rat. A review of the literature reveals that several studies have suggested an overlap of areas corresponding to MDH and Vi in a variety of mammals (Krieg, '42; Meessen and

Olszewski, '49; Crosby and Yoss, '54; Brown, '56; Friede, '59; Breazile, '67; Kusama and Mabuchi, '70; Jacquin et al., '86; Shigenaga et al., '86; and Shigenaga et al., '86), but this suggestion has not generally been accepted. Perhaps one reason for this may be the fact that none of these studies provide adequate descriptions of the region to enable other investigators to easily recognize this overlap in the same or different species.

The earliest indication of a distinct overlap of the caudal subdivisions of rat SVN was provided by Krieg ('42) who schematically illustrated that his "nucleus gelatinosis" (SG in the present study) curved at its rostral end to form a cap over the more medially located "nucleus spongiosis" (Vi in the present study), while his "main nucleus" of the SVN overlapped laterally with the "nucleus gelatinosis". Presumably this overlap is also schematically illustrated in drawings of Nissl and Golgi preparations in his Figure 140, although he does not specifically label the "main nucleus". Although Krieg's study predates Olszewski's ('50) report and therefore employs a different terminology in reference to regions within SVN, the overlap between his "gelatinosis" and "main" nuclei clearly corresponds to the MDH/Vi overlap described in the present study.

In a more recent study, Jacquin et al. ('86) report a partial overlap between rat MDH and Vi. However, these authors do not provide any details of the changes which occur in this region.

The spatial dislocation of MDH by the enlarging caudal pole of Vi in the present study includes a large portion of lamina II, although some portions still remained adjacent or interstitial to SVT at this level. However, it was difficult to determine whether lamina I was also displaced along with lamina II. While it is clear that the small bundles of myelinated fibers which characterize the border between laminae I and II (Gobel, Falls, and Hockfield, '77) were displaced by Vi, the Nissl sections did not clearly show neurons characteristic of lamina I in this region.

Retrograde transport studies indicate that numerous spinal projecting neurons, which morphologically resemble lamina I neurons in size, shape and orientation, were located adjacent to these numerous small DAB's (See Chapter Three). On the other hand, our unpublished observations of Golgi impregnated material in the rat indicates that a few neurons belonging to lamina I remain situated adjacent to SVT at this level. Anterograde transport (Shigenaga et al., '86; and Panneton and Burton, '81) and electrophysiological (Hayashi, Sumino, and Sessle, '84) studies support a similar rostral extension of lamina I neurons adjacent to SVT at Vi levels of the nucleus in the cat. However, retrograde transport studies in the rat do not support the presence of spinal or thalamic projecting neurons with similar morphologies as lamina I within SVT at this point (see Chapter Two).

The spatial displacement of lamina I has previously been reported by Krieg ('42), Bates and KIllackey ('84) and Jacquin et al. ('86) in the rat and by Shigenaga et al. ('86) in the cat. However, it must be noted that this displacement of lamina I has not yet been reported in other mammalian species. It is not clear whether Krieg's ('42) "nucleus gelatinosis" included lamina I since he did not recognize distinct laminations in the superficial part of the region corresponding to MDH. On the other hand, Bates and Killackey ('84) and Jacquin et al. ('86) specifically reported only the medial displacement of lamina II thereby implying that lamina I was not displaced. However, it is not entirely clear whether these authors were using the term SG in reference to lamina I and II, or lamina II only, since neither study specifically discusses this point. Finally, Shigenaga et al. ('86) reported that the appearance of the caudal pole of Vi displaced the subnucleus gelatinosis (i.e., laminae I and II) into SVT in the cat, while the subnucleus magnocellularis is displaced medially within the nucleus.

It should be noted that indications of the medial displacement of lamina II is also evident using several histochemical stains. Paxinos and Watson ('85) show that

lamina II exhibits a dense acetylcholinesterase staining. In their Figures there is a prominent staining of regions lying deep within the ventral part of the nucleus. which on the left half of the figure lies closer to SVT than on the right half of the figure. The changes in the location of these deep regions of intense staining correspond precisely with the medial progression of lamina II described in the present study.

The present study illustrates that the transition from MDH to Vi proceeds in an orderly fashion in the rat whereby the extreme caudal pole of Vi initially appears ventrolateral to MDH displacing it dorsomedially. In addition, at subsequent levels portions of Vi also appear dorsally within the nucleus forcing MDH ventromedially. Eventually, as the caudal pole of Vi enlarges within the medulla, it appears to lie in a position entirely lateral to the rostral pole of MDH. Krieg ('42) clearly illustrated, but did not discuss, at least a part of this arrangement in the rat. The ventrolateral appearance of the caudal pole of his "main nucleus" is similar to that shown in the present study.

The presence of a distinct overlap of MDH and Vi is a feature common to the POR of several different mammals (Meessen and Olszewski, '49; Crosby and Yoss, '54; Friede, '59; Brown, '62; Breazile, '67; and Kusama and Mabuchi, '70). It is therefore likely that a similar overlap may be present in other mammalian species.

The present study further demonstrates that the medially displaced portions of SG undergo an expansion in size followed by a rapid fractionization and subsequent dissolution as the transition from MDH to Vi progresses. The expansion of the rostralmost part of SG was previously reported by Torvik ('56) in the rat and is not entirely unexpected since similar expansions of SG are found at more caudal levels of SG in the rat. The breaking up of SG into small islands during the MDH/Vi transition has previously been reported, although not illustrated, by Olszewski ('50), Olszewski and Baxter ('54), Gerhardt and Olszewski ('69), Brown

('56) and Krieg ('42) in man and other primates, as well as Saigal et al. ('82) in the sheep and Torvik ('56) in the rat.

In a recent study in the rat, Jancso and Kiraly ('80) noted that the distribution of degenerating capsaicin sensitive primary V afferents terminated in small "islands" within the deeper layers of MDH at the level of the obex. These "islands" approximate the position of the displaced portions of the fractionated lamina II demonstrated in the present study and indicate that this region receives primary substance P containing terminals.

The present study also illustrates that the rat SG undergoes a progressive regression which initially follows a ventral to dorsal pattern in the ventral portion of the nucleus and subsequently a dorsal to ventral pattern in the dorsal portion of the nucleus. A similar pattern has been reported in the fetal human brainstem (Brown, '62). It is not known whether a similar fractionization of SG occurs in other mammalian species, however, its reported presence in such diverse species as rats and primates would certainly suggest that it may exist in other subprimate forms as well. Considering the implications that such findings would have on the interpretations of the distribution of afferent inputs and specific efferent projection neuron populations within this region as well as the general functional segregation within the SVN, it is clearly important that detailed analyses of this region of the SVN, similar to those provided in the present study, are warranted in other mammalian species.

The present study demonstrates that the dorsolateralmost portion of SG remains in a position adjacent to SVT in the rostral part of the MDH/Vi transition zone in the rat. The presence of this portion of SG was previously reported by Torvik ('56). In addition, Campbell et al. ('74) identify this region as a separate somatosensory nucleus in the lateral medulla which they referred to as the "trigeminal plate nucleus". However, the latter authors did not provide any

anatomical or electrophysiological data to support this division. Similar extensions of the rostralmost part of SG have not specifically been reported in other mammals.

Several studies have reported that SG does not appear as a distinct lamina in MDH until a level caudal to the interface of MDH and Vi, thereby indicating the presence of a rostral "alaminar" portion of MDH (Arvidsson, '82; Marfurt, '81; Wunscher et al., '65; Craig and Burton, '81; Eisenmann et al., '63; Gerhardt and Olszewski, '69; Dubbeldam and Karten, '78) The present study clearly demonstrates that although SG does, at least partially, disappear while the remaining portions of MDH do gradually regress during the transition from MDH to Vi, there always remains a clear distinction between the components of the rostral pole of MDH and the caudal pole of Vi. In addition, although the present study illustrates at least a spatial separation of the rostral portions of SG and magnocellular lamina of MDH, the distinction between the individual lamina remains clear in Nissl and myelin stained preparations. It could be argued therefore, that a true non-laminated MDH does not exist in the rat, although the normal laminar structure of MDH is disrupted somewhat. In consideration of the results of the present study, it would seem useful to discontinue the use of the term alaminar in reference to rostral levels of MDH in the rat since it creates some confusion regarding the structural organization of MDH in the POR. Rather, it would seem more valuable to provide more detailed descriptions of the structural changes which occur in this region.

In view of the results of the present study, a few remarks are necessary regarding the results of previous investigations to the structural and functional organization of the POR. In a recent study, Arvidsson ('82) identified a separate rostrally located "non-laminated" region of MDH in the rat which exhibited a pattern of vibrissae afferent termination identical to that seen in Vi and Vo and distinctly different from that seen in laminated portions of MDH. This distinction was reflected in a shift in the distribution of the terminals to a deeper location with

respect to SVT as well as a complete reversal in the somatotopy present. It seems quite probable however, that Arvidsson's's "non-laminated" rostral MDH actually represents the caudal extension of Vi. If this is the case, then a single spatial manner of representation of vibrissae afferents within MDH results, and the apparently confusing presence of two separate spatial distribution patterns reported by Arvidsson ('82) is resolved. In support of this interpretation, the cytochrome oxidase stained sections shown in Figure 10 illustrate that the caudalmost part of Vi overlaps laterally with MDH in the transition zone and exhibits a dense staining pattern representing the various vibrissae afferent segmental zones (Nomura and Mizuno, '86; Nomura et al., '86; and Ma and Woolsey, '874). In contrast, in more medial portions of the transition zone, the intensity of labeling is much less and the patterns not quite as distinct. This latter region is continuous with and resembles that seen in the more caudally located MDH. Moreover, the recent study by Jacquin et al. ('86) also supports this view since they demonstrate that the caudalmost aspect of Vi within the transition zone exhibits a distinct vibrissae afferent segmental pattern.

The POR of SVN has been well documented to be a site of dental pulp afferent (DPA) termination in the rat (Marfurt, '84) and cat (Arvidsson and Gobel, '81; and Westrum et al., '81). In particular, these terminations have been described in dorsal and ventral regions of medial Vi. It seems probable that the distinct overlap of MDH and Vi as described in the present study may account for the specific distribution of DPA's to Vi. In particular, Marfurt and Turner ('84), in describing the distribution of the first mandibular molar tooth pulp within the SVN, illustrate that the distribution of DPA afferents terminate in the extreme dorsolateral part of caudal Vi just deep to SVT. In addition, Marfurt and Turner specifically noted a continuity in the distribution of DPA's at MDH and Vi levels of the SVN. The present study clearly demonstrates that this region of Vi represents

the rostral extensions of SG. The distribution of DPA's to the rostral extension of SG is entirely congruent with the distribution of DPA's to regions of SG located in similar positions just caudal to this level of the SVN.

Similarly, if a distinct overlap of MDH and Vi occurs in the POR of the cat, then this may account for the distribution of DPA's in medial regions of dorsal and ventral Vi as illustrated by Westrum and colleagues ('81). In particular, the presence of labeling in these regions could, at least, partially represent labeling in the rostral extension of the displaced portions of SG. Westrum, Canfield and Black ('76) noted, in fact, that much of the central degeneration in Vi, following tooth pulp removal in adult cats, was confined to neuropil areas relatively devoid of fascicles and fibers which contained groups of small neurons. The present study clearly demonstrates neuropil of similar character which is identified at this level in the rat as displaced portions of SG. Further support for the contention that some of the DPA terminal labeling may actually lie within the confines of the displaced rostral portions of SG comes from the recent immunocytochemical studies of Drew, Westrum and Ho ('86) in which they report that these specific regions are selectively labeled using Substance P and Enkephalin antibodies in the cat. The high content of SP and Enkephalin in SG has been well established.

In addition, in a recent autoradiographic study of the localization of Substance P receptors in the rat medulla, Helke et al. ('84) describe a high density of SP receptors in lamina II. The SP receptor binding sites revealed in this study are coextensive with the position of the displaced portions of lamina II described in the present study.

It is interesting to note that Hayashi et al. ('84) recently reported the presence of nociceptive neurons in the lateral and ventromedial margins of caudal Vi in the cat. In addition, these authors suggested that these neurons may actually represent a rostral continuation of the marginal layer of MDH into Vi levels of the

nucleus.In view of this fact, it is clear that a reexamination of the distribution of DPA afferents within the POR must be conducted in order to determine whether DPA afferents terminate exclusively in these displaced portions of SG or whether they may also terminate as well in other portions of either MDH or Vi. Regardless, the results of the present study have a profound effect on the widespread contention that Vi is involved, albeit minimally, in the processing of dental pain.

Recent anatomical studies have provided evidence which supports the notion that an "onion skin" arrangement of primary V fibers exists in MDH (Arvidsson, '82; Jacquin et al., '84; and Panneton and Burton, '81) thus confirming early electrophysiological reports of the existence of such a topographical arrangement (Dejerine, '14; and Kunc, '70). In consideration of this arrangement of primary V fibers, the rostral pole of MDH which overlaps Vi in the POR would necessarily be involved primarily in the processing of somatosensory information from the oral parts of the head. Brown ('58a) had earlier conjectured that the most cephalic portions of MDH, at the MDH/Vi transition zone, may receive pain fibers from V as long as the pars gelatinosa was present. However, he suggested that the transition zone does not contribute to the secondary pain pathways essential for the recognition of pain at higher levels but provides for internuclear connections mediating reflexes. In this regard, recent retrograde transport studies have demonstrated that thalamic projecting neurons are not found in the rostralmost part of MDH which contributes to the transition zone (see Chapter Three). However, similar studies of intranuclear pathways in the SVN indicate that neurons within this region may actually contribute to this intranuclear pathway. It appears therefore that Brown's conjecture was correct. It is interesting to note also that Torvik ('56) had earlier noted that the expansion of SG at this level of the nucleus may be related to an expansion of afferent input. The large input of DPA afferents in this region may be the source of this expanded afferent input.

The rostral pole of MDH, as illustrated in the present study, undergoes some changes in its apparent structural organization which includes a spatial separation of its superficial and deeper lamina. This structural alteration in the normal composition of MDH raises some questions regarding the integrity of the intrinsic circuitry of MDH at this level. It is known, for example, that SG has an intimate relation with the deeper layers of MDH which includes the extension of stalk cell dendrites into SG as well as the extension of some of the dendrites of the pyramidal layer IV cells into the overlaying superficial lamina (Gobel, '82; and Gobel and Hockfield, '77). It would seem that a separation of the dorsolateralmost SG from the remaining deeper lamina of MDH should effect this intimate structural relationship. However, it remains to be determined whether these two regions actually do interact at this level of the nucleus even though they are spatially separated. In this regard, the occasional appearance of the gelatinous-like neuropil extending between the dorsolateral SG and the deeper parts of MDH may form the anatomical substrate for these connections. It must be noted however, that this rostralmost part of SG receives a unique afferent input from the glossopharyngeal and vagal primary afferent fibers, which distinguishes it from the more caudally located portions of SG. Therefore, this portion of SG is clearly functionally distinct from these more caudal levels of the nucleus. In consideration of this difference, the apparent spatial separation from the deeper layers of MDH, may actually reflect a difference in the intrinsic functional organization of this region.

In a preliminary Golgi impregnation study of Vi in the rat (Phelan and Falls, '83), Golgi type II interneurons were reported in the lateral regions of the nucleus adjacent to SVT. A reexamination of this material in light of the results of the present study, indicated that these neurons were, in fact, located in this dorsolateralmost remnant of SG. It would appear therefore, that this region does contain interneurons like the more caudal portion of SG. It is not known whether

the structural organization of this region is similar in other respects to the more caudal portions of SG. In addition, it is not known how the loss of the superficial lamina in the POR of the nucleus might effect the intrinsic organization of the rostral most portion of the deeper layers of MDH. The lack of any gross changes in the structural organization of the magnocellular layers of MDH in the peri-obex region of the nucleus, other than a gradual medial displacement and reduction in overall size is supported by retrograde transport studies which reveal that this region of the nucleus exhibits a pattern of projections which is similar and continuous with that seen in the more caudal levels of the magnocellular layers of MDH. In fact, Panneton and Martin ('83) speculated that the trigeminofacial projecting neurons located within Vi at the level of the obex represented the rostral continuation of lamina V of MDH.

The Vi/Vo Transition.

The rostral extent of Vi within the brainstem is an ambiguous inn the literature as is its caudal border with MDH. There is no general consensus concerning either the location of the Vi/Vo border or the cytoarchitectural distinction between Vi and Vo at this level. In man and other primates (Olszewski, '50; Olszewski and Baxter, '54: Gerhardt and Olszewski, '69: and Breazile, '67) it is generally agreed that the rostral pole of Vi lies at the level of the rostral third of the inferior olive. A sudden change is observed in the cell pattern, at this point, which is marked by a loss of the large neurons characteristic of Vi and the appearance in Vo of a more compact arrangement of the remaining small and medium-sized neurons. A similar description is provided by Eisenmann et al. ('63) in the cat and Meessen and Olszewski ('49) in the rabbit where they identify a Vo alpha containing large neurons scattered among smaller neurons and the transition from Vo alpha to Vo beta marked by the loss of these large neurons. This similarity has generally been interpreted to mean that the Vo alpha in each of these studies represents

Olszewski's ('50) Vi. In the studies by Taber ('61) and Ikeda ('79) in the cat, the rostral pole of Vi is located just rostral to the oral pole of the hypoglossal nucleus at the level of the rostral third of the inferior olive. Taber ('61) reports that the boundary between Vi and Vo in the cat is marked by the appearance of large-sized neurons in the ventrolateral part of caudal Vo, while Ikeda ('79) states that the rostral pole of Vi is not delimited from the caudal pole of Vo. In addition, Ikeda identifies the caudalpole of Vo in his study as corresponding to the Vo alpha of Eisenmann et al. ('63), however, he is not clear about whether he also includes his Vi in Vo alpha. Eisenmann et al. ('63) clearly stated however, that their Vo alpha extended from the obex to the caudal pole of the facial nucleus, an extent that would include the entire Vi and caudal pole of Vo identified by Ikeda ('79) in the cat. Furthermore, in the early study by Torvik ('56) in the rat, the rostral pole of Vi is located at the rostral pole of the hypoglossal nucleus. In addition, he reports that large neurons are found in Vi and Vo and that the border between them is rather indefinite.

The differences in cytological organization of Vo alpha and Vo beta in the studies by Eisenmann et al. ('63) in the cat and Meessen and Olszewski ('49) in the rabbit appear to correspond rather closely with the differences originally described in primates between Vi and Vo respectively (Olszewski, '50; Olszewski and Baxter, '54; Gerhardt and Olszewski, '69). In contrast to this however, the descriptions provided by Taber ('56) and Ikeda ('79) in the cat and Torvik ('56) in the rat are clearly inconsistent with the original descriptions in primates as well as those of Eisenmann et al. ('63) and Meessen and Olszewski ('49) in the cat and rabbit, respectively. These differences serve to illustrate the ambiguity which surrounds the cytoarchitectural distinction of borders within the rostral SVN. The possibility exists that there are distinct species differences in the cytological organization of Vi and Vo such that precise cytoarchitectural correspondences across species may be

impossible. In this regard, it should be noted that the phylogenetic study of Crosby and Yoss ('54) indicated that there are distinct species differences in the distribution and differentiation of Vi and Vo components of rostral SVN.

In a recent study in the rat, Fukishima and Kerr ('79), have proposed the redefining of the rostral boundary of Vi in accordance with their observations of Nissl cytoarchitecture and and distribution of thalamic projecting neurons as revealed in retrograde transport studies. They reported that Vi extended from the obex to the caudal pole of the facial nucleus clearly including the caudalpole of Vo as previously defined by Torvik ('56) in the rat. Cytoarchitecturally, they describe Vi as containing large, medium and small-sized neurons. However, they noted that the large neurons were consistently smaller than the "giant" cells which characterize the caudal pole of Vo. In addition, they reported that the distribution of thalamic projection neurons marked this border clearly with an absence of such labeling rostral to the caudal pole of the facial nucleus in levels defined as Vo. This particular delineation of the extent of Vi in the rat ismore consistent with that reported by Taber ('61) in the cat in extent and cytological organization of Vi and Vo. However, it still remains inconsistent with the description provided in primates (Olszewski and Baxter, '54) and rabbit (Meessen and Olszewski, '49) or cat (Eisenmann et al., '63).

More recent experimental studies have shown that this border between Vi and Vo can also be demonstrated by the differences in the distribution of the spinal projection neurons since the "giant" cells in caudal Vo in the rat project to the spinal cord (Falls, '84). In addition, the appearance of cerebellar projecting neurons in the DM nucleus (Falls et al., '85) contributes to the distinction of the border between Vi and Vo. Thus, it is clear that the border between Vi and Vo as redefined by Fukishima and Kerr ('79) reflects a cytological difference in neuronal organization as well as a difference in several different projection systems within the SVN.

The present study in general has adopted the outline proposed by Fukishima and Kerr ('79) in the rat. However, the present study provides details of the cytoarchitectural organization of this region which was lacking in Fukishima and Kerr ('79). In particular, the present study has shown that although a difference in the cytoarchitectural organization of SVN does exist at the caudal pole of the facial nucleus, there is no sudden or abrupt change as has been reported in other species. Rather, there is a gradual transition over a distance of approximately 300 μm. As few of the " giant" cells ar seen scattered among the large neurons in the rostral pole of Vi throughout this level. retrograde transport studies reveal that these neurons project to the the spinal cord (Falls, '84) while some of the remaining cells in this region of rostral Vi project to thalamus (see Chapter Three). In addition, the DM nucleus begins as a separate and distinct nucleus in the rostral pole of Vi along its medial edge and enlarges to occupy the dorsomedial region of Vo. Thus, components of Vi and Vo may be found intermingled as well as separate but overlapping within this region.

It is interesting to note that although the rostral half of Vi which was identified by Torvik as the caudal half of Vo, structurally resembles Vi more than Vo. However, there are distinct differences which support a distinction of rostral and caudal halves of Vi.

The Structural Organization of Vi

Cytoarchitecture. The results of the present study demonstrate that Vi consists of a population of small, medium and large-sized cells which exhibit a variety of somatic shapes. The histograms shown in Figure 9 illustrate that dcVi, vlVimc and dlVi share a similar distribution pattern for somatic cross sectional areas of their constituent neurons which is more widespread than the distribution in brVi, vlVipc and irVi which consists of a higher percentage of smaller neurons. Although the histograms comparing somatic cross sectional areas show only a single

distribution of cells, differences in the morphology of these cells permits the further differentiation of several different cell types within the various regions. A comparably detailed description of cell types has not previously been reported in any species.

The majority of the available cytoarchitectural descriptions of Vi in mammals have noted a rather uniform distribution of the total cell population throughout Vi. However, a few studies did note differences in the distribution of specific populations of neurons within Vi. Meessen and Olszewski ('49), for example, noted that the larger-sized neurons in Vo alpha (i.e., Vi) in the rabbit were especially common laterally within the nucleus. A similar concentration of medium-sized neurons was reported by Wunscher et al. ('65) and Fukishima and Kerr ('79) in the rat. The present study confirms that the largest of the neurons within Vi are distributed ventrolaterally, specifically within vlVimc.

In addition, Taber ('61) and Torvik ('56) reported a progressive increase in the medium and large-sized neurons proceeding from caudal to rostral levels of Vi in the cat and rat, respectively. The results of the present study confirm this pattern, especially but not exclusively in the ventrolateral regions of Vi where a caudal parvocellular and a rostral magnocellular region was recognized. A similar caudal to rostral progressive increase was also seen in dcVi and irVi.

It is interesting to note the differences in the distribution of neurons has not been reported in Vi of any higher mammal. In studies of the primate SVN, for example, Vi is consistently described as possessing a uniform distribution of large-sized neurons scattered throughout the nucleus along with other small and medium-sized neurons (Gerhardt and Olszewski, '69; Olszewski, '50; Noback and Goss, '59).

Myeloarchitecture. In the only studies to have previously described the myeloarchitecture of Vi, Gobel ('71) and Gobel and Purvis ('72) provided detailed descriptions of the distribution of myelinated fibers including DAB's and PR's

throughout Vi in the cat. These authors reported that the DAB's, along with other myelinated fibers coursing throughout Vi, constituted a major intranuclear plexus subserving ascending and descending fiber projections.

The present study provides a comparably detailed description of the myeloarchitecture of Vi in the rat. The myeloarchitectural organization of Vi in the rat is revealed to be quite similar to that present in the cat. In addition, however, the descriptions provided in the present study document regional differences in myeloarchitecture throughout each of the six cytoarchitecturally defined regions in Vi. The texture of the neuropil varied in each specific region, with the coarsest neuropil found in vlVimc and the finest found in dcVi and irVi. These regional differences may reflect differences in the organization of afferent inputs to these various regions. In fact, the dense plexus of myelinated fibers distributed to caudal brVi and vlVipc represents a unique afferent input to these regions, since none of the other regions in Vi exhibited a similar plexus.

Distinct Regions in Vi. Astrom ('53) was the first to provide a detailed morphological study proposing the presence of distinct subnuclei in the region of SVN corresponding to Vi. In his study, he identified four distinct nuclei in the mouse based on differences in the distribution of afferent fibers and variations in the somatodendritic morphology of neurons as revealed in Golgi impregnation studies. The four nuclei included: a marginal nucleus which lies along SVT at the level of the oral half of the hypoglossal nucleus (i.e., caudal Vi) and which contains large quadrilateral shaped neurons; an intermediate nucleus located medial to the marginal nucleus which contains a relatively sparse number of small round cells; a dorsomedial nucleus which contains medium-sized neurons and lies in the dorsomedial region of the nucleus in close association with the solitary nucleus; and a lateroventral nucleus containing medium and large-sized neurons which is located in the region ventrolateral to the dorsomedial nucleus.

In an earlier study in the rat, Krieg (50) also identified several nuclei including a "dorsal, small celled" group containing small, densely packed, pale oval-shaped cells. This nucleus appears to correspond to the dorsomedial nucleus of Astrom in terms of its location and cyto- and myeloarchitecture. However, it is difficult to determine the correspondence of the remaining cell groups identified by Krieg due to the brief descriptions provided in his report and the lack of any accompanying diagram.

Torvik ('56) later identified two distinct cell groups in rat Vi based primarily on observations of Nissl stained preparations. These groups included: a ventrolateral group which he believed corresponded to the "marginal nucleus of Astrom", and a dorsomedial group representing the caudal continuation of the "dorsomedial nucleus of Astrom". In addition, Torvik recognized a region corresponding to the "intermediate nucleus of Astrom" although he described it as merging with the ventrolateral cell group.

A precise correspondence between the six distinct regions identified in the present study and the subnuclei and cell groups identified by Astrom ('53) and Torvik ('56) is not readily apparent. However, some similarities can be noted. The present study identified a region in the medial part of rostral Vi which represented the "dorsomedial nucleus of Astrom". Astrom ('53), Torvik ('56) and Krieg ('50) all recognized a dorsomedial nucleus in Vi. However, while the dorsomedial nucleus of Astrom was chiefly located along the medial margin of Vi, the comparable region identified by Torvik occupied almost the entire dorsomedial two-thirds of Vi.

The "intermediate nucleus of Astrom" appears by its level in the medulla to correspond to the rostral pole of MDH at the MDH/Vi transition zone. In fact, Astrom noted a similarity in the morphology of the neurons in his "intermediate nucleus" and the more caudal parts of MDH. At more rostral levels, Astrom's "intermediate nucleus" corresponds to the medial segment of vlVipc and irVi.

The region identified as the "marginal nucleus" by Astrom corresponds to the caudal pole of Vi, in particular the caudal crescent-shaped region identified in the present study. The lateroventral nucleus of Astrom appears to correspond at least partially to the magnocellular part of MDH. The region identified by Torvik as the ventrolateral region of Vi encompassed brVi, dlVi and the lateral segments of vlVimc and vlVipc.

The present study reveals the presence of six separate regions within rat Vi based on correlative observations in Nissl and myelin stained sections. Each of these six regions exhibits a distinct cytoarchitectural and myeloarchitectural pattern of organization reflected in differences in the size, shape, density, distribution and staining intensity of their constituent neurons, as well as the size, density, and distribution of the various intrinsic myelinated fibers including the DAB's and PR's. While the results of the present study do not provide any direct evidence that these cytoarchitecturally distinct regions represent a functional compartmentalization of Vi, the detailed descriptions provided in this study allow more thorough comparisons to be made with the results of other studies which do provide information related to the functional organization of these regions.

The border region of Vi is cytoarchitecturally characterized by the presence of numerous oval to fusiform shaped neurons which are collected into bands and clusters of cells adjacent to SVT. The cytochrome oxidase stained sections through the POR which are provided in the present study reveal that the clusters within brVi exhibit a markedly higher metabolic level of activity which contrasts sharply with neighboring regions of brVi or vlVipc. This activity most likely corresponds to the presence of a specific afferent input to these clusters since no neurons were labeled. In a recent combined anterograde and retrograde labeling study, brVi was identified as one of two spinal recipient zones in Vi (see Chapter Four). In addition, the clusters of cells in brVi were revealed to consist of spinal projecting neurons which

receive a moderately dense spinal afferent input. The reciprocal spino-trigemino-spinal loop relayed through these clusters in brVi is exclusively involved with the uppermost levels of the cervical spinal cord. However, the function of this reciprocal pathway has not yet been investigated. It is known that brVi lies in a part of Vi which receives primary V afferent information relayed through the maxillary/ophthalmic divisions of the V nerve were specifically those related to posterior and lateral parts of the head. This fact suggests that these clusters may be intimately involved in trigeminal-neck reflexes. Retrograde axonal transport studies have reported that the majority of the cells in brVi project to the cerebellum and spinal cord, while few cells project to the thalamus (see Chapter Three). This projection pattern implies that the spinal input to brVi may be involved in a spino-trigemino-cerebellar pathway. This latter fact also provides supporting evidence demonstrating that brVi represents a structural and functional distinct region in Vi. A preliminary account of Golgi impregnated neurons in Vi indicates that brVi cells have dendritic fields restricted to the territory of brVi (Phelan and Fall, '83; unpublished observations). This fact indicates that the cells in brVi may function as a unit separate from other regions in Vi.

The dorsolateral region of Vi is similarly characterized by the presence of neurons preferentially oriented parallel to SVT. The Golgi impregnation of neurons in this region indicate that the cells have dendritic fields restricted to dlVi and oriented parallel to SVT (Phelan and Falls, '83; unpublished observations). This region lies in an area of Vi which receives primary V afferent fibers from the mandibular division of the trigeminal nerve (Jacquin et al., '83). In particular, it receives fibers from the lateral and posterior parts of the mandibular field represented by the auriculotemporal nerve. In addition, this region represents the second spinal recipient zone in Vi (see Chapter Four). Retrograde axonal transport studies further indicate that the majority of the cells in this region project to the

thalamus while only a few cells project to the cerebellum or the spinal cord (see Chapter Three). These facts together indicate that this region may be involved in the relay of spinal afferent information to the thalamus. Therefore, although brVi and dlVi share a common spinal afferent input, these two cytoarchitecturally distinct regions represent two functionally distinct regions in Vi which are distinguished primarily by their secondary projections. It has not yet been determined whether similar cytoarchitecturally and functionally distinct regions exist in other species.

The ventrolateral parvocellular and magnocellular regions of Vi are characterized by a complexly organized cyto- and myeloarchitecture which supports the presence of medial and lateral segments. In addition, the DAB's and cells in this region are organized into distinct patterns which characterize the various levels of the nucleus. These two regions are situated in parts of Vi which receive primary V afferents from the maxillary/ophthalmic divisions of the V nerve. The distinct topographical separation of these two division of the V nerve have not yet been reported in rat Vi. Therefore, the specific relationship between the medial and the lateral segments of these regions and particular primary V afferents is not known. Recent studies have shown that succinic dehydrogenase (Belford and Killackey, '79; and Killackey and Belford, '79) and cytochrome oxidase (Ma and Woolsey, '84; Nomura et al., '86; and Nomura and Mizuno, '86) histochemistry can be used to demonstrate the somatotopic distribution of vibrissae afferent segmental representation within the ventrolateral regions of rat Vi. In fact, a part of this pattern in the caudal pole of vlVipc can be seen in the cytochrome oxidase stained sections through the POR shown in Figure 10. This figure illustrates that the distribution of the vibrissae afferent input occupies almost the entire ventrolateral region of Vi. Thus, vlVipc and vlVimc function primarily in the relay of orofacial tactile sensory information to other nuclei along the neuraxis. a recent retrograde axonal transport study has revealed that these regions of Vi contain cells projecting

to the thalamus, the cerebellum and the spinal cord (see Chapter Three). Although vlVipc and vlVimc each contained thalamic, cerebellar and spinal projecting neurons, there were distinct differences in the regional distribution and somatodendritic morphologies of the three groups of neurons throughout the ventrolateral regions of Vi. The Golgi impregnation of neurons in these ventrolateral regions further indicates the existence of a morphologically heterogeneous group of neurons (Phelan and Falls, '83; unpublished observations). These facts together provides additional evidence supporting functional differences between vlVimc and vlVipc.

The dorsal cap and intermediate regions of Vi lie in areas of Vi which receive primary afferent information from the mandibular and the maxillary/ophthalmic divisions of the V nerve, respectively. In fact, the combined region of dcVi and dlVi together coincide precisely with the distribution of the mandibular nerve as anterogradely labeled by Jacquin et al. ('83). The precise primary V afferents terminating to irVi are not known. Retrograde transport studies indicate that thalamic and cerebellar cells exhibiting similar morphologies are distributed throughout these two regions (see Chapter Three). A large number of the thalamic projecting neurons in these two regions have recently been reported to contain the putative excitatory neurotransmitter glutamate (Magnusson et al., '87). However, little is known about the functional organization of these two regions.

The results of the present study in conjunction with other studies indicate that there are six cytoarchitecturally distinct regions in rat Vi which also largely represent functionally distinct regions. The recognition of these six distinct regions in Vi will enable future studies of this nucleus to provide more detailed information on the precise regional functional roles of Vi in overall somatosensory processing in the medulla.

CHAPTER TWO

THE INTERSTITIAL SYSTEM OF THE SPINAL TRIGEMINAL TRACT IN THE RAT: ANATOMICAL EVIDENCE FOR MORPHOLOGICAL AND FUNCTIONAL HETEROGENEITY

INTRODUCTION

The existence of "interstitial" neurons embedded within the fibers of the mammalian spinal trigeminal tract (SVT) was first reported by Ramon y Cajal ('09). The presence of this interstitial system (InSy-SVT) has since been demonstrated to be a fundamental characteristic of SVT throughout phylogenetic history (Crosby and Yoss, '54). A variety of terms have been used in reference to InSy-SVT including the "interstitial nucleus of Cajal" (Gobel and Purvis, '72; Marfurt, '81; and Ishidori et al., '86), the "interstitial nucleus of SVT" (Gobel and Purvis, '72; and Shults, Light and Donaghy, '85), and the "paratrigeminal nucleus" (Chan-Palay, '77, '78a,b). The use of the latter term, in particular, has caused a great deal of confusion in the literature, since in addition to being used in reference to InSy-SVT as a whole, it has also commonly been used to refer to spatially separate and often cytologically distinct cell groups in the lateral medulla (Rhoton, O'Leary and Ferguson, '66; Rhoton, '68; Oswaldo-Cruz and Rocha-Miranda, '68; Sobusiak, Zimny, and Zabel, '72; Campbell, Parker, and Welker, '74; Somana and Walberg, '79; Beckstead and Norgren, '79; Panneton and Loewy, '80; Mugnaini and Oertel, '85; Panneton and Burton, '85; and Paxinos and Watson, '85). This latter fact is particularly important since there has been little agreement in the literature concerning the boundaries of InSy-SVT. Although Ramon y Cajal clearly restricted

the domain of his interstitial nucleus to include only those cells lying deep within the fibers of SVT, Gobel and Purvis ('72) extended their "interstitial nucleus of Cajal" to include those regions of neuropil wedged between SVT and the restiform body (RB) or spinal cerebellar tract (SCT). Later, Chan-Palay ('78a) defined her "paratrigeminal nucleus" as also including those neurons lying among the fibers of SCT and RB. This confusion is compounded further by the fact that several additional terms, including "nucleus trigemino-cuneatus lateralis" (Fuse, '19), "nucleus insulae cuneatus lateralis" (Olszewski and Baxter, '54; Noback, '59; Taber, '61; and Ciriello, Hrycyshyn, and Calaresu, '81a), "promontorium" (Astrom, '53; Riley, '60; and Cechetto, Standaert, and Saper, '85), and "ectotrigeminal nucleus" (Campbell et al., '74; Paxinos and Watson, '85), have been used in reference to isolated groups of neurons situated entirely within SVT or lying between it and SCT or RB. This varied and often inconsistent usage of nomenclature in reference to regions within and surrounding SVT has created some uncertainty concerning the structural and functional organization of InSy-SVT.

Recent studies have implicated portions of InSy-SVT in the processing of nociceptive (Marfurt, '81; Salt, Morris, and Hill, '83; Marfurt and Turner, '84; Arvidsson and Thomander, '84; Cechetto et al., '85; Panneton and Burton, '85; and Shults et al., '85), tactile (Jacquin, Renehan, Mooney, and Rhoades, '84), chemoreceptive (Panneton and Loewy, '80; Chan-Palay, '78b; Cechetto et al., '85), and thermoreceptive (Kilduff, Sharp, and Heller, '83; and Cechetto et al., '85) information relayed through primary afferents of the trigeminal, glossopharyngeal and vagus cranial nerves. In addition, spinal (Phelan and Falls, '84b; see also Chapters Three and Four) and cortical (Dunn and Tolbert, '82) afferents have been demonstrated to terminate within various portions of InSy-SVT. Initially it was suggested solely on the basis of degeneration studies in the cat that InSy-SVT contributed to the extensive intranuclear projection system within the spinal V

nucleus (SVN) (Gobel and Purvis, '72). However, recent axonal transport studies fail to support this latter contention (Hockfield and Gobel, '82; Panneton and Burton, '82; Ikeda, Matsushita, and Tanami, '82; Ikeda, Tanami, and Matsushita, '84; Somers and Panneton, '84, and Panneton and Burton, '85). On the contrary, neurons within InSy-SVT have been demonstrated to project to several different extratrigeminal sites along the neuraxis including the thalamus (Albe-Fessard, Boivie, Grant, and Levante, '75; Burton and Craig, '79; Fukishima and Kerr, '79; Craig and Burton, '81; Pearson and Garfunkel, '83; and Somers and Panneton, '84); cerebellum (Watson and Switzer, '78; Somana and Walberg, '79; Saigal et al., '80; and Matsushita, Ikeda, and Okado, '82); parabrachial region (King, '80; Hamilton, Ellenberger, Liskowsky, and Schneidermann, '81; Ikeda et al., '84; Panneton and Burton, '85; Cechetto et al., '85; and Menetrey, Leah and dePommery, '87), and solitary nuclei (Menetrey et al., '87). This diversity in the efferent projections of InSy-SVT coupled with its varied inputs supports a complex role for this system in somatosensory processing in the lateral medulla.

The InSy-SVT has long been considered as simply an extension of lamina I and/or lamina II of the medullary dorsal horn (MDH). Regions of InSy-SVT have been reported to exhibit an ultrastructural organization similar to that found in these superficial laminae (Gobel and Purvis, '72; and Kerr, '70a). Electrophysiological studies have further demonstrated similarities in response characteristics between those interstitial neurons located at MDH levels and subjacent populations of marginal neurons (Price, Dubner, and Hu, '76; Hubbard and Hellon, '80; and Dawson, Hellon, and Hubbard, '80). Anterograde transport (Panneton and Burton, '85; Marfurt, '81; Marfurt and Turner, '84; and Shigenaga et al., '86) and intracellular horseradish peroxidase (HRP) labeling (Jacquin et al., '84) studies have also revealed a spatial continuity in the distribution of primary V afferents to portions of InSy-SVT and lamina I and/or lamina II. Finally,

immunocytochemical studies have indicated that InSy-SVT shares many common features with these superficial laminae with regard to its content of putative neurotransmitters (Chan-Palay, '78b; Jancso and Kiraly, '80; Finley, Maderdrust, Roger, and Petrusy, '81; Sakanaka et al., '82; Olschowska, O'Donoghue, Mueller, and Jacobowitz, '82; Yamazoe et al., '84; Shults, Quiron, Chronwall, Chase, and O'Donoghue, '84; DelFiacco, Dessi and Levanti, '84; Skofitsch, Jacobowitz, Eskay, and Zamir, '85; Shults et al., '85; and Drew, Westrum and Ho, '86).

Despite the large body of evidence supporting a similarity between InSy-SVT and the superficial laminae of MDH, several additional studies provide some indications to the contrary. The presence of numerous cerebellar projecting neurons within InSy-SVT, for instance, is incongruous with the notion of a functional similarity between these two structures since the superficial layers of MDH are conspicuously devoid of these cerebellar projecting neurons (Faull, '77; Steindler, '77, Watson and Switzer, '78, Ikeda, '79; Somana and Walberg, '80; and Patrick and Haines, '82). Golgi studies have additionally revealed that interstitial neurons located at rostral levels of SVN (Chan-Palay, '78a) exhibit different morphologies compared to cells in the superficial lamina of MDH (Gobel, '75a,b, '78a,b). These differences in morphology and connectivity might be explained if InSY-SVT was actually composed of several morphologically and functionally diverse collections of neurons. In this context, the results of a recent retrograde transport study in the cat support a functional heterogeneity within InSy-SVT which includes a spatial segregation of thalamic and peribrachial projecting neurons (Panneton and Burton, '85). It is not known whether a similar functional heterogeneity and spatial segregation of distinct projection neuron populations exists in rat InSy-SVT.

In view of the emerging complex role that InSy-SVT appears to fulfill in somatosensory processing in the medulla, and in light of the confusion surrounding its overall structural and functional organization, it is necessary that this entire

system be re-examined in order to clarify its cytological and connectional characteristics. The present study uses Nissl, myelin and cytochrome oxidase stained preparations, as well as Golgi impregnation and retrograde axonal transport techniques to examine the structural and functional organization of rat InSy-SVT. In particular, this study examines whether cyto- or chemoarchitecturally distinct regions can be identified within rat InSy-SVT and whether populations of thalamic and/or cerebellar projecting neurons can be localized within specific regions of this system. The present study further uses the rat as a model in order to propose a scheme of nomenclature to be used in reference to InSy-SVT which is more consistent with original definitions, and which will hopefully serve to clarify some of the existing confusion in the literature concerning the structural and functional organization of this lateral medullary region.

METHODS

Adult, male Sprague-Dawley albino rats weighing 200-300 grams were used throughout this investigation. The separate components of InSy-SVT proposed in the present study were determined on the basis of differences in their overall neuronal cytology in conjunction with differences in their chemoarchitecture and connectivity along the neuraxis.

The cyto- and myeloarchitectonic features of InSy-SVT were based on observations of Nissl and 1-2 μm thick plastic embedded semithin myelin stained sections prepared in a previous study (see Chapter One). Low power camera lucida drawings were made from representative transverse and horizontal sections in each preparation using a drawing tube attached to a Leitz Orthoplan microscope. The relative position of the various components of InSy-SVT, as revealed from a comparison of these drawings, is schematically shown in Figure 1. The cytological characteristics of individual neurons were examined using a 50X objective. Neurons

were classified into different types based on their Nissl staining characteristics and their relative somatic and nuclear size and shape. The somatic cross sectional areas of cells within the InSy-SVT were determined from transverse Nissl stained sections with the aid of a Nikon Image Analyzer, a 40X objective, and a drawing tube attached to a microscope. Sampling included all of the cells in a single field of view exhibiting a distinct nucleolus. Measurements were pooled from selected rostrocaudal areas of each identified component, grouped into block intervals of 25 μm^2 and plotted as frequency histograms of the somatic cross sectional areas (Figure 4). In addition, the maximum and minimum somatic diameters were measured for each of these cells. Sample measurements were also taken in a similar manner from lamina II of MDH at a level just caudal to the obex for purposes of comparison. The mean and standard deviations were calculated for all pooled sets of measurements.

The pattern of cytochrome oxidase staining within InSy-SVT was revealed in three animals using the histochemical modification of Wong-Riley ('79). The animals were anesthetized with an intraperitoneal injection of Nembutal (50 mg/kg) and perfused intraaortically with a brief heparanized 0.9% physiological saline wash followed by 500ml of a fixative consisting of 1% paraformaldehyde and 1% glutaraldehyde in 0.15M phosphate buffer (pH 7.4). The brains were then removed from the skull and immediately placed in a 0.15M phosphate buffer overnite at 4° C. Transverse serial sections were cut on a Vibratome at a final thickness of 50 μm and collected in 0.15M phosphate buffer. Alternate serial sections throughout InSy-SVT from all three animals were simultaneously incubated at 37° C in the dark for 1-2 hours in an incubation medium consisting of: 50 mg diaminobenzidine tetrahydrochloride (filtered), 90 ml 0.15M phosphate buffer (pH 7.4), 15-30 mg of cytochrome C, and 4 mg sucrose. The sections were then visually checked every 30 minutes for the presence of light to dark brown reaction product within the tissue

and the incubation stopped when there was a clear differentiation between reactive and nonreactive areas of the brain. The sections were then washed in 0.15M phosphate buffer, mounted onto gelatinized glass slides and air dried. In one animal the sections were counterstained with 0.5% cresyl-violet, while the sections in the remaining animals were coverslipped unstained for purposes of comparison. Cytochrome oxidase positive zones were identified as regions of relatively dark areas against a pale background. Different regions of the InSy-SVT were classified as exhibiting either intense, moderate, or relatively low levels of cytochrome oxidase activity. Differences in the relative intensity of cytochrome oxidase staining throughout InSy-SVT was taken to indicate differences in the metabolic activity of the various regions. Cytochrome oxidase positive neurons were characterized by the "pseudo-Golgi" like staining of their somadendritic tree.

Golgi impregnated neurons were obtained in InSy-SVT using the Golgi-Kopsch method as modified by Gobel ('78a). Serial sections of impregnated blocks were cut on an Oxford Vibratome in the transverse plane at a thickness of 150-300 μm and subsequently dehydrated, cleared and coverslipped. The detailed morphology of representative neurons were drawn with the aid of a drawing tube using either a 100X oil immersion or 50X objective. Neurons were classified according to differences in their somadendritic and axonal morphology.

The location of thalamic and cerebellar projecting neurons within InSy-SVT were determined following the retrograde transport of HRP. The animals used in the present study were previously used in another study (see Chapter Four). A fresh solution of 30% HRP (Sigma Type VI) dissolved in 2% dimethylsulfoxide was stereotaxically delivered through a 26 gauge Hamilton syringe as single, large unilateral injections (0.2-0.3 μl total) centered in the ventrobasal thalamic complex and adjacent regions (6 animals), or as multiple injections (1.0-3.0 μl total) into the ipsilateral cerebellar vermis and hemisphere (6 animals). The animals were allowed

to survive 1-3 days and were then perfused intraaortically with a brief, heparanized physiological saline rinse followed by 500 ml of a 1% paraformaldehyde and 1% glutaraldehyde fixative in 0.15M phosphate buffer (pH 7.4). The brainstems were blocked and postfixed in the same fixative for 1-4 hours and then sectioned on an Oxford Vibratome at a thickness of 50 μm in the transverse plane. Alternate serial sections were reacted for tetramethylbenzidine histochemistry according to the protocol of Mesulam ('78) and counterstained with 1% neutral red. The position and extent of the injection site in each case was determined from light and darkfield illumination and reconstructed from low power camera lucida drawings. The position of retrogradely HRP labeled somata throughout the rostrocaudal extent of InSy-SVT were plotted from each section using a drawing tube attachment. The morphology of HRP labeled cells were examined using a 50X objective and representative camera lucida drawings of labeled cells made from each case. Samples of the somatic cross-sectional areas of HRP labeled projection neurons in InSy-SVT were measured for comparison with those measurements obtained in Nissl stained sections.

RESULTS

The term InSy-SVT is used in the present study to refer to a diverse system of cells and neuropil which together form an extensive interweaving network situated primarily amongst the fibers of SVT, as well as in regions wedged between SVT and SCT and areas extending through SCT to reach the lateral surface of the medulla. In the rat, the InSy-SVT is primarily located at levels between rostral MDH and mid-trigeminal nucleus oralis (Vo). This interstitial system consists of five morphologically and functionally distinct components which are distributed within different parts of the lateral medulla relative to SVT. The relative position of each of these components with respect to SVT and the spinal trigeminal nucleus (SVN) is

schematically illustrated in Figure 1. The first component of InSy-SVT is represented by scattered interstitial cells and patches of neuropil which extend laterally into SVT from the substantia gelatinosa (SG) layer of MDH (Figure 1A). The second component is the dorsal paramarginal nucleus (PaMd) which consists of a small but distinct group of neurons and neuropil situated within the dorsolateral part of SVT at rostral levels MDH (Figures 1A-C). The third component represents a trigeminal extension of the parvocellular reticular formation (V-Rpc) into the ventromedial aspect of SVT from rostral levels of MDH to caudal levels of trigeminal nucleus interpolaris (Vi) (Figures 1D and E). The fourth component is the paratrigeminal nucleus (PaV) which consists of a large accumulation of neurons and neuropil situated entirely within the dorsal part of SVT at levels throughout the caudal half of Vi (Figures 1D-G). The fifth component is the insular trigeminal-cuneatus lateralis nucleus (iV-Cul) which is a discontinuous collection of neurons and neuropil located within SVT, as well as between SVT and SCT, at levels throughout the entire rostrocaudal extent of Vi and at caudal levels of Vo (Figures 1C-H). Detailed descriptions of the light microscopic morphology and connectivity of each of these regions will be provided separately below.

The Substantia Gelatinosa Contribution to InSy-SVT

A relatively few, sparsely scattered small to medium-sized neurons are present throughout SVT at MDH levels. The smaller neurons mainly exhibit oval to fusiform-shaped somata (6-10 μm in maximum diameter), a high nuclear to cyptolasmic ratio, and pale to moderately stained evenly distributed fine, granular Nissl substance. The medium-sized neurons primarily possess oval-shaped somata (10-15 μm in maximum diameter), a large centrally placed nucleus, and moderately stained flocculent appearing Nissl substance. The Nissl substance in these cells often extends into the proximal portions of large diameter dendritic processes. These neurons are especially prominent in the dorsal third of SVT with progressively fewer

cells situated in more ventral portions of the tract. The majority of these small and medium-sized interstitial neurons are situated within the medial two-thirds of the tract and are predominantly oriented with their long axis directed mediolaterally. The population of neurons within SVT at these levels morphologically resemble cells in the subjacent lamina I of MDH (Gobel, '78a,b). On the basis of this similarity in morphology, their close spatial relationship, and the dispersed nature of these cells within SVT, these interstitial neurons are considered here to represent displaced lamina I cells.

In addition to the few scattered interstitial SG cells in SVT, there is also a larger contribution of SG neuropil to InSy-SVT in the rat. Although, the medial margin of SVT primarily exhibits a relatively smooth contour in the rat, two interstitial extensions of SG neuropil invade the dorsal and ventral aspects of SVT in the peri-obex region (Figures 1A-C). During the transition between rostral MDH and caudal Vi the enlarging caudal pole of Vi medially displaces SG (Figures 1B and C). In the ventral part of SVT, strips of SG are commonly left wedged between the caudal pole of Vi and SVT. These strips of SG (particularly lamina I portions) sometimes extend into the ventral part of SVT (Figures 1B and C). Although the extension of SG is difficult to distinguish in Nissl stained preparations, they are easily recognized in myelin stained semithin sections where the relatively amyelinated fine textured SG neuropil is pale in comparison to the deeply stained myelinated SVT (Figure 5A). The contribution of lamina I, in particular, to this interstitial region is most clearly evident in cytochrome oxidase stained sections where the low to moderately stained lamina I neuropil contrasts sharply with the unstained fibers of SVT (Figure 6D). The neighboring remnants of lamina II neuropil situated more deeply within Vi are by comparison relatively unstained in cytochrome oxidase stained preparations.

In the dorsalmost aspect of SVT at this same level, other strands of SG neuropil (particularly lamina II portions) consistently extend into SVT (Figures 1C and 2C). These dorsal interstitial extensions of SG represent lamina II and not lamina I neuropil since the regions appear relatively unstained in cytochrome oxidase stained preparations (compare Figures 6A and B) and the neuropil exhibits a fine texture in myelin stained preparations. The low to moderate stained regions in SVT lateral to this dorsal interstitial extension of SG represent neuropil belonging to PaMd and not lamina I (see below).

Examples of Golgi impregnated neurons were not obtained in any of the interstitial parts of SG. In addition, large injections of HRP into the cerebellum (Figure 10B) do not retrogradely label any of these interstitial SG neurons. Furthermore, despite the presence of a few retrogradely labeled SG neurons along the medial margin of SVT at rostral MDH levels of the medulla following large injections of HRP into the contralateral thalamus (Figure 10A), no labeled cells are found in the larger interstitial islands of SG in these cases.

The Dorsal Paramarginal Nucleus

The number of small and medium-sized neurons within SVT substantially increases as one proceeds to rostral levels of MDH. A small but conspicuous collection of these neurons consistently appears in a rather restricted portion of the dorsal third of SVT at the rostral pole of MDH (Figures 1A-C, and Figures 2A and C). These neurons are part of the PaMd nucleus which extends approximately 400 Mm rostrocaudally. The small-sized neurons in this nucleus are morphologically similar to those found in more caudal and ventral portions of SVT (Figure 3D). The medium-sized neurons (10-20 Mm in diameter) mainly exhibit multipolar or fusiform-shaped somata and darkly stained, flocculent appearing Nissl substance which is evenly distributed throughout the cytoplasm (Figures 3A-C). The Nissl substance often extends into proximal dendrites. The majority of these neurons have

their long axis directed mediolaterally within SVT. Neurons in this region are especially prominent along the many blood vessels which course through SVT at this point. The neurons in PaMd are generally more intensely stained, slightly larger in size, and more densely packed than those cells situated in the subjacent Lamina I (compare Figures 4A and E). They also typically appear in clusters of four or more cells.

Golgi impregnated neurons in this region exhibit oval-shaped somata (10-20 μm in maximum diameter) which give rise to two to four relatively thick primary dendrites (Figure 8C). These dendrites course 20-200 μm before giving rise to secondary dendritic processes which also extend for long distances in the neuropil. The neurons are distinctly characterized by heavily spine-laden somata and dendrites. The spines are evenly distributed along the soma-dendritic tree and exhibit a variety of morphologies including sessile and pedunculated spines and short filamentous spine-like appendages. The axons of these cells arise from either the soma or the base of a primary or secondary dendrite.

Many of the larger cells in PaMd are retrogradely labeled following HRP injections into the contralateral thalamus (Figure 11A). These neurons range from 50 to 300 μm in somatic cross sectional area. The smaller neurons in PaMd are less frequently labeled following thalamic injections. Cerebellar injections of HRP do not label any cells in this region.

A rather unique feature of neurons in this nucleus is their tendency to exhibit a moderate intensity of soma-dendritic staining in a "pseudo-Golgi" like fashion in cytochrome oxidase stained preparations (Figures 6A and B). In fact this staining pattern is helpful in differentiating the boundaries of this region from adjacent portions of SG in which no cytochrome oxidase stained neurons are encountered. The overall intensity of staining in PaMd neuropil is also slightly lighter compared

to that of lamina I neuropil, but darker than the unstained appearance of lamina II neuropil (compare Figures 6A and B).

The Trigeminal Extension of the Parvocellular Reticular Formation

A modest collection of neurons lie embedded in a network of thin neuropil strands in the ventral medial aspect of SVT at the level of the transition from MDH to Vi. (Figures 1D and E, and Figure 2B). This region represents a trigeminal extension of the parvocellular reticular formation (V-Rpc). The nucleus extends approximately 500 μm rostrocaudally. The cells in V-Rpc range in size from 8-15 μm in maximum diameter and exhibit oval to fusiform-shaped somata with light to moderately stained fine granular Nissl substance. The spatial continuity between V-Rpc and the medially adjacent parvocellular reticular formation is most clearly evident in cytochrome oxidase stained sections in which intensely stained strands of reticular neuropil extend laterally into SVT (Figure 5E). The intensity of the cytochrome oxidase staining in V-Rpc neuropil demarcates this region from the more caudally situated low to moderately stained lamina I neuropil. (compare Figures 6D and E).

Golgi impregnated neurons in V-Rpc were not obtained due to the sparseness of cells intrinsic to this region and the difficulty in establishing the precise location of the nucleus in unstained sections. However, virtually every cell in V-Rpc is retrogradely labeled following contralateral thalamic injections of HRP (Figure 11B). These labeled neurons appear loosely distributed in SVT and exhibit thin dendritic processes which intertwine amongst the bundles of SVT fibers to form a reticular appearing network of labeled somata and processes. These neurons are morphologically similar to retrogradely labeled neurons located in medially adjacent parts of the parvocellular reticular formation.

The Paratrigeminal Nucleus

The PaV nucleus first appears as a single large mass of interstitial neurons and neuropil in SVT at the level of the transition from MDH to Vi (Figures 1C and D). The nucleus extends approximately 700 μm rostrocaudally from this level to the midrostro-caudal extent of Vi (Figure 1G). It measures approximately 600 μm at its greatest dorsoventral extent and its presence produces a prominent bulge in SVT. The caudal boundary between PaV and the rostral poles of PaMd and the dorsal interstitial SG neuropil is not easily distinguished in Nissl stained sections. However, the boundary between these nuclei is readily evident in cytochrome oxidase stained preparations since the neuropil of PaV exhibits a moderate to intense staining that contrasts sharply with the pale stained appearance of interstitial SG neuropil (compare Figures 6B and C). In addition, neurons in PaV are not stained in a "pseudo-Golgi" like fashion by cytochrome oxidase as are PaMd neurons. Myelin stained semithin sections through this region also aid in distinguishing between these nuclei since the PaV neuropil exhibits a moderately coarse texture while the neuropil of the dorsal interstitial SG is by contrast pale and gelatinous in appearance (compare Figures 5A and B).

The cells in PaV are randomly arranged in small clusters interspersed among the bundles of longitudinally coursing myelinated SVT axons. The cells are also prominently aligned along blood vessels which commonly pass through SVT at this level. A few single strands of cells sometimes extend laterally from PaV and traverse SCT to reach the lateral surface of the medulla. Occasionally, a single strand of cells also extends laterally to connect PaV with the ventrolateral edge of insular portions of the lateral cuneate nucleus (Cul) lying between the dorsal margin of SVT and SCT.

Small neurons with spherical to oval-shaped somata (8-12 μm in maximum diameter) are commonly found throughout PaV. These neurons possess large

centrally located nuclei and pale to moderately stained fine Nissl substance distributed uniformly throughout the cytoplasm (Figure 3I). Larger neurons with oval to multipolar-shaped somata measuring 15-20 μm in maximum diameter are also common. These latter neurons possess large centrally located spherical to oval-shaped nuclei and pale to moderately stained granular Nissl substance (Figures 3G and H). The Nissl substance often extends into thick primary dendrites which frequently emanate from one side of the neuron. The dendrites of these cells do not appear in Nissl stained sections to exhibit any preferential orientation within the neuropil. The presence of these dendrites accounts, in part, for the moderately coarse texture of PaV neuropil in myelin stained semithin preparations (Figure 5B).

The PaV nucleus gradually separates into two cytologically similar groups of neurons and neuropil at rostral levels of the medulla (Figures 1E and F, and Figure 2D). The dorsal group is usually larger in size than the ventral group. These two masses of neuropil subsequently become linked by a band of cells which appears medially within the tract. The majority of cells in this band have oval to fusiform-shaped somata which measure 10-20 μm in maximum diameter. The cells possess large centrally located spherical to oval-shaped nuclei and moderately stained granular Nissl substance. A few pale stained small neurons and large multipolar-shaped neurons of varying intensity, similar to those in other parts of PaV, are also present in this band. The cells in this band usually possess large primary dendrites which are primarily oriented in a dorsoventral direction along the long axis of the band. This orientation of the dendrites can be best appreciated in myelin stained semithin sections where the neuropil of the band appears striated due to the large number of dendrites bundled together compared to the more irregular arrangement of dendrites in the main body of PaV (compare Figures 5B and C).

The band of cells connecting the dorsal and ventral groups of PaV shifts medially within SVT at more rostral levels until it lies along the medial margin of

the tract adjacent to the dorsolateral subdivision of Vi (dlVi, Figure 1F). The boundary between PaV and dlVi is easily demarcated at this point due to the relatively smaller size and less intensely stained cytoplasm of PaV neurons compared to those in dlVi (see Chapter One). The band of cells in PaV gradually disperses at more rostral levels leaving only isolated patches of interstitial cells in the rostralmost pole of PaV.

Golgi impregnated sections through PaV reveals the existence of two main types of neurons. These cells can be differentiated on the basis of differences in their dendritic branching pattern and their distribution within the nucleus. Type I neurons possess primarily spherical to oval-shaped somata and two to four primary dendrites which often arise from one side of the cell body. These neurons are primarily characterized by the presence of long primary, secondary and tertiary dendrites which give rise to a columnar-shaped dendritic field that is preferentially oriented dorsoventrally within PaV especially along the lateral and medial margins of the main body of the nucleus. These cells are also particularly prominent within the medial band region of PaV. The dendrites of cells in both regions of PaV contribute to the parallel dendritic bundling pattern which characterizes this band. (Figures 7A and 8A). Type I neurons possess a sparse number of spines on their proximal dendrites and a slightly greater number on distal dendritic branches. The dendritic spines can be morphologically separated into simple spines which exhibit a variety of sizes and shapes, and more complex spines in which two spines or appendages emanate from a single common stem. These latter spines are more often distributed in distal portions of the dendritic tree. The simple spines sometimes occur in pairs which together outline a concavity giving the impression that they surround some structure possibly representing an axon terminal. Some neurons exhibit complex terminal dendritic thickets consisting of a large number of spines and spine-like appendages on the distal end of dendrites (Figures 7B and C).

The axons of these cells emerge from either the soma or the base of a proximal dendrite and are not oriented in any one particular direction within the neuropil.

Type II neurons are similar in size and shape as Type I neurons. The neurons are characterized by the presence of relatively shorter primary and higher order dendrites which branched more often compared to Type I cells. The dendrites of these cells are wavy and give rise to more of a spherical to elliptical-shaped dendritic field. The dendritic tree of these neurons is more compact compared to the widespread linearly organized dendritic field of Type I neurons. The entire dendritic field of individual Type II neurons is difficult to reconstruct due to the rather tortuous course of the dendritic arbors around the bundles of SVT axons. Type II neurons possess a slightly greater number of dendritic spines especially proximally compared to Type I neurons. In addition, a few somatic spines are sometimes present. The dendritic spines of Type II neurons are in general morphologically similar to those seen on Type I cells. Type II neurons are especially prominent throughout the center of the dorsal and ventral groups of PaV neuropil. The axons of Type II cells arise from either the soma or the base of a proximal dendrite and exhibit no particular orientation within the neuropil. None of the Type I or Type II neurons in PaV exhibit any intrinsic axon collaterals. By comparison, neighboring lamina II neurons, which are situated within Vi along the medial edge of SVT bordering PaV, characteristically give rise to extensive intranuclear axon collaterals (Figure 8B). None of the neurons in PaV are retrogradely labeled following either thalamic or cerebellar injections of HRP.

The Insular Trigeminal-Cuneatus Lateralis Nucleus

The iV-Cul nucleus consists of a discontinuous collection of cells wedged between and lying interstitial to the fibers of SVT and SCT (Figures 1C-H). The caudalmost part of the nucleus first appears in transverse sections as a small irregular-shaped compact mass of neurons and neuropil situated along the

dorsolateral margin of SCT at the level at which this tract has covered one-third to one-half of the lateral surface of SVT (Figure 1C and 2E). This level of the medulla corresponds to the transition between rostral MDH and caudal Vi. A large amount of glial membranes cover this part of iV-Cul and separates it from the surrounding cerebral spinal fluid. At progressively more rostral levels within the medulla, a large part of the iV-Cul neuropil is forced medially between SVT and SCT to form a "main" insular region of iV-Cul as the fibers of SCT continue to extend dorsally along the lateral medulla (Figures 1D and 2F). A few cells remain along the lateral surface of SCT (Figure 2F, arrows). Smaller isolated islands or nests of compactly arranged cells are also interspersed between SVT and SCT at more ventral levels in the medulla (Figures 1D-F). However, similarly located cell nests are rarely seen more dorsally. These insular collections of iV-Cul neuropil are at levels extending approximately 1mm rostrocaudally throughout the caudal two-thirds of Vi. Small cellular bridges sometimes extend laterally from the main insular portion of iV-Cul to interconnect it with isolated patches of cells lying interstitial to SCT. These extensions are clearly evident in cytochrome oxidase stained preparations where they appear as fine networks of intensely stained neuropil against a pale background of unstained SCT fibers (Figure 6F). The main insular portion of iV-Cul also consistently exhibits medially directed extensions which traverse SVT to enter the territory of the border region of Vi (brVi, Figures 1D and E; see also Chapter One). The invasion of insular parts of iV-Cul into the confines of brVi is most clearly seen when the neurons of iV-Cul are retrogradely labeled (Figure 11D). No direct neuropil connections are observed between iV-Cul and either PaV, Cul or the lateral reticular (LR) nuclei.

The neurons of iV-Cul are the most conspicuous of all five components of InSy-SVT in Nissl stained sections. They are are morphologically similar in each part of iV-Cul and consist of small to medium-sized (8-20 μm in maximum

diameter) intensely stained neurons (Figures 3J-N). The smaller cells possess primarily fusiform-shaped somata (Figures 3M and N), while the medium-sized neurons possess round to oval-shaped somata (Figures 3J-L). These neurons exhibit a high nuclear to cytoplasmic ratio, central nuclei, and evenly dispersed intensely stained coarse Nissl substance which often extends into large primary dendritic processes. The majority of the neurons and their primary dendrites are oriented either dorsoventrally within the insular portions of the nucleus or mediolaterally within the interstitial extensions of the nuclei which are directed towards Vi. Neurons in this region are also sometimes aligned along blood vessels. The caudalmost part of iV-Cul, located along the dorsal margin of SCT, predominantly contains the larger oval-shaped neurons which are often conspicuously aligned in rows. This arrangement is particularly evident in myelin stained semithin sections where they often exhibit closely apposed surfaces (Figure 5D). In general, the iV-Cul neuropil appears relatively free of myelinated fibers and is slightly less coarsely textured compared to PaV neuropil (compare Figures 5B and E).

In most of the Golgi impregnated sections through iV-Cul, the main insular body of the nucleus appears as one large mass of impregnated neurons and processes within which individual cells are not easily distinguished in their entirety due to the extensive intermingling of dendrites. In general however, neurons in this region possess spherical to oval-shaped somata which give rise to two to four relatively thick primary dendrites that usually originate from one or both poles of the cell body (Figure 9B). The dendrites of these cells give rise to disk-shaped dendritic fields which are restricted to the small area that the nucleus occupies between SVT and SCT. In contrast, neurons in some of the more ventrally located insular islands of iV-Cul have dendrites which are primarily oriented in a mediolateral direction within the tract (Figures 8C-E). These neurons also possess spherical to oval-shaped somata and two to four primary dendrites which usually

issue from the medial side of the soma. The primary and higher order dendrites of these neurons often course long distances without branching and are organized into tight mediolaterally directed columns which traverse SVT. The terminal dendrites of some of these neurons actually extend into brVi (Figure 8E). A sparse number of dendritic spines are present on the proximal dendrites. However, the terminal portions of the dendrites usually exhibit a larger number of dendritic spines. In general, the spines consist of simple and complex spines whose overall morphology is similar to the simple and complex dendritic spines on dendrites of PaV neurons. The more complex appearing spines are usually distributed at distal portions of the dendritic tree. The axons of iV-Cul neurons arise from either the somata or the base of a primary dendrite and course laterally or dorsally within the medulla to assume a final course parallel to the ascending fibers of SCT. The axons of iV-Cul neurons do not give rise to any intrinsic axon collaterals within the nucleus. Large thalamic injections of HRP do not label a single cell in iV-Cul. However, injections of HRP into the ipsilateral cerebellum labels every cell in the nucleus (Figure 11C-F). The composite diagram of camera lucida drawings of retrogradely labeled neurons in the main insular part of iV-Cul, shown in Figure 8A, clearly illustrates the restriction of the dendritic fields of the neurons within the confines of the nucleus.

Figure 1

A schematic diagram illustrating the relative position and extent of the five components of InSy-SVT in the rat from caudal (A) to rostral (H) levels of the SVN.

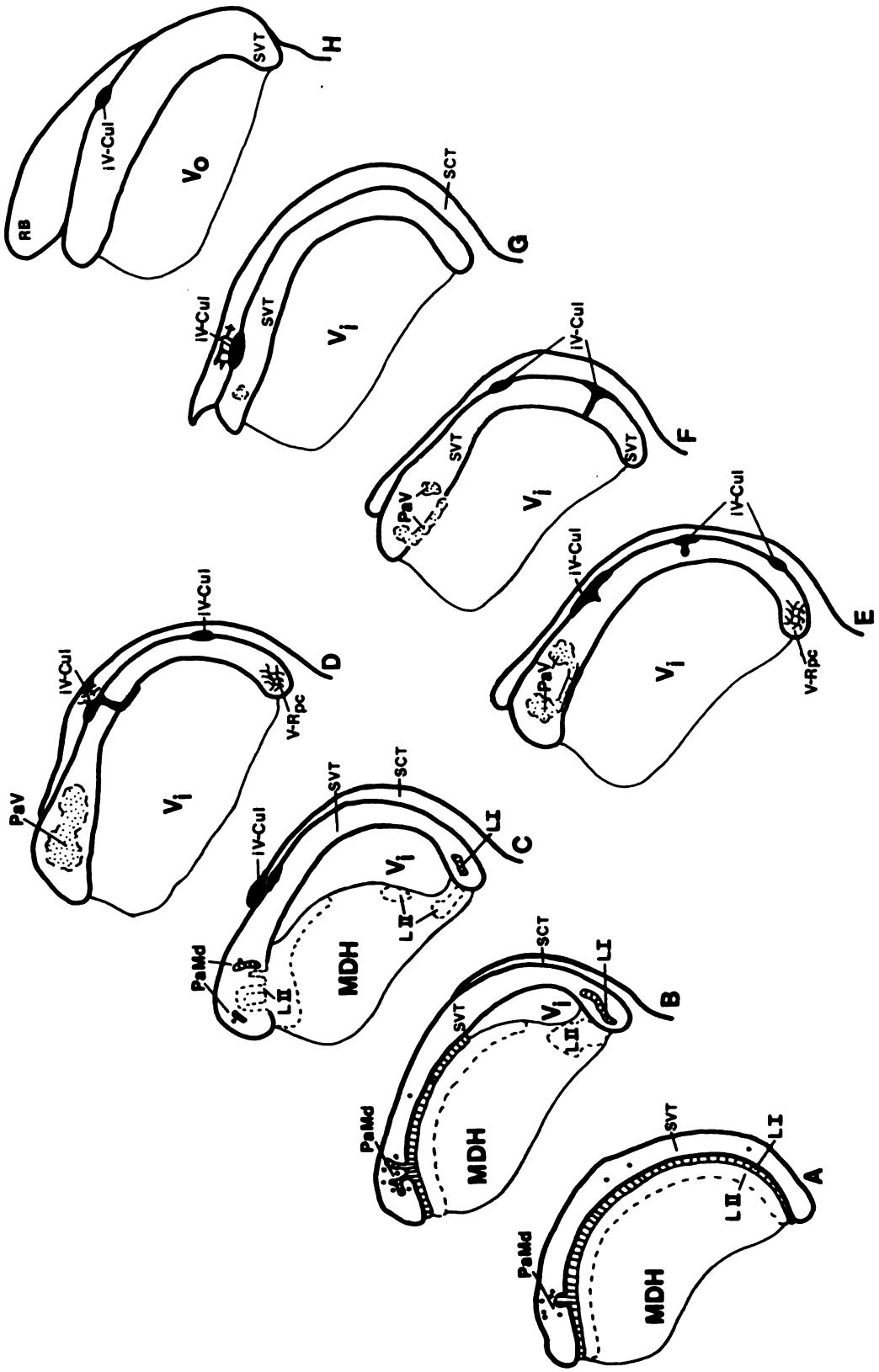
A
B
C
D
E
F
G
H
MDH
PaMd
LI
LII
SVT
SCT
lV-Cul
V-Rpc
PaV
RB
Vo
Vi

Figure 2

A series of transverse Nissl stained sections through selected levels of SVT to illustrate the cytoarchitectural appearance of various components of InSy-SVT. Arrows in E and F point to isolated cell groups of iV-Cul. X130.

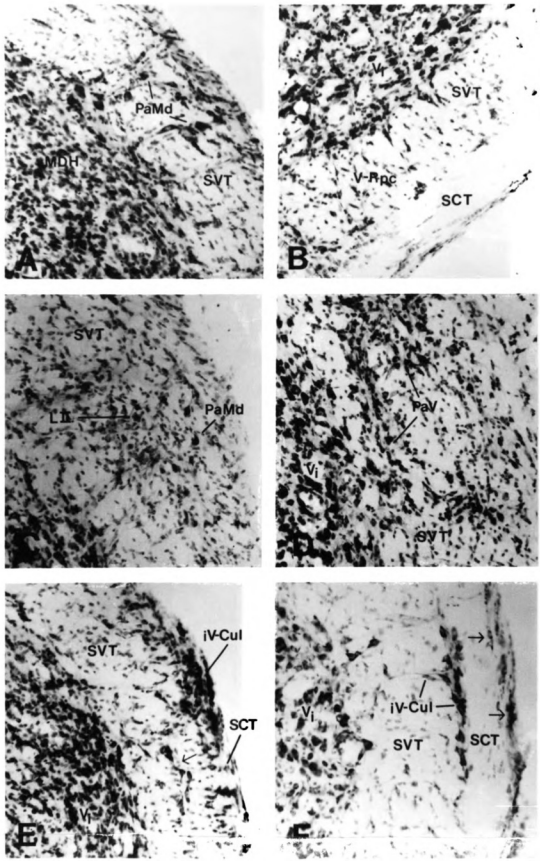
PaMd
MDL
SVT
A
Vi
SVT
V-Rpc
SCT
B
SVT
LTr
PaMd
PaV
Vi
SVT
SVT
iV-CuI
SCT
Vi
iV-CuI
SVT
SCT

Figure 3

A series of high power photomicrographs illustrating the morphology of Nissl stained cells in PaMd (A-D), PaV (E-I), and iV-Cul (J-N). X1200.

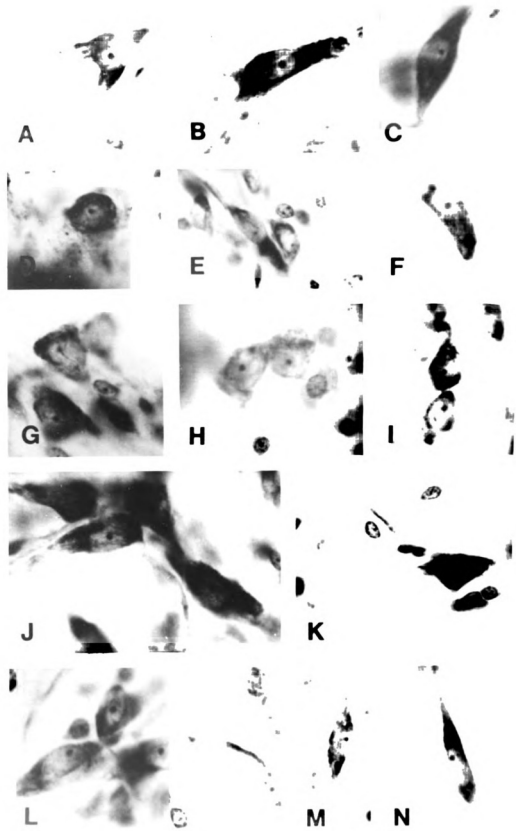
A
B
C
E
F
G
H
I
J
K
L
M
N

Figure 4

Frequency histograms comparing the somatic cross-sectional areas of Nissl stained neurons in the four major components of InSy-SVT (A-D) and in SG (E).

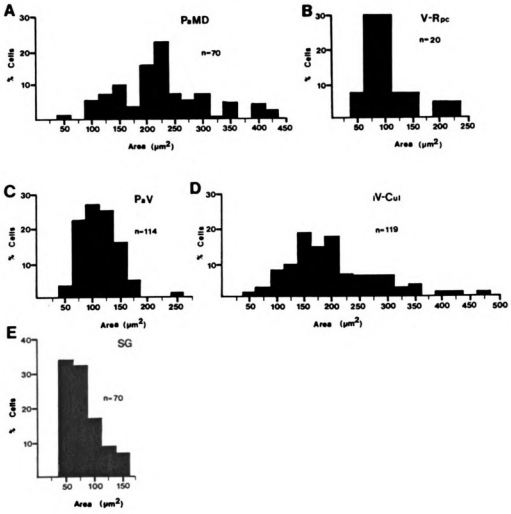
A
PaMD
n=70
% Cells
Area (μm²)
B
V-Rpc
n=20
% Cells
Area (μm²)
C
PaV
n=114
% Cells
Area (μm²)
D
iV-Cul
n=119
% Cells
Area (μm²)
E
SG
n=70
% Cells
Area (μm²)

Figure 5

A series of high power photomicrographs of myelin stained semithin sections comparing the texture of the neuropil in interstitial regions of lamina I (A), PaV (B and C), and iV-Cul (D and E). Arrows in B, C and D point to small PaV cells, dendrites, and serially aligned iV-Cul cells, respectively. X420.

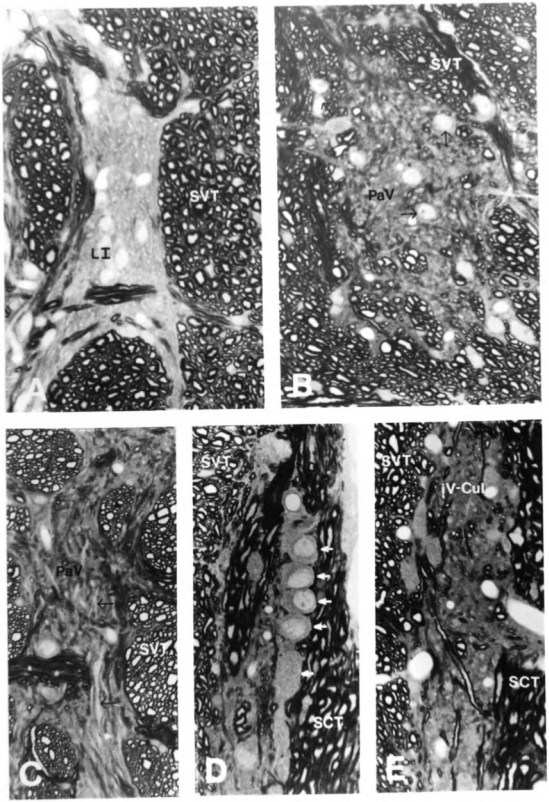
SVT
LI
A
SVT
PaV
B
PaV
SVT
C
SVT
SCT
D
SVT
V-Cul
SCT
E

Figure 6

A series of photomicrographs illustrating differences in the intensity of cytochrome oxidase staining in the five components of InSy-SVT. Arrow in B points to a "pseudo-Golgi" like staining of a PaMd cell. X130.

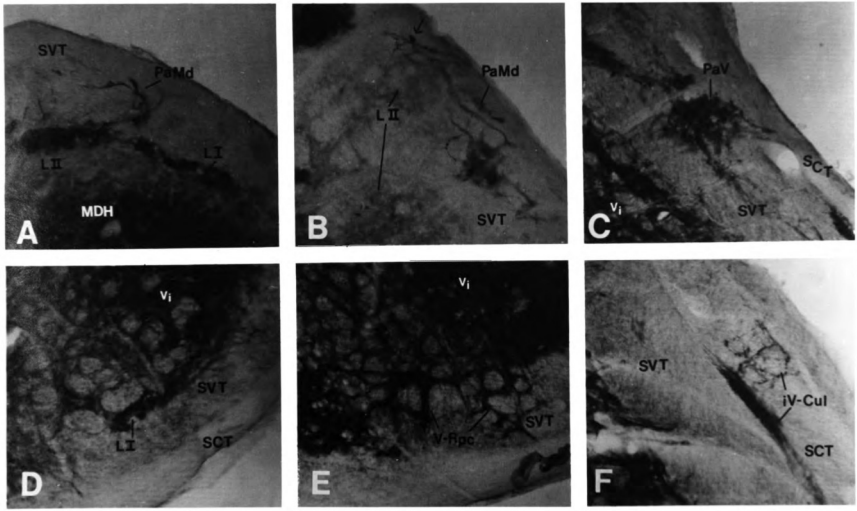
SVT
PaMd
LII
LI
MDH
A
PaMd
LII
SVT
B
PaV
SCT
Vi
SVT
C
Vi
SVT
LI
SCT
D
Vi
SVT
V-Rpc
E
SVT
iV-Cul
SCT
F

Figure 7

Two photomicrographs and a camera lucida drawing demonstrating the dendritic bundling present in the medial band region of PaV (A, open block arrows) and the terminal dendritic thicket of a PaV neuron (B and C). Golgi-Kopsch preparation. X40 (A), X1000 (B and C).

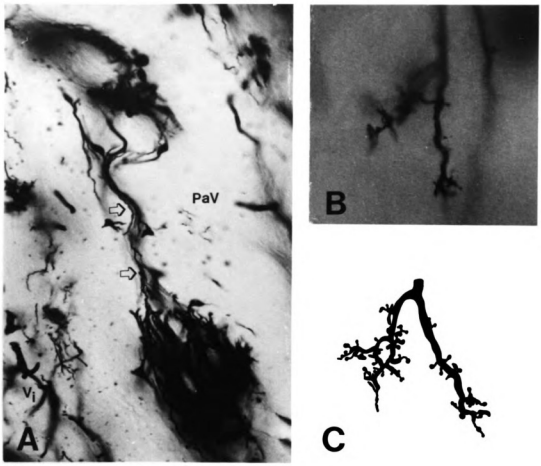
PaV
VI
A
B
C

Figure 8

A composite schematic diagram comparing camera lucida drawings of representative PaV (A and B), PaMd (C), and SG (B) cells. Open block arrows in A point to the dendritic bundling which characterizes the medial band of PaV neuropil. Golgi-Kopsch preparation.

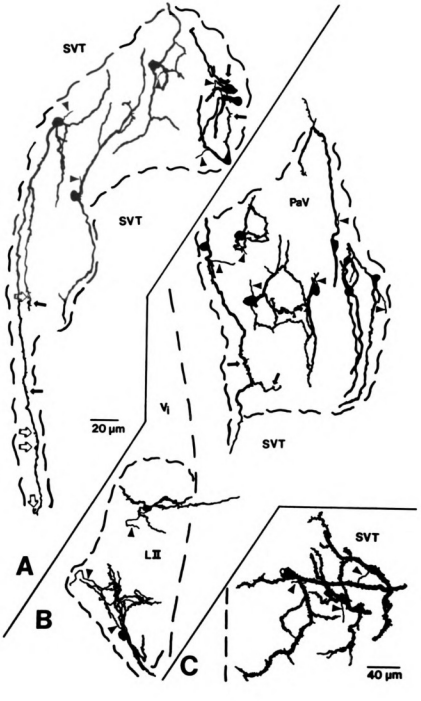
SVT
SVT
PaV
SVT
20 µm
V1
LII
A
B
C
SVT
40 µm

Figure 9

Camera lucida drawings illustrating the morphology of representative neurons in iV-Cul following either retrograde labeling from cerebellar injections of HRP (A) or Golgi impregnation (B-E). Axons (small arrowheads). Golgi-Kopsch preparation.

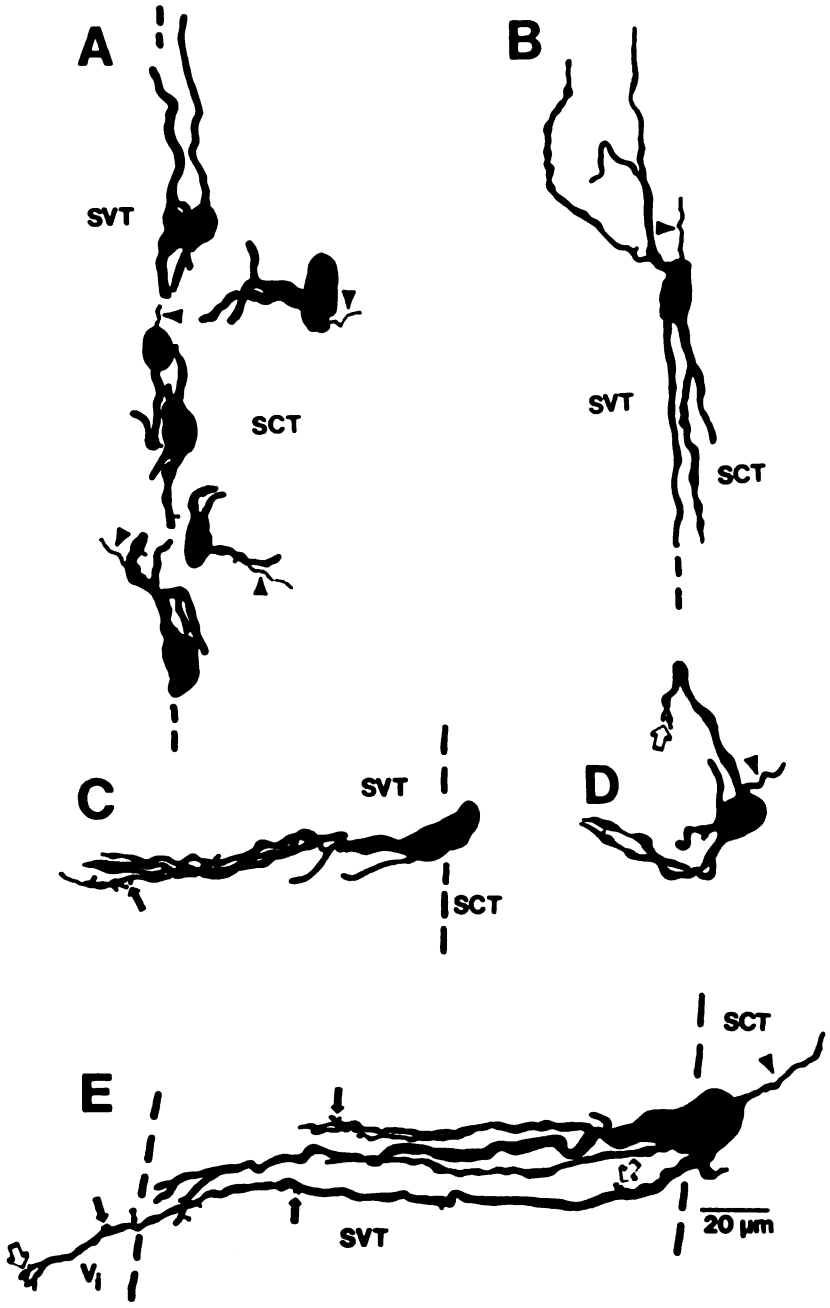
A
SVT
SCT
B
SVT
SCT
C
SVT
SCT
D
E
SCT
SVT
V_1
20 µm

Figure 10

Schematic diagram illustrating the relative size and extent of representative HRP injections into the thalamus (A) and cerebellum (B). Ventrobasal thalamic complex (VB).

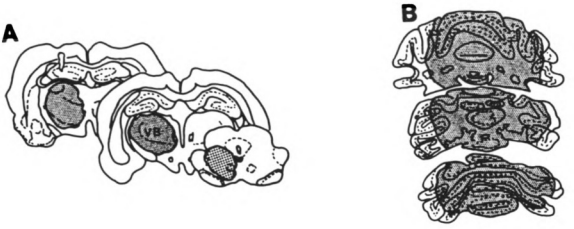
A
VB
B

Figure 11

A series of photomicrographs illustrating the distribution and morphology of retrogradely labeled neurons in various regions of InSy-SVT following HRP injections into either the thalamus (A and B) or cerebellum (C-F). X120.

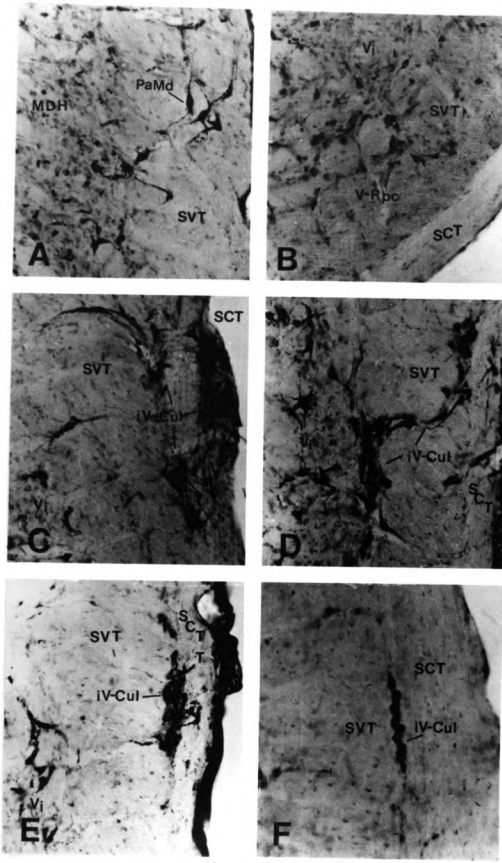
MDH
PaMd
SVT
A
Vi
SVT
V-Rpc
SCT
B
SCT
SVT
iV-CuI
Vi
C
SVT
iV-CuI
SCT
D
SVT
SCT
iV-CuI
Vi
E
SCT
SVT
iV-CuI
F

DISCUSSION

The present study represents the first to examine the cyto-, myelo-, and chemoarchitecture, the morphology, and the connectivity of the entire system of cells located in and around SVT in any species. The results of the present study document the existence of several morphologically and functionally heterogeneous components in InSy-SVT in the rat and provides detailed morphological descriptions of each of these regions which can be used to identify homologous regions of InSy-SVT in other mammalian species.

The structural and functional composition of InSy-SVT has in the past been clouded with confusion stemming primarily from a widely inconsistent usage of nomenclature in reference to this region coupled with an often incorrect assumption of homologous regions across species. This confusion has, perhaps, been perpetuated most by the rather conspicuous absence of any thorough review of the pertinent literature. Considering that it has become increasingly clear that this interstitial system plays a complex role in the processing of somatosensory information within the lateral medulla, it is imperative that this deficiency be addressed in order that these terminology related inconsistencies can be resolved.

Prior to discussing the specific results of the present study therefore, an historical review of the relevant literature is provided with an emphasis on the development of terminology presently used in reference to InSy-SVT as well as the spatial extent of this system of cells in the lateral medulla. It is intended that this review will clarify some of the existing confusion regarding nomenclature while also serving as a basis for the justification of the terminology proposed in the present investigation.

Historical Review

The earliest description of an interstitial system within mammalian SVT was provided by Ramon y Cajal ('09) who noted the presence of "interstitial cells" situated amongst the fibers of SVT in Golgi impregnated material. He further noted that in man these neurons were well organized into groups which formed a distinct "interstitial nucleus". Although Ramon y Cajal reported the presence of "interstitial cells" along the entire extent of SVT from the level of the facial nucleus to the pyramidal decussation, the only illustration included in his study was a single schematic drawing of a Golgi impregnated transverse section from newborn rabbit (see his Figure 380). The position of SVT at the superficial surface of the brain in this figure, as well as the distinct laminar organization depicted, indicate that the section lies at a level corresponding to MDH. Illustrations of the more rostrally located "interstitial cells" in rabbit medulla or the larger "interstitial nucleus" in man are conspicuously absent from this study.

In a subsequent myeloarchitectonic study of human SVN, Fuse ('19) provided the first detailed account of the organization of interstitial cells throughout the rostrocaudal extent of SVT. In particular, he indicated an especially prominent mass of interstitial gray within rostral SVT, in contrast to the more dispersed strands and nests of interstitial cells in more caudal levels of the tract. Fuse's myeloarchitectonic study was also the first to demonstrate that the interstitial neuropil within human SVT was spatially continuous with regions of neuropil bordering the ventral, lateral and dorsal edges of SVT. In particular, he noted intimate connections ventrally with LR and subtrigeminal nuclei, connections laterally with neuropil wedged between SVT and SCT which he identified as "lateral marginal gray", and connections dorsally and dorsolaterally with a region containing two nuclei which he referred to as the "trigeminocuneatus lateralis" and "trigeminocuneatus intermedius" nuclei. The latter two nuclei, along with a third nucleus referred to as the "trigeminocuneatus

medialis", derived their names from the fact that together they formed a neuropil connection between the spinal trigeminal and cuneate nuclei.

According to Fuse, the "trigeminocuneatus lateralis nucleus", in particular, corresponded to a region previously identified by Ziehen ('13) as the "nucleus marginalis dorsalis" or "promontorium". Fuse reported that this triangular-shaped region, wedged between RB, SCT and SVT, was not especially gelatinous in appearance, a fact that was later confirmed by Riley ('60). Riley, in fact, further reported that this region probably belonged to the group of "marginal" nuclei, while Fuse considered the "trigeminocuneatus lateralis" (or promontorium) as nothing more than an especially well developed ventrolateral extension of Cul. This latter belief was also subsequently held by Olszewski and Baxter ('54) since in their cytoarchitectonic atlas of human brainstem, they apparently included this particular region as part of Cul (see their Plates X and XII).

In an earlier study in marsupials, Ziehen ('01) identified a group of cells which extend along the lateral surface of SVT, as well as between it and SCT and RB, as the "nucleus marginalis dorsalis". The widespread marsupial distribution of this nucleus was in apparent contrast to the more limited position of this nucleus in man (Ziehen, '13). However, Olszewski and Baxter ('54) reported that the comparable regions of cells lying between SVT and RB in man actually represented displaced portions of Cul, and they referred to these areas as the "insulae of the lateral cuneate nucleus". This particular terminology was later adopted in studies in other primates (Noback, '59; Gerhardt and Olszewski, '69), and cat (Taber, '61) in lieu of the use of the terms "lateral marginal gray" or "nucleus marginalis dorsalis" as proposed by Fuse ('09) and Ziehen ('01), respectively. More importantly however, Olszewski and Baxter provided the first description of the cytology of these neurons indicating that the cells exhibited darkly stained Nissl substance. Interestingly, these authors illustrated that these insulae of the lateral cuneate nucleus traversed SVT to

become contiguous with neuropil of the lateral margins of Vi (See their Plate X). Although they did not specifically discuss the presence of interstitial cells within SVT, they did illustrate many such cells throughout the rostrocaudal extent of the tract. This latter fact would seem to indicate that Olszewski and Baxter believed that these interstitial cells in SVT were different from those interstitial portions of the insulae of the lateral cuneate nucleus.

A few years later, Noback ('59) reported that the "insulae of the lateral cuneate nucleus" in the gibbon were similar in appearance, although smaller and less numerous, compared to that reported by Olszewski and Baxter in man ('54). Gerhardt and Olszewski ('69) later published an extensive cyto- and myeloarchitectonic comparison of the medulla oblongata and pons among a variety of primate species in which they provided a brief comparative analysis of these "insulae of the lateral cuneate nucleus". In general, these authors reported that the cytology of cells within these insulae were similar in appearance, in all primates examined, to the descriptions provided by Olszewski and Baxter in man ('54). However, their study confirmed that these insulae in man were relatively more numerous and larger in extent and ramification than those in other anthropoids or lower primate forms. This apparent trend in the reduction of the overall size of the "nuclei insulae cuneati lateralis" is supported by Taber's ('61) study in the cat in which the feline "nuclei insulae cuneati lateralis" was reported to be represented solely by a small group of cells which extended ventrally from Cul around the lateral surface of SVT.

Craigie's discourse on the finer anatomy of the central nervous system (CNS) contains the first illustration of interstitial neuropil in SVT of the rat (Zeman and Innes, '25). The schematic drawing in Figure 4A shows a large area of neuropil lying in the dorsal part of SVT, at a level corresponding to the peri-obex region of the medulla. This region is labeled "substantia gelatinosa" indicating that it was

considered as an interstitial portion of the SG layer of MDH. However, no morphological evidence to support this view was provided; in fact, the text does not even specifically discuss this region.

Almost thirty years later, Astrom ('53) also recognized the existence of a similar region of neuropil in his Golgi impregnation study of mouse brainstem and proposed that it represented a distinct nucleus in the lateral medulla. He referred to this area as the "promontorium", since judging by its position and the appearance of its limiting trigeminal fibers, it corresponded according to him to the "promontorium" described by Ziehen ('09) and the "nucleus trigeminocuneatus lateralis" described by Fuse ('19). However, Astrom's "promontorium" in the mouse clearly lies entirely within the fibers of SVT and does not share a common position in the dorsolateral medulla with either of the nuclei described by Ziehen ('09) or Fuse ('19) which lie along the dorsal and dorsolateral margins of SVT. Nevertheless, Astrom did not discuss the significance of these differences when making his generalizations concerning the homology of this "promontorium".

A few years after the appearance of Astrom's study, Torvik ('56) provided a brief cytoarchitectural description of rat SVN in which he stated that the rostralmost part of SG is partly broken up and cell nests of gelatinous substance are seen intercalated in the dorsal part of SVT. Torvik noted that this region apparently corresponded to the "promontorium" identified by Astrom ('53) in the mouse. Torvik's identification of this region as SG indicates that the cells in these interstitial nests were cytologically similar in appearance to the densely packed, small pale staining neurons which he described in more caudal parts of SG. It is important to recognize that the pale appearance of these neurons is in obvious contrast to the reportedly intensely stained appearance of neurons in the "promontorium" or "nucleus trigeminocuneatus lateralis" described by Ziehen ('09) and Fuse ('19), respectively. Torvik's cytological description of neurons in this region clearly

indicates that Astrom had assumed an incorrect homology between his "promontorium" in mouse and the "promontorium" previously described in man by Ziehen ('09).

In their cytoarchitectural atlas of opossum brain, Oswaldo-Cruz and Rocha-Miranda ('68) introduced the term "paratrigeminal" nucleus to refer to a collection of small, pale stained neurons located at posterior bulbar levels between the restiform body and SVT. The authors noted that their "paratrigeminal" nucleus, previously observed but left unnamed by Voris and Hoerr ('32) roughly corresponded as to its anatomical level with the "nuclei insulae cuneati lateralis" of Taber ('61). However, they emphasized that there was no similarity in cell types between these two regions, rather the cells in their "paratrigeminal" nucleus resembled those in the outer parts of pars caudalis of SVN. They also noted that cell strands crossed SVT to interconnect their "paratrigeminal" nucleus with the outer aspects of the pars interpolaris (Vi) and pars caudalis (MDH) subdivisions of SVN. It is important to note the striking similarity in the descriptions provided by these authors for neurons in their "paratrigeminal" nucleus and that provided by Torvik ('56) for neurons in the interstitial portions of SG. It would appear from these descriptions that these two regions may represent homologous regions in opossum and rat, respectively. The only difference is that in the opossum the "paratrigeminal" nucleus extends more laterally and includes large regions wedged between SVT and RB.

In a later study, Rhoton et al. ('66) redefined the term "paratrigeminal" nucleus to refer to a separate small collection of ovoid-shaped neurons in the monkey which are situated dorsal to SVT at the level where the vestibular nerve passes over the dorsal margin of SVT. This use of the term was subsequently adopted by Sobusniak et al. ('72) in the dog. Rhoton et al. ('66) noted that the neurons in this nucleus differed from the scattered vestibular neurons in adjacent

regions in that they were smaller and showed less densely stained chromatin. They further demonstrated a previously unidentified projection of degenerating facial afferents to this area following facial rhizotomy. This pathway was later confirmed using autoradiographic techniques in the monkey (Beckstead and Norgren, '79). Rhoton et al. ('66) suggested that their "paratrigeminal" nucleus may actually be an oral extension of Cul and participate in afferent cerebellar systems. In addition, they noted that this nucleus does not exist in rat or cat.

The term "paratrigeminal" nucleus has subsequently been used in numerous studies in reference to a variety of cell groups related to the trigeminal sensory system (Campbell et al., '74; Chan-Palay, '77a, 78a,b; Somana and Walberg, '79; Panneton and Burton, '85; Mugnaini and Oertel, '85; and Menetrey et al., '87). The term was used by Campbell et al. ('74) to refer to a small group of cells lying between SVT and SCT in the peri-obex region of the rat. These authors distinguished this nucleus from a larger mass of interstitial gray positioned in the dorsal aspect of SVT which they referred to as the "ectotrigeminal" nucleus. They further distinguished a third nucleus lying on the medial side of the "ectotrigeminal" nucleus which they referred to as the "trigeminal plate" nucleus. These three nuclear groups were considered by these authors to represent three separate somatosensory nuclei. However, the authors failed to provide any morphological or functional evidence to support either the parcellation of these three separate nuclear groups or their implications in somatosensory functions. Since these authors do not reference the earlier Oswaldo-Cruz and Rocha-Miranda ('68) study or any other morphological or functional study in this region, the origin of their terminology as well as the basis for their proposed subdivision remains obscure. Nevertheless, the "ectotrigeminal" nucleus of Campbell et al. ('74) clearly occupies a position within SVT similar to those regions previously described as interstitial portions of SG in the rat (Zeman and Innes, '25; Torvik, '56) and as the "promontorium" in the mouse

(Astrom, '56). In addition, Campbell et al.'s "trigeminal plate" nucleus appears to correspond at least in position with the rostralmost extension of SG as illustrated in Figures 1 and 3 (levels 3) of Torviks earlier study ('56). However, the "paratrigeminal" nucleus of Campbell et al. ('74) represents the first report of the presence of a distinguishable group of neurons lying between SVT and SCT in rodents since neither Craigie, Torvik, nor Astrom reported the presence of such a region in any of their studies. The application of the term "paratrigeminal" nucleus to this region in the rat appears to be based on the fact that the cells were present in a position between SVT and SCT in which Oswaldo-Cruz and Rocha-Mirandas' "paratrigeminal" nucleus was reported to lie. However, Campbell et al. do not even reference this latter study. The fact that Campbell et al. ('74) did not provide any cytological description of the neurons in their "paratrigeminal" nucleus prohibits any further comparisons of this region with similar studies in other species.

A few years later, Chan-Palay ('77) introduced the term "paratrigeminal" nucleus as an alternative term to be used in reference to the "nuclei insulae of the lateral cuneate" which according to her represented one of numerous nuclei in the brain exhibiting a rich indoleamine innervation. Although Chan-Palay indicated that this nucleus is situated in the dorsal half of SCT and RB, she did not provide any accompanying descriptions of the precise extent and cytological organization of this nucleus rendering it difficult to determine precisely which region she was referring to in the rat. In two subsequent studies appearing the following year, Chan-Palay (78a,b) provided details of the cytology, synaptic structure and putative neurotransmitter content of her "paratrigeminal" nucleus. In these studies she defines more precisely the extent of the nucleus stating that the term refers to the entire diffuse collection of neurons which lie embedded in the fibers of RB, SVT and SCT. In addition, she extended the use of the term to similar regions existing in monkey and man in addition to those in rat. In the first of her two papers, Chan-

Palay provides a brief review of this region in which she stated that her "paratrigeminal" nucleus corresponds in position with Ramon y Cajals' ('09) "interstitial nucleus", Olszewski and Baxters' ('54) and Tabers' ('66) "insulae nucleus cuneati lateralis", and Oswaldo-Cruz and Rocha-Mirandas' ('68) "paratrigeminal" nucleus. Several points are worth mentioning in regard to this initial literature review. First, although purporting to include all known references concerning this region, it is now obvious that Chan-Palays' background review was quite incomplete. Second, she incorrectly reported that Ramon y Cajal described his "interstitial nucleus" as approaching the superficial surface of the brain, which directly contradicts Ramon y Cajals specific statement that he did not include any cells near the superficial surface of the brain in his "interstitial nucleus". Finally, Chan-Palay assumes an homology between Oswaldo-Cruz and Rocha-Mirandas' "paratrigeminal nucleus", and Olszewski and Baxters' and Tabers' "insulae nuclei cuneati lateralis" without offering any explanation regarding the reported differences in the cytological appearance of these regions. These misleading and incorrect statements by Chan-Palay coupled with the incompleteness of her background review of the literature has caused considerable confusion since subsequent studies relied heavily on her review of this region for their own justification of homologous regions and choice of terminology. Despite these incorrect and misleading statements however, the specific details offered in this study are invaluable since they provide the only morphological descriptions of the cells within this region since that provided by Ramon y Cajal. Although implying that the cells that she illustrates are representative of all cells within her "paratrigeminal" nucleus, it is important to realize that she only illustrates the morphology of those cells located within the dorsal aspect of SVT. In this regard it is interesting to note that the myeloarchitectural photograph that she shows in Figure 1 (Chan-Palay, '78b) appears similar to that shown by Campbell et al. ('74) in Figure 7a. It would appear

from a comparison of the two photographs that Chan-Palay "paratrigeminal" nucleus corresponds in part to the combined area occupied by Campbell et al.s' "paratrigeminal", "ectotrigeminal", and "trigeminal plate" nuclei.

Somana and Walberg ('79) were the first to adopt the term "paratrigeminal" nucleus in the cat. However, these authors used the term to refer to a specific collection of cerebellar projecting neurons situated within the ventral part of RB as well as between RB and SVT. They further indicated that this region in cat may actually represent dislocated aggregations of Cul neurons since both nuclei exhibited similar efferent distribution patterns within the cerebellum and, in fact, were sometimes spatially continuous with each other in the lateral medulla. Although purporting to use the term in the same sense as Chan-Palay, these authors clearly adopted a more restricted use of the term since they exclude those regions lying interstitial to SVT.

Kilduff et al. ('83) indicate the presence of a "paratrigeminal" nucleus intercalated between the fibers of RB and SVT in the ground squirrel. They reported that this nucleus was the only brain structure to significantly increase its relative 2-deoxyglucose uptake during hibernation. In particular, they reported that a zone of increased metabolic activity was present whenever there was neuropil between SVT and SCT and that this active region was contiguous with the marginal layer (lamina I) of MDH suggesting the possibility of a functional homology between these two structures.

In a more recent study in the cat, Panneton and Burton ('85) use the term "paratrigeminal" nucleus to refer to a collection of peribrachial projecting neurons located within interstitial pockets of neuropil in the dorsal part of SVT as well as along the medial edge of SVT at the level of the obex. These authors also purport to use the term in the same manner as Chan-Palay but did not include the cells located

along the lateral margins of SVT or within RB. However, their study is the first to report the projection of interstitial neurons to the peribrachial region in any species.

In a more recent study in the rat, Menetrey et al. ('87) reported the presence of parabrachial projecting neurons in a region which they identify as "paratrigeminal" nucleus in accordance with Chan-Palay's ('78a) definition. However, the authors further distinguish a basal part of PaV which is the rostralmost extension of SG and a dorsal part which forms irregular regions in SVT and between it and RB. The basal part of PaV in this study clearly corresponds with the rostral remnant of SG as defined by Torvik ('56) and the "trigeminal plate" nucleus of Campbell et al. ('74). However, because of the short nature of this report, the remaining borders of PaV, other than its prominent part in the dorsal part of SVT remains unclear.

Mugnaini and Oertel ('85) identify a region situated entirely within the dorsolateral part of RB as the "paratrigeminal" nucleus in the rat. They report that this region exhibits a moderate density of immunocytochemically defined gamma-aminobutyric acid (GABA) containing terminals and that almost 50% of the cells exhibited GABA immunoreactivity.

A number of additional studies, too numerous to list here, have identified a patch of interstitial neuropil in the dorsal part of SVT as the "paratrigeminal" nucleus in accordance with the recently published experimental rat atlas of Paxinos and Watson ('85). In addition, an "ectotrigeminal" nucleus was also recently defined in this rat atlas (Paxinos and Watson, '85) as a region lying between SVT, SCT at its mid dorsoventral extent of the medulla. However, no descriptions of the morphology of these regions is provided. It is unclear why these authors chose to refer to the region as the "ectotrigeminal" nucleus since the term was originally used by Campbell et al. ('79) to refer to the region which Paxinos and Watson identify as the "paratrigeminal" nucleus.

In addition to these numerous studies which apply the term "paratrigeminal" nucleus to the regions in and around SVT, a few recent studies have also used other terminologies in reference to this region. In a study comparable to the Panneton and Burton ('85) in the cat, Cechetto et al. ('85) recently described a dense cluster of parabrachial projecting neurons within the dorsal part of SVT at the level of the obex in the rat. However, these authors chose to adopt Astroms' terminology and referred to this region as the "promontorium" primarily because of what they believed was a possibility of confusion surrounding the use of the term "paratrigeminal" nucleus since it had also been used by Rhoton et al. ('66) to refer to an entirely different population of cells in monkey brainstem. It is interesting to note that Cechetto et al. illustrate a few parabrachial projecting neurons situated in the ventral part of SVT which they apparently did not specifically include in their "promontorium" but which nevertheless represented parabrachial projecting interstitial neurons. In addition, Ciriello et al. ('81a) recently adopted the term "insulae nuclei cuneati lateralis" to refer to neurons lying between SVT and SCT. In an earlier study, Gobel and Purvis ('72) adopted the term "interstitial nucleus of Cajal" or "interstitial nucleus of the SVT" to refer to the entire system of cells in and around SCT, SVT and RB. The latter terminology was also adopted by Shults et al. ('84) in cat and Ishidori et al. ('86) in the dog.

This historical review clearly illustrates that an interstitial system exists within and around SVT in the lateral medulla (i.e., InSy-SVT). In addition, this review suggests that this system contains several morphological distinct regions. The important findings of this review are that there has been no consistent usage of nomenclature when referring to these interstitial regions and that there has been some assumptions made on homologies between various nuclei which may not be entirely accurate. These inconsistencies in nomenclature as well as the erroneous assumptions of homology among different regions in the lateral medulla has been

perpetuated by the lack of any detailed descriptions of the various regions which might aid in comparative studies to identify homologous regions across species.

The Interstitial Regions of the Substantia Gelatinosa

It has long been agreed that SG contributes to the interstitial neurons and neuropil of SVT. The issue however, is whether or not the entire system of interstitial cells throughout the rostrocaudal extent of SVT represent displaced portions of SG. The results of the present study indicate that SG contributions to InSy-SVT in the rat are restricted to levels of SVT caudal to the obex. In particular, the interstitial contributions from SG in the rat are represented by a relatively diffuse collection of scattered cells at MDH levels of the tract and by larger more prominent extensions of neuropil into the dorsal and ventral aspects of SVT in the peri-obex region of the medulla. The combined cyto-, myelo- and chemoarchitectural approach utilized in the present study provides anatomical evidence supporting the existence of a morphological similarity between these interstitial SG regions and SG proper. In addition, this approach has further enabled a finer distinction that allows the identification of specific laminar contributions to this neuropil. These results generally confirm previous reports of the presence of interstitial regions of SG in the rat (Torvik, '56; and Fukishima and Kerr, '79). However, the present study provides the first detailed account of the full extent of the interstitial SG neuropil in this animal. In particular, Torvik ('56) reported that the interstitial region in the dorsal part of SVT was cytologically similar to SG, but he did not include a further distinction between the specific laminar contributions to this neuropil. In addition, Torvik considered the entire interstitial neuropil in dorsal SVT as SG, in contrast to the results of the present study in which the rostral interstitial neuropil has been identified as comprising nuclei distinct from SG (see PaMd, PaV and iV-Cul below). Fukishima and Kerr ('79), on the other hand, only

reported the presence of marginal-like neurons in the dorsal part of SVT at rostral levels of MDH.

Interstitial extensions of SG into SVT, at MDH levels of the medulla, have also been reported in the cat (Hockfield and Gobel, '78; Panneton and Burton, '81; Marfurt, '81; Shigenaga et al., '81, '86) and dog (Ishidori et al., '86). However, the extent of the interstitial contributions from SG at levels caudal to the obex in the rat appears to be less than that observed in these animals. In the cat, for example, the medial border of SVT at MDH levels of the medulla is irregular in outline due to the presence of numerous extensions of SG which form large patches of interstitial neuropil in SVT (Hockfield and Gobel, '78). This situation contrasts sharply with the relatively smooth appearance of the medial border of SVT in the rat and the relatively small number of interstitial cells at this level of SVT. These differences may reflect a heavier reliance on somatosensory processing at this level of SG in higher mammalian species relative to the rat.

In contrast, the presence of relatively large regions of interstitial SG in restricted parts of the dorsal and ventral aspects of SVT in the peri-obex region of the medulla appears to be a feature common to rat (Torvik, '56), cat (Hockfield and Gobel, '78; Panneton and Burton, '81; Marfurt, '81; Shigenaga et al., '81, '86) and dog (Ishidori et al., '86). In fact, the appearance of interstitial regions of SG at this point provides a reliable landmark for the level of the transition between MDH and Vi (see Chapter One). The reason for the appearance of these interstitial regions at this particular level is not yet known. It is possible though that the appearance of the caudal pole of Vi may cause some spatial restrictions in the medulla which simply results in the subsequent pushing of SG neuropil into SVT.

The results of the present study support the presence of spatially separate contributions from laminae I and II to the peri-obex portions of interstitial SG neuropil. A similar distinction between laminae I and II neuropil in ventral and

dorsal interstitial regions of SVT, respectively, has not previously been reported in any species. In an early study in the cat, Kerr ('70b) reported that the interstitial neuropil in SVT at MDH levels of the medulla was ultrastructurally more similar to lamina II than to the marginal layer. However, in a more recent study, Shigenaga et al. ('81, '86) reported that the interstitial regions of neuropil at the peri-obex region of the medulla in the cat were cytologically and myeloarchitecturally similar to lamina I. Ishidori et al. ('86) also reported that ventral interstitial regions of SVT in the dog represent interstitial extensions of lamina I. However, none of these studies have specifically reported the extension of lamina II into any part of SVT. This difference may reflect a true species difference in the specific laminar contributions of SG to InSy-SVT.

The cytochrome oxidase staining pattern reported in the present study supports a similarity in metabolic activity between laminae I and II and the ventral and dorsal interstitial regions of SG, respectively. In addition, it suggests that the ventral region of interstitial SG is metabolically more active than the dorsal interstitial region. These differences in the intensity of cytochrome oxidase staining enabled a clear distinction between these interstitial regions of SG and the PaMd, PaV and iV-Cul nuclei. The application of this technique to other animals may prove useful in determining homologous regions of interstitial SG neuropil across species.

One important issue that has not previously been raised in regard to the existence of these interstitial regions of SG is what impact the spatial isolation of the neuropil in these regions has on the intrinsic circuitry that presumably exists between it and the deeper laminae of MDH. It is known for example that there are extensive interconnections between the superficial laminae and the deeper magnocellular laminae of MDH (Gobel et al., '82; and Gobel and Hockfield, '77). It is not known whether or not these interconnections still exist between the islands of

interstitial SG and the spatially separated deeper parts of MDH. This issue will only be resolved when more detailed studies are conducted on the intrinsic circuitry of these interstitial regions.

Although none of the neurons in the interstitial regions of SG were identified in the present study as cerebellar projecting neurons, the presence of a few thalamic projecting neurons in this region confirms previous studies in the rat (Granum, '86; and Kemplay and Webster, '86). However, these latter studies only illustrated and did not specifically discuss the presence of these interstitial neurons. Unfortunately, the precise locus of termination of these cells in the thalamus cannot be determined in the present study since only large injections of HRP were used in the diencephalon. Comparable groups of retrogradely labeled thalamic projecting neurons have also been reported in the cat (Hockfield and Gobel, '78). In addition, in recent retrograde transport studies in the rat (Menetrey et al., '87; and Cechetto et al., '85) and cat (Panneton and Burton, '85), parabrachial projecting neurons were demonstrated to be present in interstitial regions of SVT which appear to include those areas arising from SG. It is not known however, whether the parabrachial projecting neurons in these regions represent collaterals of the thalamic projecting neurons or whether they form a separate population of neurons in the rat. However, Panneton and Burton ('85) report that these two projections arise from two different populations of cells in the cat. No other efferent projections of neurons in these interstitial regions of SG have been reported in any species.

A number of primary trigeminal afferent inputs have been anatomically demonstrated to terminate in the interstitial SG regions of the tract at rostral levels of MDH. In particular, corneal afferents have been shown to terminate in ventral parts of the tract at this level in the cat (Panneton and Burton, '81; and Marfurt, '81). In addition, this region of SVT has been shown to receive fibers from the infraorbital, lacrimal, frontal, and infratrochlear branches of the trigeminal nerve

(Panneton and Burton, '81). On the other hand, the dorsal group of SG neuropil has been shown to receive dental tooth pulp afferents in the rat (Marfurt and Turner, '84). In addition, the studies cited above also demonstrated that the primary trigeminal afferent input to interstitial regions of SG are contiguous with that to regions of SG proper. The reception of tooth pulp and corneal afferent fibers, both of which are primarily concerned with the transmission of nociceptive impulses, suggests the involvement of these interstitial SG regions in medullary pain processing mechanisms. In this regard, recent immunocytochemical studies have reported that fibers containing substance P (SP), a putative neurotransmitter peptide long known to be associated primarily with pain processing pathways, are distributed to these interstitial regions and to contiguous regions of SG proper (Drew et al., '86; and South and Ritter, '86).

In addition to the primary trigeminal inputs to this region, a descending cortical input originating in the primary somatosensory cortex has also been reported to terminate in the ventral interstitial region of SVT at the peri-obex level of the medulla in the cat (Dunn and Tolbert, '82). It is interesting to note that cortical afferents have not been reported to terminate in any of the more rostrally situated interstitial regions of SVT which are considered in the present study to represent nuclei separate from SG. The absence of any cortical input to these more rostral regions lends further support to the functional distinction of these nuclei from interstitial regions of SG.

There has as yet been no specific electrophysiological analysis of cells located in the larger dorsal and ventral interstitial regions of SG neuropil in the rat. However, some of the electrophysiological studies which focused on cells in the dorsolateral part of SVT at the MDH level of the medulla may have included these areas in their recording sites (Craig and Burton, '81; Burton et al., '81; Hubbard and Hellon, '80; and Salt et al., '83). These studies have generally reported that

interstitial neurons in these regions primarily represent cells with small receptive fields that respond to either noxious and non-noxious stimuli or cells that respond only to noxious stimuli.

The role of these interstitial regions of SG is not entirely clear at this time. However, the afferent and efferent connectivity of these regions coupled with the immunocytochemical detection of SP in this region implicates these interstitial extensions of SG in the processing and relay of nociceptive impulses from trigeminal receptive fields to the thalamus and parabrachial regions in the rat. This overall function is congruent with the origin of these areas from the superficial lamina of SG proper.

The Dorsal Paramarginal Nucleus

The presence of thalamic projecting neurons in the interstitial region of SVT identified here as PaMd has previously been demonstrated in the rat (Fukishima and Kerr, '79; Granum, '86; and Kemplay and Webster, '85). In addition, comparable regions of thalamic projecting neurons have also been reported in the cat (Craig and Burton, '81; and Burton et al., '81), and monkey (Albe-Fessard et al., '75). These interstitial thalamic projecting neurons have generally been considered to simply represent displaced neurons of the marginal layer of MDH. In fact, the overall morphology of Golgi impregnated PaMd neurons revealed in the present study coupled with their projection to the thalamus supports at least a partial structural and functional similarity between PaMd and the marginal layer of MDH. However, the results of the present study further suggest that this region should be considered a separate and distinct nucleus in the lateral medulla. This conclusion is based on several factors. First, in Nissl stained preparations these cells stand out quite distinctly since they are slightly larger in size and more intensely stained than any of the neurons in the marginal layer proper. Second, the cells in this region are prominently clustered into groups of four or more cells within SVT which contrasts

sharply with the widely separated typically linear arrangement of marginal cells in MDH. Third, the cells in PaMd exhibit a distinct soma-dendritic "pseudo-golgi" like staining in cytochrome oxidase stained preparations which is not present in any of the neurons in lamina I. This latter difference suggests that PaMd neurons may be functionally more active compared to other marginal neurons. In fact, the more intense Nissl staining appearance of these cells may indicate a greater amount of Nissl substance reflecting their higher metabolic activity compared to other marginal cells. These differences coupled with the unique position of this group of "marginal" neurons in SVT suggests that it may represent a specialized interstitial region of lamina I in the rat. The name proposed in the present study to refer to this region reflects the similarity to and spatial relationship of this group of neurons with the marginal layer of MDH.

In a recent study, numerous parabrachial projecting neurons were demonstrated in the dorsolateral aspect of SVT in regions which may encompass PaMd in the rat (Cechetto et al., '85; and Menetrey et al., '87). The population of small-sized neurons in PaMd which remained unlabeled following thalamic injections of HRP in the present study may, in fact, represent these parabrachial projecting neurons. It is also possible though that the axonal projection of PaMd neurons to the thalamus may collateralize to the parabrachial region. In the cat however, thalamic and parabrachial projecting interstitial neurons have recently been shown to represent spatially separate populations of cells (Panneton and Burton, '81).

Sources of afferent inputs to PaMd are not easily determined from the literature since previous studies have not generally differentiated this nucleus from other interstitial regions of SVT. The region occupied by PaMd has been reported to receive an input from the trigeminal nerve in the rat (Salt et al., '83). In particular, electrophysiological analysis of neurons in this region indicates that they

represent wide dynamic range, polymodal, temperature sensitive, noxious and non-noxious cells which respond to stimulation of trigeminal receptive fields. In addition, Contreras et al. ('82) illustrate the presence of primary afferent fibers in the region occupied by PaMd following lesions of the facial nerve in the rat. However, it is not known whether these fibers contact cells in this region or whether they simply represent fibers of passage.

Recent immunocytochemical studies demonstrate the presence of several different putative neurotransmitters in the region occupied by PaMd (Yamazoe et al., '84; and Fallon and Leslie, '86). In particular, SP, enkephalin, cholicystokinin, and avian pancreatic polypeptide immunoreactive fibers have been illustrated to terminate in the dorsal part of SVT. The source of these putative neurotransmitters is not known. In addition, the region occupied by PaMd contained some enkephalinergic and avian pancreatic polypeptide immunoreactive neurons, but it lacked any of the neurotensin or SP immunoreactive neurons which populate neighboring regions of SG. The presence of SP and enkephalin fibers coupled with the identification of nociceptive neurons in this region of the lateral medulla supports an involvement of PaMd in medullary pain processing mechanisms. However, the precise role of PaMd in somatosensory processing remains to be determined.

The Trigeminal Extension of the Parvocellular Reticular Formation

An extension of the parvocellular reticular formation into SVT has not previously been recognized in any species. However, the presence of thalamic projecting neurons in the ventral aspect of rat SVT has previously been illustrated but not discussed by Granum ('86). The specific thalamic nuclei which are the targets of V-Rpc cells cannot be determined from either study since large injections were utilized in order to maximize the retrograde labeling of thalamic projecting

cells. A comparable group of thalamic projecting neurons has not yet been identified in any other species.

The pattern of cytochrome oxidase staining reported in the present study reveals a clear continuity between the neuropil of V-Rpc and that of the parvocellular reticular formation. In addition, the similarity in the intensity of these two regions suggests a relatively similar level of metabolic activity. In fact, it is the relative intensity of cytochrome oxidase staining coupled with the presence of thalamic projecting neurons which distinguishes this region from other interstitial components of InSy-SVT.

The afferent inputs to V-Rpc remain unknown. It is not known, for example, whether V-Rpc receives a direct primary trigeminal afferent input. The position of V-Rpc in the ventromedial aspect of SVT indicates that if it does, then it would most likely receive inputs from ophthalmic areas of the trigeminal nerve since these fibers travel in this region of SVT. In this regard, it has not yet been determined whether the corneal afferents that terminate in the ventral part of SVT might possibly contact the thalamic projecting neurons of V-Rpc. The answer to this question must await the use of a combined anterograde and retrograde labeling study.

In a recent study describing the distribution of immunoreactive SP fibers in SVN, a dense amount of SP immunoreactive fibers were detected in the interstitial regions of SVT near V-Rpc (Drew et al., '86). In addition, this labeling extended into the parvocellular reticular formation. It has not yet been determined whether V-Rpc lies within this region of SP immunoreactive terminals. The presence of SP fibers in this region coupled with the thalamic projection of these cells would indicate that this nucleus may represent another medullary center for the relay of nociceptive impulses to the thalamus. Since the afferent and efferent connections of V-Rpc have not yet been fully determined and no electrophysiological studies have

yet been conducted on V-Rpc cells in any species, the functional role of this lateral medullary nucleus remains unknown.

The Paratrigeminal Nucleus

The region identified in the present study as PaV corresponds in position to the "promontorium' of Astrom ('56) and Cechetto et al. ('84) in the mouse and rat respectively, and the "ectotrigeminal nucleus" of Campbell et al. ('74), and "paratrigeminal nucleus" of Paxinos and Watson ('85) in the rat. The combined cyto-, myelo-, and chemoarchitectural as well as Golgi impregnation descriptions of PaV provided in the present study represent the first such detailed analysis of this nucleus in any species. The interstitial region of SVT occupied by PaV has long been believed to simply represent a dorsolateral extension of SG. In fact, a morphological similarity between this region and SG in the rat was first recognized by Torvik ('56) in Nissl stained sections. However, the structural features of PaV revealed in the present study suggests that this region represents a nucleus which should be regarded as distinct from SG proper. In particular, the cells of PaV are larger in their overall size compared to SG cells and the neuropil is more coarser in appearance than the gelatinous SG neuropil. This coarseness is primarily due to the many relatively thick dendrites of PaV neurons which permeate the neuropil. In addition, the cytochrome oxidase staining pattern of this region indicates a higher metabolic activity in PaV relative to lamina II. Finally, the morphology of PaV neurons as revealed by Golgi impregnation is distinctly different from the morphology of cells which populate either laminae I or II (Gobel, '78a,b; and Gobel et al., '80).

The soma-dendritic morphology of Golgi impregnated PaV neurons has previously been reported in the rat (Chan-Palay, '78a). Although Chan-Palays' "paratrigeminal" nucleus included cells outside of the region defined in the present study as PaV (see Historical review above), the cells that she illustrates clearly lie in

the region of PaV. However, Chan-Palay provides only a cursory description of PaV neurons stating that they generally exhibit a fusiform-shaped cell body with long primary dendrites that emerge from the poles of the soma and do not branch more than once or twice. She further states that the cells for the most part are aspiny, although some of the smaller cells may be spiny in appearance. It would appear from her brief descriptions and her schematic diagram that Chan-Palay was primarily referring to the Type I neurons identified in the present study. It is possible that her small spiny neurons may represent Type II neurons. However, Chan-Palay does not distinguish separate cell types in her "paratrigeminal" nucleus and does not provide enough detailed descriptions of the soma-dendritic morphologies of these cells to allow detailed comparisons with the cell types described in the present study.

The observations in the present study, in conjunction with those of Chan-Palay ('78), illustrate that the soma-dendritic tree of the vast majority of PaV neurons is morphologically different than that reported for cells in either lamina I or lamina II (Gobel, '78a,b; and Gobel et al., '80). However, it must be mentioned that some Type II neurons bear a striking resemblance to stalk cells located in lamina II (Gobel, '78b). In addition, these two studies demonstrate that none of the neurons in PaV are Golgi Type II interneurons. Since interneurons form an integral part of the morphological substrate for somatosensory processing in lamina II (Gobel, '78b), their absence in PaV supports the notion that this region is not entirely structurally or functionally similar to lamina II. The absence of interneurons in PaV further indicates that all of the neurons in this region represent projection neurons. The results of the present study provide no indication whether or not the different cell types in PaV may represent functionally distinct neurons.

One of the most intriguing aspects of the structural organization of PaV was the presence of dendritic bundles which were especially prominent in the band

region of the nucleus. Dendritic bundling has been reported to be a feature common throughout many regions of the CNS (for complete review see Roney, Scheibel, and Shaw, '79). The generalized distribution of dendritic bundles in the CNS suggests that this structural feature must serve an important role in brain function. It has been proposed that this structural phenomenon may function as a basic electrophysiological processing unit, a mechanism for synchronization of cell activities, or as a structure involved in developmental or metabolic maintenance activities (Roney et al., '79). It is not known whether any of these functions may be subserved by the dendritic bundling which characterizes PaV.

The retrograde axonal transport experiments in the present study reveal that none of the cells in PaV project to either thalamus or cerebellum in contrast to many such projections from cells in neighboring components of InSy-SVT (eg., see PaMd, V-Rpc and iV-Cul nuclei). However, a recent study has shown that there are a large number of parabrachial projecting neurons in PaV in the rat (Cechetto et al., '85; and Menetrey et al., '87), and cat (Panneton and Burton, '85). These studies report that the parabrachial projecting neurons are distributed in a continuous band of cells connecting PaV regions of SVT and the more caudal levels of SG proper. This fact has contributed to the belief that PaV simply represents an interstitial extension of SG. In addition, PaV cells have been reported to project to the solitary, lateral reticular, and reticular formation nuclei in the rat (Menetrey et al., '87). The projection of PaV to the parabrachial region and solitary nuclei suggests that this nucleus may be involved in autonomic functions since these areas mediate the relay of cardiopulmonary afferents to the forebrain (for review see Smith and deVito, '84).

An input to PaV from the glossopharyngeal and vagal nerves was first reported by Torvik ('56) and Astrom ('56) in the rat and mouse, respectively. This projection has since been confirmed in the rat (Contreras et al., '82), cat (Panneton

and Loewy, '80; Arvidsson and Thomander, '84; and Nomura and Mizuno, '82) and monkey (Beckstead and Norgren, '79). None of the other components of InSy-SVT have been reported to receive any input from primary glossopharyngeal or vagal fibers. In an early study in the rat, Rustioni et al. ('71) reported that the region occupied by PaV does not appear to receive any primary trigeminal inputs as revealed by the lack of changes in the histochemical detection of acid phosphatase activity following sectioning of specific branches of the trigeminal nerve. However, an additional source of afferent fibers to PaV may arise from the dorsal column nuclei since a contralateral input has been reported by Massopust et al. ('85) to terminate in the vicinity of PaV in the rat. In this latter study however, it must be noted that the authors mislabel PaV as the "parabrachial" nucleus. No other source of afferent fibers to this region have yet been identified.

Immunocytochemical studies indicate that PaV receives a prominent input from monoamine fibers (Chan-Palay, '78b). Numerous studies have also reported the presence of SP immunoreactive fibers in PAV (Shults et al., '84, Ljundahl et al., '78; Chan-Palay, '78a,b; Jancso and Kiraly, '80; Sakanaka et al. '82; and Yamazoe et al., '84). In addition, enkephalin immunoreactive fibers have been demonstrated in the region occupied by PaV (Fallon and Leslie, '86). The source of these various putative neurotransmitters has not yet been identified. Furthermore, SP and somatostatin containing neurons have been reported in the region occupied by PaV (Chan-Palay, '78a; and Finley et al., '81). These studies clearly indicate that PaV is a region exhibiting a heterogeneity of putative neurotransmitter containing fibers and cells, a fact which reflects the complex role that this nucleus must play in somatosensory processing.

The PaV nucleus has been briefly examined at the ultrastructural level in the monkey (Chan-Palay, '78a,b). In that study, the neuropil in PaV was described as complex consisting of a heterogeneous population of axon terminals which display a

variety of different morphologies in which dense-core vesicle containing terminals predominate. The axon terminals were reported to form axo-dendritic, axo-spinous, axo-somatic and axo-axonic synaptic relationships. Our unpublished observations of PaV at the ultrastructural level in the rat confirm the heterogeneous nature of bouton terminals, the predominance of dense-core vesicle containing terminals, and the heterogeneity of synaptic relationships. In addition, PaV in the rat is characterized by the presence of numerous complex synaptic glomeruli. Chan-Palay ('78b) further identified the serotonin, noradrenalin, and SP fibers in PaV at the ultrastructural level. In particular, she reported the existence of a heterogeneous population of synaptic and non-synaptic serotonergic and noradrenergic fibers. A similar heterogeneity of serotonergic fiber terminals has also been reported to be present in SG (Ruda and Gobel, '80).

No electrophysiological analysis has yet been performed on PaV cells in any species. However, it is interesting to note that the nucleus represents the only region in the brain to exhibit changes in its glucose utilization during hibernation in ground squirrels (Kilduff et al., '82, '83, '84). This fact indicates that this nucleus must play an important role in the hibernation process. It has been suggested that this nucleus may function in the regulation of autonomic activity through the monitoring of peri-oral temperature (Menetrey et al., '87; and Cechetto et al., '85). The precise role of this nucleus in non-hibernating animals such as the rat has yet to be determined. Nevertheless, its involvement in autonomic function is clearly supported by its relay of primary glossopharyngeal and vagal inputs to the parabrachial and solitary nuclei. In addition, its receipt of SP and enkephalin fibers and the presence of SP neurons in the nucleus may also implicate it in medullary pain processing mechanisms.

The Insular Trigeminal-Cuneatus Lateralis Nucleus

The region identified in the present study as iV-Cul corresponds in position to the "paratrigeminal nucleus" of Campbell et al. ('74) and the "ectotrigeminal

nucleus" of Paxinos and Watson ('85) in the rat. Homologously similar regions in other mammals include the "nuclei insuli cuneati lateralis" in man and other primates (Olszewski and Baxter, '54; and Gerhardt and Olszewski, '69), the "trigeminocuneatus lateralis nucleus" in man (Ziehen, '13), and the "paratrigeminal nucleus " in the cat (Somana and Walberg, '79). The choice in terminology used in the present study was based on several factors. First, the terminology previously used in the rat to refer to this region was unacceptable. In particular, the use of the term "paratrigeminal" nucleus by Campbell et al. ('74) to refer to this nucleus is inconsistent with the original definition of that term as introduced by Oswaldo-Cruz and Rocha-Miranda ('65) in the oppossum and later adopted in other animals to refer to a group of pale stained neurons located in and around SVT (see Historical Review above). The results of the present study clearly indicate that iV-Cul neurons are one of the most intensely Nissl stained group of neurons in the lateral medulla. In addition, the term "ectotrigeminal" nucleus as used by Paxinos and Watson ('85) is also unacceptable since the term was originally proposed by Campbell et al. ('74) to be used in reference to what is identified in the present study and by Paxinos and Watson ('85) as the "paratrigeminal" nucleus. Second, the term "nuclei insulae cuneati laterali" was first reported by Olszewski and Baxter ('54) and Gerhardt and Olszewski ('69) to refer to a group of intensely stained neurons located in an homologous region of lateral medulla in man and other primates. In addition, the term "trigeminocuneatus lateralis" was earlier introduced by Ziehen ('13) to refer to a similar group of neurons in man. In the present study, the name "insular trigeminal-cuneatus lateralis" was chosen to refer to the homologous region in the rat in order to reflect the use of both of these latter terms in higher species as well as the spatial and functional relationship between this nucleus and Cul and SVN nuclei.

In the past, this group of neurons in the lateral medulla has generally been regarded as merely displaced cells of neighboring nuclei (ie., Cul, SVN, and LR; see Historical Review). However, the present study represents the first to provide a detailed description of the morphology of this region in any species. The results of the present study suggest that this nucleus represents a separate somatosensory nucleus in the lateral medulla. In this regard, a correlative electron microscopic analysis of iV-Cul in the rat provides ultrastructural evidence supporting the contention that this region represents a distinct and separate nucleus in the lateral medulla (Phelan and Falls, '86; see also Chapter Five).

The Golgi impregnation of neurons in iV-Cul illustrate that the morphology of these neurons is different from any other component of InSy-SVT or SG proper. In addition, since none of the neurons in iV-Cul are Golgi Type II interneurons, the cells in this nucleus must all represent projection neurons. The retrograde transport experiments in the present study confirm this, since every neuron in the nucleus was demonstrated to project to the cerebellum. This fact indicates that iV-Cul represents a previously unrecognized precerebellar medullary nucleus. In a previous study, cerebellar projecting neurons were illustrated but not discussed to lie in the region occupied by iV-Cul in the rat (Watson and Switzer, '78). However, in a more recent study the existence of cerebellar projecting neurons in this region of the rat was specifically denied (Menetrey et al., '87). On the other hand, the presence of similar accumulations of cerebellar projecting neurons in this region of the lateral medulla has been reported in the cat (Somana and Walberg, '79; and Matsushita et al., '82) and sheep (Saigal et al., '80). While Somana and Walberg ('79) identified this group of neurons as the "paratrigeminal" nucleus, neither Matsushita et al. ('82) nor Saigal et al. ('80) specifically recognized these interstitial cerebellar neurons as a distinct nucleus. The results of the present study do not indicate which part of the cerebellum is the target site of iV-Cul neurons since large injections were used in

order to maximally label medullary cerebellar projecting neurons. This latter fact is what probably accounts for the presence of such cells in this study and their absence in a previous study of rat medulla (Menetrey et al., '87). However, in a comparable study in the cat, Somana and Walberg ('79) reported a similar distribution of cells which projected to cerebellar lobules I, II, V, VIIIB and IX, and the paramedian lobule. We have also observed retrograde labeling of iV-Cul neurons in the rat following smaller injections of HRP into some of these regions of the cerebellum (unpublished observations).

The iV-Cul nucleus can be distinguished from neighboring somatosensory nuclei by the presence of a spinal input. In a recent study of the spinotrigeminal pathway in the rat, it was revealed that spinobulbar fibers, which originate in the upper cervical spinal cord and terminate in the border region of Vi (brVi), also extend into iV-Cul (Phelan and Falls, '85; see also Chapter Three). Neighboring regions of InSy-SVT do not receive a similar spinal input. It is interesting to note that the present study documents that some of the cells in iV-Cul extend into the territory of brVi. This region of Vi has also been demonstrated to contain a large population of cerebellar projecting neurons (see Chapter Four). The significance of the intimate spatial relationship and similarity of projection between iV-Cul and brVi neurons remains to be determined. An electron microscopic analysis of the spinal afferents to iV-Cul indicate that they represent a central input to synaptic glomeruli in iV-Cul and that they establish asymmetrical synaptic contacts with iV-Cul dendrites (Phelan and Falls, '86; see also Chapter Five). In addition, the ultrastructural morphology of these spinal inputs suggests that they may be providing an excitatory synaptic input to iV-Cul neurons.

Sources of afferent inputs to iV-Cul other than those arising from the spinal cord have not yet been established. A few primary trigeminal fibers are present in iV-Cul following injections of HRP into the trigeminal root (unpublished

observations). However, it is not known whether these fibers actually establish synaptic contact with iV-Cul neurons or whether they represent fibers of passage.

The iV-Cul nucleus can be histochemically distinguished from adjoining areas by its intense staining for acetylcholinesterase (Paxinos and Watson, '85; and Butcher and Woolf, '84). The absence of immunocytochemical staining of neurons in this region, using antibodies to the more specific cholinergic marker choline acetyltransferase (Kimura, McGeer and Peng, '84), suggests that iV-Cul receives an extrinsic cholinergic input. It has previously been demonstrated that cholinergic neurons are present in the spinal cord (Phelps et al., '84; Satoh et al., '83; and Kimura et al., '84). It is possible therefore that the spinal input to iV-Cul may represent a source of acetylcholine to this nucleus.

The putative neurotransmitter content of iV-Cul neurons is not known since the nucleus has only recently been recognized as a distinct nucleus and many of the immunocytochemical studies to date have not specifically reported the distribution of identified neurotransmitter containing neurons in this region of the lateral medulla. However, in a recent immunocytochemical study describing the distribution of 4-aminobutyrate:2-oxoglutarate transaminase (GABA-T) intensive neurons in the rat hindbrain (Nagai, Maeda, Imai, McGeer and McGeer, '85), GABA-T intensive neurons were schematically illustrated in a region which may correspond to iV-Cul. In another study, glutamic acid decarboxylase (GAD) positive cell bodies were also illustrated in a similar region of the lateral medulla (Mugnaini and Oertel, '85). The presence of GABA-T (the enzyme which catabolizes the inhibitory transmitter GABA) and GAD (the enzyme responsible for the synthesis of GABA through the decarboxylation of glutamic acid) have proven to be reliable endogenous markers for GABAergic neurons in the CNS. The immunocytochemical detection of these two enzymes in neurons in or near iV-Cul raises the possibility that some of the neurons in this nucleus may represent GABAergic medullary

neurons. The presence and extent of GABAergic neurons in iV-Cul is an important point worthy of future study since it would suggest that some part of the iV-Cul projection to the cerebellum may have a GABA mediated "inhibitory" influence over the activity of cerebellar neurons.

In an earlier investigation of the distribution of immunocytochemically identified SP containing neurons in interstitial parts of SVT, Chan-Palay ('78b) reported that up to 30% of the interstitial neurons contained SP. Since Chan-Palay did not distinguish between iV-Cul and PaV it is not clear whether or not neurons in iV-Cul themselves represent SP containing cells. Nevertheless, a moderately dense amount of SP immunoreactive fibers was also reported by Chan-Palay ('78a) in the region occupied by iV-Cul. This was later confirmed in the rat by Yamazoe et al. ('84). This latter study also demonstrated enkephalin immunoreactive fibers in iV-Cul. The presence of SP and enkephalin fibers in iV-Cul might indicate the involvement of this nucleus in medullary nociceptive pathways since these putative neurotransmitters have long been associated with pain processing pathways in the brainstem.

No electrophysiological analysis have yet been performed on iV-Cul neurons in any species. Therefore, the precise role of this nucleus in somatosensory processing in the medulla is not known at this time. Nonetheless, the presence of a prominent spinal afferent input and the projection of all iV-Cul neurons to the cerebellum indicates that this nucleus represents a previously unrecognized precerebellar medullary spinal relay nucleus. The distinction of this nucleus from other precerebellar medullary relay nuclei, such as Cul or LR, is based on several factors. First, the Nissl staining characteristics of cells in iV-Cul is different from any of these other nuclei in their size, shape and intensity of staining. Second, the region receives a spinal input which does not project to these other nuclei (Phelan and Falls, '85; see also Chapter Three). Third, it exhibits a strong acetylcholinesterase

activity which is not seen in either LR or Cul. Fourth, the ultrastructural organization of the nucleus is distinctly different from any of these nuclei (Phelan and Falls, '86; see also Chapter Five). These factors together suggest that this nucleus should be considered a distinct precerebellar medullary nucleus.

Summary and Conclusions

The results of the present study demonstrate that InSy-SVT is composed of several morphologically and functionally distinct regions. The present study thus confirms the heterogeneity of interstitial neurons in SVT as previously reported in the cat (Panneton and Burton, '85). However, the present study provides far more detailed descriptions of each of these regions than has previously been available. Although it has long been held that these regions may represent dislocated cells of SG, the results of the present study in conjunction with previous studies provides clear evidence supporting the distinction of four spatially separate nuclei which do not represent simple extensions of SG into SVT. These four nuclei appear to subserve a number of different functions in the lateral medulla as revealed by differences in their afferent and efferent projections. In fact, the variety of functions ascribed to InSy-SVT in the past can be easily explained by the presence of these various nuclei. Further studies on the electrophysiology, pharmacology and connectivity of each of these regions is clearly needed in order to fully understand the role of these interstitial regions in somatosensory processing in the lateral medulla.

The present study utilized differences in the levels of cytochrome oxidase staining to support the distinction of the individual nuclei in InSy-SVT. In the last ten years, the histochemical demonstration of cytochrome oxidase, a mitochondrial enzyme essential for oxidative phosphorylation, has proven to be a useful anatomical marker in assessing the relative metabolic activity of regions within the CNS (Wong-Riley, '76, '79; Wong-Riley, Merzenich, and Leake, '78; Wong-Riley et

al., '81; Wong-Riley and Carrol, '84; Wong-Riley and Kageyama, '86; and Kageyama and Wong-Riley, '87). These studies have firmly established a close correlation between the level of enzymatic activity and the functional state of neurons. In addition, these studies indicate that high levels of cytochrome oxidase reactivity are correlated with intense localized convergence and/or pathway specific excitatory synaptic inputs. The histochemical demonstration of cytochrome oxidase activity was also reported in these studies to be sensitive to altered states of neuronal activity in developing and mature sensory systems in mammals. In particular, impulse blockade and deafferentation have been shown to cause a decrease in the level of cytochrome oxidase activity in the affected postsynaptic neurons along the entire sensory chain (Wong-Riley, '79; Wong-Riley and Riley, '83). In the highly ordered trigeminal sensory system, the histochemical demonstration of cytochrome oxidase activity has reliably been used to examine functional changes in the organization of the vibrissae related inputs to the SVN, thalamus and somatosensory cortex (Nomura and Mizuno, '86; Nomura et al., '86; and Wong-Riley and Welt, '80). In fact, this anatomical marker correlates well with cytoarchitectural patterns in rat SVN (Ma and Woolsey, '84). The present study reveals the existence of different levels of cytochrome oxidase activity throughout InSy-SVT which supports the non-homogeneity of this system. The results of the present study also indicate that the cytochrome oxidase delineated boundaries of individual components of InSy-SVT precisely parallels those boundaries defined by differences in the cyto- and myeloarchitecture and connectivity of the nuclei. This fact suggests that it may be advantageous to apply this technique to the lateral medulla of other mammals in order to define the boundaries of homologous regions of InSy-SVT.

Finally, it is interesting to note that a rather conspicuous interstitial nucleus has been identified in those snakes possessing sensory pit organs (Molenaar, '74, '77, '78a; and Schroeder and Loop, '76). This nucleus, referred to as the "nucleus of the

lateral descending tract", is the sole target for primary trigeminal fibers transmitting infrared sensory information from the pit organs to the trigeminal complex (Molenaar, '78b). It appears that this nucleus represents a highly specialized region of the trigeminal somatosensory system in snakes (Gruberg et al., '79). It is not clear whether this nucleus is specifically analogous to any of the components of InSy-SVT reported in the present study. Perhaps a more detailed description of the morphological organization of this nucleus might provide some indication as to which, if any, of the various nuclei in InSy-SVT this nucleus represents. Nevertheless, the presence of this important sensory processing nucleus in an interstitial location in the lateral medulla of the snake illustrates how significant other interstitial nuclei may be in the processing of somatosensory information in other animals, and points out the need for a more complete understanding of this complex region across species.

CHAPTER THREE

A COMPARISON OF THE DISTRIBUTION AND MORPHOLOGY OF THALAMIC, CEREBELLAR AND SPINAL PROJECTING NEURONS IN RAT TRIGEMINAL NUCLEUS INTERPOLARIS

INTRODUCTION

Numerous axonal transport studies conducted during the last decade have revealed that the efferent projections of trigeminal nucleus interpolaris (Vi) are directed towards a number of different targets along the neuraxis, including the thalamus (Cheek, Rustioni, and Trevino, '75; Basbaum, Giesler, and Menetrey, '77; Kruger, Saporta, and Feldman, '77; Karamanlidis, Michaloudi, Mangana, and Saigal, '78; Fukishima and Kerr, '79; Burton and Craig, '79; Feldman and Kruger, '80; Berkley, Blomquist, Pelt, and Fink, '80; Erzurumlu and Killackey, '80; Erzurumlu, Bates, and Killackey, '80; Stritzel, RoBards, and Richardson, '80; Kruger and Young, '81; Matsushita, Ikeda, and Okado, '82; Hill, Morris, and Salt, '82; Shigenaga, Nakatani, Nishimori, Suemune, Kuroda, and Matano, '83; Pearson and Garfunkel, '83; Somers and Panneton, '84; Peschanski, '84; Silverman and Kruger, '85; Roger and Cadusseau, '85; Shammah-Lagnado, Negrao, and Ricardo, '85; and Kemplay and Webster, '86), superior colliculus (Edwards et al., '79; Berkley et al., '80; Bull and Berkley, '80; Stritzel et al., '80; Killackey and Erzurumlu, 81; Huerta, Frankfurter, and Harting, '83; and Silverman and Kruger, '85), inferior colliculus (RoBards, '79; and Stritzel et al., '80), cerebellum (Cheek et al., '75; Eller and Chan-Palay, '76; Faull, '77; Steindler, '77; Watson and Switzer, '78; Ikeda, '79; Saigal, Karamanlidis, Voogd, Mangana, and Michaloudi, '80; Somana, Kotchabhakdi, and

Walberg, '80; Gould, '80; Matsushita et al., '82; Patrick and Haines, '82; Huerta et al., '83; Somers and Panneton, '84; and Silverman and Kruger, '85), parabrachial region (Ikeda, Tanami, and Matsushita, '84; Panneton and Burton, '85; and Cechetto, Standaert, and Saper, '85), pontine nuclei (Swensson, Kosinski, and Castro, '84), reticular formation (Shammah-Lagnado, Ricardo, Sakamoto, and Negrao, '83; and Ross, Ruggiero, and Reis, '85), facial motor nucleus (Senba and Tohyama, '83; Panneton and Martin, '83; Hinrichsen and Watson, '83; and Erzurumlu and Killackey, '79), inferior olive (Boeston and Voogd, '75; Brown, Chan-Palay, and Palay, '77; Feldman and Kruger, '80; Walberg, '82; Huerta et al., '83, and Huerta, Hashikawa, Gayoso, and Harting, '85), and spinal cord (Crutcher, Humbertson and Martin, '78; Craig, '78; Matsushita, Okado, Ikeda, and Hosoya, '80, '81; Matsushita et al., '82; Ruggiero, Ross, and Reis, '81; Cabana and Martin, '84; and Leong, Shieh, and Wong, '84a,b); as well as various intranuclear sites within the spinal V nucleus (SVN) (Kruger et al., '77; Kruger and Young, '81; Ikeda, Matsushita, and Tanami, '82; Panneton and Burton, '82; Hockfield and Gobel, '82; Lovick and Wolstencraft, '83; Ikeda et al., '84; Somers and Panneton, '84; and Silverman and Kruger, '85).

The presence of these divergent projections coupled with the apparent overlap in the distribution and morphology of specific projection neuron populations within Vi, prompted widespread speculation regarding the possible existence of collateralization among the axonal projections of this nucleus. In this regard, recent anatomical (Stritzel et al., '80; Huerta et al. '83; Somers and Panneton, '84; Patrick and Robinson, '84; Steindler, '85; Silverman and Kruger, '85; and Bruce, McHaffie, and Stein, '84, '85) and electrophysiological (Woolston, LaLonde, and Gibson, '82; Hayashi, Sumino, and Sessle, '84; Jacquin, Woerner, Mooney, and Rhoades, '85; Mantle-St.John and Tracey, '87) studies, designed specifically to test for the presence of axon collaterals, have provided direct

evidence indicating that some Vi neurons possess branched axons directed towards multiple targets. However, there is no clear consensus concerning the precise pattern and extent of divergent axon collaterals in Vi. The greatest controversy surrounds whether or not trigeminothalamic (TT) and trigeminocerebellar (TC) projection neurons represent independent cell populations. Anatomical studies utilizing retrograde double labeling techniques have indicated that up to 80% of TC neurons in rat Vi possess branched axons directed towards the thalamus (Silverman and Kruger, '85; and Patrick and Robinson, '84),whereas similar studies have failed to detect such neurons in mouse (Steindler, '85) and cat (Somers and Panneton, '84). On the other hand, electrophysiological studies employing the antidromic activation technique have demonstrated that less than 1% of TC neurons in rat Vi send axon collaterals to the thalamus (Woolston et al., '82; and Jacquin et al., '85), while almost 13% of TC neurons in cat Vi possess branched axons directed towards the thalamus (Hayashi et al., '84). While some of these differences may be attributed to the differing sensitivities and inherent limitations of the techniques employed (e.g., retrograde transport of flourescent dyes versus antidromic activation techniques), it is also possible that these differences may reflect a species difference in the organization of collateral projections originating from Vi neurons. This latter concept however, has recently been challenged by Silverman and Kruger ('85) based on their belief that existing anatomical double labeling studies, in general, fail to reveal the total population of specific projection neurons due to injection sites which do not encompass the entire area of the intended target nuclei. Therefore, the extent of collateralization between TT and TC pathways remains a matter of debate. Nevertheless, it is clear that Vi does possess a heterogeneous population of projection neurons including some which do exhibit divergent axonal projections.

In view of the heterogeneity of neurons within Vi, the question has been raised whether specific populations of projection neurons can be identified based on

differences in their morphology or distribution within the nucleus. In this regard, Matsushita et al. ('82) recently utilized the retrograde transport of horseradish peroxidase (HRP) to examine and compare the regional distribution and morphology of TT, TC and trigeminospinal (TS) projection neurons throughout cat SVN. They indicate that although TT and TC neurons in Vi cannot be separated on the basis of their somatic size alone, the bulk of these neurons are spatially segregated along the rostrocaudal axis of the nucleus. In particular, TC cells were more concentrated in the rostral half of Vi and TT cells were more numerous in the caudal half of the nucleus with the are in between having some partial overlap of neurons.. In addition, these authors report that TS cells possess relatively larger somata than either TT or TC neurons and are spatially restricted to lateral regions of the nucleus. These differences in the distribution and morphology of TT, TC, and TS neurons results support the findings of the previously mentioned double labeling studies in the cat which failed to detect significant populations of Vi neurons with branched axons directed towards thalamus and cerebellum. In addition, this study further suggests that, based on differences in morphology and distribution, TS neurons in cat Vi may represent a cell population distinct from either TT or TC cell populations. However, this latter point has yet to be examined using anatomical double labeling techniques. A comparably detailed regional analysis of the distribution and morphology of retrogradely labeled TT, TC and TS projection neurons in rat Vi is conspicuously lacking in the literature. This is especially surprising in view of the fact that species differences have been reported in the distribution of specific projection neuron populations in Vi (McHaffie, Bruce, and Stein, '84) and that such information would clarify questions about the extent of collateralization between different projection neuron populations in Vi by providing indications of the extent of overlap in the distribution and morphology of these cell populations. In addition, a detailed examination of the distribution and morphology

of retrogradely labeled neurons in rat Vi would be invaluable since it might enhance our understanding of the comparative functional organization of Vi in mammals.

It has recently been suggested that a strong structure-function-connectivity relationship exists for individual neurons in rat Vi (Jacquin et al., '85). In particular, preliminary evidence based on combined intracellular recording and HRP labeling techniques, suggests that TT and TC cells exhibit distinct somadendritic morphologies in rat Vi and that the receptor field size of individual projection neurons can be correlated with the size of their dendritic fields. In particular, TT cells were reported to have large somata, large dendritic fields and large receptive fields, while TC cells generally have smaller somata, smaller dendritic fields and smaller receptive fields. This structure-function-connectivity hypothesis clearly has strong implications regarding the structural and functional organization of Vi. However, due to the inherent limitations in the degree of population sampling associated with the combined intracellular recording and HRP labeling technique, it is not clear whether this hypothesis holds true for all TT and TC projection neurons in Vi. The fact that this study only describes the presence of large, multipolar thalamic projecting neurons in Vi, even though previous retrograde transport studies observed large as well as small TT cells in the nucleus (Fukishima and Kerr, '79; and Erzurumlu, Bates, and Killackey, '80), certainly raises some concerns about the generality of this hypothesis. Moreover, the recent report of extensive collateralization between TT and TC cell populations in rat Vi (Silverman and Kruger, '85) casts some serious doubts about the validity of this hypothesis. However, since there is as yet no information regarding the distribution or morphology of branched TT and TC neurons in Vi, it remains difficult to interpret the results of this study. It is certainly possible that Jacquin et al. ('85) sampled from regions of Vi in which the TT and TC populations exhibit different morphologies and therefore represent the independent TT and TC cell populations, while the

remaining portions of Vi contain the majority of the collateralized TT and TC neurons. Some information about this latter possibility could easily be obtained through a regional analysis of the distribution and morphology of TT and TC projection neurons in rat Vi.

The need for a detailed analysis of the regional distribution and morphology of specific projection neuron populations in rat Vi gains additional importance considering the fact that several cytoarchitecturally distinct regions have been identified within the nucleus (Phelan and Falls, '84; see also Chapter One). However, it has not yet been determined whether regional differences in the distribution and/or morphology of specific projection neuron populations may provide further support for the presence of these cytoarchitecturally heterogeneous regions. Although two of these regions, the dorsolateral and border regions, have been further substantiated as distinct regions based on their identification as spinal recipient zones in Vi (Phelan and Falls, '84; see also Chapter Four), the distribution of specific Vi projection neuron populations within these regions has not fully been examined. Information regarding the spatial relationship between the termination of spinotrigeminal afferents and the distribution of trigeminal efferent projection neurons would not only provide insights into the functional nature of the spinotrigeminal projection itself, but also enhance our understanding of the regional functional organization of rat Vi.

The present study was designed to examine and compare the regional distribution and morphology of retrogradely labeled TT, TC and TS neurons in rat Vi following large injections of HRP into the respective targets. In particular, the density, distribution and somadendritic morphology of TT, TC and TS neurons were examined and compared throughout the rostrocaudal extent of Vi, using the cytoarchitecturally defined regions proposed in an earlier study (see Chapter One)

as a guide in determining the relative position of these projection neurons within the nucleus.

METHODS

Adult, male Sprague-Dawley rats (200-300 gms.) were used throughout this investigation. Each animal was anesthetized by an intraperitoneal injection of Nembutal (50 mg/kg). Large injections of a fresh 30-60% solution of HRP (Sigma Type VI) dissolved in 2% dimethylsulfoxide were stereotaxically injected using a 26 guage Hamilton syringe. Injections into the diencephalic target sites were positioned according to the coordinates of Paxinos and Watson ('85) while injections into the cerebellum and spinal cord were placed under visual guidance. In 6 animals, single, unilateral injections (0.2-0.3 μl total) were centered within the ventrobasal thalamic complex. In 6 animals, multiple injections (1.0-3.0 μl total) were positioned within various regions of the ipsilateral cerebellar vermis and hemisphere. In 12 animals, single or multiple unilateral injections (0.05-1.0 μl total) were positioned in the upper cervical levels of the spinal cord. Each animal was allowed to survive 1-3 days and then perfused intraaortically, using a Masterflex pump delivery system, with a brief, heparanized physiological saline rinse followed by 500 ml of a fixative consisting of 1% paraformaldehyde and 1% glutaraldehyde in 0.12 M phosphate buffer (pH 7.4). The brains were then immediately removed from the skull, hand blocked into 4-6 mm blocks of tissue in the transverse plane and either postfixed in the same fixative for an additional 1-3 hours or immediately placed in 0.12 M phosphate buffer for 1-24 hours. Serial 50 μm thick sections were then cut on an Oxford Vibratome in the transverse plane and collected in fresh 0.12 M phosphate buffer. Alternate, serial sections were processed for localization of HRP reaction product using tetramethylbenzidine (TMB) histochemistry according to the protocol of Mesulam ('78) and counterstained with 1% neutral red. The remaining sections

were either reacted with TMB or left unreacted and counterstained with either 1% neutral red or 0.5% cresyl-violet.

The full extent of the injection sites were determined by comparison under bright and darkfield illumination. Representative camera lucida drawings of the spread of the HRP within the target sites were made from each case for subsequent comparison. The position of retrogradely labeled neurons within the brainstem were plotted from representative sections throughout the rostrocaudal extent of the nucleus using a drawing tube and a 40X objective in order to preserve relative cell morphology. Retrogradely labeled neurons were identified by their content of HRP granules distributed throughout the somatic and dendritic cytoplasm. Only those profiles exhibiting a distinct nucleus or clearly situated entirely within the section were plotted. Camera lucida drawings of individual retrogradely labeled neurons throughout the rostrocaudal extent of the nucleus were made using a 50X objective. In those cases with long survival times, the course of individual axons, identified on the basis of their uniform diameter, their course within the neuropil and their origin from the soma or proximal dendrite were reconstructed from serial sections whenever possible.

The somatic cross sectional areas of retrogradely labeled neurons were measured using a Bioquant Image Analysis system which computed these areas from tracings of the perimeters of labeled neurons drawn with the aid of a camera lucida using a 40X objective. Retrogradely labeled neurons were sampled throughout the rostrocaudal extent of the nucleus at 100 μm intervals and grouped according to their position within the various cytoarchitecturally defined regions proposed in a previous study (see Chapter One). The neurons included in this sampling were only those which exhibited a nucleus or were clearly situated entirely in the section. These measurements were grouped into block intervals of 25 μm^2 and plotted as frequency histograms for each of the proposed regions (Figure 6B-

G). The total somatic cross-sectional area histograms for a specific projection neuron population (Figure 6A) were compiled from the combined percentages calculated from each separate region within the nucleus. In addition, the maximum and minimum somatic diameters were also measured for each of these cells. The mean and standard deviations were calculated for all pooled sets of data and appropriate statistical tests were applied to these data as necessary.

RESULTS

The present study utilized relatively large injections of HRP, coupled with long post-injection survival times, in order to maximize the number and intensity of retrogradely labeled TT, TC and TS neurons in Vi. This approach resulted in a consistent pattern of retrograde labeling in all cases examined. The density of retrograde labeling in individual neurons as a result of this method facilitated the localization of labeled neurons at low magnification and allowed comparisons of their respective soma-dendritic morphologies. In view of the consistent pattern of labeling obtained in these experiments, the results of only a single representative case, from each of the series of HRP injections into the diencephalon, cerebellum, or cervical spinal cord will be presented below.

The distribution and morphology of retrogradely labeled TT, TC, and TS neurons were compared throughout the rostrocaudal extent of Vi at eight representative levels of the nucleus (Figure 1). The specific regional distribution of labeled neurons was compared at each of these levels in reference to the various cyto- and myeloarchitecturally distinct regions previously defined in Vi (Phelan and Falls, '83; see also Chapter One). A detailed description of the morphological characteristics distinguishing each of these regions has been provided elsewhere (see Chapter One). Briefly, six morphologically distinct regions are present in Vi. The topographical relationship of these regions throughout the rostrocaudal extent

of the nucleus is schematically illustrated in Figure 1. Vi extends from the peri-obex region of the medulla, where it exhibits a spatial overlap with MDH (Levels 1 and 2), to the level of the caudal pole of the facial motor nucleus, where it exhibits a more gradual transition with the various subdivisions of Vo (Levels 7 and 8). The border (brVi) and the dorsolateral (dlVi) regions of Vi are represented by relatively thin bands of cells subjacent to SVT. These regions differ from each other by the size and shape of their constituent neurons. The ventrolateral part of Vi consists of a caudal, parvocellular (vlVipc) and a rostral, magnocellular (vlVimc) region. The latter region contains the largest of the neurons within Vi. Each of these two regions also possess a medial and a lateral segment (not shown). These segments exhibit slight differences in the size and density of their constituent cells. The dorsal cap (dcVi) and intermediate (irVi) regions of Vi together occupy the dorsomedial third of the nucleus. The caudal part of irVi appears cytoarchitecturally similar to vlVipc, while its rostral part more closely resembles dcVi.

In order to facilitate comparisons between the distribution of the retrogradely labeled TT, TC and TS neurons, caudal (Levels 1-4) and rostral (Levels 5-8) halves of Vi will be referred to in the present study. The boundary between these two halves of the nucleus lies at the transition from vlVipc and vlVimc. The division of Vi into two halves is not entirely arbitrary, since there are some distinct differences in the morphological characteristics of the various regions of Vi in the caudal and the rostral half of the nucleus (see Chapter One).

Trigeminothalamic Projection Neurons

The schematic diagram in Figure 2A illustrates the spread of HRP following a single unilateral injection centered in the ventrobasal (VB) complex of the thalamus. The spread of HRP in this representative case covered the entire thalamic complex including the posterior thalamic nuclei, the intralaminar nuclei, the zona incerta, and the medial geniculate body. The spread of HRP also included a small

part of the contralateral thalamus along the midline, as well as parts of the ipsilateral hypothalamus, the ipsilateral subthalamus, and the ipsilateral substantia nigra and entopeduncular nuclei. There was only minimal involvement of the mesencephalic reticular formation. The spread of HRP in this case was typical for all of those cases involving a thalamic injection. In addition, the relative number and distribution of retrogradely labeled neurons was similar in each of these cases.

Several extra-trigeminal medullary nuclei contained retrogradely labeled neurons. These regions included a massive number of labeled cells in the contralateral dorsal column nuclei (i.e., nucleus gracilis, Gr; and nucleus cuneatus, Cun); a moderate number of labeled cells in the contralateral lateral cuneate nucleus (Cul); a few lightly labeled cells in the ipsilateral caudal dorsolateral solitary complex; a small number of labeled cells in the ventrolateral parvocellular reticular formation (pcRF) bilaterally; and a few cells in the ipsilateral vestibular nuclear complex.

The distribution of retrogradely labeled neurons in those regions of SVC, other than Vi, included a massive number of contralaterally located neurons in Vms, a moderate number of neurons in the superficial and deeper layers of contralateral MDH, and a few neurons in the caudal, dorsolateral part of the ipsilateral border zone (BZ) of Vo (Falls, Rice and VanWagner, '85; and Falls, '86). In addition, retrogradely labeled neurons were present in the contralateral dorsal paramarginal nucleus (PaMD) and the trigeminal extension of pcRF (V-Rpc). These latter two nuclei, which are located within the confines of SVT, represent separate components of the interstitial system of SVT (InSy-SVT).

A considerable number of retrogradely labeled TT neurons were present throughout the rostrocaudal extent of contralateral Vi, although the density of neurons decreased at the extreme rostral pole of the nucleus (Level 8). Retrogradely labeled neurons were found in the entire dorsoventral and

mediolateral extent of the nucleus. In addition, all six regions of Vi contained retrogradely labeled neurons. The densest concentration of labeled neurons occurred in the dorsomedial aspect of caudal Vi and in the ventrolateral aspect of rostral Vi.

The distribution, somatic size and relative somadendritic morphology of TT cells in this case is illustrated in Figures 3, 6, and 7. The entire population of retrogradely labeled TT cells exhibited a variety of somatic sizes and shapes. Small (<15 μm in diameter), medium (15-25 μm in diameter), and large (>25 μm in diameter) neurons were retrogradely labeled. The somatic cross sectional areas of these neurons ranged from 25-450 μm^2 (Figure 6A). The small, medium, and large-sized neurons exhibited somatic cross sectional areas of <150 μm^2, 150-300 μm^2, and >300 μm^2, respectively. The vast majority of the retrogradely labeled neurons consisted of those neurons in the small to medium-sized range. The somatic cross sectional areas of neurons varied within specific regions of Vi (Figure 6B-G). The mean and standard deviation for these regions were (μm^2): brVi (142,88), dlVi (169,69), vlVipc (123,55), vlVimc (238,825), dcVi (152,54) and irVi (128,43). Each of the six regions of Vi contained small-sized retrogradely labeled neurons. However, although these cells formed the predominant cell type in brVi, vlVipc, and irVi; the medium cells predominated in dlVi, dcVi, and vlVimc.

A variety of different types of retrogradely labeled TT neurons could be distinguished on the basis of the combination of their somatic size and shape. These included small-sized oval and polygonal-shaped neurons, medium-sized oval, fusiform, spindle, and polygonal-shaped neurons, and large-sized polygonal or stellate-shaped neurons. These various types of neurons exhibited distinct differences in their regional distribution within Vi (Figure 7; and see below).

The most conspicuous feature characterizing the caudal half of Vi was the presence of a relatively dense number of retrogradely labeled neurons in dcVi, irVi,

dlVi and the medial part of vlVipc compared to the relative paucity of retrogradely labeled neurons in the lateral part of vlVipc and brVi. In addition, the majority of the retrogradely labeled neurons in the lateral part of vlVipc were consistently lightly labeled in comparison to the more dense labeling of TT cells in other regions of Vi. This light labeling of vlVipc neurons was not affected by changes in either the position of the injection site in the thalamus or the length of the post-injection survival time.

The presence of retrogradely labeled neurons in the caudal pole of vlVipc contrasted sharply with the relative absence of such neurons in the medially adjacent portions of MDH at the MDH/Vi transition (Figures 1 and 3, level 1). However, a few intensely labeled medium-sized spindle to fusiform-shaped neurons were present along the MDH/Vi border. These neurons had their long axes oriented parallel to SVT and were morphologically similar to those retrogradely labeled neurons found in the marginal layer of MDH. Since similar retrogradely labeled neurons were not present in the adjoining regions of vlVipc, these neurons are considered to represent marginal neurons.

A number of different types of retrogradely labeled neurons were present in vlVipc. These included small oval-shaped neurons with thin radiating dendrites or bipolar-shaped dendritic fields, and medium-sized neurons with multipolar-shaped dendritic fields. The axons of these neurons primarily originated from the soma and coursed medially within the nucleus. Each of these cells were distributed throughout vlVipc. However, the largest neurons in this region were preferentially distributed to its dorsolateral tip.

There was a rather striking paucity of retrogradely labeled neurons in brVi. The labeled neurons that were present in this region consisted mainly of small oval-shaped neurons with bipolar-shaped dendritic fields oriented parallel to SVT. A few

small oval-shaped cells with thin radiating dendrites were also present. The axons of these cells arose from the soma.

The number of retrogradely labeled neurons in dlVi was much greater than that found in brVi. In addition, the retrograde labeling of these neurons was comparatively very intense. These cells were primarily small and medium-sized fusiform-shaped neurons; small oval-shaped cells with radiating or bipolar-shaped dendritic fields; or larger medium-sized multipolar cells. However, the majority of the TT cells in dlVi were primarily bipolar-shaped neurons. The dendrites of each of these cell types were preferentially oriented along the dorsoventral extent of dlVi parallel to SVT.

Many retrogradely labeled neurons were scattered throughout dcVi and irVi. These cells primarily consisted of small oval-shaped cells with radiating dendritic fields. A few medium-sized multipolar-shaped cells were also present. The neurons in irVi were generally smaller than those in dcVi.

The most striking feature of the retrograde labeling in the rostral half of Vi was the presence of a large number of medium-sized multipolar-shaped neurons in the lateral part of vlVimc and the presence of a modest number of retrogradely labeled neurons in dcVi, irVi and the medial part of vlVimc. The presence of numerous retrogradely labeled neurons in the lateral part of vlVimc contrasted sharply with the relative paucity of labeled neurons in the lateral part of vlVipc. This difference clearly marked the transition from the caudal to the rostral half of Vi.

The retrogradely labeled neurons in vlVimc consisted primarily of large multipolar-shaped neurons as well as a few smaller oval-shaped neurons. These latter neurons were morphologically similar to those in the caudal half of Vi. However, the number of small neurons in vlVimc was greatly reduced in comparison to the number found in vlVipc. While the large multipolar-shaped neurons were preferentially distributed to the lateral parts of vlVimc, the smaller neurons

predominated in the medial aspect of vlVimc. The density of retrogradely labeled neurons in vlVimc gradually decreased at more rostral levels within the medulla. The number of retrogradely labeled large multipolar-shaped cells accounted for approximately 80% of the total population of large multipolar-shaped cells in this region.

The number of retrogradely labeled neurons in dlVi increased in the rostral half of the nucleus and continued throughout the rostrocaudal extent of Vi. The neurons at these levels were morphologically similar to those found at more caudal levels, although a larger proportion of medium sized neurons were now present. The number of retrogradely labeled neurons in brVi also was slightly greater in the rostral half of the nucleus. The majority of the neurons in this region were morphologically similar to those found in the caudal half of brVi. In addition, however, a few medium-sized polygonal-shaped neurons with multipolar-shaped dendritic fields were also present. These latter neurons exhibited two to four relatively thick primary dendrites which were primarily oriented perpendicular to SVT. The axons of these neurons originated from the soma or the base of a primary dendrite. These neurons were morphologically similar to those in the adjoining regions of vlVimc and are considered to represent displaced vlVimc cells. The smaller neurons in brVi were occasionally organized into small groups of three or more cells.

The retrogradely labeled neurons in dcVi and irVi were morphologically similar to those in more caudal levels of the nucleus, although they were generally slightly larger in size and fewer in number.

Trigeminocerebellar Projection Neurons

The schematic diagram in Figure 2B illustrates the spread of HRP following multiple unilateral injections placed in the cerebellar vermis and hemisphere. The spread of HRP covered almost the entire vermal cortex and subjacent white matter

excluding only the lingula, nodulus and ventral part of the uvula. There was a slight spread across the midline into the contralateral vermal lobules. The spread of HRP also included the majority of the hemispheric cortex with the exception of the lateral part of the hemisphere and the flocculus and paraflocculus. In addition, the spread of HRP encroached upon the ipsilateral deep cerebellar nuclei. There was no visible involvement of regions outside of the cerebellum. The spread of HRP in this case was typical for those cases of cerebellar injections. The distribution of retrogradely labeled neurons was relatively similar in each of the cases examined.

The distribution of retrogradely labeled neurons in extratrigeminal brainstem nuclei included a massive number of neurons in the ipsilateral Cul and lateral reticular (LR) nuclei, as well as a few cells in the contralateral LR. In addition, the contralateral inferior olive and the ipsilateral reticular formation, including the nucleus linearis (Lin), contained retrogradely labeled neurons.

The presence of retrogradely labeled neurons in regions of SVC, exclusive of Vi, included a large number of cells in ipsilateral Vo, especially in its dorsomedial region (DM, Falls, Rice and VanWagner, '85) and a few cells in BZ; as well as a few scattered cells in the deep layers of MDH. In addition, every cell in the insular trigeminal-cuneatus lateralis nucleus (iV-Cul) was retrogradely labeled. This latter nucleus has recently been identified as a distinct component of InSy-SVT (Falls and Phelan, '84; see also Chapters Two and Five).

A considerable number of retrogradely labeled TC neurons were distributed throughout the rostrocaudal extent of ipsilateral Vi. A few scattered cells were also present contralaterally. The density of retrogradely labeled neurons was extremely sparse in the rostral pole of the nucleus (Level 8). However, retrogradely labeled neurons were present throughout the entire dorsoventral and mediolateral extent of the nucleus. All six regions of Vi contained retrogradely labeled neurons, although

there was a conspicuously low number of TC cells in dlVi compared to the remaining regions.

The distribution, size and somadendritic morphology of retrogradely labeled TC neurons is illustrated in Figure 4, 6 and 7. The entire population of retrogradely labeled TC cells exhibited a similar heterogeneity of somatic size and shape as did the population of TT cells. Small, medium and large sized neurons were retrogradely labeled. The somatic cross sectional areas of these neurons ranged from 50-450 μm^2 (Figure 6A). These neurons could also be generally grouped into three categories of cell sizes and ranges of somatic cross sectional areas similarly to the TT cells. The overall distribution of somatic cross sectional areas of TC neurons was slightly shifted towards the medium-sized neurons compared to the TT cell population. This shift was also reflected regionally (Figure 6B-G). The mean and standard deviation for these regions were (μm^2): brVi (138,46), dlVi (170,52), vlVipc (132,55), vlVimc (298,95), dcVi (190,50) and irVi (196,51). The smallest neurons predominated in brVi and dlVi, while the medium-sized neurons predominated in vlVipc, irVi, and dcVi. The largest of the TC cells were present in vlVimc.

A variety of TC neurons could also be classified on the basis of somatic size and somatic shape. These included small oval and fusiform-shaped neurons, medium oval, spindle and fusiform-shaped neurons, and large polygonal shaped neurons. These neurons exhibited distinct regional differences in their distribution within Vi (Figures 6 and 7; also see below).

The caudal pole of vlVipc, at the level of the transition from MDH to Vi, contained a modest number of intensely labeled TC neurons. However, at the same level brVi contained a rather conspicuous collection of retrogradely labeled neurons. These neurons were small oval and fusiform shaped neurons with primarily bipolar-shaped dendritic fields oriented parallel to SVT, and a few small cells with

multipolar-shaped dendritic fields. The axons of the cells in this region usually arose from the lateral aspect of the soma. Similar types of neurons were present in more rostral levels of brVi.

The distribution of retrogradely labeled neurons in vlVipc was such that there were often large areas of neuropil which lacked retrogradely labeled neurons. This gave the impression that there was a patchy distribution. However, no specific pattern could be detected in any of the TC cases examined. The types of retrogradely labeled neurons in vlVipc included a similar group of small and medium sized cells as was reported above in the thalamic injection cases. However, the largest number of retrogradely labeled neurons consisted of a population of medium-sized multipolar-shaped neurons. The majority of these neurons had their primary dendrites oriented mediolaterally within Vi. The axons of the multipolar-shaped neurons in vlVipc usually arose from the lateral aspect of the soma. In many instances, they could be followed for great distances in the neuropil. A large number of these axons were easily detected at low power magnification and formed a network of thin fibers which traveled laterally in Vi, entered SCT, and assumed a dorsolaterally directed course in the tract. The axons of these cells traversed SVT only at the points where bundles of fibers entered Vi. These latter structures, referred to as penetrating rays, represent bundles of myelinated fibers which represent primary trigeminal fibers leaving SVT to enter the various V nuclei (Gobel and Purvis, '72). No intrinsic axon collaterals were detected in any of these neurons.

A similar group of retrogradely labeled neurons were distributed throughout dcVi and irVi (Compare 6C, D and G). These neurons also displayed a patchy distribution in the neuropil. The origin and course of the axons of these cells was similar to that found in vlVipc cells.

The few retrogradely labeled neurons that were present in dlVi were primarily small oval to fusiform-shaped neurons with bipolar-shaped dendritic fields oriented parallel to SVT. These neurons were primarily restricted to a location within 50 μm of SVT. The axons of these neurons usually arose from the soma.

The pattern of retrograde labeling in the rostral half of Vi paralleled that in the caudal half of the nucleus. In brVi, the relatively large number of TC cells continued into the rostral pole of Vi, except for the most rostral level in which no cells were found. The types of neurons present were morphologically similar to those found in the caudal half of brVi.

In vlVimc, a similarly patchy distribution of primarily medium and large-sized neurons was present. The majority of these cells possessed 4-8 primary dendrites which emerged from the medial side of the soma and formed a cone shaped dendritic arbor with the cell body at the apex. The axons of these cells arose from the opposite side of the cell body and traveled laterally within Vi. No intrinsic axon collaterals were apparent in any of these cells. In many cases, the dendritic fields of these neurons appeared slightly arced due to their coursing around a deep axon bundle (DAB) in the neuropil. These DAB's have previously been reported to represent pathways for the axons of cells contributing to the extensive intranuclear projection system in SVC. There were approximately an equal number of retrogradely labeled and unlabeled large multipolar-shaped cells in this region.

There was virtually no difference in the type or distribution of retrogradely labeled neurons in dcVi or irVi compared to that found in caudal parts of the nucleus. However, the numbers of retrogradely labeled cells in irVi was less than that found at more caudal levels of the medulla.

An occasional group of retrogradely labeled neurons were also seen in dlVi immediately adjacent to SVT. These neurons were morphologically similar to those found at more caudal levels of the nucleus.

Trigeminospinal Projection Neurons

The schematic diagram in Figure 2C illustrates the spread of HRP in two separate injection loci in the cervical spinal cord. The two series of injections were utilized in the present study in order to maximize the density of retrograde labeling of TS neurons. The injection into the upper cervical spinal cord was centered between C1 and C2 levels, while the injection in the mid to lower cervical spinal cord was centered at C3-C6 levels of the cord. In both cases, the spread of HRP included the entire ipsilateral gray matter and varying portions of the white matter. A slight spread of HRP also encroached upon the medial aspect of the contralateral spinal cord central gray matter at some levels. Due to the dorsal approach of the injection needle, and the depth of penetration into the cord, the lateral funiculus was partially interrupted at various levels of the cord in each case. In order to facilitate comparison between the distribution and morphology of TS, TT, and TC cell populations, the results of upper and lower cervical injections were grouped together. However, the specific differences between the two series of experiments will be noted when necessary.

The distribution of retrogradely labeled neurons in extratrigeminal brainstem nuclei included the ipsilateral reticular formation, especially at positions bordering the deep layers of MDH, and the ventral part of ipsilateral Cun.

The presence of retrogradely labeled neurons in regions of SVC, exclusive of Vi, included a few scattered cells in ipsilateral Vms, a large number of cells bilaterally in the ventrolateral part of Vo, and a number of cells in ipsilateral MDH. In addition, moderate to dense anterograde labeling of the ascending spinotrigeminal fiber pathway also occurred. The specific regional distribution of this anterograde labeling and its spatial relationship to the distribution of TS neurons throughout SVC has been described in detail elsewhere (Phelan and Falls, '84; see also Chapter Four).

A modest number of retrogradely labeled neurons were present in Vi following injections into the cervical spinal cord. The greatest number of retrogradely labeled neurons occurred after the upper cervical injections. The majority of retrogradely labeled neurons were restricted to lateral and ventral parts of the nucleus. There were some distinct differences in the number, distribution and intensity of retrogradely labeled TS neurons between the upper cervical and the mid to lower cervical injections. The mid to lower cervical injection consistently labeled a number of neurons in dlVi and vlVimc. However, rostral injections resulted in a greater density of retrogradely labeled neurons in brVi, vlVimc, dlVi and vlVipc. A detailed description of the topographical relationship between Vi and the cervical spinal cord has been provided elsewhere (see Chapter Four).

The entire population of retrogradely labeled TS neurons exhibited a similar heterogeneity of somatic size and shape as that described above for the TT and TC cell populations. Small, medium and large sized neurons were retrogradely labeled. The somatic cross sectional areas of these neurons ranged from 25-750 μm^2. The overall distribution of somatic cross sectional areas for TS neurons more closely paralleled the population of TT cells than the population of TC cells (figure 6A). However, the population of TS cells clearly had a wider range. In addition, there were distinct differences in the somatic cross sectional areas of TS neurons within the various regions of Vi. The mean and standard deviation for these regions were (μm^2): brVi (122,56), dlVi (178,56), vlVipc (202,79) and vlVimc (341,98). The small neurons predominated in brVi and vlVipc, while small and medium sized cells formed the majority of cells in dlVi. In vlVimc, however, a large proportion of the cells were large-sized neurons with the smallest neurons being the least frequently labeled of the cells. The large-sized neurons in vlVimc were the largest of all retrogradely labeled neurons in Vi following either thalamic, cerebellar or spinal injections.

The population of TS neurons could be classified into several types on the basis of their somatic size and somatic shape. These neurons included small oval-shaped neurons with primarily radiating dendrites; small fusiform-shaped cells with bipolar-shaped dendritic fields; medium-sized multipolar cells and large polygonal-shaped neurons with multipolar-shaped dendritic fields. These neurons exhibited distinct differences in their regional distribution throughout Vi (Figures 6 and 7; also see below).

The most striking feature of the pattern of retrogradely labeling in the caudal half of Vi was the presence of two to three clusters of 5-20 small retrogradely labeled neurons in brVi. These clusters of neurons were evenly distributed along the dorsoventral extent of brVi. They were not organized into rostrocaudally directed columns but rather represented discrete structures which appeared periodically along the rostrocaudal extent of the caudal half of brVi. The neurons in these clusters were small oval-shaped cells with thin radiating dendrites or conical-shaped dendritic fields. The dendrites of these neurons were restricted to the area within the clusters. The axons of these cells arose from the soma. In addition to these clusters of cells, a few small to medium-sized neurons with bipolar-shaped dendritic fields were also present within the remaining parts of brVi.

A few scattered cells were present in vlVipc especially in its lateral aspect. These neurons consisted of a small population of small neurons with thin radiating dendrites and a large population of medium-sized neurons with pyramidal-shaped dendritic fields. The majority of the TS cells in vlVipc were distributed to the dorsolateral part of the region. Those cells in the medial parts of the region had their dendritic fields oriented mediolaterally while those in the dorsolateral parts were oriented dorsoventrally. These patterns appeared to mimic the arcing contour of fiber bundles in vlVipc which changes from a mediolateral to a dorsoventral direction in the nucleus (see Chapter One). The axons of TS cells in vlVipc

originated from the soma and coursed ventromedially in the neuropil towards the ventromedial border of Vi with pcRF.

Numerous retrogradely labeled neurons were present in dlVi. These neurons were primarily fusiform with bipolar-shaped dendritic fields oriented parallel to SVT. A few multipolar cells were also present.

A few rare scattered cells were present in dcVi and irVi. The cells in dcVi were positioned mainly in the lateral aspect of the region near its border with dlVi. The neurons in fact exhibited morphologies similar to those in dlVi (Figure 7).

The most notable feature characterizing the rostral half of Vi was the presence of numerous medium and large-sized neurons with multipolar-shaped dendritic fields in vlVimc. These cells were distributed throughout the entire rostrocaudal extent of vlVimc and were particularly prominent in its lateral aspect. It appeared that approximately 60 % of the large multipolar-shaped cell in this region were retrogradely labeled. A few small neurons were also present in this region. These latter cells exhibited morphologies similar to those cells found in vlVipc. The axons of the TS cells in vlVimc arose from the soma or the base of a large primary dendrite and coursed ventromedially in the nucleus. Some of these axons could be followed for long distances. In these cases, the axons traveled ventromedially in Vi and entered the ventrolateral part of the reticular formation where they entered a bundle of myelinated fibers. No intrinsic axon collaterals were observed in any of these neurons. A few of the medium-sized neurons in vlVimc were also present within the confines of brVi. However, the clusters of small neurons which characterized the caudal half of brVi were no longer present. A few small cells with bipolar-shaped dendritic fields were scattered through brVi.

Numerous cells were present in dlVi. These cells had similar somadendritic morphologies as those present in the caudal half of the nucleus. In addition, a few scattered cells were also present in dcVi and irVi.

Figure 1

Schematic diagram illustrating the topographical relationship of the various regions within Vi at eight rostrocaudal levels. The inset shows the shading patterns used in the Figure. The borders of the various regions are based on the results of a previous study (Phelan and Falls, '84a; see also Chapter One).

Figure 2

Schematic diagram illustrating the spread of HRP in representative cases in which the injection was centered in the thalamus (A), cerebellum (B) or the cervical spinal cord (C). Two separate spinal cord injections (Cases ST-5 and ST-8) were pooled in the present study for purposes of comparison with the thalamic and cerebellar cases.

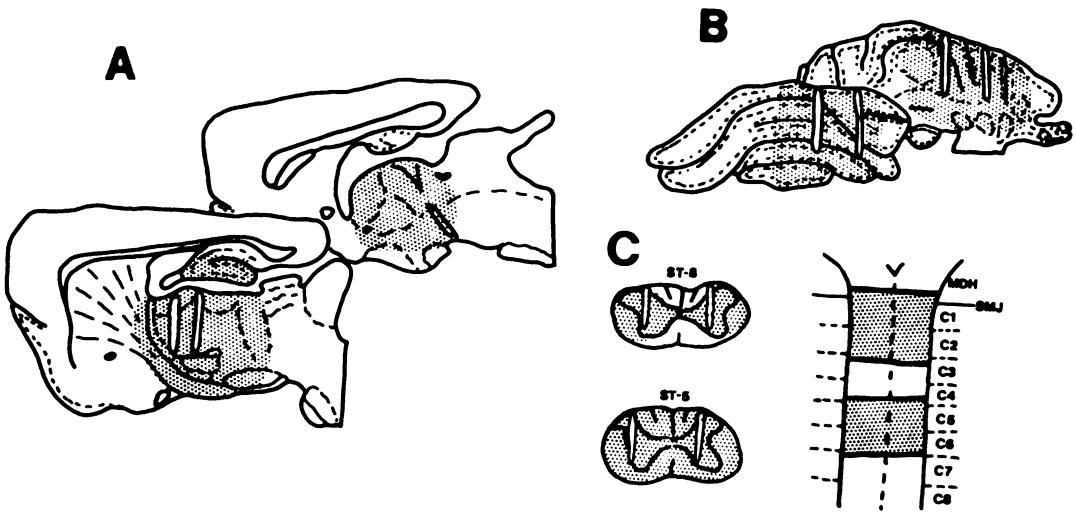
A
B
C
ST-6
ST-5
MDH
SMJ
C1
C2
C3
C4
C5
C6
C7
C8

Figure 3

Schematic diagram illustrating the distribution and relative morphology of retrogradely labeled TT neurons throughout the rostrocaudal extent of Vi. The boundaries between the various regions of Vi, in this and subsequent figures, were determined based on differences in the cyto- and myeloarchitecture of these regions as previously described (Phelan and Falls, '84a; see also Chapter One).

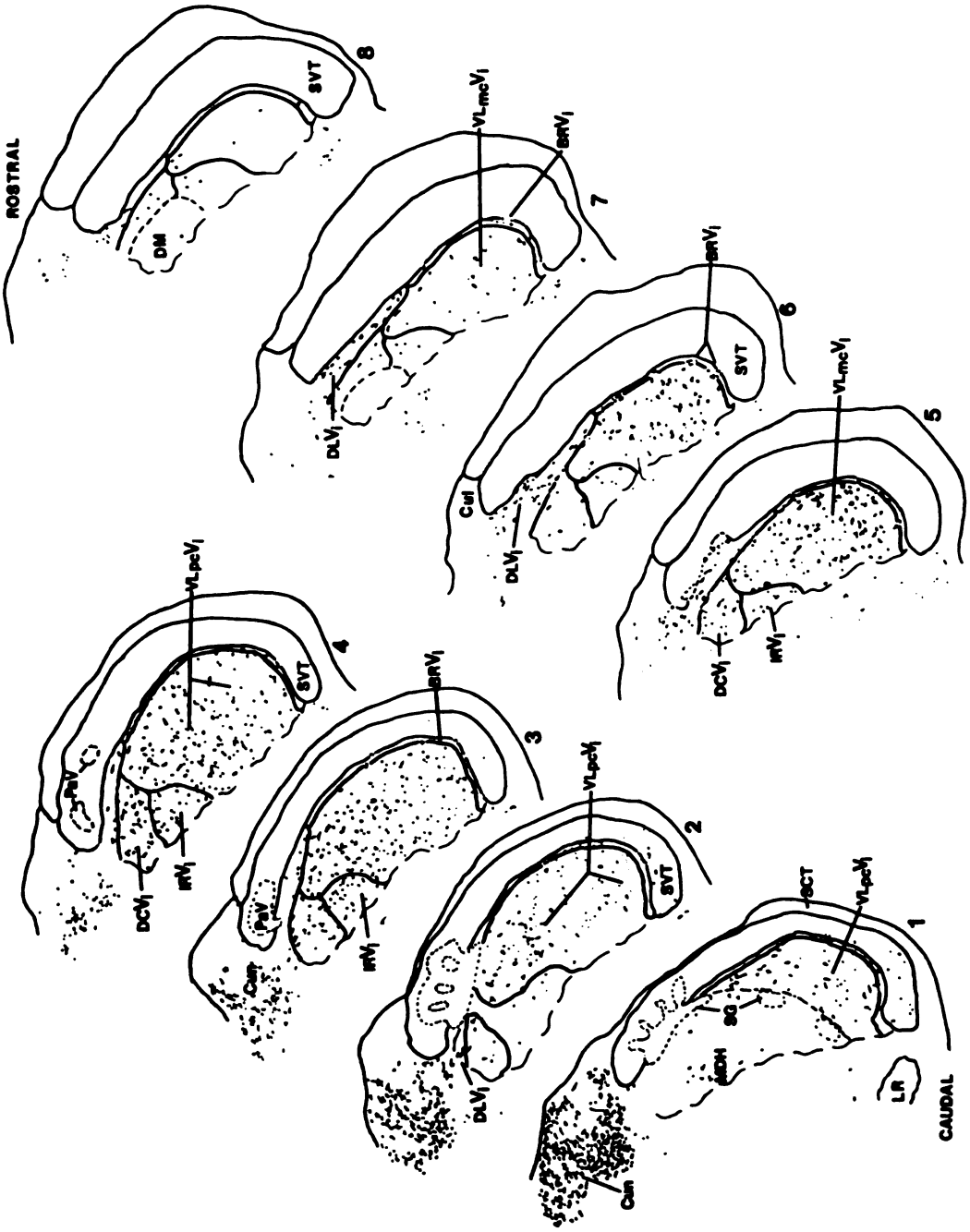
ROSTRAL
CAUDAL
8
7
6
5
4
3
2
1
SVT
DM
VL_mcV_i
BrV_i
DLV_i
Cul
DCV_i
IrV_i
VL_pcV_i
PaV
Cun
SG
MDH
LR
SCT

Figure 4

Schematic diagram illustrating the distribution and relative morphology of retrogradely labeled TC neurons throughout the rostrocaudal extent of Vi.

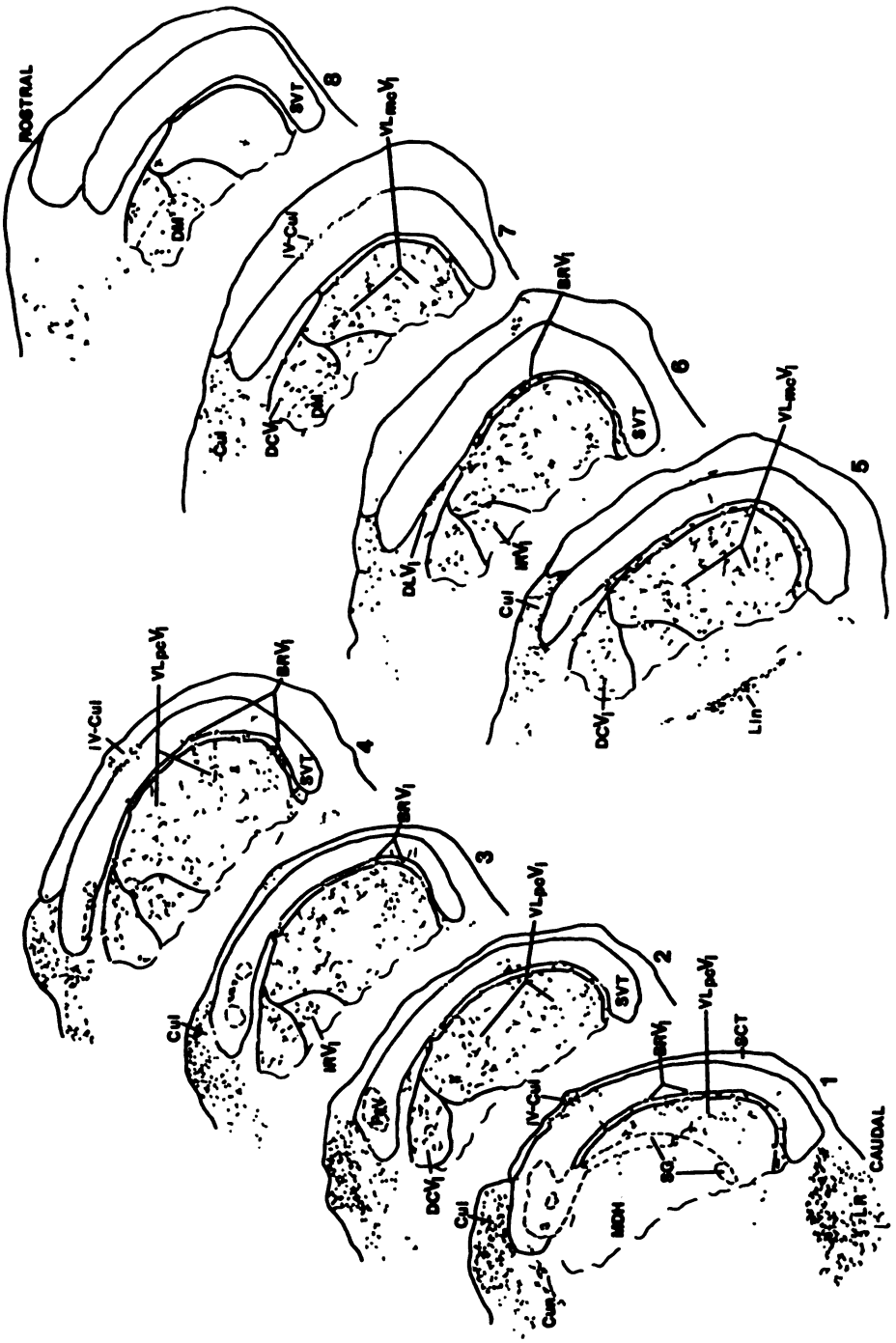
ROSTRAL
CAUDAL
SVT
VL-mcVl
IV-Cul
DMV
Cul
DCVl
BRVl
DLVl
MVVl
Lin
VL-pcVl
VL-poVl
SBCT
SG
MDH
Cun
8
7
6
5
4
3
2
1

Figure 5

Schematic diagram illustrating the distribution and relative morphology of retrogradely labeled TS neurons throughout the rostrocaudal extent of Vi.

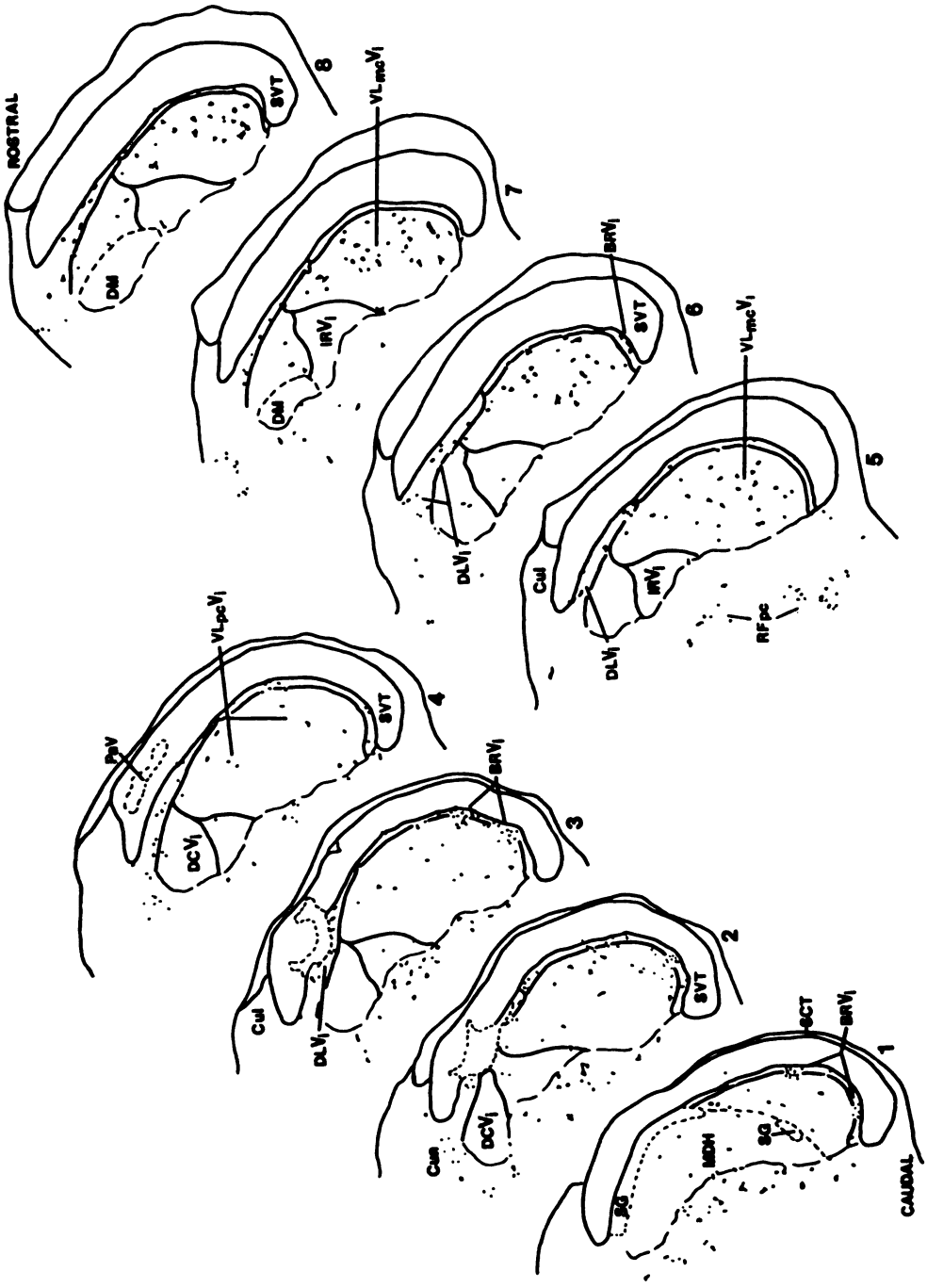
ROSTRAL
CAUDAL
8
7
6
5
4
3
2
1
SVT
DMI
VL$_{mc}$V$_1$
IRV$_1$
BRV$_1$
DLV$_1$
RFpc
VL$_{pc}$V$_1$
PaV
DCV$_1$
Cul
Cun
SCT
MDN
SG

Figure 6

Frequency distribution histograms comparing the somatic cross sectional areas of the entire population of TT, TC and TS projecting neurons in Vi (A) and the regional distribution of these cells (B-G). The few TS cells described in the text within dcVi were not included in this Figure.

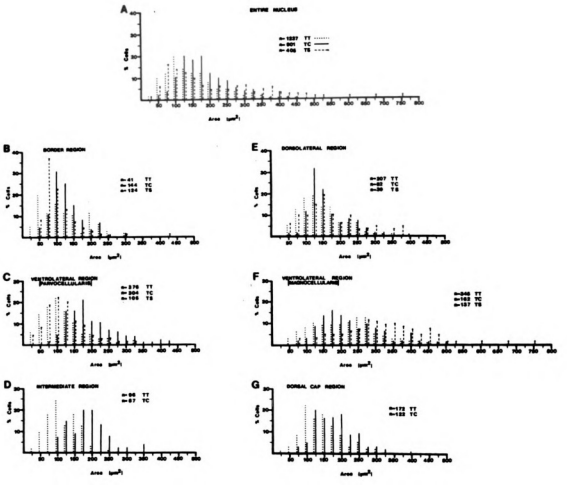
A
B
C
D
E
F
G

Figure 7

Camera lucida drawings of representative retrogradely labeled TT, TC and TS neurons in the various regions of Vi. The scale bar applies throughout. The dotted lines in brVi and dlVi indicate the border with SVT. The dotted lines in dcVi indicate the border with Cun. The dotted lines in vlVipc indicate the border with MDH. The arrowheads indicate axons.

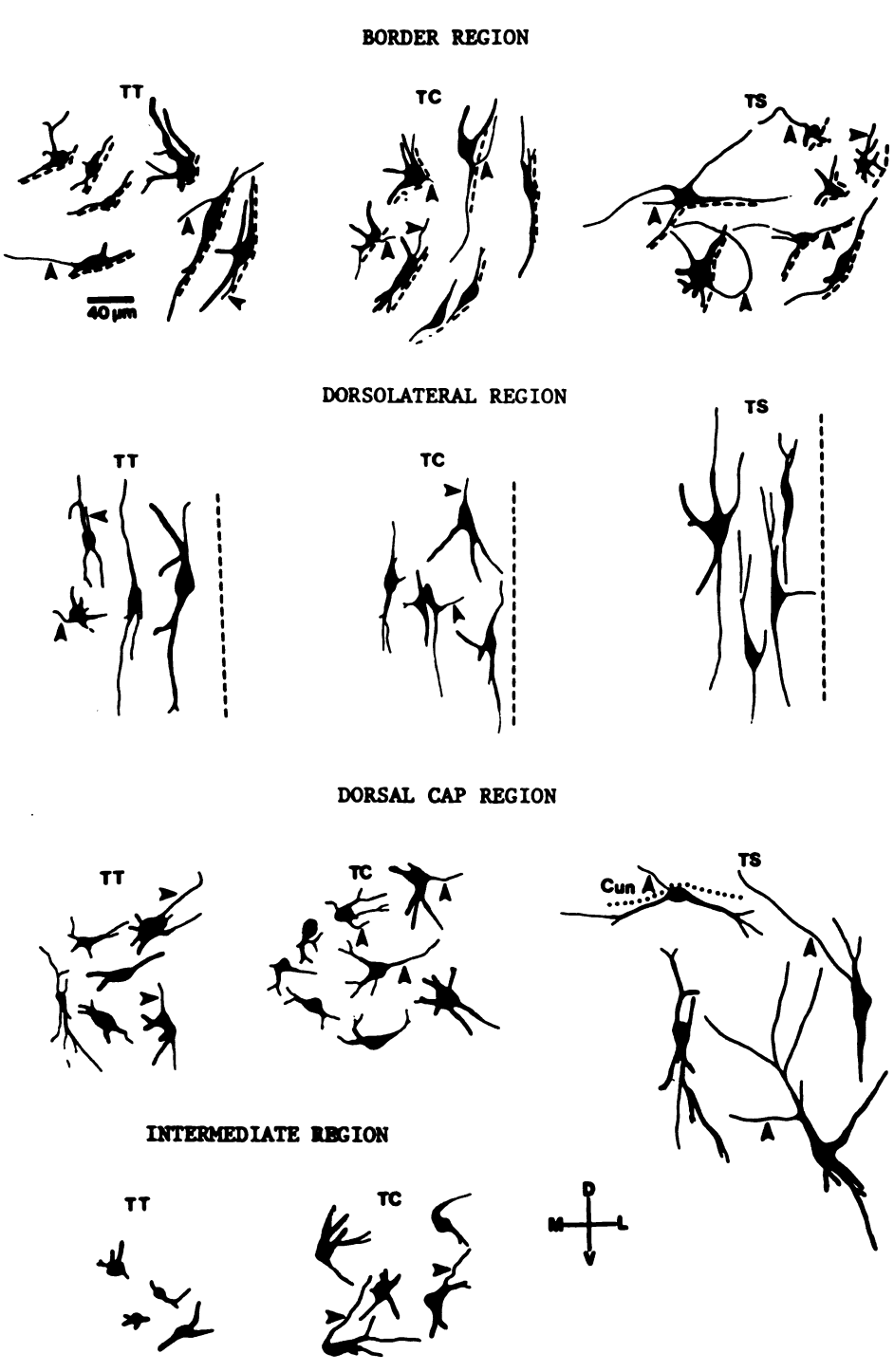
BORDER REGION
TT
TC
TS
40 µm
DORSOLATERAL REGION
TT
TC
TS
DORSAL CAP REGION
TT
TC
TS
Cun A
INTERMEDIATE REGION
TT
TC
D
M
L

DISCUSSION

The present study represents the first study to provide a detailed description of the distribution and morphology of retrogradely labeled TT, TC and TS neurons throughout the rostrocaudal extent of rat Vi. In particular, the present study is the first to examine the distribution of these projection neurons with respect to the six cyto- and myeloarchitecturally defined regions recently reported in rat Vi (see Chapter One). The results of the present study indicate that there are regional variations in the distribution and morphology of TT, TC and TS neurons which parallel these cytoarchitectural regions. This fact provides the first indication of distinct differences in the functional organization of these regions in Vi. In addition, the regional distribution of TT, TC and TS neurons provides strong evidence suggesting the possibility of collateralization among these three projection systems within specific regions of the nucleus.

Trigeminothalamic Projections

A diencephalic projection originating in Vi has been well established in the rat (Woolston, LaLonde, and Gibson, '82; Silverman and Kruger, '85; Roger and Cadusseau, '85; Erzurumlu, Bates and Killackey, '80; Kruger, Saporta, and Feldman, '77; Erzurumlu and Killackey, '80; Shammah-Lagnado, Negrao and Ricardo, '85; Peschanski, '84; Fukishima and Kerr, '79; Magnusson, Clements, Larson, Madl and Beitz, '87; Jacquin, Mooney and Rhoades, '86; and Mantle-St. John and Tracey, '87). These studies demonstrate that Vi projects to the VB complex, the posterior group of thalamic nuclei, the zona incerta, and the medial geniculate body. The results of the present study confirm the presence of an extensive thalamic projection originating in rat Vi. However, the specific targets of the TT cells labeled in the

present study cannot be determined since the large injections used encompassed all of the known diencephalic target nuclei.

The results of the present study indicate that the thalamic projecting neurons in Vi exhibit a variety of somatic sizes and shapes. Thus, these morphological features are not sufficient criteria alone to allow the identification of TT cells in Vi. However, despite this morphological heterogeneity, the present findings also indicate the presence of distinct regional differences in the distribution of TT cells throughout Vi. The differences in the regional distribution of these morphologically distinct neurons supports the presence of each of the six cytoarchitecturally distinct regions previously defined within rat Vi. In particular, large multipolar-shaped neurons were especially concentrated in vlVimc, medium fusiform-shaped cells were prominent in dlVi, small oval to fusiform-shaped cells inhabited brVi, and small oval-shaped cells were distributed throughout the dorsomedial two-thirds of Vi. In addition, differences in the density and morphology of cells in the ventrolateral regions of Vi appeared to support the presence of distinct medial and lateral segments within vlVipc and vlVimc.

The specific distribution and morphology of TT cells revealed in the present study throughout the rostrocaudal extent of Vi, differs significantly from the results of previous retrograde axonal labeling studies in the rat. In particular, Kruger et al. ('77) reported that the large cells in rostral Vi were retrogradely labeled following injections into the thalamus, however the majority of the cells in Vi, especially those in the caudal portions of the nucleus, remained unlabeled. On the other hand, Fukishima and Kerr ('74) reported that the majority of the large neurons, a moderate number of the medium sized cells, and an occasional small cell were retrogradely labeled following thalamic injections. Erzurumlu et al. ('80) reported that the rostral pole of Vi contained large retrogradely labeled cells which were gradually replaced at more caudal levels of the nucleus by small and medium-sized

retrogradely labeled cells. Finally, Mantle-St. John and Tracey ('87) reported that the majority of the large multipolar neurons as well as some of the smaller cells were retrogradely labeled following thalamic injections. These studies disagree with the present study with regard to the rostrocaudal distribution of TT cells. One important difference between the present study and these other studies is that none of these studies provide as detailed a description of the distribution or morphology of retrogradely labeled TT cells as that provided in the present study. This fact alone may account for the reported differences.

However, another plausible explanation to specifically account for the difference in the reported density of TT cells in the caudal pole of Vi may be that the present study was able to distinguish between Vi and MDH at this level of the medulla. Previous retrograde transport studies have not reported such a distinction. The inability to distinguish Vi from MDH at this level, coupled with the preferential distribution of TT cells in caudal Vi compared to rostral MDH, would certainly support the erroneous conclusion that TT cells are not common in the caudal pole of Vi. This fact clearly demonstrates the importance of providing detailed descriptions of the distribution of retrogradely labeled cells with respect to cytoarchitecturally defined boundaries in any nucleus.

The results of the present study are in agreement with the general distribution pattern reported for TT cells in the rabbit (Karamanlidis et al., '75). However, it differs significantly from the distribution pattern reported to exist in the cat (Shigenaga et al., '87; Matsushita et al., '82; Burton and Craig, '79) and the monkey (Burton and Craig, '79). In these latter studies TT cells were reported to be particularly concentrated in the caudal half of Vi. The reason behind this difference is not known. Perhaps one explanation may be found in differences in the effective spread of HRP in the diencephalon of these studies. It is easier in the rat to include the entire thalamic region in a large injection of HRP, while it is much more

difficult to do so in other mammals due to the comparatively large size of the diencephalon. It may be possible that large injections in the cat, comparable in extent to those in the present study, may result in the retrograde labeling of a larger number of cells distributed throughout Vi. On the other hand, the differences between the rat, the cat and the monkey might reflect a true species difference in the functional organization of the thalamic projection system. If this is the case, then perhaps the fact that the vibrissae region in rat occupies a relatively large percentage of the entire trigeminal facial representation may account for the larger number of TT cells in Vi compared to the situation in the cat and the monkey in which the vibrissae sensory regions occupy a much smaller proportion of the nucleus. Since there has yet been no reported distinction of specific cytoarchitectural regions in cat Vi as has recently been defined in the rat, it is impossible to compare the specific regional distribution of TT cells in these two species.

The most conspicuous feature of the thalamic distribution pattern revealed in the present study is the relative paucity of retrogradely labeled neurons in the lateral part of vlVipc compared to the lateral part of vlVimc. This distinct pattern gains particular importance because these regions of Vi receive a somatotopically organized primary vibrissae afferent input (Belford and Killackey, '79; Killackey and Belford, '79; and Arvidsson, '82). The existence of small TT cells in the caudally located vlVipc and large TT cells in the rostrally located vlVimc suggests the presence of two separate projections relaying vibrissae afferent information from Vi to the thalamus. The morphological differences between the cells of origin of these two pathways is particularly important in view of the implications that these differences have on their receptive fields. In a preliminary account of the morphology of cells in rat Vi, based on the Golgi impregnation technique, several morphologically distinct cell types were reported (Phelan and Falls, '83). Although it

is not known which cell types specifically represent thalamic projection neurons, this study did report that the small cells generally had small dendritic fields, while the larger cells generally had large dendritic fields. It is known that the size of a dendritic field may be strictly related to the size of the receptive field of a neuron. Therefore, the small TT cells in vlVipc may be relaying a more specific vibrissae afferent information to the thalamus compared to the larger cells in vlVimc.

In a recent study in the rat, the response properties and morphology of identified TT cells were reported (Jacquin et al., '86). This study revealed that TT cells in rat Vi possessed large receptive fields resulting from the convergence of primary afferents subserving a number of different vibrissae. Furthermore, intracellular labeling of these neurons revealed that they had large dendritic fields which spanned large areas of the ventrolateral portion of Vi. According to their figures, these TT cells were situated in a region corresponding to the rostral part of vlVimc. These authors suggested that these TT cells could not play a significant role in the organization of the specific thalamic receptive fields in VB in which individual cells respond to only a single vibrissae. The authors concluded that Vms must be primarily responsible for the receptive field pattern in the thalamus. However, in light of the results of the present study, the conclusion of these latter authors may have been premature. It may be possible that the smaller TT cells distributed throughout vlVipc may also contribute to the specific receptive field pattern in VB.

The second most notable feature of the distribution of TT cells in Vi was the prominent appearance of TT cells in dlVi and the comparatively small number of such cells in brVi. This fact supports a functional difference in these two regions. It is interesting to note that these two regions have recently been identified as spinal recipient zones in Vi. The predominant presence of TT cells in dlVi compared to brVi supports the idea that the spinal input to dlVi may be involved in a spino-trigemino-thalamic pathway while that to brVi is not (see also Chapter Four).

Finally, a recent study has reported that a large proportion of the thalamic projecting neurons in rat Vi contain the putative excitatory neurotransmitter glutamate (Magnusson et al., '87). In particular, this study reported that these cells were distributed to the dorsomedial two-thirds of Vi. However, no indication of the cell morphology is given. The results of this study indicate that TT cells in dcVi, irVi and possibly the medial segment of the ventrolateral part of Vi contain glutamate. On the other hand, the TT cells which populate the lateral parts of vlVimc and vlVipc may not utilize glutamate as its neurotransmitter.

Trigeminocerebellar Projections

A cerebellar projection originating in Vi has previously been demonstrated in the rat using electrophysiological (Woolston, Kassel, and Gibson, '81; and Woolston, LaLonde, and Gibson, '82) and anatomical (Watson and Switzer, '78; Huerta, Frankfurter and Harding, '83; Silverman and Kruger, '85; Race and Falls, '86) techniques. These studies demonstrate the projection of cells in Vi to four specific regions of the cerebellum (i.e., crus I, crus II, the paramedian lobule, and the uvula). In the present study, the use of large injections in the cerebellum prevented the identification of the specific target sites for the retrogradely labeled TC cells. However, a preliminary account of the topographical projection of TC cells in Vi has been reported elsewhere (Race and Falls, '86).

The available information in the literature regarding the distribution and morphology of TC cells in rat Vi is extremely limited. It has been suggested that the cells in Vi which project to crus I and crus II are located primarily in the dorsal two-thirds of the nucleus (Huerta et al., '83) and that these cells are primarily small and medium-sized neurons. On the other hand, Watson and Switzer ('78) illustrated a wider distribution of cells in Vi following an injection which encompassed a wider region of the cerebellum. In a more recent study, Race and Falls ('86) revealed the presence of four morphologically distinct populations of neurons in Vi which

projected to one or more areas in the cerebellum. However, there has yet been no study providing a detailed description of the distribution and morphology of TC cells throughout the rostrocaudal extent of Vi especially with regard to their distribution within the specific cytoarchitecturally defined regions recently identified in rat Vi. Finally, Mantle-St. John and Tracey ('87) reported that TC cells were distributed only to lateral regions of Vi.

The present study reveals that TC cells are distributed throughout the entire rostrocaudal extent of Vi including each of the six cytoarchitecturally defined regions. The present findings also indicate that cerebellar projecting neurons are morphologically heterogeneous. Thus, TC cells like TT cells cannot be distinguished solely on the basis of somatic size or shape. However, the present study also indicates that there are distinct differences in the regional distribution of TC cells in Vi.

The most striking feature of this pattern was the large number of TC cells in brVi and the relative absence of TC cells in dlVi. This distribution appears to be complementary to the distribution of thalamic projecting neurons described above. This difference provides further support for basic differences in the functional organization of these two regions. In fact, while the spinal input to dlVi may represent a spino-trigemino-thalamic pathway, the spinal input to brVi may be involved in a spino-trigemino-cerebellar pathway.

The precise pattern of distribution of TC cells reported in the present study differs significantly from that reported in the cat (Ikeda, '79; and Matsushita et al., '82) in which TC cells are concentrated in the rostral half of the nucleus. It is not known whether this difference might reflect a basic difference in the functional organization of Vi in the rat and the cat.

It has been demonstrated that the trigeminal target areas in the cerebellum also exhibit a somatotopically organized vibrissae afferent input (Joseph et al., '78;

and Shambes et al., '78). The numerous medium-sized cells distributed throughout vlVipc and vlVimc may relay this primary afferent information to the cerebellum, since these cells are situated within vibrissae afferent regions of Vi.

Trigeminospinal Projections

A spinal projection originating in Vi has previously been reported in only a few studies in the rat (Ruggiero et al., '81; and Leong et al., '84a,b). These studies indicate that neurons in rat Vi project to all levels of the spinal cord. The injections in the present study were restricted to the cervical spinal cord, however because of the possibility for retrograde labeling of TS neurons by damaged fibers of passage, the precise termination of most of the cells in the present study are not known. The only exception to this was those cells which only labeled following injections centered in the upper cervical spinal cord (e.g., brVi). These latter cells appear to only terminate in this region and do not project to lower levels of the cord. The topographical projection of cells in Vi to the cervical spinal cord has been described in detail elsewhere (see Chapter Four).

The present study reveals that TS neurons consist of a heterogeneous population of cells. In addition, the results of the present study indicate a rather restricted distribution of TS cells to ventral and lateral parts of Vi. This result generally confirms the distribution pattern reported in previous studies in the rat (Leong et al., '84a,b; and Ruggiero et al., '81) and cat (Matsushita et al., '82). However, the precise regional distribution of TS cells revealed in the present study is distinctly different from that reported in any species. The most significant difference is the presence of discrete clusters of neurons in the caudal half of brVi. The presence of these clusters in this region has not previously been reported in any species. The significance of this clustered arrangement of TS cells in Vi is not yet known. It is interesting to note that previous cytoarchitectural studies have noted the presence of similar clusters of cells in caudal brVi (see Chapter One). In addition,

these clusters are known to receive a spinal afferent input (see Chapter Four). The second most significant difference between the present study and previous studies is the large number of TS cells distributed throughout dlVi, vlVipc and vlVimc. Previous studies in the rat have only noted TS cells in regions of Vi which would correspond to the rostral pole of vlVimc (Leong et al., '84a) or along the ventromedial aspect of caudal Vi (Ruggiero et al., '81). The present study indicates a distribution of TS cells which encompasses a wider portion of Vi than previously suggested. This discrepancy may partially be explained by the fact that these other studies did not include injections centered in the uppermost levels of the cervical spinal cord.

Collateral Projections within Specific Regions of Vi

It has long been known that Vi is unique among the various nuclei of SVN in that its efferent projections are widely distributed throughout the neuraxis. This fact has prompted speculation regarding the possible existence of collateralization among the secondary projections of this nucleus. Although there has not yet been any study directed towards investigating whether TS cells send collaterals to the thalamus or the cerebellum, several electrophysiological (Jacquin et al., '86; and Woolston et al., '82) and anatomical (Patrick and Robinson, '84; Silverman and Kruger, '85; and Mantle-St. John and Tracey, '87) studies have specifically investigated whether the thalamic and the cerebellar projections originating in rat Vi represent collateral pathways. However, the results of these studies have been contradictory. In particular, Woolston et al. ('82) reported that only 1 out of 80 cells were antidromically activated following VB and uvular stimulation. This result was confirmed by Jacquin et al. ('86) in which none of the 11 identified TT cells could be antidromically activated from the cerebellum. In a more recent study, Mantle-St. John and Tracey ('87) reported results of double retrograde labeling experiments which indicated that the thalamic and cerebellar projections originating in Vi

represent separate populations of neurons. However, Patrick and Robinson ('84) and Silverman and Kruger ('85) both reported that a large number of TT and TC cells were double labeled following injections into VB and the cerebellum. In fact, Silverman and Kruger stated that more than 80% of the TC cells in Vi also sent collaterals to the thalamus. However, neither of these two studies provide any detailed information regarding the regional distribution or morphology of these neurons. In addition, comparable studies in the mouse (Steindler, '85) and in the cat (Somers and Panneton, '84) deny the presence of any collateralization between the thalamic and cerebellar projection in these species. However, one electrophysiological study in the cat reported that up to 13% of TC cells also send collaterals to the thalamus (Hayashi et al., '84). The discrepancies between the rat, mouse and cat may represent real species differences, however the discrepancies among the various studies in the rat itself are more difficult to reconcile. It has been suggested that the differences in these studies may be the result of differences in the relative size of the injection sites (Silverman and Kruger, '85).

The results of the present study do not provide any direct evidence concerning the collateralization among these pathways in rat Vi. However, if the results of Silverman and Kruger ('85) and Patrick and Robinson ('84) are correct, then it should be possible to determine, through a detailed comparison of the distribution and morphology of TT, TC and TS projecting neurons, which of the specific regions of Vi may contain cells contributing to this collateralization.

In general, the somatic cross sectional areas of TT, TC and TS cell populations exhibited an extensive overlap in the present study. In addition, all three projections consisted of a morphologically heterogeneous population of cells. Therefore, somatic size and shape cannot be used to distinguish among these neurons. However, the largest of the multipolar-shaped cells in rostral vlVimc

exclusively represented TS neurons. This finding indicates that there are at least some distinct TS cells which do not project to either the thalamus or the cerebellum.

The overall distribution pattern revealed in the present study indicates an extensive overlap of TT and TC cells in all six regions of Vi. However, since TS cells were restricted to ventral and lateral regions of the nucleus, if there is collateralization between this pathway and the others, then it must occur in cells situated in dlVi, vlVipc, vlVimc or brVi. Conversely, the TT and TC cells in dcVi and irVi do not collateralize with TS cells.

The border region of Vi. The number of TT cells in this region was very low compared to the large number of TC and TS cells. In fact, TC cells outnumbered TT cells 3.5:1, while there were an even number of TC and TS cells in the region. This fact indicates that the majority of TC and TS cells cannot collateralize to the thalamus. The morphology of TT, TC and TS cells was not significantly different in this region. However, the few TT cells that were present gave rise to medially directed axons, while the majority of TC cells gave rise to laterally directed axons. This suggests that the vast majority of TT and TC cells represent separate populations of neurons in brVi. The majority of the large TS cells in rostral brVi also gave rise to medially directed axons. However, the morphology of these TT cells was entirely different than the TT cells in the same region, therefore these cells must also represent separate populations of neurons. In addition, the TS cells in caudal brVi were characteristically organized into discrete clusters. This arrangement was not seen in either TT or TC cells suggesting that the majority of TS cells in these clusters represent a separate group of Vi neurons. The results of the present study cannot rule out the possibility that there may be a few cells which do collateralize in this region, however if they exist then they would constitute only a minor percentage of the total cell population in brVi and may not be functionally significant.

The dorsolateral region of Vi. The number of TT cells in this region far outnumbered either TC or TS cells. In fact, the ratio of TT to TC cells was 2.5:1, while that of TT to TS cells was approximately 5.3:1. This fact indicates that the majority of TT cells in dlVi cannot send collaterals to the cerebellum or the spinal cord. The largest neurons in this region represented TS neurons, therefore these cells also represent a separate group of neurons in this region. The TC cells were most commonly found immediately adjacent to SVT, while TT and TS cells were more common in lateral regions of dlVi. This indicates that the TT and TS cells most probably do not also project to the cerebellum. These findings suggest that collateralization in dlVi may not be extensive and if present will most likely be between TT and TS cells.

The ventrolateral parvocellular region of Vi. The TT cells were predominantly distributed to the medial segment of this region, while TS cells were primarily distributed to the lateral segment and TC cells evenly distributed throughout both segments. This distribution pattern suggests that TT and TS cells are largely independent projections in vlVipc. The somatic cross sectional areas of TT, TC and TS neurons in this region indicates that approximately 50% of the total population of TT or TS cells have small somatic sizes which were not present in the TC cell population. This indicates that the small TT and TS neurons in this region do not send collaterals to the cerebellum. In the lateral segment of this region, the TT and TS cells were predominantly small in size while the TC cells were predominantly medium in size. This indicates that the majority of the TT and TS cells in the lateral segment of vlVipc do not send collaterals to the cerebellum. On the other hand, the medial segment of this region does not exhibit any distinct differences which preclude the existence of neurons projecting to the thalamus and the cerebellum. It is possible that cells in this region may account at least in part for the double labeled cells reported in this region by Patrick and Robinson ('84).

The ventrolateral magnocellular region of Vi. The largest cells in this region were TS which do not send collaterals to either the thalamus or the cerebellum, since these large cells did not label following thalamic or cerebellar injections. The majority of the TT and TS cells were distributed to the lateral segment of vlVimc, while TC cells were distributed throughout the medial and the lateral segments. In addition, the TT cells in the medial segment were primarily small neurons, while the TC cells in this region were mainly medium-sized neurons. Thus, the majority of TT and TC cells in the medial segment of this region represent separate populations of cells. Furthermore, the TT and TC cells were restricted to the caudal three-quarters of vlVimc, while TS cells were fairly common throughout the rostral half of Vi. This distribution pattern indicates that the TS cells in the rostral quarter of vlVimc represent a separate population of cells which do not send collaterals to either the thalamus or the cerebellum. In the lateral segment of vlVimc, many of the TC cells were morphologically distinct from either TT or TS cells. However, there was also an extensive overlap in the size and shape of labeled neurons in this region. The fact that approximately 80% of the large cells in the lateral segment were TT cells, 50 % were TC cells and 50 % were TS cells indicates that there must be collateralization of at least 30% of the large multipolar-shaped cells in this region. This is underscored by the fact that the axonal morphology of the large labeled neurons in each of the three projection groups was similar. The collateralization of TT and TS cells has not previously been reported in any species. The collateralization that must necessarily exist between TT and TC cells in this region may account for at least part of the double labeled cells that were reported by Silverman and Kruger ('85) and Patrick and Robinson ('84).

The dorsal cap and intermediate regions of Vi. The extremely few number of spinal cells that were present in these regions were far outnumbered by TT and TC cells and exhibited morphologies not seen in these latter groups. The size, shape,

somadendritic morphology and distribution of TT and TC cells in these regions were not significantly different to preclude the possibility of collateralization in these regions of Vi. The cells in this region may also represent some of the double labeled cells reported by Silverman and Kruger ('85) and Patrick and Robinson ('84).

The results of the present study clearly indicate several regions where collateralization of TT, TC or TS cells is not possible because of differences in the size, shape, or distribution of individual neurons. In addition, the present study provides some indication of regions of Vi in which collateralization of these pathways may occur. Finally, the present study provides evidence which indicates that some collateralization must exist in vlVimc.

A series of preliminary double labeling experiments designed to determine the extent of collateralization of TS and TC projections in rat Vi indicates that these two cell populations represent entirely separate cell groups (unpublished observations).

It is interesting to note that the two spinal recipient regions in Vi (dlVi and brVi) appear to represent regions containing separate populations of thalamic and cerebellar projecting neurons, respectively.

The significance of the fact that the possible sites of collateralization are located predominantly in dorsomedial aspects of Vi as compared to ventrolateral regions is not known. These dorsomedial regions are involved mainly in the processing of orofacial sensory information from oral regions of the face. Perhaps the importance of these regions in normal activity necessitates the integration of cerebellar and thalamic activities. The significance of extensive collateralization in vlVimc is not yet known. However, this region receives a topographical vibrissae input in which the cells have large receptive fields responsive to multiple vibrissae. Therefore, the information transmitted by these cells may be more involved in

complex integrative functions as compared to the simple relay of sensory information. It appears from this study, that vlVipc contains predominantly separate TT and TC populations of cells. It is interesting to note that this region also receives a topographical input from the vibrissae. The possibility that the cells in this region may have smaller receptive fields which respond to only one or a few vibrissae may underlie the necessity for separate relay of this information to the thalamus and the cerebellum.

CHAPTER FOUR

THE SPINOTRIGEMINAL PATHWAY AND ITS SPATIAL RELATIONSHIP TO THE ORIGIN OF TRIGEMINOSPINAL PROJECTIONS IN THE RAT

INTRODUCTION

In the last decade, anatomical and electrophysiological studies have firmly established the existence of a direct trigeminospinal (TS) projection in a number of mammals, including rat (Burton and Loewy, '76, '77; Satoh, '79; Ruggiero, Ross and Reis, '81; and Leong, Shieh and Wong, '84a,b), hamster (Bruce, McHaffie, and Stein, '84), cat (Kuypers and Maisky, '75; Burton and Loewy, '77; Craig, '78; Burton, Craig, Poulos, and Molt, '79; Tohyama et al., '79; Matsushita, Ikeda, and Okado, '82; Matsushita, Okado, Ikeda and Hosoya, '80, '81; Rustioni, Schmechel, Cheeks, and Fitzpatrick, '84; and Hayashi, Sumino, and Sessle, '84), dog (Craig, '78), opossum (Crutcher, Humbertson and Martin, '78; and Cabana and Martin, '84) and monkey (Burton and Loewy, '77). These studies have reported the presence of spinal projection neurons in all three subdivisions of the spinal trigeminal nucleus (SVN) (i.e., trigeminal nucleus oralis, Vo; trigeminal nucleus interpolaris, Vi; and the medullary dorsal horn, MDH) as well as in the main sensory V nucleus (Vms). These neurons have been reported to project to the entire length of the spinal cord in the rat (Ruggiero et al., '81). However, it has not yet been determined whether this also holds true for other species. Although the precise locus of termination of this descending pathway within the spinal cord has not yet been determined, it has been speculated that this pathway may contribute to the modulation of neurons in the dorsal horn giving rise to ascending sensory projections; influence the output of

motor neurons involved in withdrawal reflexes, such as the trigemino-neck reflex; or contribute to the expression of other reflexes which may involve the integration of trigeminal (V) and spinal somatic and autonomic systems (Humphrey and Hooker, '59; Manni, Palmieri, Marini and Petterossi, '75; Burton and Loewy, '77; Sumino and Nozaki, '77; Abrahams and Richmond, '77; Abrahams, Anstee, Richmond and Rose, '79; Rose and Sprott, '79; and Ruggiero et al., '81).

A direct projection from the spinal cord to the sensory trigeminal nuclear complex (SVC) (i.e., SVN and Vms) has been demonstrated using experimental degeneration studies in the rat (Torvik, '56), cat (Johnson, '54; Rossi and Brodal, '56; Nauta and Kuypers, '58; and Rustioni and Molenaar, '75), hedgehog (Jane and Schroeder, '71; and Ring and Ganchrow, '83) and monkey (Kerr, '75; and Rustioni, Hayes and O'Neill, '79). In general, these studies reported degenerating spinal afferents within restricted regions of one or more of the SVC nuclei following lesions at various spinal cord levels. Additional experiments utilizing dorsal rhizotomies (Hand, '66; Rustioni and Macchi, '68; Shriver, Stein and Carpenter, '68; Imai and Kusama, '69; Keller and Hand, '70; Kerr, '72b; Rustioni, '74 and Rustioni and Molenaar, '75) or successive degeneration techniques (Rustioni, '74; and Rustioni and Molenaar, '75) demonstrated a widespread contribution to this projections from primary as well as non-primary spinal afferents, particularly within those projections to MDH and Vi. However, there is no consensus among these studies regarding the origin, course or distribution of spinal afferents within the individual SVC nuclei. Although much of this variability in distribution patterns within SVC may be due to the inherent difficulties and limitations of the experimental degeneration techniques employed in these studies, it is also possible that specific species differences may exist within this projection. Nevertheless, the specific details of the origin and distribution of the ascending spinal projection to SVC remains equivocal.

Electrophysiological studies have not confirmed the presence of spinal afferents within the specific regions of SVC identified in the anatomical studies, and therefore provide little insight into the functional nature of this projection. However, it has been suggested that the spinotrigeminal projection may serve as a link in ascending sensory pathways through SVC, in parallel with other ascending spinobulbar pathways to the thalamus and cerebellum (Rossi and Brodal, '56; and Hand, '66). In addition, it has been proposed that this direct spinotrigeminal projection may, in conjunction with the direct TS pathway, form the anatomical substrate for a reciprocal spino-trigemino-spinal feedback system (Rossi and Brodal, '56; and Hand, '66) similar to other spino-bulbar-spinal loops which subserve a variety of reflexes (Shimamura and Livingston, '63; Cervero and Wolstencroft, '84).

Considering the important role that the spinotrigeminal pathway might play in overall sensory processing in the pons and medulla, it is rather surprising that this system has largely been ignored in recent years. In fact, the organization of the spinotrigeminal pathway has not specifically been investigated using any of the modern anterograde transport techniques. A determination of the precise distribution of spinal afferents within SVC as well as the spatial relationship of this input with the cells of origin of secondary V projections, in particular those projections to the thalamus, cerebellum and spinal cord, is clearly essential, in order to obtain a more complete understanding of the functional nature of this ascending spinal pathway.

The present study was designed to examine the distribution and light microscopic morphology of spinotrigeminal afferents in the rat using the anterograde transport of horseradish peroxidase (HRP) and tritiated amino acids. In addition, the present study directly examines the spatial relationship between the distribution of spinal afferents and the location of TS efferent neurons in SVC, by

taking advantage of the simultaneous anterograde and retrograde transport of HRP which occurs following injections into the spinal cord.

METHODS

Adult, male Sprague-Dawley rats (200-300 grams) were used throughout this investigation. In 20 animals, a fresh 30-60% solution of HRP (Sigma Type VI), dissolved in 2% dimethylsulfoxide, was injected into the cervical and/or upper thoracic levels of the spinal cord using a 26 gauge Hamilton syringe. The injections consisted of either relatively small, single, unilateral injections (.05-0.2 μl total) centered at or between specific spinal cord segments; or larger, unilateral or bilateral injections (0.2-1.0 μl total) located in upper, middle or lower cervical and/or upper thoracic cord levels. In each case, the injection needles approached from the dorsal aspect of the cord and penetrated the dorsal and/or ventral horns. Three animals received multiple, bilateral injections of HRP (2.0-3.0 μl total) centered in the dorsal funiculi, and dorsal and ventral horns at C2-C5 levels of the cord. One animal received a unilateral injection (0.1 μl total) in the dorsal funiculi at the C1 level of the cord. The spinal cord was transected in one animal at the level of T2 and an HRP soaked gel was placed between the two cut ends of the cord. In addition, several injections of HRP (2.0 μl total) were placed in the proximal end of the transected cord. After a survival time of 24-48 hours each animal was perfused intraaortically, using a Masterflex pump delivery system, with an initial, brief heparanized physiological saline wash followed by 500 ml of a fixative consisting of 1% paraformaldehyde, 1% glutaraldehyde and 0.5% $CaCl^2$ in 0.12 M phosphate buffer (pH 7.4). The brainstems and spinal cords were then removed, blocked in the transverse plane and either postfixed an additional 1-4 hours or immediately serially sectioned on an Oxford Vibratome at a thickness of 50 Mμ. The brainstems were specifically cut in the transverse plane while the spinal cords were cut in either the

transverse or horizontal plane depending upon the size and extent of the expected injection sites within the spinal cord. Alternate serial sections were reacted for tetramethylbenzidine (TMB) according to the histochemical protocol of Mesulam ('78) and counterstained with 1% neutral red. In most cases, the remaining sections were either reacted with TMB and left unstained, or else left unreacted and stained with a 0.5% cresylecht violet solution and subsequently dehydrated and coverslipped. In those animals receiving the multiple injections at C2-C5 levels of the cord, the alternate sections were processed for visualization of HRP using the cobalt-glucose oxidase (Co-GOD) method of Itoh et al.('79). These sections were then cleared through a series of graded glycerin solutions (Gobel et al., '80) and coverslipped with 100% glycerin. Examples of well isolated HRP labeled spinal afferent fibers were drawn using a drawing tube attached to a Leitz microscope and a 100X oil immersion objective lens at a final magnification of 1,250X. Several samples of labeled spinotrigeminal fibers were selected and processed for subsequent electron microscopic analysis (see Chapter Five). The remaining sections were rehydrated through a graded series of glycerin, stained with 0.5% cresylecht violet, dehydrated and coverslipped.

The actual position of the injection site as well as the spread of the HRP was reconstructed from serial sections in each case using a drawing tube attached to a Leitz Orthoplan microscope. The position of retrogradely labeled somata within SVC were plotted from representative TMB reacted sections in each case. The distribution of retrogradely labeled neurons within other brainstem nuclei were noted for subsequent comparisons with previously established patterns and used as an indication of the spread of HRP within the spinal cord. In most animals, the anterograde transport of HRP was detected as grains of TMB reaction product accompanied by an occasional labeling of fibers. The distribution of the anterograde labeling was charted from representative sections onto the same camera lucida

drawings illustrating the distribution of retrogradely labeled neurons. The distribution patterns of anterograde labeling within other brainstem regions (eg., spinoreticular, spinofacial, spino-olivary, spino-dorsal column) were also noted and used to distinguish differences in the spread of the injection sites. In those cases reacted with the Co-GOD method of HRP visualization, examples of well isolated axons and their terminal collaterals were drawn whenever possible to illustrate the morphology and collateralization patterns of spinotrigeminal fibers within SVC.

The anterograde transport of tritiated amino acids was also used to document the origin of the spinotrigeminal pathway from secondary spinal neurons in the uppermost cervical levels of the spinal cord. Seven animals were injected with .05-0.4 μl of a mixture of tritiated proline and leucine (50-80 μCi/μl) using a 26 gauge Hamilton syringe alone or one fitted with a glass micropipette (50 μm tip diameter). Single, unilateral injections were centered in the dorsal horn at C1-C5 levels of the spinal cord. Two injections were centered approximately at the border between MDH and C1. The animals were allowed to survive 3-5 days and were then perfused intraaortically using an identical procedure as that previously described for the HRP experiments, except that the fixative contained 2% paraformaldehyde and 2% glutaraldehyde. The brains were removed, blocked in the transverse plane and postfixed overnite at 4° C. Serial sections were then cut on an Oxford Vibratome at a thickness of 30-50 μm. Two to three sets of alternating sections were mounted on gelatin subbed slides and air dried. The slides were then dehydrated through chloroform and an alcohol series, rehydrated and dried in a 30° C oven for one hour. The injection sites from one alternating series of sections were used for the rapid detection of the size and location of the injection sites according to the protocol of Imai, Steindler and Kitai ('83). The entire series of alternating sections were subsequently dipped in Kodak NTB-2 emulsion at 43° C and allowed to slowly dry in a humidity chamber overnite. The slides were then placed in light tight boxes

and stored at -70°C for 6, 12 or 18 weeks. They were then developed in D-19, rinsed, fixed with Kodak rapid fix and extensively washed. The slides were then directly placed into a 0.5% cresylecht violet acetate solution for counterstaining and subsequently dehydrated and coverslipped. In addition, several blank control slides were processed along with the other slides for purposes of determining the amount of general background noise due entirely to the processing procedures.

The analysis of the autoradiographically developed slides were performed under brightfield and darkfield illumination in order to determine the position of silver grains in relation to the cell and fiber patterns previously described within SVC (Gobel, Falls and Hockfield, '77; Falls and King, '80; Falls et al., '86; see also Chapter One). Vibratome sections were specifically used because of the clearer delineation of myelinated fiber systems in these sections under darkfield illumination compared to that seen in frozen sections. The density of silver grains located within presumed anterogradely labeled terminal fields were compared with background levels in other regions of the brainstem. Only those regions exhibiting consistent labeling in consecutive sections at a density well above background levels were considered positive for anterograde transport. Representative camera lucida drawings of the distribution of silver grains were made from each case for subsequent comparisons. The maximum extent of the injection sites were determined from reconstructions of the serial sections using bright- and dark-field illumination.

RESULTS

Horseradish Peroxidase Studies

The injection of HRP into various levels of the cervical spinal cord consistently resulted in the anterograde labeling of spinotrigeminal fibers. The density and distribution of this labeling varied with the size and location of the

injection site within the cervical spinal cord. In those cases with small, primarily unilateral injections of HRP, only sparse anterograde labeling occurred within some of the spinal recipient regions in SVC. In order to maximize the density of labeling within these regions, and thereby localize the full extent of the spinotrigeminal projection, larger bilateral injections were also placed at various levels of the cervical spinal cord. In all of those cases with a bilateral spread of HRP, the density of anterograde labeling was rarely symmetrical and the pattern of labeling in SVC was consistent with that obtained using smaller, more localized, unilateral injections. The use of the larger injections allowed the direct examination of the spatial relationship between the distribution of retrogradely labeled TS neurons and the distribution of the spinotrigeminal afferents within SVC. The different survival times used in the present study had no specific effect on the precise distribution pattern of labeling throughout SVC. However, the longer survival times did result in a relatively more dense labeling of the spinotrigeminal afferent fibers and TS efferent neurons in SVC.

The results of the series of injections utilized in the present study will be summarized through the presentation of five representative cases which together illustrate specific features of the organization of the spinotrigeminal pathway in the rat and its spatial relationship to the distribution of TS neurons in SVC. An additional case will be presented to summarize the morphological features of spinotrigeminal fibers revealed through the use of the Co-GOD method of HRP visualization. The specific morphological features of retrogradely labeled TS neurons will not be provided here since they have been previously reported elsewhere (Phelan and Falls, '86; Leong et al., '84a,b; Ruggiero et al., '81; Satoh, '79; and Burton and Loewy, '77; see also Chapter Three).

Case ST-12. A series of small unilateral injections of HRP were centered in the dorsal and ventral horns at levels corresponding to C7 through T1 in this animal.

The needle tracks coursed through the medial half of the dorsal and ventral horns and caused slight damaged to the lateral funiculus. The spread of HRP encompassed the entire ipsilateral gray and white matter (Figure 1A). Labeled fibers were present in the dorsal column funiculi (DCF) and in the dorsal and ventral parts of the lateral funiculus (LF). These labeled fibers continued into the medulla. The extratrigeminal brainstem regions exhibiting anterograde labeling included the contralateral dorsal accessory inferior olive (DAO), the ipsilateral lateral reticular (LR) nucleus, the ipsilateral medial part of the facial nucleus, the ipsilateral lateral cuneate (Cul) nucleus, and the ipsilateral dorsal column nuclei (DCN, i.e., nucleus gracilis, Gr; and nucleus cuneatus, Cun). In addition, diffuse anterograde labeling was present throughout the majority of the reticular formation. A small number of anterogradely labeled fibers coursed within ipsilateral SCT. However, the SVT was free of any anterogradely labeled fibers throughout its entire extent in the medulla.

No anterograde labeling was detected in any part of MDH. However, an occasional retrogradely labeled neuron was observed in the deeper magnocellular layers of caudal MDH, as well as in the medially adjacent parvocellular reticular formation (pcRF). A sparse amount of anterograde labeling was present in ipsilateral Vi (Figure 2). This was primarily confined to a narrow band of labeling, measuring approximately 50 μm wide, which bordered SVT in the rostral pole of the dorsolateral subdivision of Vi (dlVi). An occasional anterogradely labeled fiber was also present in the border region of Vi (brVi). These two regions have previously been identified as separate and distinct regions within Vi based on cyto- and myeloarchitectural and connectional criteria (Phelan and Falls, '84a, '85; see also Chapters One and Three). There were no retrogradely labeled neurons in either of these regions. The remaining regions in Vi were devoid of any anterograde labeling.

However, a few lightly labeled spinal projecting neurons were scattered throughout the ventrolateral regions of ipsilateral Vi.

No anterograde labeling was observed in any region of Vo. A few retrogradely labeled neurons were present bilaterally in the ventromedial aspect of the nucleus. In the dorsolateral aspect of ipsilateral Vms, at the level corresponding to the transition from Vo to Vms, a sparse amount of anterograde labeling was present in an area immediately adjacent to SVT.

The main insular portion of the ipsilateral insular trigeminal-cuneatus lateralis nucleus (iV-Cul) also exhibited a moderate density of anterograde labeling in this case. This nucleus is located between SVT and the spinocerebellar tract (SCT) at levels lateral to Vi. It represents a separate and distinct component of the interstitial system of SVT (InSy-SVT; Falls and Phelan, '84; see also Chapter Two). There were no retrogradely labeled neurons in this region.

The overall pattern of anterograde and retrograde labeling in this case was typical for those cases in which HRP injections were centered in the lower cervical and upper thoracic levels of the spinal cord. Larger injections and longer post-injection survival times had no significant effect on either the density or the distribution of spinotrigeminal fibers in these cases. In addition, the injection of HRP into the upper thoracic level of the cord in one animal in which the spinal cord was transected in order to maximize labeling of cut fibers of passage, still resulted in a similar pattern of anterograde labeling of spinotrigeminal fibers as that described in this case.

Case ST-5. A large bilateral injection of HRP was placed between C5 and C6 levels of the spinal cord in this animal (Figure 1A). The needle tracks penetrated through the medial half of the dorsal and ventral horns. Several small injections were made at various depths of the needle track and the resultant spread of HRP included the entire gray and white matter bilaterally at C5 and C6 spinal levels. A

moderate density of anterogradely labeled fibers were conspicuously present in the DCF at levels rostral to the injection site. This labeling continued into the medulla where it gave rise to a moderate density of anterograde labeling in the DCN. The distribution of anterograde labeling in Cun was especially prominent in the ventral "cap" region of the nucleus (Kuypers and Tuerk, '64). In addition, a sparse amount of labeled fibers were present in the LF. These fibers continued into the medulla and gave rise to anterograde labeling localized in the ventrolateral pcRF. The various extratrigeminal brainstem nuclei exhibiting anterograde labeling in case ST-12 were also labeled in this case, although the density of this labeling was now slightly greater.

There was no anterograde labeling detected in any part of MDH. However, several retrogradely labeled neurons were present within the deeper magnocellular layers of MDH especially in the caudal half of the nucleus. A few retrogradely labeled neurons were also situated in the more superficial layers of MDH. In addition, a number of retrogradely labeled neurons in the reticular formation lined the medial border of MDH.

A moderate density of anterograde labeling was present throughout dlVi (Figures 3 and 7A). This was particularly evident in the rostral half of Vi. A few retrogradely labeled neurons were situated within the confines of this anterograde labeling in dlVi. These TS neurons exhibited fusiform-shaped somata and were oriented with their long axis directed dorsoventrally in dlVi. The labeling throughout this dorsolateral region of Vi consisted primarily of terminal-like labeling through which coursed a few HRP labeled fibers in a dorsoventral direction parallel to SVT. The anterograde labeling in dlVi was spatially contiguous with that found more dorsally in the ventral part of Cun.

A sparse amount of anterograde labeling, consisting primarily of a few HRP labeled fibers, was also present in brVi within 50 μm of SVT. However, no

anterograde labeling was detected in any of the remaining parts of Vi. Although, several retrogradely labeled spinal projecting neurons were scattered throughout the ventrolateral regions of the nucleus, no retrogradely labeled neurons were present in brVi.

A sparse amount of anterograde labeling was present in iV-Cul. This anterograde labeling was continuous with that found in brVi through a mediolaterally directed strand of neuropil which traversed SVT. Although a few anterogradely labeled fibers were present in SCT at this level of the medulla, these fibers were chiefly located within the lateral aspect of the tract and were not contiguous with the anterograde labeling in iV-Cul.

The anterograde labeling in dlVi extended rostrally into the caudal 100-200 μm of the dorsolateral aspect of the border region (BZ) of Vo (Falls, Rice and VanWagner, '85; and Falls, '86). This labeling represented the only spinotrigeminal input to Vo in this case. Although there was retrograde labeling of many of the large multipolar-shaped neurons which populate the ventrolateral subdivision of Vo, there were no retrogradely labeled neurons within the confines of the anterograde labeling in dorsolateral BZ.

Two separate regions in the lateral aspect of caudal Vms exhibited a sparse-to-moderate density of anterograde labeling. In the dorsolateral aspect of Vms, a plexus of HRP labeled fibers and terminals was present in a region similar to that described in case ST-12. Another plexus was present in the ventromedial aspect of Vms bordering SVT. An occasional retrogradely labeled neuron was present immediately adjacent to SVT within the confines of the dorsolateral region of spinal input to Vms. However, no retrogradely labeled neurons were located in either the ventrolateral region of anterograde labeling or in the remaining unlabeled portions of Vms.

Case ST-7. A small, unilateral injection of HRP was placed in the dorsal and ventral horns between C2 and C3 levels of the spinal cord in this animal (Figure 1A). The needle tract coursed through the medial part of the lateral funiculus. The spread of HRP included the entire ipsilateral half of the spinal cord. The resultant pattern of anterograde labeling in extratrigeminal brainstem nuclei was similar to that obtained in case ST-12.

No anterograde labeling was detected in MDH. However, retrogradely labeled spinal projecting neurons were present in similar numbers and in similar locations as that described in case ST-5, although they were now slightly less intensely labeled.

A moderate density of anterogradely labeled fibers and terminals were present throughout the rostrocaudal extent of ipsilateral dlVi. A number of retrogradely labeled neurons were distributed within the confines of this anterograde labeling at the mid-rostrocaudal extent of Vi (Figures 2 and 3B). An isolated patch of anterograde labeling was present in the extreme caudal pole of Vi adjacent to SVT (Figure 2, open block arrow). This area represented an isolated part of caudal dlVi which was separated from the anterograde labeling situated more dorsally by a rostral remnant of SG. A few HRP labeled fibers coursed around this rostral remnant of SG to reach this region. The anterograde labeling in this isolated patch became continuous with that in the more dorsal part of dlVi as the remnant of SG disappeared at more rostral levels of the medulla. The spatial relationship between dlVi and this rostral remnant of SG has been described in detail elsewhere (see Chapter One).

A moderate density of anterograde labeling was present in ipsilateral brVi. The labeling in this region extended throughout the entire length of Vi and was quite conspicuous in the caudal half of the nucleus where it formed a distinct band of anterograde labeling throughout the entire dorsoventral extent of brVi. The

density of anterograde labeling within brVi at this level contrasted sharply with the absence of anterograde labeling within the superficial layers of MDH and clearly marked the level of the transition between Vi and MDH. Although no retrogradely labeled neurons were present in brVi, a few retrogradely labeled neurons were distributed throughout the ventrolateral regions of Vi. The ipsilateral iV-Cul nucleus also contained a few scattered anterogradely labeled fibers.

The anterograde labeling within dlVi extended rostrally into the caudal 200-300 μm of the dorsolateral part of ipsilateral BZ. Although no retrogradely labeled neurons were present in this region, numerous retrogradely labeled neurons were distributed bilaterally throughout the ventrolateral aspect of Vo.

A moderate density of anterograde labeling was present in the dorsolateral and ventromedial regions of ipsilateral Vms. These regions of anterograde labeling extended approximately 400 μm in the caudal pole of Vms and were similar to those described in case ST-5. The anterograde labeling in the dorsolateral aspect of Vms was contiguous with a sparse amount of labeled fibers and terminals present in the dorsally adjoining region of the ventral vestibular complex. A few retrogradely labeled neurons were scattered ipsilaterally throughout the ventral regions of caudal Vms. However, none of these neurons were situated within the confines of the anterograde labeling.

Case ST-10. A small, unilateral injection of HRP was placed of the DCF between C1 and C2 levels of the spinal cord in this animal (Figure 1A). This site was specifically chosen in order to determine the contribution of fibers traveling in the DCF to the spinotrigeminal pathway in the rat. The injection site encompassed the entire ipsilateral DCF and the majority of the fibers in the funiculi were intensely labeled. There was also a slight spread of HRP into the ipsilateral gray matter immediately subjacent to the DCF. Anterograde labeling in extratrigeminal

brainstem nuclei included a moderately dense labeling in the contralateral DAO, the ipsilateral ventral regions of Gr and Cun, and the ipsilateral Cul.

A moderate density of anterograde labeling was present throughout the ipsilateral pcRF. This labeling was particularly prominent along the medial margin of MDH. In addition, anterogradely labeled fibers arising from the DCF coursed ventrolaterally through the pcRF to form a group of labeled fibers in the ventrolateral region of pcRF subjacent to SVT. This latter group of fibers extended rostrally to Vms levels of the medulla. A few lightly labeled spinal projecting neurons were distributed throughout the pcRf and the ventral regions of Gr and Cun.

No anterogradely labeled fibers or retrogradely labeled neurons were detected in any part of MDH. However, a relatively dense amount of anterogradely labeled fibers and terminals were present throughout the entire rostrocaudal extent of ipsilateral dlVi (Figure 2). This labeling appeared to arise from the adjoining ventral part of Cun. An occasional retrogradely labeled neuron was present in caudal ipsilateral dlVi within the confines of the anterograde labeling.

A moderate density of anterogradely labeled fibers and terminals was also present in the caudal half of ipsilateral brVi. The anterograde labeling in this region was discontinuously distributed throughout brVi. A moderate density of anterograde labeling was also present in the main insular portion of iV-Cul. However, no retrogradely labeled neurons were detected in either of these two regions.

The anterograde labeling in dlVi extended into the caudal part of ipsilateral BZ. No retrogradely labeled neurons were detected in any part of Vo.

Anterograde labeling, consisting primarily of fine terminal-like labeling, was present in two very dense bands measuring approximately 50 μm wide in the same dorsal and ventral regions of ipsilateral Vms which were identified as spinal recipient zones in case ST-7. The anterograde labeling in the ventromedial aspect of

Vms appeared to arise from the group of labeled fibers situated in the ventrolateral pcRF.

Case ST-8. A series of bilateral injections of HRP were placed in the dorsal and ventral horns at C1 and C2 levels of the spinal cord in this animal (Figure 1A). The spread of HRP involved the entire gray matter at this level of the spinal cord and slightly extended rostrally past the spinomedullary junction (SMJ). The pattern of anterograde labeling in extratrigeminal brainstem nuclei was identical to that obtained in case ST-5, although the density of anterograde labeling was now much greater.

The SCT and SVT contained numerous HRP labeled fibers in this case. The labeled fibers in SCT extended throughout the entire rostrocaudal extent of SVC and continued rostrally into the restiform body. The labeled axons in SVT were primarily located within medially parts of the tract and did not extend past rostral levels of Vi.

A sparse amount of anterograde labeling was present in caudal levels of MDH immediately rostral to SMJ. This labeling was especially concentrated in SG, but did not extend into the more rostral levels of the medulla. A large number of retrogradely labeled neurons were distributed throughout the reticular formation bordering MDH. In addition, some retrogradely labeled neurons were present in the superficial and deeper magnocellular layers of caudal MDH. However, no retrogradely labeled neurons were present in more rostral levels of MDH.

An extremely dense amount of anterograde labeling filled the entire region occupied by dlVi (Figure 2). This region also contained numerous retrogradely labeled neurons possessing primarily fusiform-shaped somata. The anterograde and retrograde labeling in dlVi together with that in the ventral regions of Cun formed a continuous band of labeling in the dorsolateral medulla. In addition, numerous bundles of HRP labeled axons were present in the region immediately dorsal to Vi.

These bundles of labeled axons continued rostrally throughout the entire extent of SVC.

A relatively dense amount of anterograde labeling was present throughout the entire rostrocaudal extent of brVi (Figure 3C-F) and was continuous with the anterograde labeling present in the ventrolateral aspect of pcRF. This labeling formed a dense band measuring up to 100 μm in diameter. However, the continuity of this band of labeling was conspicuously interrupted by the presence of up to three oval-shaped regions of relatively less dense anterograde labeling (Figure 3D, arrowheads; and Figure 3E). These oval-shaped regions, measuring approximately 120 μm by 200 μm in diameter, were evenly spaced along the dorsoventral extent of brVi. The anterograde labeling in these regions consisted primarily of a fine plexus of terminal-like labeling as well as a few large HRP labeled fibers. These oval-shaped regions did not form continuous rostrocaudal columns in brVi, rather they represented discrete structures. Numerous retrogradely labeled neurons with fusiform to oval-shaped somata were distributed throughout the band of labeling in brVi. In addition, retrogradely labeled neurons possessing small oval-shaped somata were widely distributed throughout each of the oval-shaped regions and formed conspicuous clusters of cells in brVi (Figure 7E). The asymmetrical density of retrograde labeling in brVi, coupled with a similar asymmetry in the density of the HRP injection in the spinal cord, suggested that these latter neurons projected primarily to the ipsilateral cervical cord.

The dense anterograde labeling in brVi was contiguous with the numerous islands of interstitial neuropil embedded among the fibers of SVT (Figure 3C, arrowheads). These islands represent interstitial regions of iV-Cul. The main insular and more ventral insular regions of iV-Cul also exhibited dense anterograde labeling. Retrogradely labeled neurons were not present in any of the interstitial or insular portions of iV-Cul.

The ventrolateral region of Vi also exhibited a sparse amount of anterogradely labeled fibers and terminals. In addition, a large number of retrogradely labeled neurons were distributed throughout this region of Vi. The majority of the labeled fibers in this region were present in the deep axon bundles (DAB's) which permeated the neuropil. These DAB's have previously been described as representing bundles of axons interconnecting rostral and caudal subnuclei of SVC (Gobel and Purvis, '72).

The anterograde labeling in dlVi, brVi and the ventrolateral regions of Vi all extended rostrally throughout the entire rostrocaudal extent of Vo. However, the density of labeling in these regions of Vo was less than that in the similar regions of Vi. The extensions of brVi into BZ formed a continuous band of labeling throughout the entire lateral aspect of Vo. Numerous retrogradely labeled neurons were distributed throughout the ventrolateral regions of Vo. In addition, a few retrogradely labeled neurons were present within the confines of the anterograde labeling in ventral parts of BZ (Figure 3G). However, the oval-shaped clusters of retrogradely labeled cells which characterized brVi were not present in BZ. In addition, the dorsolateral part of BZ did not contain any retrogradely labeled neurons.

The same two spinal recipient zones identified in Vms in previous cases also exhibited a dense amount of anterograde labeling (Figure 3H-I). A few retrogradely labeled neurons with small fusiform or larger multipolar-shaped somata were distributed within the confines of this dorsolateral region of anterograde labeling (Figure 3H). In addition, a few retrogradely labeled neurons were distributed throughout the ventral half of Vms in areas clearly outside of the ventromedial region of anterograde labeling which bordered SVT.

Case ST-24. A series of large injections of HRP were centered in the DCF and the dorsal and ventral horns at C2-C5 levels of the spinal cord in this animal

(injection site not shown). The spread of HRP included the entire gray and white matter bilaterally and extended up to the SMJ. The axonally transported HRP was visualized using the Co-GOD method in order to examine in more detail the morphology of spinotrigeminal fibers. This histochemical method resulted in a more uniformly dense and diffuse filling of spinotrigeminal fibers and terminals in this case compared to the granular type of labeling obtained in previous cases using the TMB method of HRP visualization. The results of the present case were typical for the type of labeling obtained using this protocol.

The resultant pattern of anterograde labeling in extratrigeminal brainstem and SVC nuclei was identical to that predicted from the combined results of the previously described cases. In addition, numerous retrogradely labeled neurons were distributed throughout the medulla, although they were more lightly labeled compared to the retrogradely labeled neurons visualized with TMB.

The spinal input to dlVi consisted primarily of thin fibers measuring less than 1.5 μm in diameter. These fibers clearly originated from the ventral Cun and coursed in a fairly straight fashion through dlVi (Figure 4). These fibers gave rise to a few thin collaterals which formed a diffuse plexus of lightly labeled fibers throughout dlVi. These collaterals exhibited small oval-shaped boutons en passant and terminal boutons measuring less than 1.0 μm in diameter. Some of these terminals were closely apposed to retrogradely labeled TS neurons in this region (Figure 4A, arrows). Individual fibers and their collaterals were difficult to reconstruct in dlVi due to the vast number and intermingling of the fibers in this region.

The spinal input to brVi consisted of two morphologically different types of fibers. The first type was similar to those present in dlVi, although they gave rise to a greater number of en passant swellings than did the fibers in dlVi (Figure 4B, arrows). The en passant boutons measured less than 1.0 μm in diameter. The second

type of labeled axons were relatively thicker fibers measuring approximately 1.5-2.0 μm in diameter. These larger fibers coursed through brVi and sometimes gave rise to thinner axon collaterals. This second type of fiber traveled through the entire region of brVi. However, the oval-shaped clusters of retrogradely labeled neurons in brVi exhibited mainly a fine plexus of thin fibers and terminal-like endings (Figure 4C). Individual fibers and their collaterals were also difficult to reconstruct in brVi (Figure 8C).

The spinal input to iV-Cul consisted of relatively thick axons which were morphologically similar to those in brVi. These fibers emitted thin axon collaterals, measuring 1.0-1.5 μm in diameter and could extend up to 200 μm in length. These axon collaterals gave rise to numerous irregularly spaced small-to-large sized boutons en passant and terminal bouton-like swellings (Figure 4D-F). These boutons ranged in size from 1.0-3.0 μm in diameter. The smaller boutons were spherical to ovoid in shape while the larger boutons were primarily irregular in outline. The largest of these boutons were larger than any of those present in any other spinal recipient zone in SVC. Individual axons and their collaterals were easily reconstructed in this nucleus. A single large axon could give rise to several thin axon collaterals which usually coursed in a straight path in the neuropil and did not branch further (Figure 5). These collaterals could exhibit up to ten or more boutons en passant with interbouton distances ranging from 5.0 to 50.0 μm.

The spinal inputs to BZ consisted of fibers which exhibited a similar morphology as those present in the respective zones of dlVi and brVi. The spinal inputs to Vms were also morphologically similar to those fibers present in Vi and Vo. Individual fibers and their collaterals were also difficult to distinguish in these subnuclei of SVC.

Autoradiographic Studies

It is well known that the HRP technique utilized in the series of experiments described above has the disadvantage that fibers of passage through the injection site can contribute to the resulting pattern of anterograde and retrograde labeling. In view of this, the spinotrigeminal projection revealed above could have originated from a variety of sources including secondary cells in the upper cervical spinal cord, secondary cells located at more caudal levels of the cord, or primary spinal dorsal root fibers. In an attempt to distinguish among these possibilities, a series of unilateral injections of tritiated amino acids were placed at various levels of the cervical spinal cord. The anterograde transport of tritiated amino acids is particularly useful in resolving this question since it does not have the fiber of passage problem associated with the HRP technique.

In those animals which received injections of tritiated amino acids in C3-C5 levels of the spinal cord, there was no detectable labeling in any region of SVC well above background levels. However, in those animals in which the injections were centered in more rostral levels of the cervical cord, there was a consistent labeling of the spinotrigeminal projection. The results of these latter injections will be summarized through the presentation of three representative cases.

Case AR-21. A single unilateral injection of tritiated amino acids was centered in the dorsal horn between C2 and C3 levels of the spinal cord (Figure 1B). The injection site spread into the dorsal and ventral horn of the cord at these levels sparing only the central gray matter surrounding the central canal. Autoradiographically detected silver grains were distributed well above background levels in several extratrigeminal nuclei including the contralateral DAO, the ipsilateral LR, and the ipsilateral DCN.

Anterogradely labeled fibers ascended from the level of the injection site into the medulla where they were localized to the ventral regions of the DCN and in

the ventrolateral region of pcRF near SVT. Silver grains were especially concentrated in the reticular formation along the medial margin of SVC. In addition, anterograde labeling was present throughout SCT, but noticeably absent from SVT.

A sparse density of silver grains was present throughout ipsilateral dlVi and brVi. The labeling in these regions did not extend rostrally into Vo. The distribution of silver grains in dlVi was often organized into small discrete clusters which encircled neuronal somata (Figure 6A, arrowheads). These clusters presumably represented labeling of axon terminals, Some silver grains were concentrated within the main insular portion of ipsilateral iV-Cul. A sparse amount of labeling was also present in the same dorsolateral and ventromedial aspects of ipsilateral Vms which were identified as spinal recipient zones in the HRP cases described above.

Case AR-20. A single, unilateral injection of tritiated amino acids was centered in the dorsal horn between C1 and C2 levels of the spinal cord (Figure 1B). The injection site spread into the dorsal and ventral horn of the cord at these levels sparing only the central gray matter surrounding the central canal and the ventralmost part of the ventral horn. Silver grains were distributed well above background levels in the same extratrigeminal nuclei labeled in Case AR-21. The SCT also exhibited a moderate density of silver grains.

A moderate density of silver grains were present in dlVi (Figure 6B) and brVi. A sparse amount of silver grains was also concentrated over the caudal ventrolateral region of Vi, including some of the DAB's in this region. The anterograde labeling in dlVi and brVi extended rostrally into the caudal half of BZ. In addition, a moderate density of silver grains was distributed in the same two regions of Vms as obtained in case AR-21.

Case AR-17. A single, unilateral injection of tritiated amino acids was centered in the dorsal horn at the transition from C1 to SMJ (Figure 1B). The

spread of the injection encompassed the dorsal horn of the spinal cord at this level, but spared the central gray matter surrounding the central canal and most of the ventral horn.

A dense amount of anterograde labeling was present throughout SCT as well as in the medial part of SVT. A sparse amount of silver grains was present in MDH at levels just rostral to the injection site. In addition, many of the DAB's in this region were heavily labeled.

A moderate concentration of silver grains was localized in dlVi (Figure 6C and D) and throughout the dorsolateral part of BZ (Figure 6E). The silver grains in dlVi were often organized into distinct pericellular clusters (Figure 6C, arrows) or serially aligned over fibers (Figure 6D, arrows). In addition, a moderate density of silver grains was present in brVi and throughout the ventral part of BZ. Although the density of anterograde labeling in BZ was less than that in either dlVi or brVi, it formed a distinct band of continuous labeling in BZ. A sparse amount of silver grains was also concentrated in the main insular portion of iV-Cul. The two spinal recipient zones in Vms also exhibited a moderate density of silver grains (Figure 6F). In addition, a moderate density of silver grains was distributed throughout the ventrolateral region of Vi, Vo and caudal Vms. The greatest amount of this labeling was present in the caudal pole of ventrolateral Vi, with progressively less found at more rostral levels of the medulla. The majority of this labeling was present over the numerous DAB's which permeated the neuropil.

Figure 1

Schematic diagram illustrating the position and extent of representative injections of HRP (A) and tritiated amino acids (B) in cervical levels of the spinal cord.

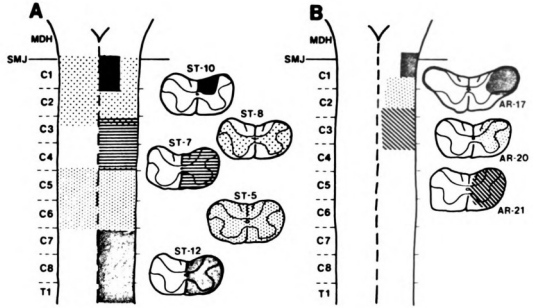
A
MDH
SMJ
C1
C2
C3
C4
C5
C6
C7
C8
T1
ST-10
ST-8
ST-7
ST-5
ST-12
B
MDH
SMJ
C1
C2
C3
C4
C5
C6
C7
C8
T1
AR-17
AR-20
AR-21

Figure 2

A series of schematic diagrams illustrating the distribution of anterograde and retrograde labeling at different levels of SVC following the injection of HRP into the cervical spinal cord. The case numbers refer to the injection sites depicted in Figure 1A. The open block arrow in case ST-7 marks an isolated patch of dlVi at the level of the transition between MDH and Vi.

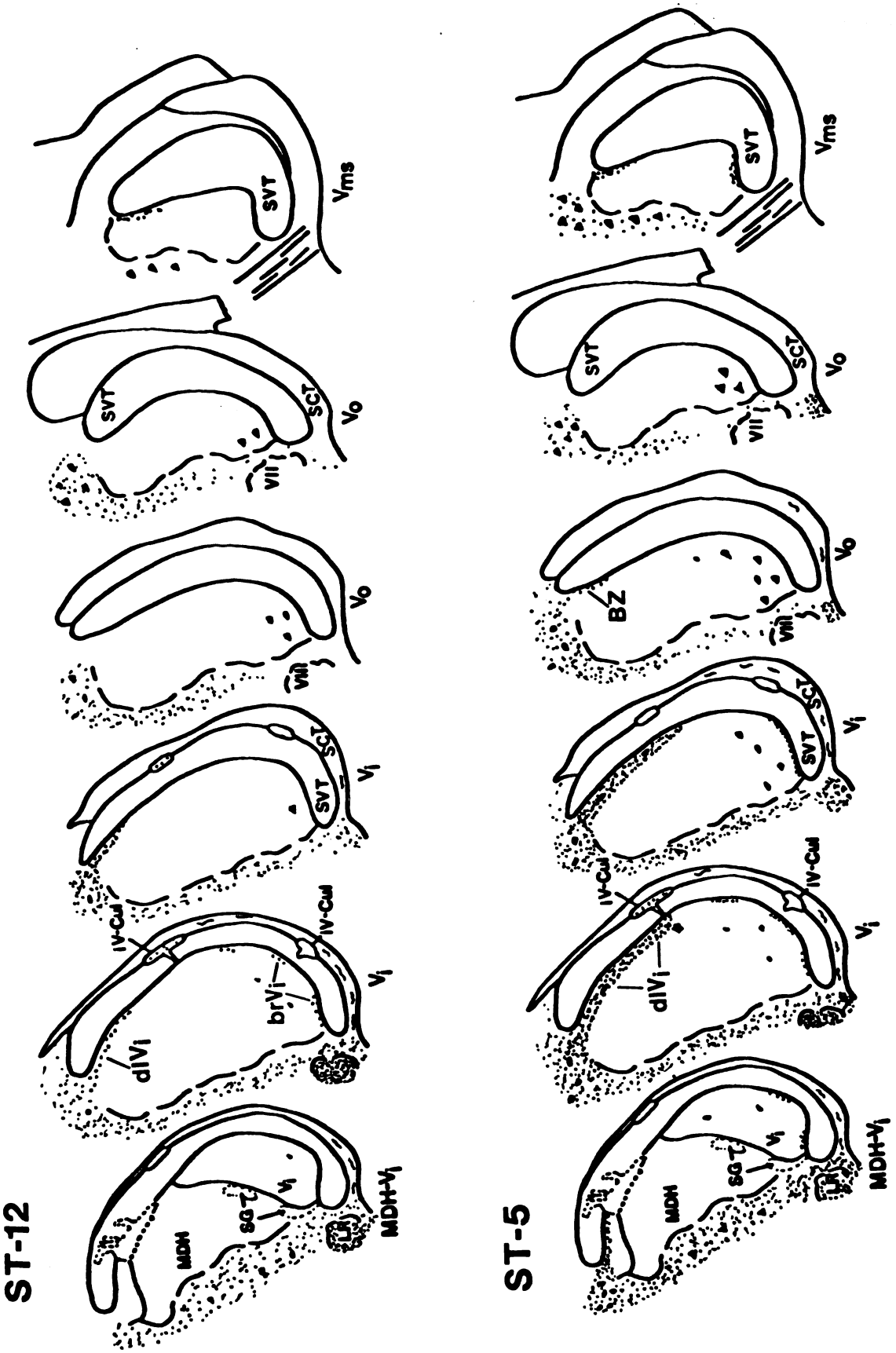
ST-12
MDH
SG
LR
MDH+V1
dlV1
brV1
IV-Cu
V1
SCT
SVT
Vo
VII
Vms
ST-5
BZ

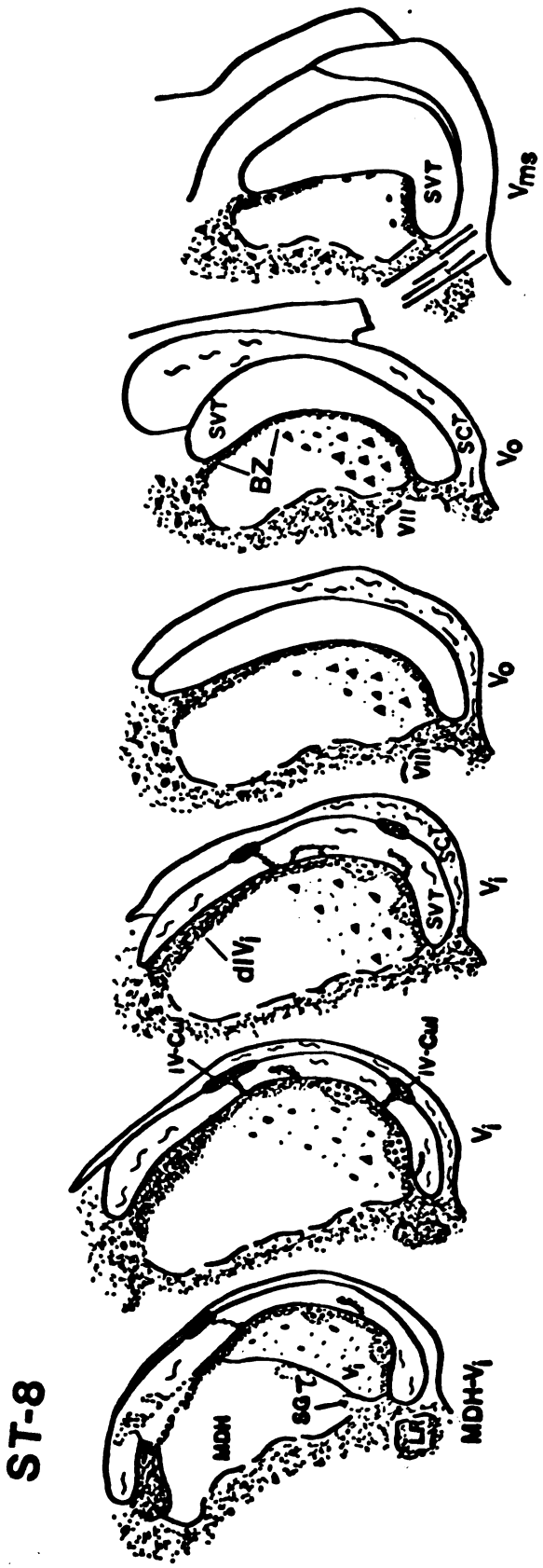
ST-8
MDH
SGT
LR
MDH-V$_l$
IV-Cm
IV-Cm
V$_l$
pIVl
SVT
SCT
V$_l$
V$_o$
VIII
SVT
BZ
SCT
V$_o$
SVT
V$_{ms}$

Figure 3

A series of photomicrographs showing examples of anterograde labeling of spinotrigeminal fibers and retrograde labeling of TS neurons through various levels of SVC.

A. Anterograde labeling in dlVi in case ST-5 (X120).

B. Anterograde and retrograde labeling in dlVi in case ST-7 (X120).

C-I. Anterograde and retrograde labeling in case ST-8 (C, D and F-I X120; E X480). Anterogradely labeled spinotrigeminal fibers are illustrated in brVi (C-F) including the oval-shaped regions which contain clusters of TS neurons (D and E, arrowheads); the interstitial and insular portions of iV-Cul (C, arrowheads); the caudal part of ventromedial BZ; and the dorsolateral (H) and ventromedial (I) regions of Vms bordering SVT.

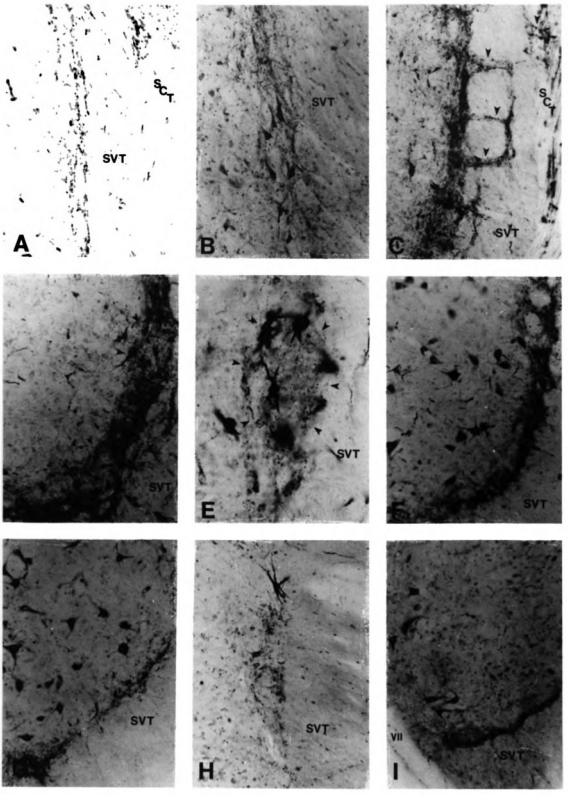
SCT
SVT
A
SVT
B
SCT
SVT
C
SVT
D
SVT
E
SVT
F
SVT
G
SVT
H
VII
SVT
I

Figure 4

A series of photomicrographs showing the morphology of spinotrigeminal fibers visualized using the Co-GOD method in case ST-24. HRP-labeled spinotrigeminal fibers are illustrated in dlVi (A), brVi (B) including the oval-shaped clusters of retrogradely labeled cells (C, arrowheads), and the main insular portions of iV-Cul. The open block arrows in A mark the location of retrogradely labeled dlVi neurons. The arrows in B point to thin fibers in brVi which give rise to several en passant boutons (X480).

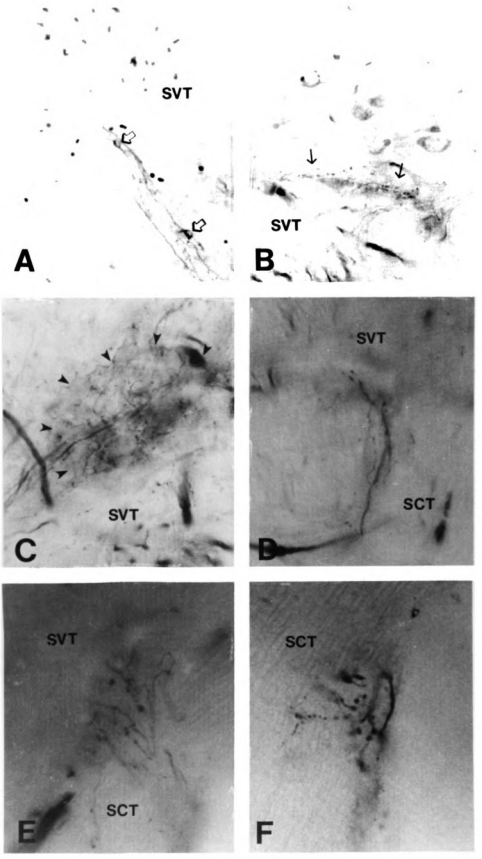
SVT
A
SVT
B
SVT
C
SVT
SCT
D
SVT
SCT
E
SCT
F

Figure 5

Camera lucida drawings illustrating the morphology of representative spinotrigeminal fibers in iV-Cul visualized using the Co-GOD method. The fiber in A corresponds to that shown in Figure 8D; while the plexus shown in C corresponds to that shown in Figure 8E. The inset diagrams illustrate the position of these labeled fibers at rostral (B) and caudal (D) levels of the medulla. The scale bar in A also applies to C.

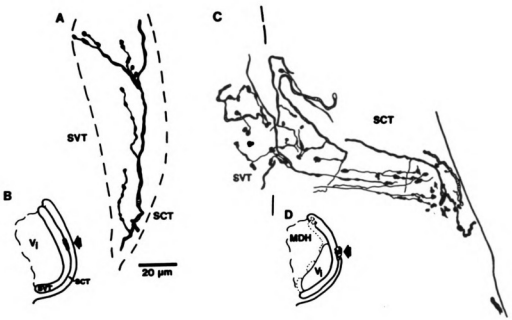
A
SVT
SCT
20 µm
B
VI
SVT
SCT
C
SCT
SVT
D
MDH
VI

Figure 6

A series of photomicrographs showing examples of the resultant pattern of anterograde labeling of the spinotrigeminal pathway following the injection of tritiated amino acids into the cervical spinal cord as viewed under darkfield (A, case AR-21; and B, case AR-20) and brightfield (C-F, case AR-17) illumination. Anterograde labeling is depicted in dlVi (A-D), the caudal dorsolateral part of BZ (E), and the ventromedial region of Vms (F). The arrows in A and C mark the pericellular distribution of silver grains, while those in D mark a labeled fiber (x480).

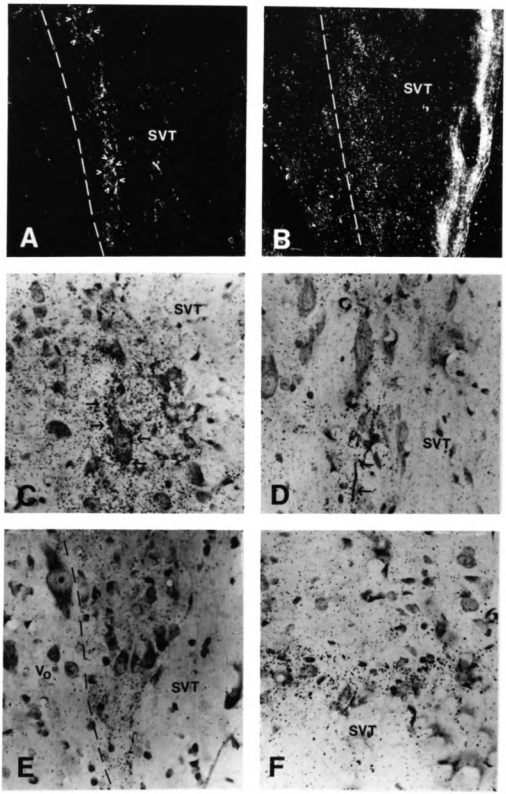
SVT
A
SVT
B
SVT
C
SVT
D
V_o
SVT
E
SVT
F

Figure 7

A schematic diagram summarizing the location of the spinal recipient zones in Vi, Vo and Vms levels of SVC (solid filled areas) and the known secondary projections of cells in these areas to the thalamus, cerebellum, MDH, and spinal cord. The thick lines represent the existence of a major projection, while the thin lines represent a relatively minor contribution to the pathway. The projections illustrated in this diagram were based on the results of the present study in conjunction with several other studies cited in the discussion.

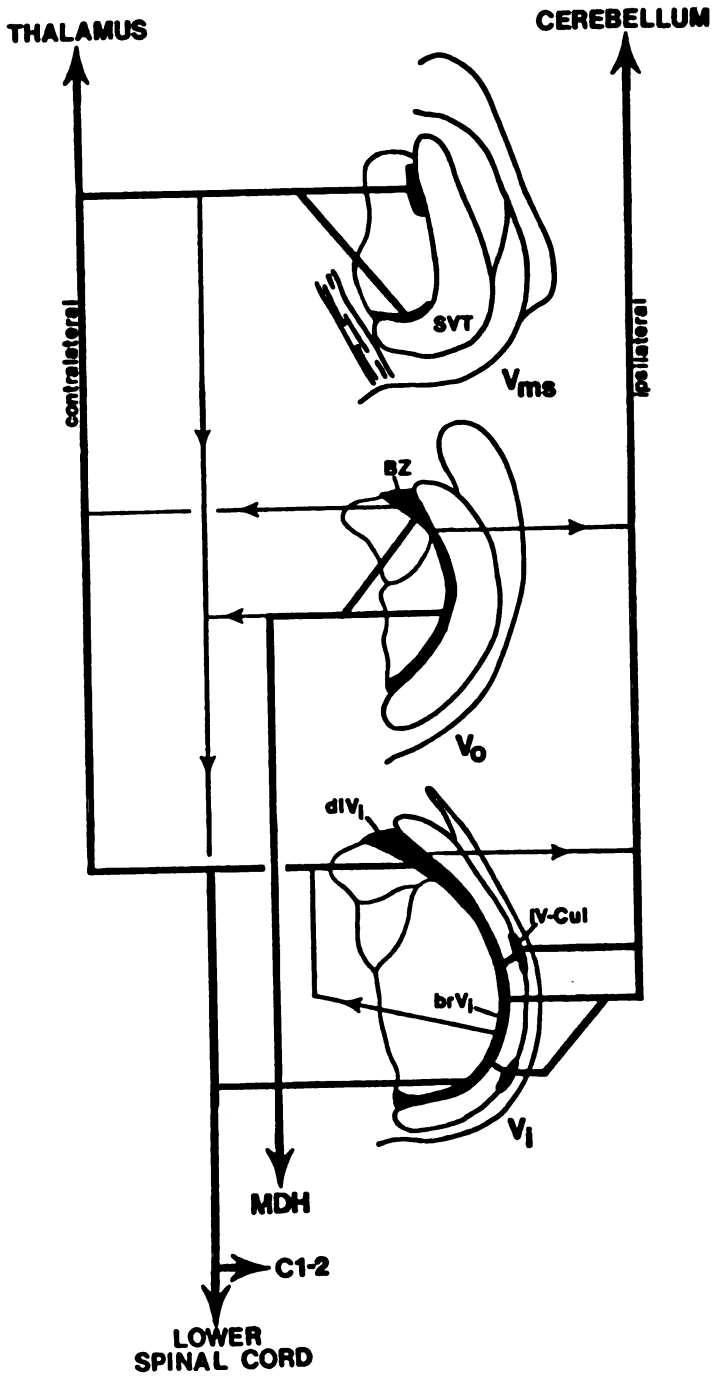
THALAMUS
CEREBELLUM
contralateral
ipsilateral
SVT
V_{ms}
BZ
V_o
dlV_l
lV-Cul
brV_l
V_l
MDH
C1-2
LOWER
SPINAL CORD

DISCUSSION

In recent years, the presence of a direct projection from the spinal cord to SVC has received relatively little attention. Nevertheless, the literature contains numerous references to studies which provide anatomical evidence supporting the presence of a direct spinotrigeminal pathway in mammals. However, these investigations, for the most part, include only experimental degeneration studies employing various silver impregnation methods. Considering the number of conflicting results reported in these studies, it is quite surprising that the distribution of spinal afferents within SVC has not been re-examined using any of the modern anterograde transport techniques. It is possible that the conspicuous lack of any comprehensive literature review of experimental evidence supporting the presence of a spinotrigeminal pathway in mammals may have contributed to the fact that this pathway has recently been overlooked. In view of this, an historical survey of the relevant literature is provided prior to discussing the specific findings of the present study.

Historical Review

The presence of a direct spinal input to SVC was first suggested by Astrom (1953) in his Golgi impregnation study of mouse brainstem, in which he identified a number of thin fibers which coursed concentrically along the medial border of SVT. These fibers contributed to a dense axonal plexus which delineated a "marginal nucleus", representing one of several subnuclei he distinguished in SVN. These fibers were traced to the cuneate fasciculus and some of them exhibited terminations within the 'marginal nucleus'. On the basis of these observations, Astrom proposed that at least some of the fibers represented an ascending spinal input to his "marginal nucleus". Although he recognized, but did not choose to

adopt, the terminology proposed several years earlier by Olszewski ('50) identifying three separate subdivisions in primate SVN (i.e., Vo, Vi and MDH), it is clear that the location of the "marginal nucleus of Astrom" corresponds to the level of Vi (see Chapter One).

Spinal Cord Lesion Studies. The first experimental anatomical evidence in support of a spinotrigeminal pathway was published by Johnson ('54) in an abstract describing the use of the silver impregnation method of Nauta ('57) to to determine the distribution of ascending spinobulbar connections in the cat following spinal cord hemisections. This report indicated that, in addition to widespread spinoreticular connections, a principally ipsilateral distribution of degenerating axons was present within Vo. However, no details are provided on the extent or precise distribution of these spinal afferents.

Two years later, the studies of Rossi and Brodal ('56), using the silver impregnation method of Glees ('46), and Torvik ('56), using the Nauta method ('57), provided the first detailed accounts of the distribution of spinal afferents within SVC following partial or complete spinal cord hemisections in cat and rat, respectively. Rossi and Brodal concluded that spinal afferents arose from cervical, thoracic and lumbar levels of the cord, ascended in the ventrolateral funiculus (VLF) and distributed bilaterally and diffusely to all SVC nuclei. In particular, they noted that Vms (primarily its ventralmost part) and nucleus caudalis (that is, MDH, especially its caudalmost part) received more spinal afferents than the other nuclei in SVC. Torvik ('56), on the other hand, demonstrated a rather restricted distribution of spinal afferents to SVC. In particular, he reported a moderate number of thin degenerating fibers distributed ipsilaterally within SVN following partial hemisection at C2 and C3 levels of the spinal cord. These spinotrigeminal fibers ascended chiefly in the VLF and curved along the concave side of the dorsal

part of SVT to terminate exclusively in the dorsolateralmost part of Vo subjacent to SVT, at the level of the transition from Vi to Vo.

A number of similar experimental degeneration studies were conducted in a variety of mammals during the last thirty years. Although some of these studies denied the existence of spinotrigeminal fibers in a number of mammals, other studies did report the presence of degenerating fibers within SVC following lesions of the spinal cord. Breazile and Kitchell ('68), for example, reported degenerating fibers and terminals in SVN of the domestic pig following lesions primarily of the VLF at cervical and thoracic cord levels. In particular, they reported that MDH, Vi and Vms received a bilateral projection from cervical and thoracic levels, while Vo only received an ipsilateral projection from the cervical cord. These authors further noted that the latter projection to Vo might actually have represented intrinsic intratrigeminal connections which may have appeared due to the possible involvement of MDH within the lesion site. In addition, Breazile and Kitchell noted that there was a greater ipsilateral concentration of degenerating fibers in MDH following cervical lesions, that there was a generally increased density of degenerating fibers in caudal portions of Vi, and that degenerating fibers were present within the dorsal and ventral parts of Vms with very few seen in the center of the nucleus. In other studies, Kerr ('75) described a small cluster of degenerating fibers in the ophthalmic area of ipsilateral MDH at a level just below the obex, following lesions of the VLF at C4 in the monkey. More recently, Ring and Ganchrow ('83) reported degenerating fibers in a similar location following lesions at C7-T1 in the hedgehog. However, in the latter case, the projection appeared entirely contralateral to the side of the lesion.

Several additional studies, conducted primarily to identify the distribution of spinal inputs within the dorsal column nuclei, illustrated but did not directly discuss, the presence of degenerating fibers within SVN (Nauta and Kuypers, '58; Rustioni,

'74; Rustioni and Molenaar, '75; Jane and Schroeder, '71; Rustioni et al., '79) following transections at various spinal cord levels. Nauta and Kuypers ('58), for example, illustrated the presence of sparse degeneration within the rostral levels of SVN following partial transection of the VLF at C1 in the cat (see their Figures 2 and 3). On the other hand, Rustioni ('74) and Rustioni and Molenaar ('75) illustrated projections to ipsilateral MDH and Vi following lesions at C2 and C4 in the cat (see their Figure 7, levels 2,3,5,and 6), while Rustioni et al. ('79) illustrated similar projections following transections at C3 in the monkey (see their Figures 9 and 10). In addition, Jane and Schroeder ('71) illustrated degenerating fibers in rostral levels of SVN following cervical cord transection in the hedgehog (see their Figure 4).

Dorsal Rhizotomy and Successive Degeneration Studies. Over the last thirty years, a number of additional experimental degeneration studies were conducted in order to determine the relative contribution of primary and non-primary fibers to the spinobulbar projection. Several of these studies specifically reported the distribution of primary spinal inputs to SVN in cat (Hand, '66; Rustioni and Macchi, '68; Imai and Kusama, '69; Keller and Hand, '70, Kerr, '72b) and monkey (Shriver et al., '68). Hand ('66), for example, reported a bilateral projection, with an ipsilateral predominance, to rostral MDH and caudal Vi from L1, L5 and L6 but not S1 dorsal roots. In particular, a moderate L1 input and a sparse input from L5 and L6 terminated in the ventral and ventromedial aspects of rostral MDH and caudal Vi. In addition, L1 appeared to contribute a sparse input to the dorsolateral aspect of Vi. In contrast, Rustioni and Macchi ('68) reported that the only primary spinotrigeminal projection arose exclusively from the S3 dorsal root and distributed bilaterally to Vi. Imai and Kusama ('69) reported a spinotrigeminal projection which arose from C2 but not C1, C3 or C4 dorsal roots. They noted that although a small number of degenerating fibers ascended in the medial part of SVN to terminate in

the dorsomedial part of MDH, additional degenerating fibers, which ascended in the ventral funiculus, entered the ventrolateral corner of Cun and continued ventrolaterally along the lateral border of Vi where they consistently terminated in clusters adjacent to SVT. Keller and Hand ('70) reported the presence of a sparse number of degenerating fibers in the dorsolateral edge of ipsilateral Vi following section of the C3 dorsal root while sectioning of the other lower cervical and upper thoracic dorsal roots did not appear to contribute any spinotrigeminal afferent fibers. These authors further noted that occasional degenerating fibers exited from the dorsal funiculus and coursed through the ventrolateral edge of Cun to terminate in the dorsomedial edge of MDH. Kerr ('72b) identified two discrete groups of fibers which arose from the first four cervical dorsal roots and contributed to a spinotrigeminal projection which distributed to a region extending from the obex to three millimeters anterior, which he identified as MDH. The first group ascended in the dorsal funiculi and crossed the medial aspect of SVN to distribute bilaterally, with an ipsilateral predominance, to an area which he identified as "area C". This region, located in the ophthalmic portion of the nucleus received a variable projection from the first four cervical roots which consisted of a small collection or fairly pronounced cluster of degenerating fibers. Kerr further noted that this region appeared gelatinous and presented other structural characteristics suggestive of the SG layer of MDH. The second group of fibers consisted of an ipsilateral projection to a region, situated in the dorsolateral aspect of the nucleus adjacent to SVT, which he designated as "area L". Although this area received projections from C2 and C3 dorsal roots, as well as a poorer projection from the C4 dorsal root, it never received a contribution from the C1 dorsal root. In addition, Kerr noted that "area L" had previously been shown to receive fibers from the glossopharyngeal and vagus nerves ('62). A small projection arising from the C2 dorsal root was reported by Shriver et al. ('68) in the monkey. These fibers ascended in the cuneate fasciculus and

terminated in the magnocellular portion of caudal SVN. In the only study involving dorsal root rhizotomies in the rat, Torvik ('56) denied a contribution from the first four cervical dorsal roots to the spinotrigeminal projection.

A non-primary source of fibers from lower cervical to upper thoracic levels of the cord was discovered by Rustioni ('73) and Rustioni and Molenaar ('75) using successive degeneration techniques in the cat. In particular, these authors reported that fibers ascended in the ventral funiculus and terminated bilaterally in the ventromedial edge of rostral MDH and caudal Vi as well as ipsilaterally in the dorsolateral part of Vi.

Electrophysiological Studies. The spinotrigeminal pathway has remained relatively unexamined from an electrophysiological standpoint. In fact, only a few studies can be found in the literature which refer to this pathway. All of these studies were conducted in the cat. In 1956, Rossi and Brodal referred to an unpublished study by Palestini, Rossi and Zanchetti, in which some extracellularly recorded units in SVN, responded to natural stimulation of the limbs. Ten years later, Kerr ('66a) referred to an unpublished study (Kerr, Schwassman, Stern and Kruger), which denied the presence of SVN cells responsive to physiological stimulation of fields other than those of the trigeminal distributions. He suggested, in fact, that Palestini and associates may have recorded from ascending spinal fibers in SVN rather than from neurons. In an earlier study, Kruger, Siminoff and Witkovsky ('61) tentatively suggested that there was some indication of upper cervical dorsal root representation within SVN. Kruger and Michael ('62a) later identified this as a tactile representation from C1 and C2 dorsal roots which was distributed to the dorsum of the ear and the top and caudal surface of the head immediately below the peripheral representation of the ophthalmic division of the trigeminal nerve. In a later study, Kerr, Kruger, Schwassman and Stern ('68) reported that C2 is represented in the lateral portions of SVC, however they did not

provide any indication of the level of this input within the SVC. In addition, Gordon, Landgren and Seed ('61) reported that a few neurons, located deep within MDH, exhibited wide receptive fields which responded to squeezing of the forepaw, hindpaw and trunk. In subsequent studies, Darian-Smith, Proctor and Ryan ('63), Darian-Smith, Phillips and Ryan ('63) and Eisenmann, Landgren and Novin ('63) reported the presence of similar neurons located deep within the ventromedial parts of Vms, Vo and Vi. These latter studies presumed however, that these ventromedially located cells represented parvocellular reticular neurons. In a more recent study, Azerad, Woda and Albe-Fessard ('82) reported that some neurons were found in various parts of Vo which exhibited receptive fields activated by tap and/or pressure partially within and partially outside of the trigeminal fields. However, Hayashi et al. ('84) recently denied the presence of neurons in Vi with receptive fields outside of the peripheral representation of the V nerve.

Summary. This review of the literature reveals the existence of numerous studies reporting the distribution of degenerating fibers within SVC following spinal cord transections or dorsal rhizotomies. These studies support the presence of a direct spinotrigeminal pathway in several different mammals. However, it is clear from this review that there is no general consensus among these studies regarding the origin, course or distribution of spinotrigeminal fibers within any species. The majority of these studies indicated a rather restricted distribution of spinal afferents within SVC which does not support the original reports of Rossi and Brodal ('56) and Breazile and Kitchell ('68) suggesting a more widespread bilateral projections in cat and pig, respectively. The majority of the inconsistencies amongst these anatomical studies may likely be attributed to the inherent difficulties and limitations of the experimental degeneration techniques employed (see Bowsher, Brodal, and Walberg, '60 for review). However, the existence of a variable input of spinal afferents to SVC, from animal to animal, as reported by Kerr ('72b) may have

partially contributed to these inconsistencies. In addition, the possibility must also be considered that some of these inconsistencies may be due to the existence of a true species difference in the organization of spinal afferents to SVC.

This review also illustrates that electrophysiological studies have not yet provided confirmation of the presence of a direct spinal trigeminal projection. In particular, the available electrophysiological studies provide no indication that cells in these anatomically defined spinal recipient regions exhibit any responses to stimulation of fields outside of the peripheral distribution of the V nerve. The functional nature of the spinotrigeminal pathway therefore, remains as much of a mystery as does the precise details of its organization.

The Distribution of Spinal Afferents in SVC.

The results of the present study confirm the existence of a direct projection from the spinal cord to SVC in the rat using modern anterograde transport techniques. These findings reveal that the spinotrigeminal pathway in this animal consists of an ipsilateral projection distributed exclusively to relatively narrow regions subjacent to SVT in Vi, Vo and Vms, with the densest and most consistent anterograde labeling of spinal afferents occurring in Vi.

In addition, however, the spinal recipient zones in SVC can be separated into two groups. The first group received an increasing density of spinal afferents following injections centered in progressively more rostral levels of the spinal cord. This group included Vms, the band region of brVi, and the caudal dorsolateral part of BZ. The second group received a spinal afferent input only when the injection involved C1-C2 levels of the spinal cord. This group included the ventral part of caudal BZ and the entire rostral half of BZ. This particular distribution pattern has not previously been reported in any species (see "The Origin and Course of Spinotrigeminal Afferents" for further discussion).

The present study indicates that two spinal recipient zones exist in Vi. These two regions, dlVi and brVI, have previously been identified as distinct regions of rat Vi based on differences in their cyto- and myeloarchitecture and connectivity (Phelan and Falls, '84a, '85; see also Chapters One and Three). The results of the present study thus provide additional anatomical evidence supporting the distinction of these two regions from other regions in Vi.

The present results confirm the initial suggestion by Astrom ('53) that a spinotrigeminal projection exists within rodent Vi. Furthermore, the combined distribution of spinal afferents in dlVi and brVi provides experimental evidence supporting Astrom's initial contention that spinal afferents are distributed to the entire lateral region of the nucleus.

The present study is in complete agreement with the study of Torvik ('56) regarding the exclusive ipsilaterality of the spinotrigeminal pathway in rat, but differs significantly with regard to the overall distribution pattern for spinotrigeminal afferents. In particular, Torvik reported the presence of a single spinal recipient zone in SVN which was situated in the dorsolateral aspect of the nucleus at a level designated as caudal Vo near the Vi/Vo transition. However, since Fukishima and Kerr ('79) recently redefined the rostral extent of rat Vi, based on differences in cytoarchitecture and thalamic connectivity, the level of the distribution of spinal afferents indicated by Torvik is now considered to lie near the middle of the rostrocaudal length of Vi. Therefore, the dorsolateral spinal recipient zone of Torvik ('56) corresponds to dlVi in the present study. The present study, therefore, confirms the existence of a spinal recipient zone in the dorsolateral part of Vi. However, the present study is the first to describe the presence of spinal afferents in brVi, Vo and Vms in the rat. The difference between the overall distribution of spinotrigeminal afferents as reported by Torvik ('56) and in the

present study may simply be explained by inherent differences in the sensitivity of the experimental techniques employed.

The overall distribution pattern for spinotrigeminal afferents reported in the present study has not previously been described in any of the experimental degeneration studies conducted in other mammalian species. However, previous studies have reported the distribution of spinal afferents within some of these specific regions of SVC. In particular, several studies in the cat illustrated spinal afferents which terminated specifically within the dorsolateral region of Vi (Hand, '66; Imai and Kusama, '69; Keller and Hand, '70; Kerr, '72b; Rustioni, '74; and Rustioni and Molenaar, '75). Although there have been no cytoarchitectural studies to suggest the presence of a region of Vi analogous to rat dlVi in any other species, this dorsolateral region of Vi in the cat may, in fact, represent a feline homologue of dlVi.

Two studies in the cat (Imai and Kusama, '69; Kerr, '72b), deserve particular attention because they reported that the distribution of primary spinal afferents within the dorsolateral region of Vi (Kerr's "area L") appeared in clusters. This arrangement was not observed in the present study, rather the anterograde labeling filled the entire region of dlVi. However, some of the anterograde HRP labeling did appear as an isolated patch in the caudal part of Vi. This region actually represented an isolated part of dlVi. It is possible that the clusters described by Kerr ('72b) may reflect similar islands of neuropil in the cat. However, the differences in the organization of spinal afferents in the dorsolateral region of Vi in the rat and cat may have another explanation. Since the large injections of HRP used in the present study potentially included primary as well as non-primary spinal afferents to SVC, the continuous pattern of HRP labeling observed in the present study may be the result of these combined inputs. It is possible therefore, that the specific anterograde labeling of primary dorsal root fibers alone might result in a clustering

pattern of spinal afferents in rat dlVi. On the other hand, the possibility must be considered that this difference in distribution represents a true species difference in the organization of spinal afferents within the dorsolateral regions of Vi in rat and cat. Finally, the differences in the sensitivities of the techniques used may account, at least in part, for these differences. The experimental degeneration technique, for instance, labels only terminal and preterminal endings while the anterograde HRP technique labels fibers and terminals. The density of labeled fibers and terminals in the present study, therefore, may have obscured the presence of any patchy distribution pattern.

The presence of spinal afferents in ventrolateral regions of Vi has been illustrated, but not specifically discussed by Rustioni ('74) in the cat and Rustioni et al. ('79) in the monkey. In their Figures 2 (section D) and 10 (sections C-E), respectively, a few degenerating fibers are shown in the ventrolateral part of SVN adjacent to SVT at levels which appear to correspond to Vi. These regions may be analogous to brVi. Several additional studies have reported the presence of spinal afferents in the ventromedial edge of Vi (Hand, '66; Kerr, '75; Rustioni, '75; Rustioni and Molenaar, '75; Rustioni et al., '79; and Ring and Ganchrow, '83) and may also correspond to brVi. In another study, Kerr ('72b) described a spinal input to a gelatinous-like region which he identified as "area C" located in the ventromedial edge of SVN at the level of the obex in the cat. Although similarly gelatinous regions representing displaced portions of SG have been described in similar regions of the rat (see Chapter One), these particular regions were conspicuously devoid of anterograde labeling in the present study and contrasted sharply with the presence of anterograde labeling in adjacent portions of brVi.

Previous degeneration studies have reported the distribution of spinal afferents to the rostral pole of MDH, particularly its ventromedial aspect (Rossi and Brodal, 56; Hand, '66; Breazile and Kitchell, '68; Imai and Kusama, '69; Shriver et

al., '68; Keller and Hand, '70; Rustioni, '73; Rustioni, '74; Rustioni and Molenaar, '75; Kerr, '75; and Ring and Ganchrow, '83). The results of the present study do not confirm this projection in the rat. The lack of anterograde labeling within the ventromedial aspect of MDH in the present study may solely be due to a more accurate identification of MDH and Vi components at their interface in the peri-obex region (see Chapter One). Since similar distinctions have not yet been made in other species, some of the degenerating fibers reported to lie in the ventromedial aspect of rostral MDH, may have actually been in regions belonging to the caudal part of Vi. It must be pointed out however, that the placement of HRP injections in the uppermost cervical spinal cord resulted in the appearance of anterograde labeling within MDH only in those cases in which the injection site invaded the caudal pole of the nucleus. In these cases, the labeling within MDH is considered to represent a part of the extensive intratrigeminal projection system within SVC (see "Intratrigeminal Pathways" below).

The presence of a spinal input to Vo has previously been reported only by Rossi and Brodal ('56) in the cat and Breazile and Kitchell ('68) in the pig. However, the latter authors concluded that since their lesion may have included parts of caudal MDH, the ipsilateral projection to Vo from the upper cervical cord may not have been part of a spinotrigeminal pathway, but rather a part of the extensive intratrigeminal system in SVC. However, the results of the present study clearly document the presence of a spinotrigeminal projection to lateral regions of Vo. In particular, this projection terminates in BZ. This subdivision of Vo has recently been distinguished in the rat on the basis of differences in its cyto- and myeloarchitecture and connectivity (Falls, '83, '84a,b, '86; and Falls et al., '85). The exclusive termination of spinal afferents to BZ provides additional anatomical evidence supporting the distinction of this region from other regions in Vo. A similar distinction has not yet been reported in any other species.

The present study demonstrates a direct spinal input to Vms. This projection has been previously denied in the rat (Torvik, '56), but has been reported to be present in the cat (Rossi and Brodal, '56) and the pig (Breazile and Kitchell, '68). The restricted distribution of spinal afferents to lateral regions of Vms in the rat is in contrast to the reported widespread distribution of these afferents in the other two species. Although this may reflect a species difference in this projection, it is not easy to overlook the fact that the overall results of Rossi and Brodal ('56) and Breazile and Kitchell ('68) do not agree with any other previous experimental degeneration study (see Historical Review above). It is likely therefore, that the results of these particular studies were spurious in nature and should not be considered further.

The present study also indicates a projection of spinal afferents to insular and interstitial portions of iV-Cul. This nucleus has recently been identified as one of several distinct components of the InSy-SVT in the rat (Falls and Phelan, '84; see also Chapter Two). A spinal input to iV-Cul has not previously been reported in any species. It is interesting to note that other components of InSy-SVT which lie within SVT at the same levels as iV-Cul, particularly the paratrigeminal nucleus, do not receive a similar spinal input. This differential distribution of spinal afferents within the InSy-SVT, provides additional support for the presence of functional heterogeneity within this system (Falls and Phelan, '84; see also Chapter Two). It remains to be seen whether similar patterns of spinal projections exist within the InSy-SVT of other mammalian species. It should be noted in this regard that Rustioni and Macchi ('68) observed degenerating fibers in a small ipsilateral cell group situated between RB and SVT at caudal Vo levels in the cat following C3 hemisection of the cord. In addition, Rustioni ('73) illustrated (his Figure 7, level 5) degenerating fibers in a similar location at caudal Vi levels following lesion of the lateral funiculus at L2 levels of the cord. Although comparable regions to those

described by Rustioni and Macchi ('68) and Rustioni ('73) exist in the rat, neither of these regions corresponds to iV-Cul (see Chapter Two).

The Origin and Course of Spinotrigeminal Afferents

Previous experimental degeneration studies have provided evidence suggesting the origin of spinotrigeminal afferents from all levels of the spinal cord including contributions from primary and non-primary sources (see "Historical Review" above). In the present study, the placement of HRP injections was limited to cervical and/or upper thoracic levels of the cord, in order to maximize the simultaneous labeling of spinotrigeminal and trigeminospinal pathways within SVC. Therefore, the precise level of origin of the spinotrigeminal projections revealed by these injections is difficult to determine, since it is possible that damaged fibers of passage originating at lower levels of the cord may have partially contributed to the anterograde labeling pattern. However, there was generally a progressive increase in the density of anterograde labeling in SVC following injections into progressively more rostral levels of the cervical spinal cord. This pattern may reflect an increased origin of spinotrigeminal fibers at these levels of the cord, since variations in the injection size or post-injection survival time of injections in lower levels of the cord did not significantly affect the density of this anterograde labeling. In addition, some regions in SVC received a spinal input only when the injection was centered at C1-C2 levels of the spinal cord, suggesting that at least part of the spinotrigeminal pathway originates only at this level.

On the other hand, the results of the series of tritiated amino acid injections unequivocally confirms the pattern of an increasing amount of spinotrigeminal fibers arising from progressively more rostral levels of the cervical spinal cord. In addition, these latter experiments document the origin of at least part of the spinotrigeminal projection from secondary cells located in the dorsal horns of the uppermost levels of the cervical spinal cord. In fact, these studies reveal that

secondary spinal neurons at these levels contribute projections that distribute to each of the spinal recipient zones identified in the anterograde HRP labeling studies.

The lack of anterograde labeling in SVC following injections of tritiated amino acids into C3-C5 levels of the spinal cord suggests that secondary cells at these levels do not contribute to the spinotrigeminal pathway in the rat. However, this negative result must not be taken as definitive, since the lack of anterograde labeling may reflect a limitation of the autoradiographic technique. It is possible, for instance, that a weak projection originating from these levels might have been lost in the background level of noise. A more complete series of autoradiographic experiments is needed in order to resolve this question.

In support of the origin of spinotrigeminal projections from cervical rather than lower levels of the spinal cord, the overall extratrigeminal pattern of spinobulbar labeling in the present study was consistent with known spinobulbar patterns originating from cervical levels of the cord (see Brodal, '81 for review). In the facial nucleus, for instance, it is known that spinal inputs are organized such that medial parts of the nucleus receive projections from cervical levels of the cord, while lateral parts of the nucleus receive projections from more caudal levels of the cord. In the present study, anterograde labeling was distributed exclusively to the medial parts of the facial nucleus. This fact suggests that the spinotrigeminal afferents demonstrated in the present study may also primarily arise from the cervical levels of the spinal cord.

The anterograde labeling within dlVi appeared in the present study to be a ventrolateral extension of the anterograde labeling within the adjacent ventral part of Cun. This was particularly evident in the distribution pattern resulting from a limited HRP injection into the DCF. Recent retrograde transport studies have demonstrated a non-primary spinal input to Cun in the rat (Giesler, Nahin, and

Madsen, '84; and dePommery, Roudier, and Menetrey, '84). The non-primary cells of origin were revealed to reside predominantly in lamina IV at levels throughout the spinal cord. It is possible that the population of retrogradely labeled neurons identified in these studies may also have included neurons projecting to dlVi, since injections into Cun may likely result in the inclusion of fibers passing through this region on their way to dlVi.

The anterograde labeling observed in brVi appeared in the present study to be spatially continuous with the anterograde labeling observed in the ventrolateral pcRF. This continuity may also indicate similar origins of inputs from within the spinal cord. The origin of secondary spinoreticular projections has been demonstrated in the rat to arise from lamina VII and VIII at levels throughout the spinal cord (Shokunbi, Hrycryshyn, and Flumerfelt, '85). It is again possible that this population of cells includes those cells that project to brVi, since injections into pcRF are likely to involve those fibers passing through on their way to brVi.

The anterograde labeling of spinal afferents in Vo appeared in the present study to be an extension of that found in dlVi and brVi and thus may more than likely arise from similar groups of cells. Finally, it is likely that the origin of the anterograde labeling observed in Vms is also similar to that found in more caudal regions of SVC.

The results of previous experimental degeneration studies have not agreed concerning a specific route for the spinotrigeminal pathway. In particular, spinotrigeminal fibers have been reported to ascend in the SVT (Hand, '66; and Rossi and Brodal, '57), the LF (Kerr, '75; Rossi and Brodal, '56; Rustioni, '73, '74; and Rustioni and Molenaar, '75), and the DCF (Hand, '66; Shriver et al., '68; Imai and Kusama, '69; Kerr, '72b; and Rustioni, '74).

In the present study, anterograde labeling was often detected in various regions of SVC without any apparent labeling of fibers in SVT. In fact, labeled

fibers were present in SVT only in those cases where the injections involved the caudal part of MDH. In these instances, labeled fibers were also seen throughout the ventrolateral aspect of SVC, particularly within the DAB's which permeate the neuropil. The anterograde labeling of SVT and the DAB's are considered in the present study to represent the involvement of part of the intratrigeminal projection system and is not considered to be part of the spinotrigeminal projection (see "Intratrigeminal Pathways" below).

The results of the present study clearly indicate two major routes of spinotrigeminal fibers in the medulla. In particular, spinal afferents projecting to dlVi, dorsolateral BZ and dorsolateral Vms arise from fibers traveling in an area lying ventral to the DCN and dorsal to SVC. The fibers in this region appear to arise primarily from the DCF. On the other hand, the spinotrigeminal fibers projecting to brVi, ventromedial parts of BZ, ventromedial parts of Vms and iV-Cul arise from fibers traveling in an area in the ventrolateral aspect of pcRF. The fibers in this region appear to arise from the DCF as well as the dorsal and ventral parts of LF.

It is interesting to note that in this regard, many of the secondary spinal neurons projecting to the DCN have branched axons which travel in both the DCF and LF (Lu et al., '85). It is not known to what extent the different routes of the spinotrigeminal inputs identified in the present study may represent a collateralization of secondary spinal neurons.

The Morphology of Spinotrigeminal Fibers

The only available information regarding the morphology of spinotrigeminal fibers is the description provided by Astrom ('53) that the spinotrigeminal fibers in the mouse were relatively thin fibers. The results of the present study confirm the relatively thin nature of the spinotrigeminal fibers in the rat. In fact, the use of Co-GOD reacted sections enabled the distinction of two separate types of anterogradely labeled spinotrigeminal fibers in the rat. The first type was a

relatively thin fiber, measuring less than 1.5 μm, which was distributed to each of the spinal recipient zones in SVC. It is not known whether these thin fibers represent myelinated or unmyelinated fibers. The second type of fiber was a relatively thicker axon, measuring up to 2.0 μm in diameter, which was distributed only to brVi and iV-Cul. These fibers have been demonstrated at the ultrastructural level to represent myelinated axons in iV-Cul. In addition, the thinner axon collaterals of these fibers in iV-Cul have been demonstrated to be unmyelinated.

The axon collaterals of spinotrigeminal fibers in SVC gave rise to numerous en passant and terminal bouton-like swellings. These swellings are presumed to represent synaptic endings. The en passant and terminal boutons in iV-Cul have been examined at the ultrastructural level and been determined to represent morphologically distinct synaptic endings (Phelan and Falls, '86; see also Chapter Five). In fact, these boutons constitute a single type of axonal ending in the nucleus which contains primarily spherical-shaped synaptic vesicles and establishes asymmetrical synaptic contacts with the dendritic shafts and dendritic spines of iV-Cul neurons. It is not known whether the spinal afferents to SVC establish direct synaptic contacts with SVC neurons or whether they are primarily involved in presynaptic modulatory mechanisms. The distribution of silver grains in distinct pericellular clusters in dlVi is highly suggestive that the spinal input to this region direct contacts the somata of dlVi neurons. However, a similar pattern was not observed in any of the other regions in SVC. It is possible that the spinotrigeminal input to these regions may directly contact parts of the dendritic tree rather than the somata. The spinal afferents to iV-Cul were, in fact, demonstrated to contact primarily the peripheral portions of the dendritic tree of iV-Cul neurons.

The spinal afferents in SVC exhibited only a simple branching pattern which consisted of the presence of several unbranched axon collaterals which gave rise to numerous en passant boutons. This simple branching pattern is morphologically

similar to that which has been described for the primary V inputs to the ventrolateral subdivision of Vo (Falls, '86) and the primary spinal inputs to lamina I of the spinal dorsal horn (Gobel et al., '81). However, it is distinctly different from the elaborate branching patterns of primary cutaneous and vibrissae afferent inputs which terminate in MDH and Vi (Hayashi, '82; '85a,b).

A more detailed study of the morphology of individual spinotrigeminal fibers in each of the spinal recipient zones is clearly needed in order to allow comparisons between these fibers and other afferent inputs to SVC.

The Spatial Convergence of Spinal Afferents with Primary and Non-Primary Afferents in SVC

Primary Trigeminal Afferents. It has been well established that primary V afferents are organized somatotopically within SVC in an essentially inverted fashion such that mandibular afferents terminate dorsally while maxillary and ophthalmic afferents terminate at intermediate and ventral levels, respectively (Torvik, '56; Kruger et al., '61, Kruger and Michels, '62a; Kerr, '63a; Nord, '67; Marfurt, '81; and Yokota and Nishikawa, '77). The anterograde labeling demonstrated within the present study encompassed regions receiving inputs from all three divisions of the trigeminal nerve. In particular, the spinal afferents identified within dlVi, its rostral extension into BZ, as well as the dorsolateral labeling in Vms, all lie primarily within the terminal field of mandibular primary afferents (Jacquin et al., '83). The spinal afferents identified within brVi, its rostral extension into BZ, as well as the ventrolateral labeling in Vms are all situated within regions receiving maxillary/ophthalmic primary afferents. Since the precise distribution patterns of the latter divisions of the trigeminal nerve have not yet been demonstrated in the rat, the boundary between these two divisions within brVi, BZ, and Vms are not known.

It is also well known that a mediolateral intradivisional somatotopy exists within the distribution of trigeminal afferents to the rostral subnuclei of the SVC

such that the oral and rostral facial fields are represented medially while the posterior and lateral portions of the head and face are represented laterally (Kruger et al., '61; Nord, '68; and Jacquin et al., '83).

In view of this somatotopic organization the distribution of spinotrigeminal afferents to the lateral regions of Vi, Vo and Vms suggests that these afferents are in a position to modulate the activity of secondary SVC neurons which are primarily concerned with the relay of sensory information from posterior and lateral parts of the head and neck.

The position of iV-Cul in the ventral two-thirds of SVT places it in a position to maximally receive primary afferents from the maxillary and ophthalmic divisions of the trigeminal nerve. It is not yet known whether primary trigeminal afferents terminate in iV-Cul in the rat. Some HRP labeled fibers are present in iV-Cul following large injections of HRP into the V root (unpublished observations). However, it is not known whether these fibers actually establish synaptic contacts with iV-Cul neurons or whether they may simply represent fibers of passage.

Non-Trigeminal Primary Afferents. In his experimental degeneration study, Kerr ('72b) noted the convergence of spinal afferents and non-trigeminal primary afferents within SVC of the cat. In particular, he demonstrated that the uppermost cervical dorsal roots distributed to his "area L" which he had previously reported to receive inputs from glossopharyngeal and vagal cranial nerves (Kerr, '62). In a more recent HRP study in the cat, Arviddson and Thomander ('84) also noted a similar convergence of spinal and non-trigeminal primary afferents within SVC. In particular, these authors demonstrated that vagal afferents were distributed within a region of lateral Vi which had previously been shown by Imai and Kusama ('69) to receive afferents from the C2 dorsal root. These two studies demonstrate that the spinotrigeminal projection to Vi exhibits a close spatial relationship with the distribution of glossopharyngeal and vagal afferents in the cat.

A similar convergence of spinotrigeminal afferents and non-trigeminal primary afferents has not previously been suggested in the rat. In his experimental degeneration study, Torvik ('56) reported the presence of a modest number of degenerating fibers in the rostrodorsal part of SG following the combined lesions of the glossopharyngeal and vagal cranial nerves. The region identified in his Figure 3 (level 3) corresponds to the rostral remnant of SG described in the present study at a level corresponding to the transition from MDH to Vi. However, the region identified in the present study as caudal dlVi was noticeably free from degenerating fibers. A more recent autoradiographic study conducted by Contreras, Beckstead and Norgren ('82) in the rat reported that the only distribution of these two cranial nerves in SVC was to the marginal subnucleus of MDH. Their Figures 6E and 7 illustrate that these fibers terminate in the same rostrodorsal remnant of SG identified by Torvik ('56). These two studies in conjunction with the results of the present study, demonstrate that the distribution of spinotrigeminal afferent in SVC of the rat are not coextensive with the distribution of glossopharyngeal or vagal cranial nerves.

The apparent differences in the convergence of these two system in Vi of the rat and cat may simply reflect a species difference in either the distribution of spinotrigeminal afferents or non-trigeminal afferents within SVC. In this regard, it must be reiterated that there is no clear consensus regarding the distribution of spinotrigeminal afferents in other species since modern anterograde transport techniques have not yet been used to describe this pathway.

The contribution of primary afferents from the facial nerve to the SVC has been well established (Torvik, '56; and Rhoton, '68). In the rat, Torvik ('56) reported the presence of facial afferents solely within the rostrodorsal part of SG (His Figure 5, level 1). However, Rhoton ('68) reported that following facial rhizotomy a few degenerating fibers entered MDH and Vi. In fact, his Figure 1C illustrates that

these fibers are distributed to the dorsolateral aspect of SVC at a level which is just rostral to the obex (i.e. at the level of the transition from MDH to Vi. However, since the precise extent of these fibers within Vi and MDH is not discussed, it is not clear whether these regions represent the caudal pole of dlVi or the rostral remnant of SG. Nevertheless, there is no anatomical evidence to suggest a convergence of facial and spinal afferents in Vi.

On the other hand, Rhoton ('68) and Contreras et al. ('82) illustrated the distribution of facial fibers in dorsolateral regions of Vms. The results of these studies, in conjunction with the results of the present study, therefore suggest the existence of a spatial convergence between spinotrigeminal fibers and primary facial fibers in Vms. It is generally assumed that the facial afferents which terminate in Vms represent the tactile components of the cutaneous auricular roots of the facial cranial nerve. The significance of this potential convergence of these afferents on neurons in the dorsolateral aspect of Vms remains to be determined. However, if the spinal afferents distributed to this region represent those from primary as opposed to non-primary spinal afferents, than this convergence may simply reflect a close proximity in the peripheral distribution of the cervical spinal and facial afferents.

It has been reported that the facial, glossopharyngeal and vagal afferents are distributed to some of the interstitial components of InSy-SVT in the rat (for a complete review see Chapter Two). However, non-trigeminal primary afferents have never been reported within the region occupied by iV-Cul. The presence of spinotrigeminal afferents in iV-Cul and the absence of such labeling in any of the other components of InSy-SVT indicates that there is no convergence of any spinotrigeminal afferents and non-trigeminal primary afferents in the InSy-SVT. Although a similar distribution of non-trigeminal primary afferents has been

demonstrated in the InSy-SVT of other species, the distribution of spinotrigeminal afferents to InSy-SVT has not yet been investigated in any species.

Non-Primary Afferents. The cerebral cortex has been demonstrated to project upon SVC in a somatotopic fashion (Kuypers and Tuerk, '64; Wold and Brodal, '74; Kawana and Kusama, '64; Kusama, Otani and Kawana, '66; Dunn and Tolbert, '72; and Tolbert, Dunn and Vogler, '84). Imai and Kusama ('69) noted that C2 dorsal roots terminate in lateral aspects of SVC in a region which overlapped with the termination site for cortical areas concerned with upper face areas. The distribution of cortical afferents to SVC in the rat has not yet been demonstrated using modern anterograde transport techniques. Torvik ('56) suggested that cortical afferents terminated medially in SVC. In conjunction with the results of the present study, this would indicate a lack of any overlap between spinotrigeminal and cortical afferents to SVC. However, since cortical afferents have been demonstrated to terminate throughout all parts of cat SVC, it is possible that if modern labeling techniques are used to examine the corticotrigeminal projection, a more widespread distribution of corticotrigeminal afferents may be uncovered.

Cortical afferents have been demonstrated to distribute to regions within InSy-SVT in the cat (Dunn and Tolbert, '72). However, since this projection has not yet been demonstrated in the rat, it is not known whether iV-Cul represents a potential site of convergence of cortical and spinal inputs in the lateral medulla.

In this regard, the corticobulbar pathway has long been thought to be important in the control of ascending sensory information in the medulla (Darian-Smith and Yokota, 68a,b). However, since electron microscopic observations of iV-Cul demonstrates the conspicuous absence of axo-axonic relationships, if there is a cortical input to this nucleus it cannot function in the presynaptic modulation of spinal afferent inputs.

A previous experimental degeneration study has also indicated the distribution of parabrachial afferents to lateral regions of Vi (Saper and Loewy, '80). In particular, these authors illustrate but do not discuss the presence of a projection from the Kolliker-Fuse nucleus to a region in SVC which appears to corresponds to brVi. In addition, a similar study of th Edinger-Westfall nucleus in the cat demonstrated a projection to lateral regions of SVC bordering SVT (Loewy and Saper, '78). The results of the present study, in conjunction with these latter studies, indicate that a spatial overlap exists between midbrain tegmental and spinal inputs in dlVi and brVi. Since the parabrachial and Edinger-Westfall nuclei are primarily involved in autonomic functions, it is possible that the convergence of spinal and parabrachial afferents in this regions indicates the involvement of spinal afferents in autonomic functions of the head and neck.

Reciprocal Spinotrigeminal and Trigeminospinal Pathways

The results of the present study generally confirm and extend previous observations regarding the distribution of TS neurons in SVC of the rat (Falls, '84; Ruggiero et al., '81; Satoh, '79; Burton and Loewy, '77; Leong et al., '84a,b;). In particular, the present findings confirm the existence of TS neurons in the deeper magnocellular layers of MDH and the ventral and lateral regions of Vi, Vo and Vms. In addition, however, the present study reveals the existence of three separate groups of TS neurons in SVC. The first group consisted of those regions which usually contained a relatively consistent number of retrogradely labeled neurons regardless of the level of the injection site in the cervical spinal cord. This group included MDH and Vms. The second group consisted of those regions which contained a noticeably increasing number of retrogradely labeled neurons following injections centered at progressively more rostral levels of the cervical spinal cord. The regions in this group included dlVi, the band region of brVi, and the ventrolateral regions of Vi and Vo. The third group consisted of those regions which

contained retrogradely labeled neurons only after injections centered in C1-C2 levels of the spinal cord. The regions in this group included the oval-shaped clusters in brVi and BZ.

The retrograde labeling pattern in the first group may indicate that the neurons in these regions project only to levels caudal to the upper cervical cord. The increase in the number of retrogradely labeled cells in the second group could simply be explained by the fact that the injection sites in the upper levels of the spinal cord involve more fibers of passage than injections centered more caudally in the cervical spinal cord. However, large injections in more caudal levels, coupled with longer post-injection survival times, did not significantly alter the relative number of TS cells in these regions. This suggests that there is a real increase in the number of retrogradely labeled cells in these regions which results from the inclusion of those cells which terminate in the upper levels of the cervical spinal cord. Finally, the pattern of labeling in the third group supports the idea that these regions project only to the upper cervical spinal cord.

A similar distribution pattern for TS neurons projecting to the cervical spinal cord has not previously been reported. In fact, the present study represents the first to report a clustered arrangement of TS neurons in brVi in any species. The significance of the clustering of the cells in this region is not yet known. However, it has been demonstrated that the primary afferents terminate in a similar clustered fashion in the region occupied by brVi (Belford and Killackey, '79a). It is not known whether the clusters of TS neurons in brVi lie within the confines of these vibrissae inputs.

The TS pathway in the rat has previously been shown to contain ipsilateral and contralateral components. While the ipsilaterality of the TS projection was not a primary concern of the present study, it is worth noting that the TS neurons in BZ and Vms were only labeled following ipsilateral injections in the cervical spinal

cord. In addition, the results of the present study suggest that the cells in brVi also project primarily to the ipsilateral spinal cord. On the other hand, the TS neurons in ventrolateral parts of Vi and Vo, and dlVi all contributed at least a partial contralateral projection.

The significance of these differences in the laterality of these TS projections to the cervical spinal cord may reflect an inherent difference in the functional role of these various groups of TS neurons. In this regard, the TS neurons in ventrolateral regions of Vi and Vo have previously been demonstrated to project bilaterally to the entire length of the cord (Ruggierro et al., '81; and Leong et al., '84a). These regions are thus able to influence the activity of neurons throughout the spinal cord. However, those neurons which have been identified in the present study as projecting only to the ipsilateral upper cervical spinal cord can influence the activity of only a small population of spinal neurons. These differences clearly reflect a basic difference in the functional organization of the spinal projections of these neurons.

The simultaneous anterograde and retrograde labeling obtained in the present study has allowed a direct examination of the spatial relationship between the spinotrigeminal and TS pathways. The results of the present study document the existence of a complex spatial relationship between these two systems. Although the ventrolateral regions of Vi and Vo contain a large population of TS neurons, they do not receive any projection from the spinotrigeminal pathway. However, spinal afferents are distributed in an organized fashion to each of the laterally located regions of SVC which contain TS neurons. In fact, the pattern of spatial overlap between spinotrigeminal and TS pathways in lateral regions of SVC supports the existence of anatomical substrates which may underly functional reciprocal loops between SVC and the cervical spinal cord. In particular, three of the laterally located spinal recipient regions received a spinal input from the cervical cord and

projected back upon the cervical cord. These regions included Vms, dlVi, and the band region in brVi. In addition, two regions received a spinal input which originated only from the uppermost levels of the cervical cord and contained cells which projected back only to the uppermost levels of the cervical cord. These regions included the oval-shaped clusters in brVi and the ventral part of caudal BZ. It should also be noted that two regions, the rostral half of BZ and the caudal dorsolateral part of BZ, received a spinal input but did not contain any TS neurons. The former received a spinal input only from the upper level of the cervical spinal cord, while the latter received an input from lower levels of the cervical spinal cord.

The significance of these reciprocal relationships between SVC and the cervical spinal cord is not known. However, the existence of these loops may suggest that the spinotrigeminal pathway functions largely in the integration of spinal and V information through a feedback mechanism.

It is interesting to note that a similar spatial relationship between spinotrigeminal afferents and TS neurons in lateral regions bordering SVT has been illustrated by Panneton and Burton ('85) in the cat. In particular, these authors report the distribution of anterograde and retrograde labeling in ipsilateral parts of the ventral and lateral regions of Vi, Vo and Vms following an injection of wheat germ agglutinin conjugated HRP into the MDH at the level of the SMJ (see their Figure 9). However, this labeling was considered by these authors to represent a part of the intratrigeminal projection system in SVC (see "Intratrigeminal Pathways" below).

The Spatial Relationship between Spinal Afferents and Other Trigeminal Efferent Neurons in SVC.

Retrograde transport studies in the rat have documented the presence of trigeminothalamic (TT), trigeminocollicular, and trigeminocerebellar (TC) projection neurons in dlVi (Phelan and Falls, '85; Huerta, Flumerfelt and Harding, '83: see also Chapter Three). However, the vast majority of projection neurons in

this region clearly represent TT cells (see Chapter Three). Retrograde transport studies have further suggested that some of the TT cells in Vi collateralize to the superior colliculus and may also contribute collaterals to the trigemino-olivary projection (Huerta et al., '83). However, the extent of collateralization of these pathways in dlVi has not specifically been examined in the rat. Furthermore, double labeling studies indicate that the TT and TC cells in dlVi represent separate populations of neurons (unpublished observations).

The spinal input to dlVi may primarily represent part of a spino-trigemino-thalamic pathway (see Figure 7) since the overwhelming majority of cells in this region represent TT neurons. However, the possible existence of collateralization in the efferent projections of neurons in dlVi suggests that the spinal input to dlVi may simultaneously influence activity in the thalamus, the superior colliculus and the inferior olive.

Although the presumed interaction of spinotrigeminal afferents and the trigeminal efferent neurons in dlVi remains to be confirmed through electrophysiological or ultrastructural techniques, the pericellular distribution of anterograde labeling in this region strongly suggests a direct axo-somatic input to dlVi neurons.

Retrograde transport studies have also documented the existence of TT and TC projection neurons in brVi (Phelan and Falls, '85; see also Chapter Three). However, the vast majority of the neurons in this region represent cerebellar projecting neurons. Double labeling studies further indicate that the TC and TT cells in this region represent separate populations of neurons in the rat (unpublished observation). This suggests that the spinal input to brVi may primarily reflect a spino-trigemino-cerebellar pathway (see Figure 7).

The dorsolateral aspect of BZ has also been reported to contain TC projecting neurons (Falls et al., '85). In addition, BZ has been demonstrated to

contain numerous MDH projecting neurons (Falls, '84b). A few TT cells have also been noted in the dorsolateral part of BZ (see Chapter Three). The spinal projection to BZ may thus represent another site for the relay of spinal information to the thalamus or the cerebellum (see Figure 7). In addition, the spinal input to this region may influence activity in the extensive intratrigeminal projection system in SVC (see "Intratrigeminal Pathways" below).

It has long been known that a major secondary TT projection originates in Vms (Smith, '73). Retrograde transport studies in the rat demonstrate that virtually all of the neurons in Vms represent TT projecting cells (Kruger et al., '79; and Erzurumlu et al., '80). The spinal afferent input to Vms may therefore represent another anatomical substrate for a spino-trigemino-thalamic pathway (see Figure 7).

Finally, the iV-Cul nucleus has recently been identified as a separate precerebellar nucleus in which all of the cells project to the cerebellum (Falls and Phelan, '84; see also Chapter Two). No other projections of iV-Cul neurons have yet been identified. The spinal afferent input to this nucleus therefore represents a spino-medullary-cerebellar pathway (see Figure 7).

The spatial relationship between the distribution of the spinotrigeminal projection and the location of identified trigeminal efferent neurons supports the existence of several potential anatomical substrates for the relay of spinal afferent information to the thalamus, cerebellum and intratrigeminal sites. It is not yet known to what extent these anatomical substrates may represent functionally active routes in the rat.

Intratrigeminal Pathways

Anatomical and electrophysiological studies have documented the presence of an extensive intranuclear projection system within mammalian SVC (Kruger et al., '77; Ganchrow, '78; ; Hu, Dostroevsky, and Sessle, '81; Ikeda, Matsushita and Tanami, '82; Ikeda, Tanami, and Matsushita, '84; and Panneton and Burton, '82; see

also Brodal, '81). This system includes ascending as well as descending projections. It has been suggested that the ascending pathways are primarily involved in the modulation of the transmission of orofacial information through rostral SVC nuclei (Yu and King, '74; Greenwood and Sessle, '76; Sessle and Greenwood, '76b; and Hu et al., '81). It has further been demonstrated that the fibers contributing to this ascending intranuclear V projection system travel primarily in SVT and in the numerous DAB's which permeate the neuropil (Stewart and King, 63; Gobel and Purvis, '72; and Ganchrow, '78).

In the present study, anterograde labeling was present in the ventrolateral regions of Vi, Vo and Vms only in those cases in which there was concommittant labeling of the fibers in SVT and the DAB's. In these cases, the injection sites were centered in the uppermost level of the spinal cord and always included a spread into the caudal pole of MDH just rostral to SMJ. The anterograde labeling in these regions of SVC is considered here to represent part of the intranuclear V projection system which was labeled because of the spread of the injection site into caudal MDH.

The cervical spinal cord has been long known to be a site of convergence of primary V and spinal fibers (Kerr, '72b). Recent electrophysiological studies have, in fact, demonstrated a reciprocal inhibitory interaction between V and spinal systems in the cat (Saade et al., '85; and Atweh et al., '85). The results of the present study confirm an intricate reciprocal relationship between secondary V and spinal systems. Nevertheless, it could be argued that the spinotrigeminal projection, particularly that originating in the upper cervical spinal cord, may simply represent an extension of the intranuclear projection system in SVC. In fact, a strikingly similar pattern of anterograde and retrograde labeling in lateral regions of SVC has been reported in the cat following the injection of wheat germ agglutinin conjugated HRP into caudal MDH at the level of SMJ (Panneton and Burton, '85). The authors

in the latter study reported that this particular anterograde and retrograde labeling pattern represented part of the intranuclear projection system in SVC.

Nevertheless, there are several facts which together argue against the suggestion that the spinotrigeminal projection in the rat may represent a simple extension of the intranuclear V projection system. First, the anterograde labeling of the spinotrigeminal pathway could occur in the absence of labeled fibers in either SVT or any of the DAB's. Second, the results of the present study clearly demonstrate that part of the spinotrigeminal projection originates from fibers traveling in the DCF which do not contribute fibers to the intranuclear V projection system. Third, the distribution pattern of retrogradely labeled neurons in the present study does not agree with the previously established patterns of descending intranuclear projections. In particular, only a few rare retrogradely labeled neurons were present in BZ, even though this region of Vo has been documented to contain a large number of descending neurons following injections of HRP into MDH (Falls, '84b; and Panneton and Burton, '85). Contrarily, the present study reveals a unique distribution of retrogradely labeled neurons in clusters within brVi. This particular pattern has not previously been reported following the injection of HRP into MDH in any species. These facts together suggest that the spinotrigeminal projection in the rat does not represent a simple extension of the intranuclear projection system in SVC. However, it is difficult to entirely rule out the possibility that a small part of the spinotrigeminal projection defined in the present study may actually represent a part of the intranuclear V projection system. If this is the case, then the results of the present study provide evidence to suggest that the organization of the intranuclear connections in the uppermost levels of the cervical spinal cord is dramatically different from that found in the adjacent parts of MDH. This difference may reflect a basic difference in the functional role that these

ascending and descending projections play in the processing of somatosensory information in the region of the spinomedullary junction.

Functional Implications

A variety of functions have been ascribed to the spinotrigeminal system in the past. It has been suggested that it may serve as a link in ascending sensory pathways through SVC, in parallel with other ascending spinobulbar pathways to the thalamus and cerebellum (Rossi and Brodal, '56; and Hand, '66). In addition, it has been proposed that the direct spinotrigeminal projection may, in conjunction with the direct TS pathway, form the anatomical substrate for a reciprocal spino-trigemino-spinal feedback systems (Rossi and Brodal, '56; and Hand, '66) similar to other spino-bulbar-spinal loops which subserve a variety of reflexes (Shimamura and Livingston, '63; Cervero and Wolstencroft, '84). The results of the present study provide no direct evidence concerning the function of the spinotrigeminal pathway in the rat. However, the specific distribution of this pathway in SVC, coupled with the spatial relationship between this projection and known afferent and efferent inputs to SVC, provides some indirect indications of the possible role of this spinomedullary projection in the rat. In particular, the results of the present study reveal that the spinal inputs to SVC are distributed exclusively to regions of SVC which are primarily concerned with the processing of sensory information from lateral and posterior regions of the trigeminal receptive fields in the face. This finding, coupled with the preferential origin of the spinotrigeminal pathway from cervical levels of the spinal cord, and the existence of anatomical pathways which would allow reciprocal interactions between SVC and the cervical spinal cord, supports the involvement of the spinotrigeminal projection in the integration of head and neck functions.

The spatial relationship between the spinotrigeminal projection and the secondary projections of neurons in the spinal recipient zones of SVC suggests the

likely involvement of this pathway in the relay of spinal information to the thalamus and the cerebellum. In particular, the results of the present study indicates that an anatomical substrate exists for the spinal relay through SVC to the thalamus in three of the spinal recipient zones (i.e., dlVi, Vms, and dorsolateral BZ), and to the cerebellum in two of the spinal recipient zones (i.e., brVi and dorsolateral BZ).

Although the spinotrigeminal pathway in the rat does not appear to terminate in MDH, which has long been regarded as the primary site for the processing of orofacial pain in SVC, the lateral regions of Vi bordering SVT have also been implicated in nociceptive mechanisms in the cat (Sessle et al., '86). If this situation holds true for the rat, then the spinal input to Vi may play a role in nociceptive mechanisms. In this regard, it has been reported that the application of nociceptive conditional stimuli to lower parts of the body results in the diffuse noxious inhibitory control of pain-related events in the V system at MDH levels of SVC (Cadden et al., '86; Villanueva et al., '86; for a review see Sjolund and Eriksson, '80). It is possible that the rostral nuclei in SVC may also contribute to this phenomenon. In that event, the spinotrigeminal pathway may represent an important part of the circuitry underlying this phenomenon.

In addition, the present study reveals the projection of spinal afferents to iV-Cul. This nucleus has recently been demonstrated to represent a separate and distinct precerebellar relay nucleus in the medulla. Correlative electron microscopic analysis of identified spinal afferents in this region has demonstrated that the terminal endings of these fibers are positioned as a central ending in synaptic glomeruli where they establish direct synaptic contacts with iV-Cul neurons (Phelan and Falls, '86; see also Chapter Five). In particular, the synaptic boutons associated with these endings possess morhological characteristics (i.e., central position in glomerulus, predominance of spherical-shaped synaptic vesicles, and asymmetrical synaptic junctions) which are suggestive that these endings provide an excitatory

synaptic input to iV-Cul neurons. However, the type of sensory information conveyed by these fibers remains unknown.

In summary, the results of the present study provide evidence for the existence of an extensive and precisely organized spinotrigeminal projection in the rat which may be involved in a multitude of functions. It is clear that more detailed investigations regarding the specific origin, postsynaptic targets and electrophysiological characteristics of this spinotrigeminal projection is needed, in order to more fully understand the various roles that it may play in somatosensory processing in the medulla. Nevertheless, although the exact role of the spinotrigeminal pathway remains elusive at this time, the termination of this projection in each of the rostral SVC nuclei indicates that it must play a fundamentally significant role in integrative V somatosensory functions in the rat.

CHAPTER FIVE

A SURVEY OF THE CYTOLOGY AND SYNAPTIC ORGANIZATION OF THE INSULAR TRIGEMINAL-CUNEATUS LATERALIS NUCLEUS IN THE RAT INCLUDING AN IDENTIFICATION OF SPINAL AFFERENT INPUTS

INTRODUCTION

The insular trigeminal-cuneatus lateralis nucleus (iV-Cul) has recently been established as one of several cytoarchitecturally distinct components of the interstitial system of the spinal trigeminal tract (InSy-SVT) (Falls and Phelan, '84; see also Chapter Two). The bulk of the nucleus lies at the level of trigeminal nucleus interpolaris (Vi) with a smaller portion present at the level of trigeminal nucleus oralis (Vo). The nucleus consists of insular neuropil wedged between SVT and the spinocerebellar tract (SCT) which often extends laterally through the SCT to reach the medullary surface, and interstitial neuropil situated within the ventral half of SVT which is sometimes contiguous with neuropil in the lateral border of Vi.

Retrograde horseradish peroxidase (HRP) axonal transport studies have firmly established that all iV-Cul neurons project to the cerebellum (Falls and Phelan, '84; Somana and Walberg, '79; see also Chapter Two). In addition, anterograde axonal transport studies have demonstrated that iV-Cul receives a prominent spinal afferent input (Phelan and Falls, '84b; see also Chapter Four). This pattern of connectivity suggests that iV-Cul represents a newly recognized precerebellar medullary nucleus. Although the morphology of neurons within iV-Cul has been described at the light microscopic level using Nissl, Golgi

impregnation, and retrograde axonal transport preparations (see Chapter Two), the cytology and synaptic organization of this nucleus have not yet been examined.

The present study evaluates and compares the normal cytology and synaptic organization within iV-Cul with that previously reported for neighboring somatosensory medullary nuclei (i.e., the lateral cuneate, Cul; the lateral reticular, LR; and Vi). In addition, the present study examines and compares the morphology and synaptic relations of anterograde HRP labeled spinal afferent fibers which terminate in iV-Cul with those previously described to terminate in other precerebellar nuclei. The results of this analysis should provide important insights into not only the functional organization of iV-Cul, but also aid in determining whether or not this newly recognized somatosensory nucleus shares any structural or functional similarities with adjacent medullary nuclei.

METHODS

The brains of adult, male Sprague-Dawley rats (250-300 gms.) were used throughout this investigation. Three animals were used to characterize the normal cytology and synaptic organization of iV-Cul. Each animal was anesthetized with an intraperitoneal injection of Nembutal (50mg/kg) and perfused intraaortically, using a Masterflex pump delivery system, with a brief heparanized, isotonic 0.1M cacodylate buffer wash followed sequentially by 250 ml each of fixatives consisting of 1% paraformaldehyde-1% glutaraldehyde and 2% paraformaldehyde-2.5% glutaraldehyde in 0.1M cacodylate buffer. The brains were immediately removed from the skull and placed in fresh fixative for an additional hour at 4^{o} C. The brainstems were handblocked and placed in fresh 0.1M cacodylate buffer for at least one hour. Blocks of tissue were sectioned on an Oxford Vibratome at a thickness of 100 μm in either the transverse or horizontal plane, collected in 0.1M cacodylate buffer and subsequently osmicated in a 1% osmium tetroxide solution in 0.1M

cacodylate buffer. The sections were handtrimmed with a razor blade under a dissecting microscope to include insular and interstitial parts of iV-Cul as well as adjacent portions of SVT and SCT. These sections were stained en bloc in 0.5% aqueous uranyl acetate, dehydrated through a graded series of acetone and flat embedded in an Epon-Araldite mixture in order to maintain orientation for subsequent sectioning. The infiltrated blocks were polymerized for 24 hours at 30' C, 24 hours at 60° C and 48-72 hours at 80° C. A single, 1 μm thick section was cut from the face of each block and stained with P-phenylenediamine according to the procedure of Hollander and Vaaland ('68). Each block was retrimmed using the 1 μm sections as a guide. Thin sections were cut from the face of each block, mounted on either copper mesh grids or Formvar-coated slotted grids and stained with lead citrate. Random as well as serial sections were examined in a JEOL 100CX electron microscope and micrographs were taken at rostral and caudal levels of the nucleus. Quantitative measurements reported in this study were made directly upon the micrograph negative whenever possible for the largest of the neuronal elements. The measurements of synaptic vesicles and the smallest neuropil elements were made using a 10X ocular micrometer on micrographs enlarged to final magnifications of 29,800-57,780X.

One additional animal was used for the anterograde HRP labeling and characterization of spinal afferents in iV-Cul. Multiple injections (2.0-3.0 μl total) of a freshly prepared 60% solution of HRP (Sigma Type VI) dissolved in 2% dimethylsulfoxide were centered in the dorsal and ventral horns and dorsal funiculi at upper cervical (C2-C5) levels of the spinal cord. Following a survival time of 24 hours, the animals were perfused intraaortically with a brief heparanized physiological saline wash followed by 500 ml of a fixative consisting of 1% paraformaldehyde and 1% glutaraldehyde in 0.12 M phosphate buffer (pH 7.4). The brains were immediately removed from the skull, handblocked into 4-6 mm

transverse blocks of tissue and serially sectioned on an Oxford Vibratome at a thickness of 50 μm. Alternate sections were collected in 0.12 M phosphate buffer and reacted for the visualization of HRP using the cobalt-glucose oxidase method of Itoh et al. ('79). The sections were then dehydrated through a graded series of glycerin solutions and coverslipped in 100% glycerin (Gobel, Falls, Bennett, Abdelmoumene, Hayashi, and Humphrey, '80). Each section was preliminarily examined at this point for the presence of HRP labeled spinal axons collaterals and terminals. Several sections containing representative examples of spinal afferent fibers were chosen for subsequent electron microscopic analysis. All of these sections were rehydrated through a graded series of glycerin solutions. Those sections chosen for subsequent electron microscopic analysis were then covered with 0.12 M phosphate buffer and examined under a dissecting microscope. The iV-Cul was then handtrimmed from these sections using a razor blade and subsequently processed for electron microscopy according to the procedure of Gobel et al. ('80). Selected blocks were serially sectioned throughout the entire 50 μm thick section. Ribbons of serial sections were collected on formvar-coated slotted grids, stained with lead citrate, and viewed in a Phillips EM 201 or JEOL 100CX electron microscope. The quantitative analysis of HRP labeled spinal afferent terminals was performed in a manner similar to that described for the normal material.

RESULTS

Neuronal Somata and Neuropil

Somata. A single class of oval-shaped neuronal somata are evident (Figure 1). The majority of the perikaryal surface is encapsulated by single, or rarely multiple, thin astrocytic lamellae which often contain dense neurofibril bundles (Figure 1). Remaining portions of the somatic surface are apposed mainly by myelinated axons and occasional dendritic shafts. Although neuronal somata are

often found in close proximity to each other, they are usually prevented from establishing direct contact by an intervening glial process. The somatic surface is typically smooth to slightly irregular in contour and may give rise to a few somatic spines (Figure 3). These spines possess small bulbous heads (measuring 0.2 μm in diameter) which arise from short, thin necks, and exhibit a relatively dark flocculent appearing cytoplasmic matrix compared to that of the soma. Somatic spines contain a few free ribosomes and single coated vesicles. Neuronal somata are characterized by large eccentrically positioned oval-shaped nuclei which occupy much of the area at one end of the cell body. The nuclear envelope typically exhibits several prominent invaginations of varying extents. The nucleus is further characterized by the presence of a prominent centrally or eccentrically located nucleolus, scattered clusters of chromatin, and occasional perinucleolar chromatin aggregates or patches of dense chromatin material positioned at the nuclear membrane. The cytoplasm is densely packed with numerous mitochondrial, extensive golgi complexes, free ribosomes, as well as lysosomes and lipofuscin granules of varying sizes. In addition, several Nissl bodies, isolated patches of granular endoplasmic reticulum (GER), strands of agranular endoplasmic reticulum (SER), and microtubules are present.

The majority of somata are devoid of axosomatic synapses. On occasion, a somatic profile which exhibits a single axosomatic synapse may be observed (Figure 2). The somatic spines when present also receive an axospinous synapse (Figure 3).

Neuropil. The most prominent feature of iV-Cul neuropil is the extensive amount of astrocytic processes which interdigitate throughout the neuropil to surround each neuronal element (Figures 5-18). These glial processes occur as either thick irregular-shaped processes (Figures 5, 11, and 16), or as thin compactly arranged lamellae (Figures 6, and 13). The latter type of astrocytic processes frequently encapsulate single dendrites, boutons or synaptic complexes to form "isolated" neuronal elements (Figure 14). These "isolated" structures are very

conspicuous in the neuropil at low magnification and do not exhibit any apparent preferential distribution.

Dendritic profiles in iV-Cul exhibit diameters which range from 0.5 μm for the smallest distal dendrites to 4.0 μm for the largest proximal dendrites. They contain mitochondria, free ribosomes, SER, GER, microtubules, multivesiculate bodies, coated vesicles, and an occasional dense-core vesicle. The proximal portions of primary dendrites often contain single golgi complexes and small lipofuscin granules. A general decrease in the number of organelles is apparent as one progresses distally within the dendritic tree. The surfaces of dendrites appear predominantly smooth, although small bump-like protuberances may be seen. These dendritic protuberances often receive synaptic contacts. Dendrites are often organized into small groups or clusters within the neuropil (Figure 11).

The dendritic trees of iV-Cul neurons give rise to a modest number of spines the majority of which are distributed on distal dendrites (see Chapter Two). Although the morphology of dendritic spines varies, a few basic types can be discerned. One type of dendritic spine is a small, bulbous pedunculated spine which possesses a round to oval-shaped head (measuring 0.2-0.4 μm in diameter) and a short, thin neck (Figures 9 and 12). These spines which occur singly emanate primarily from small to medium sized dendritic profiles and are often distributed close to dendritic branch points. The spines exhibit a flocculent appearing cytoplasmic matrix which may contain a few ribosomal complexes, dilated cisternae or sacs of SER, and a few (1-4) large vesicles.These vesicles are never associated with presynaptic membrane specializations. A second and more prevalent type of spine is the complex spine which is involved in synaptic glomeruli. They appear as pairs of appendages emanating from a common short, stout dendritic stem measuring 0.2-0.4 μm in diameter and 0.4-0.5 μm in length (Figures 4 and 24). The appendages in complex spines vary in morphology from long, uniformly thin

structures measuring 0.1 μm in diameter and up to 1.2 μm in length to bilobed, or multilobulated, structures measuring 0.4 μm in diameter and up to 1.7 μm in length. Each of these two types of appendages in complex spines exhibit a relatively dark flocculent appearing cytoplasmic matrix containing dilated cisternae and sacs of SER, mitochondria, multivesiculate bodies, and sometimes a few scattered agranular spherical vesicles and/or a single spherical-shaped dense-core vesicle. A third and less frequently encountered type of spine appears similar in size and shape to the individual appendages found in complex spines (Figures 8, 13, and 14). However, these spines arise singly, or in pairs, directly from dendritic shafts of varying sizes. In some cases, these spines emanate from dendritic shafts at points close to the origin of complex spines. Some of these spines are engaged in synaptic glomeruli (Figure 8), while others are not. A few of these spines are encountered in "isolated" synaptic complexes (Figure 13). The fourth and rarest type of spine occurs as short, straight, uniformly thin structures, measuring 0.1-0.2 Mm in diameter and 0.4-0.5 Mm in length, which emanate exclusively from the base of large diameter proximal dendritic shafts. These spines are distributed singly or as pairs on opposite sides of dendritic shafts and exhibit a flocculent cytoplasmic matrix containing tubules and sacs of SER.

Myelinated axons, ranging from 0.15 to over 1.0 μm in diameter and possessing myelin sheaths ranging from 0.02 to 0.1 μm in diameter, are commonly seen coursing throughout iV-Cul neuropil. These usually occur singly or in loosely organized small groups (Figure 7). In addition, numerous unmyelinated axons of various sizes course throughout the neuropil. The smallest of these unmyelinated axons, measuring 0.1-0.2 μm in diameter, often occur in small clusters (Figure 11). The vast majority of myelinated and unmyelinated axons of all sizes are oriented rostrocaudally within the neuropil.

Synaptology

Eight morphologically distinct categories of presynaptic terminals are found throughout iV-Cul neuropil. These terminals can be differentiated on the basis of differences in their synaptic vesicle size, shape, granularity, and distribution; the type of synaptic membrane specialization; the bouton size, shape, and postsynaptic target; as well as the density of the cytoplasmic matrix in the bouton. Table 1 summarizes the morphology of each of the eight terminal types. All of these endings are presumed to arise from axons and to be involved in axosomatic, axodendritic, or axospinous synaptic contacts. There is a striking absence of any axo-axonic synaptic contacts in iV-Cul neuropil.

Type 1 Endings (Figures 4-6). These terminals represent the most prevalent axonal ending containing predominantly large spherical-shaped synaptic vesicles. They are found as centrally positioned boutons in synaptic glomeruli where they establish asymmetrical synaptic contacts with several peripherally distributed small and large diameter dendritic shafts (0.6-2.3 μm in diameter), as well as invaginating dendritic spines. One or more astrocytic processes surround the glomerulus (Figure 6; arrowheads). Type 1 boutons frequently establish synaptic contacts with a complex spine of one dendrite and the shaft of another (Figure 4). The complex spines in these glomeruli do not usually receive synaptic contacts from other axonal endings, however the dendritic shafts are often postsynaptic to other types of axonal endings. Non-synaptic desmosomal attachment sites are occasionally observed between some Type 1 endings and dendritic shafts. Type 1 endings typically exhibit a cytoplasmic matrix containing a central core of mitochondria surrounded by a large number of densely packed synaptic vesicles and occasional neurotubules. The synaptic vesicle population consists primarily of large, spherical to slightly ovoid-shaped agranular synaptic vesicles ranging 40-60 nm in maximum diameter. The vast majority of these vesicles measure 40-50 nm in diameter. The ovoid-shaped synaptic

vesicles exhibit maximum width-to-length ratios of 1:1.5. The agranular synaptic vesicles are evenly distributed throughout the terminal and exhibit prominent clustering at the synaptic junctions. Occasionally, these endings also contain a few spherical-shaped dense-core vesicles measuring 50-80 nm in diameter with centrally positioned granules measuring 40-50 nm in diameter (Figure 5). These dense-core vesicles are scattered throughout the bouton as well as positioned at or near the presynaptic membrane. Type 1 endings are oval to irregular in shape and measure 1.6 to 4.2 μm in maximum diameter. Some appear in the form of en passant boutons with interbouton axon segments measuring less than 0.2 μm in diameter. These en passant boutons may be encapsulated by several thin astrocytic processes to form "isolated" structures. Some Type 1 endings arise from myelinated axons and unmyelinated preterminal axon segments measuring 0.6-0.7 μm in diameter

Type 2 Endings (Figures 7 and 8). These boutons are the second most frequently encountered ending containing predominantly large spherical-shaped synaptic vesicles. They are also involved in synaptic glomeruli and occur as large centrally positioned endings which establish asymmetrical synaptic contacts with one to several peripherally distributed dendritic spines and small diameter dendritic shafts. Some Type 2 endings simultaneously establish synaptic contact with a dendritic spine and its parent dendritic shaft. Invaginating spines are not usually present in these glomeruli. The Type 2 endings possess an electron lucent cytoplasmic matrix containing a few centrally positioned mitochondria and neurotubules surrounded by a modest number of synaptic vesicles in comparison to Type 1 endings. The synaptic vesicle population consists of agranular synaptic vesicles similar in size and shape as those found in Type 1 endings.The density of synaptic vesicles varies slightly among endings, but is generally low relative to the total area of the bouton. The synaptic vesicles are organized into prominent clusters at the synaptic junctions and are often aligned in distinct rows and chains. A few

vesicles are seen scattered throughout the remaining portions of the bouton. Occasionally, these endings also contain a single, spherical-shaped dense-core vesicle, measuring 82-108 nm in diameter with a centrally positioned granule measuring 60-70 nm in diameter. Type 2 endings are round to oval in shape and range from 1.5 to 4.2 μm in maximum diameter. Some Type 2 endings are seen in continuity with unmyelinated axon segments measuring 0.2 μm in diameter (Figure 7; u).

Type 3 Endings (Figures 9, 10, and 13). These endings are the least frequently observed terminals containing predominantly large spherical-shaped synaptic vesicles. They establish asymmetrical synaptic contacts with dendritic shafts measuring less than 1.0 μm in diameter as well as non-invaginating dendritic spines. They are often positioned at regions of dendritic shafts which receive multiple synaptic contacts from several morphologically different types of axonal endings (Figures 10, 13). Type 2 endings contain numerous densely packed large, spherical, agranular synaptic vesicles organized in clusters which fill the region of the bouton overlying the synaptic junctions. These vesicles are similar in overall size as those found in Type 1 and Type 2 endings, however a more uniform population of spherical-shaped synaptic vesicles (measuring 40 nm in diameter) predominates in most of these bouton profiles. A few spherical-shaped dense-core vesicles, measuring 50-90 nm in diameter with centrally located granules measuring 30-60 nm in diameter, may also be present in these endings. These dense-core vesicles exhibit a wide range of granule-to-vesicle ratios. Type 3 endings are dome-shaped profiles which range 1.0-1.6 μm in maximum diameter. Some Type 3 endings are seen in continuity with unmyelinated axon segments measuring 0.1-0.2 μm in diameter.

Type 4 Endings (Figures 11-13 and 14). This type of bouton represents the sole terminal in iV-Cul neuropil containing predominantly small spherical-shaped synaptic vesicles. They are as prevalent in the neuropil as Type 1 endings. They

establish asymmetrical synaptic contacts with small diameter dendritic shafts (0.9-1.6 μm in diameter) as well as dendritic spines. One or two invaginating or non-invaginating spines may arise from these dendrites and receive axospinous synaptic contacts from the bouton (Figures 11 and 12; s). Some Type 4 endings establish synaptic contacts with dendritic spines and are simultaneously enveloped by several compact astrocytic lamellae (Figure 13). Type 4 boutons commonly occur in clusters in the neuropil (Figure 11). They exhibit a flocculent appearing cytoplasmic matrix containing a dense number of synaptic vesicles and a few peripherally located mitochondria. The synaptic vesicle population consists of spherical to slightly ovoid-shaped small, agranular synaptic vesicles ranging 35-55 nm in maximum diameter with the majority measuring less than 35-40 nm in diameter. The ovoid-shaped synaptic vesicles exhibit maximum width-to-length ratios of 1:1.5. The agranular synaptic vesicles are distributed in clusters at the presynaptic membrane as well as throughout the central portions of the bouton. These boutons frequently contain one to several spherical-shaped dense-core vesicles measuring approximately 80-90 nm in diameter with centrally located granules measuring 50-70 nm in diameter. Less frequently, the largest of these boutons may contain several dense-core vesicles with larger central or smaller eccentrically positioned granules. Type 4 endings measure approximately 1.1-2.0 μm in maximum diameter and vary in morphology from small, dome-shaped boutons to larger round or irregular-shaped boutons. Some Type 4 endings are seen in continuity with unmyelinated axon segments measuring less than 0.3 μm in diameter.

Type 5 Endings (Figures 2, 3, 10, and 13). These endings are frequently encountered in iV-Cul neuropil and are the sole axonal ending containing pleomorphic-shaped synaptic vesicles. They establish symmetrical synaptic contacts with dendritic shafts of all sizes, non-invaginating spines, somata and somatic spines. Type 5 endings commonly establish synaptic contact with the shaft and spines of

proximal portions of primary dendrites. They are also commonly situated near dendritic branch points. In addition, they may establish synaptic contacts with the common dendritic stems which give rise to complex spines involved in glomeruli. They are also distributed at points along dendritic shafts which receive multiple axodendritic synapses from different morphological types of axonal endings (Figures 10 and 13). Some Type 5 endings simultaneously establish synaptic contacts with a soma and an adjacent somatic spine. They possess a flocculent appearing cytoplasmic matrix containing a large number of densely packed synaptic vesicles. Mitochondria are rarely present. The synaptic vesicle population consists of a varied admixture of pleomorphic-shaped vesicles. The majority of these are spherical, elliptical or irregular in shape, although a few scattered flattened vesicles are also usually present. The spherical, elliptical, and irregular-shaped vesicles range 35-50 nm in maximum diameter with maximum width-to-length ratios of 1:3. The synaptic vesicles are distributed throughout the boutons, although there is a slightly greater concentration centrally. Dense-core vesicles are rarely encountered in these endings. Non-synaptic desmosomal junctions are sometimes present between the presynaptic bouton and its postsynaptic target. Type 5 endings are usually dome-shaped and measure 0.7-1.5 μm in maximum diameter. Some endings are seen in continuity with unmyelinated axon segments measuring less than 0.2 μm in diameter.

Type 6 Endings (Figures 10, 14, and 15). These bouton profiles are commonly encountered in iV-Cul neuropil. They establish symmetrical synaptic contacts with small diameter dendritic shafts measuring less than 1.5 μm in diameter. Some endings establish synaptic contact with the common dendritic stem of complex spines. The boutons exhibit a relatively dark cytoplasmic matrix containing a heterogeneous population of densely packed synaptic vesicles and a few mitochondria. The synaptic vesicle population consists of elliptical and flattened agranular synaptic vesicles. The elliptical-shaped vesicles measure 40-60 nm in

diameter with maximum width-to-length ratios of 1:3, while the flattened vesicles measure 45-65 nm in maximum diameter and possess maximum width-to-length ratios of 1:3.5. Dense-core vesicles are not usually present in these terminals. Type 6 endings are dome-shaped and measure 0.6-1.6 μm in diameter. Some boutons are seen in continuity with unmyelinated axon segments measuring less than 0.2 μm in diameter (Figure 14).

Type 7 Endings (Figures 16 and 17). These boutons are more frequently encountered than Type 6 endings. They establish symmetrical synaptic contacts with dendritic shafts (0.5-2.0 μm in diameter) as well as dendritic spines. They are often positioned near synaptic glomeruli where they establish axodendritic synapses with large dendritic shafts and common dendritic stems which give rise to spines involved in these synaptic glomeruli. They may occur as en passant boutons and often establish multiple synaptic contacts with one to several dendrites. The boutons usually possess a pale cytoplasmic matrix similar to that of Type 2 endings and contain several mitochondria and a few neurotubules. Type 7 endings contain a modest number of spherical, elliptical, and flattened agranular synaptic vesicles distributed throughout the terminal, although prominent clustering occurs at the synaptic junctions. The spherical-shaped synaptic vesicles measure 35-40 nm in diameter, while the elliptical and flattened vesicles are similar in size and shape as those present in Type 6 endings. The elliptical and flattened vesicles are commonly oriented with their long axes perpendicular to the synaptic junctions. Some endings contain a few spherical-shaped dense-core vesicles measuring 70-85 nm in diameter with centrally positioned granules measuring 30-60 nm in diameter. Type 7 endings are oval to elongate in shape and measure up to 2.6 μm in maximum diameter. Some Type 7 endings are seen in continuity with unmyelinated axons measuring less than 0.1-0.2 μm in diameter.

Type 8 Endings (Figure 18). These boutons represent the rarest type of presynaptic terminal in iV-Cul neuropil. They occur as en passant axons which exhibit intermittant bouton swellings. These swellings establish asymmetrical synaptic contacts with small diameter dendritic shafts (measuring less than 1.5 μm in diameter). Type 8 endings exhibit a flocculent appearing cytoplasmic matrix densely packed with a heterogeneous population of spherical to elliptical-shaped, large dense-core vesicles and a few mitochondria. The dense-core vesicles, which can number over 100 per profile, are distributed throughout the bouton as well as positioned in close proximity to the presynaptic membrane specialization at synaptic junctions. The spherical-shaped dense-core vesicles range 70-92 nm in diameter, while the elliptical-shaped dense-core vesicles measure 90-140 nm in maximum diameter and exhibit maximum width-to-length ratios of 1:2. These dense-core vesicles possess spherical to elliptical-shaped centrally positioned granules ranging 46-96 nm in maximum diameter. Although the granule-to-vesicle ratio varies among the dense-core vesicles, in most cases the granule practically fills the entire vesicle. A smaller number of large spherical to elliptical-shaped agranular synaptic vesicles (measuring 40-65 nm in maximum diameter) are scattered throughout these endings and are especially prominent at the synaptic junctions. The elliptical-shaped agranular synaptic vesicles exhibit maximum width-to-length ratios of 1:3. Type 8 boutons are oval to elliptical in shape and measure 1.1-2.3 μm in diameter.

Distribution of Synaptic Profiles

Axosomatic synaptic contacts constitute only a minor portion of the synaptic relationships in this nucleus. Less than 1% of the surfaces of somatic profiles are involved in axosomatic synapses which arise exclusively from Type 5 endings.

Axodendritic and axospinous synaptic contacts constitute the majority of the synaptic population in iV-Cul. Dendrites of all sizes receive axodendritic synaptic contacts. All eight types of presynaptic terminals are engaged in axodendritic

synaptic relationships. Type 1, Type 4 and Type 5 boutons possess the widest distribution along the dendritic tree, while the remaining types are confined to the smaller diameter dendrites. The extent of dendritic surfaces covered by axon terminals varies depending upon the size and plane of sectioning of the dendrite. Cross-sections of the largest diameter dendrites are rarely covered by presynaptic boutons, while the smaller diameter dendrites more frequently receive multiple axodendritic synapses. The extent of dendritic surfaces apposed by synaptic or non-synaptic boutons in longitudinally-sectioned profiles ranges from 5-15% of the available surface. The remaining portions of these dendrites are usually covered by astrocytic processes. The smallest diameter longitudinally-sectioned dendritic profiles often exhibit small clusters of boutons of differing morphologies. These multiple axodendritic synapses may be composed of 2 to 4 separate morphological types of boutons. All of the presynaptic bouton types, with the exception of Type 8 endings, are observed in these types of relationships. There is commonly a mixture of asymmetrically and symmetrically associated endings in these clusters. Type 1 profiles are commonly associated with Type 3 and Type 7 endings; Type 4 profiles with Types 5, 6, and 7 endings; and Type 3 profiles with Type 5 and Type 6 endings. In some instances, multiple profiles of Type 4 or Type 5 endings are found with one or more morphologically different types of boutons in these relationships.

Axospinous synaptic contacts arise from all but Type 3 and Type 8 endings. Invaginating spines receive axospinous synaptic contacts exclusively from Type 1 and Type 4 endings. Type 1 and Type 6 endings often establish synaptic contact with a dendritic spine as well as its parent dendritic shaft. In some instances, these two bouton types simultaneously establish synaptic contact with a single pedunculated spine and they may also contact the parent dendritic shaft.

The numerous synaptic glomeruli in iV-Cul contain exclusively either Type 1 or Type 2 endings at their core. Type 5 or Type 7 boutons are occasionally involved

in glomeruli in those instances where they form synaptic contacts with either a dendritic shaft or one of the complex spines in these glomeruli. The remaining six types of bouton profiles are confined to extraglomerular synaptic relationships. Types 5, 6 and 7 endings are commonly found in axodendritic synaptic relationships with either the large diameter dendritic shafts or the common dendritic stems which give rise to the spines engaged in synaptic glomeruli with Type 1 endings.

The extensive astrocytic encapsulation of synaptic boutons to form "isolated" structures in the neuropil are usually associated with Types 1, 2 or 4 endings. Although the extent of astrocytic processes present in iV-Cul necessarily precludes close apposition between two vesicle containing profiles, a few rare instances are found. In these cases, the two profiles are usually morphologically similar and represent Type 3 or Type 5 endings. Although, macula adherens are occasionally observed between these latter profiles, no clustering of synaptic vesicles, widened synaptic cleft or presynaptic membrane specializations are seen in either profile.

Spinal Afferent Inputs

The light microscopic morphology of the HRP-labeled spinal afferents examined in the present study have been described in detail elsewhere (see Chapter Four). At the electron microscopic level, HRP-labeled myelinated axon collaterals, unmyelinated preterminal axon segments and presynaptic endings are evident throughout the iV-Cul neuropil (Figures 19-23).

The HRP-labeled myelinated axon collaterals range in size from 0.5 to 1.8 μm in diameter (Figure 19). They exhibit myelin sheaths ranging from 0.04 to 0.1 μm thick which generally decreases along with the decreasing size of the axons. These myelinated axons occur singly in the neuropil as well as in groups with 2 or more unlabeled myelinated axons.

The HRP-labeled unmyelinated preterminal segments range in size from 0.1 to 0.45 μm in diameter (Figures 20, 22, and 23) and course for varying distances

within the neuropil before giving rise to boutons. These unmyelinated axons occur singly in the neuropil as well as in small groups with several unlabeled unmyelinated axons. Some of these labeled preterminal segments travel along the shafts of dendrites before giving rise to boutons engaged in synaptic glomeruli with the spines of these dendrites.

The entire population of HRP-labeled spinal afferent endings in this material appears morphologically similar to Type 1 endings (Figures 21-23). The largest of the Type I endings remained unlabeled in the present experimental material. The endings contain centrally located mitochondria, numerous large, spherical-shaped, agranular synaptic vesicles measuring 40-50 nm in maximum diameter, and are primarily involved in synaptic glomeruli (Figures 21 and 22). They establish asymmetrical synaptic contacts with dendritic spines as well as parent dendritic shafts (measuring 0.5 to 2.3 μm in diameter) or the common dendritic stems of complex spines. The HRP-labeled boutons are oval to irregular in shape and range from 0.9 to 2.9 μm in diameter. The smallest labeled boutons may exhibit irregular contours and establish synaptic contacts with up to four separate small diameter dendrites or single pedunculated spines. Some dendritic shafts which lie postsynaptic to labeled Type 1 endings also receive axodendritic synapses from single unlabeled Type 5 endings (Figure 22). Some non-complex spines involved in synaptic glomeruli with labeled Type 1 profiles also receive axospinous synapses from unlabeled Type 5 endings. In one instance, a labeled Type 1 ending forms an axodendritic synapse with a dendritic shaft before it enters into a synaptic glomerulus with its complex spines. The shaft of this same dendrite also receives an axodendritic synapse from an adjacent unlabeled Type 1 ending which is engaged in a synaptic glomerulus with the spines of another dendrite. Some labeled en passant boutons establish synaptic contacts with single dendritic shafts and/or their pedunculated spines (Figure 23).

Table 1. Summary of Bouton Morphology and Distribution

Presynaptic Boutons			Synaptic Vesicles					Postsynaptic Targets				Synaptic	Afferent
			Agranular		Granular								
Type	Shape	Size	Shape	Size	Shape	Size	Number	Soma	Dendrite	Spine	Glomeruli	Junctions	Sources
1	oval to irregular	1.6–4.2[a]	s–o[b]	40–60[c] (1:1.5)[d]	s	50–80[c]	a few	–	+	+	+C[e]	Asym	Spinal
2	round to oval	1.5–4.2	"	"	s	82–108	a few	–	+	+	+C	Asym	?
3	dome	1.0–1.6	"	"	s	50–90	several	–	+	–	–	Asym	?
4	dome to irregular	1.1–2.0	s–o	35–55 (1:1.5)	s	80–90	many	–	+	+	–	Asym	?
5	dome	0.7–1.5	s,p e	35–50 (1:3)	–	–	–	+	+	+	+P[f]	Sym	?
6	dome	0.6–1.6	e	40–60 (1:3)	–	–	–	–	+	+	–	Sym	?
			f	45–65 (1:3.5)									
7	oval to elongate	2.6	s	35–40	s	70–85	a few	–	+	+	+P	Sym	?
			e	40–60 (1:3)									
			f	45–65 (1:3.5)									
8	oval to elongate	1.1–2.3	s,o e	40–65 (1:3)	s e	70–92 90–140 (1:2)	dense	–	+	–	–	Asym	?

[a] All bouton measurements are given in um. [b] s, o, e, p, and f = spherical, ovoid, elliptical, irregular, and flattened synaptic vesicles. [c] All synaptic vesicle measurements are given in nm. [d] Maximum Width-to-Length ratios. [e] = Central bouton in glomerulus. [f] = May be present as peripheral bouton in glomerulus. Asym, Sym = Asymmetrical, Symmetrical synaptic junctions. + = An observed synaptic relationship. – = Not found. ? = Source unknown.

Figure 1

An electron micrograph illustrating the somatic morphology of a typical iV-Cul neuron. Most of the somatic surface is apposed by astrocytic processes (arrowheads) which also intervene between it and an adjacent neuronal somata. The cytoplasm contains numerous organelles including mitochondria (m), golgi complexes (G), nissl bodies (NB), free ribosomes, granular endoplasmic reticulum and lipofuscin granules. The nucleus is characterized by a large centrally placed nucleolus (n) and prominent nuclear invaginations. X 8,390.

Figure 2

A Type 5 ending forms a symmetrical synapse with a neuronal somata (S). Astrocytic processes (a) surround the synapse. The small arrows in this and subsequent figures represent the location and direction of the synaptic contact. X 23,240.

Figure 3

A somatic spine (s) receives a symmetrical synapse from a Type 5 ending. The spine exhibits a relatively dark, flocculent appearing cytoplasmic matrix compared to the cell body (S) and contains several vesicular structures including a coated vesicle. Astrocytic process (a). X 23,240.


n
NB
1
2
a
S
a
S
3
S
a
S'

Figure 4

A Type 1 ending is centrally positioned in a synaptic glomerulus and establishes asymmetrical synaptic contacts with the shaft of one dendrite (D) and the complex spine (s) of another. X 23,240.

Figure 5

A centrally located Type 1 ending possessing a few dense core vesicles establishes asymmetrical synaptic contacts with two dendritic spines (s) and a dendritic shaft (D). The synaptic glomerulus is encapsulated by an astrocytic process (a). X 23,240.

Figure 6

A large Type 1 ending establishes asymmetrical synaptic contacts with several peripherally distributed spines (s). The entire synaptic glomerulus is encapsulated by several thin astrocytic glial processes (a). X 23,240.

Figure 7

A Type 2 bouton arises from a thin unmyelinated preterminal axon segment (u) and establishes a single asymmetrical synaptic contact with a small spine (s). Astrocytic process (a). X 23,240.

Figure 8

A large Type 2 ending lying adjacent to a large diameter dendrite (D) establishes asymmetrical synaptic contacts with the spine-like appendages (s) which arise from the parent dendritic shaft. X 23,240.

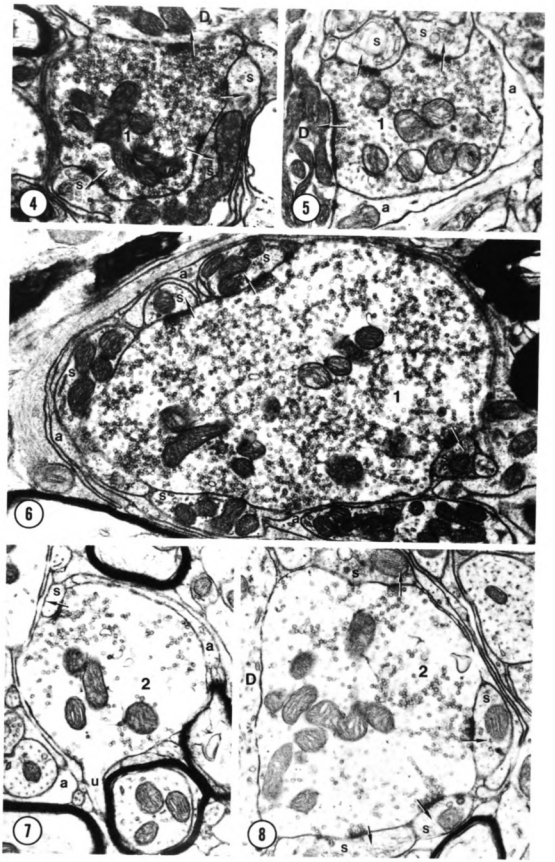
D
s
1
a
2
u
4
5
6
7
8

Figure 9

A Type 3 ending establishes an asymmetrical synaptic contact with a spine (s) of a small diameter distal dendritic shaft. Astrocytic process (a). X 23,240.

Figure 10

A Type 3 ending establishes an asymmetrical synaptic contact with a small diameter dendritic shaft which also receives asymmetrical synaptic contacts from several Type 5 and Type 6 endings. Astrocytic processes (a). X 23,240.

Figure 11

Several Type 4 endings establish asymmetrical synaptic contacts with a series of small diameter dendrites (D). An invaginating spine (s) is present in one of the boutons. Several astrocytic processes (a) surround each of the axodendritic synapses. The neuropil exhibits several unmyelinated preterminal axon segments (u). X 23,240.

Figure 12

A Type 4 ending establishes asymmetrical synaptic contacts with a dendritic spine (s) and its parent dendritic shaft (D). X 23,240.

Figure 13

A Type 4 ending establishes an asymmetrical synaptic contact with a bilobed spine (s) arising from a small diameter dendritic shaft (D). The axospinous synapse is encapsulated by several compactly arranged glial lamellae (a). Several Type 5 and Type 3 endings surround the parent dendritic shaft and establish asymmetrical synaptic contacts. X 23,240.

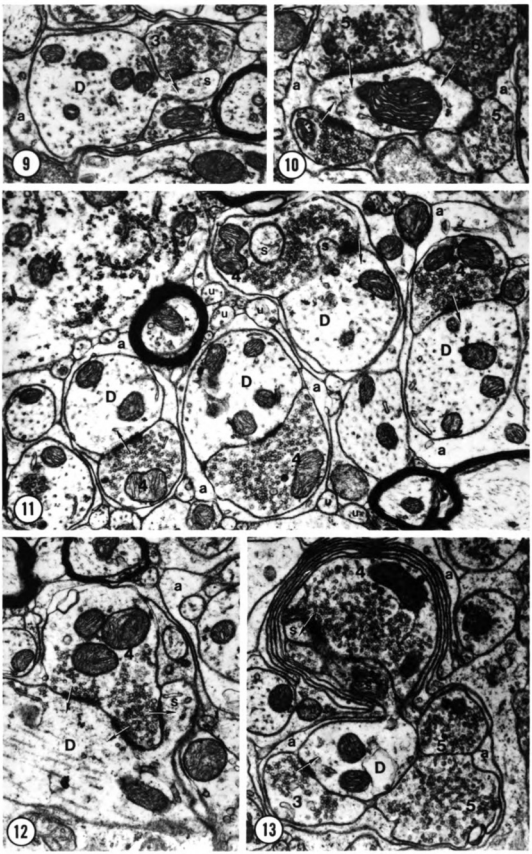
9
D
a
s
3
10
a
s
3
5
11
D
a
s
u
4
12
D
a
4
5
13
D
a
s
3
5

Figure 14

A Type 6 ending arising from an unmyelinated preterminal segment (u) establishes a symmetrical synaptic contact with a small diameter dendrite (D). A Type 4 ending is nestled between two dendritic spines and establishes an asymmetrical synaptic contact with the parent dendrite. Astrocytic processes (a) tightly envelope the terminals and their postsynaptic targets to isolate them from neighboring structures. X 23,240.

Figure 15

A Type 6 ending establishes a symmetrical synaptic contact with a small diameter dendrite. Astrocytic processes (a). X 23,240.

Figure 16

A Type 7 ending establishes symmetrical synaptic contacts in an en passant fashion with two separate dendritic profiles (D). X 23,240.

Figure 17

A Type 7 ending establishes symmetrical synaptic contacts with the shaft of a dendrite (D) and with the head of a spine (s) arising from this dendrite. X 23,240.

Figure 18

A Type 8 ending establishes an asymmetrical synaptic contact with a dendrite (D). Fibrous astrocytic processes (a). X 23,240.

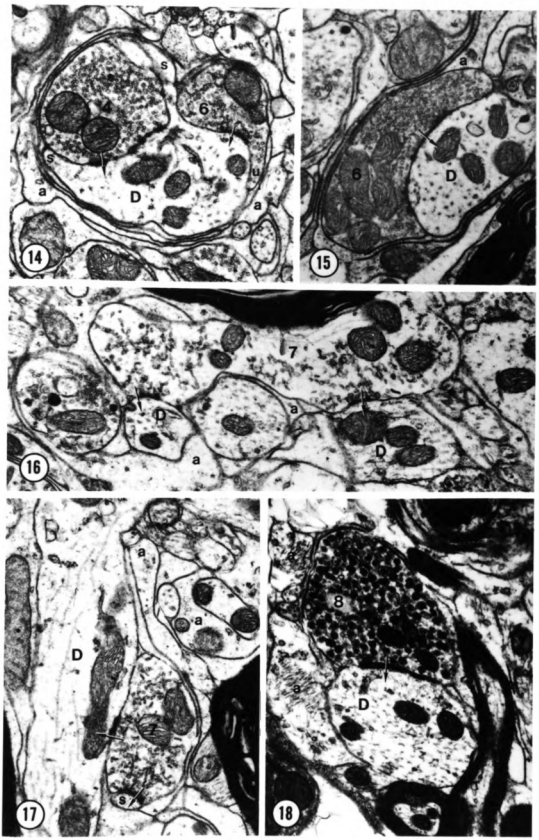
14
s
6
s
a
D
a
15
a
6
D
16
7
D
a
a
D
17
a
a
D
8
18
8
D

Figure 19

An HRP-labeled myelinated axon collateral arising from the cervical level of the spinal cord. X 23,240.

Figure 20

An HRP-labeled unmyelinated preterminal axon segment (u). X 23,240.

Figure 21

A centrally positioned HRP-labeled Type 1 ending establishes asymmetrical synaptic contacts with a parent dendritic shaft (D) and two of its spine-like appendages (s) in a typical synaptic glomerulus. Astrocytic processes (a) surround the glomerulus. X 23,240.

Figure 22

A typical HRP-labeled Type 1 ending is engaged in a synaptic glomerulus with the shaft of one dendrite (D) and the complex spine of another. A Type 5 ending forms a symmetrical synapse onto the base of the complex spine emanating from the dendrite (D). An HRP-labeled unmyelinated preterminal axon segment (u) is also present in the neuropil. Astrocytic processes (a). X 23,240.

Figure 23

An HRP-labeled en passant Type 1 ending arises from an unmyelinated preterminal axon segment (u) and establishes an asymmetrical synapse with a small diameter dendrite (D). X 23,240.


19


u
20


a
D
s
1
s
s
s
a
21

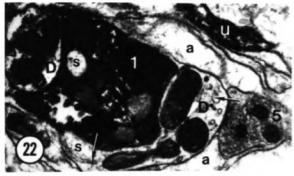
u
a
D
s
1
D
5
22
s
a

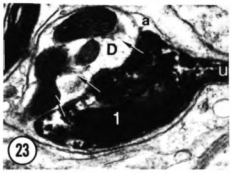
a
D
u
1
23

Figure 24

A schematic diagram illustrating the synaptic relationships present in a representative synaptic glomerulus in iV-Cul neuropil. A centrally positioned Type 1 ending establishes asymmetrical synaptic contacts with the shaft of one dendrite (D1) and the complex spine (s) of a second dendrite (D2). The base of the complex spine of D2 receives a symmetrical synaptic contact from a Type 7 ending, while the parent dendrite receives a symmetrical synaptic contact from a Type 5 ending. The entire synaptic glomerulus is ensheathed by several astrocytic glial lamellae (a). X 23,240.

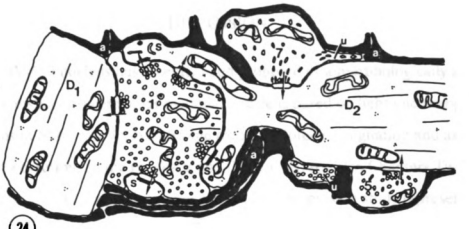

(24)

DISCUSSION

The iV-Cul nucleus has recently been proposed as a morphologically and functionally distinct precerebellar medullary nucleus based on light microscopic observations in Nissl, myelin, cytochrome oxidase, Golgi impregnation and axonal transport preparations in the rat (Falls and Phelan, '84; see also Chapters Two and Four). The ultrastructural observations reported in the present study represent the first detailed electron microscopic examination of this nucleus in any species.

The region occupied by iV-Cul has for a long time been erroneously considered to represent a simple extension of neighboring somatosensory nuclei such as Cul, LR, paratrigeminal (PaV), substantia gelatinosa (SG, laminae I and II) layer of the medullary dorsal horn (MDH) and Vi (see Chapter Two for complete review). However, the results of the present study reveal an overall ultrastructural organization of iV-Cul neuropil which is distinctly different from any of these neighboring nuclei to unequivocally support the recent light microscopically derived recognition of iV-Cul as a separate precerebellar medullary nucleus. Considering the importance of this distinction, the findings of the present study will be discussed with an emphasis on comparing and contrasting the ultrastructural organization of iV-Cul with those somatosensory nuclei with which it has long been wrongly associated in the literature.

Neuropil and Neurons

The rodent iV-Cul is one of several components of the InSy-SVT. It consists of insular and interstitial patches of neuropil distributed lateral to and amongst the fibers of SVT (Falls and Phelan, '84; see also Chapter Two). The present findings reveal that the "main insular" as well as the isolated "insular" and "interstitial" patches of neuropil within iV-Cul are relatively uniform in their ultrastructural

appearance. This observation confirms the overall homogeneous nature of iV-Cul neuropil as previously reported at the light microscopic level.

The ultrastructural appearance of iV-Cul neurons is typical for central nervous system (CNS) neurons and does not differ significantly from that of neurons in neighboring medullary somatosensory nuclei. In the previous light microscopic analysis of iV-Cul, it was proposed that this nucleus contains a homogeneous neuronal population based on the overall uniform cytological appearance and similarity in projections of its constituent neurons. The absence of any detectable ultrastructural differences in cytology among the constituent neurons of iV-Cul provides additional evidence favoring a morphologically homogeneous neuronal population. However, since there is a conspicuous absence of any correlative electrophysiological or pharmacological information on iV-Cul neurons, any statement regarding the extent of their functional homogeneity remains speculative at this time. Nevertheless, the fact that every neuron in the nucleus contributes axonal projections to the cerebellum (Phelan and Falls, '84c; see also Chapter Two) indicates that all of these neurons at least share in a common fundamental function as precerebellar medullary "relay" neurons.

The soma-dendritic morphology of iV-Cul neurons revealed at the electron microscopic level confirms and extends previous light microscopic descriptions based on observations of Golgi impregnated and retrograde axonal transport labeled neurons (see Chapter Two). The present study confirms the presence of somatic and dendritic spines and spine-like appendages on iV-Cul neurons. The frequent appearance of these structures throughout the neuropil in the present study suggests that they may be more common than previously reported based solely on observations made in Golgi impregnated preparations (see Chapter Two). In agreement with light microscopic observations, these spines and spine-like appendages were more often seen emanating from the smallest diameter distal

dendrites rather than the relatively larger diameter proximal dendritic processes or somata.This distribution pattern may underlie the observed differences in spine frequency since complete impregnation of isolated distal dendritic arbors were difficult to obtain in the Golgi impregnated material whereas the sampling in the present study was free of such problems. The ultrastructural variety in morphology and distribution of the spines and spine-like appendages in iV-Cul parallels the heterogeneity previously reported at the light microscopic level. The present study specifically documents the presence of two main morphological types of dendritic spines referred to as "simple" and "complex" spines. The simple spines represent single spines or spine-like appendages which exhibit a variety of morphological forms usually consisting of distinct spine heads and necks. The complex spines, on the other hand, represent two single spine-like appendages which arise from a single common short spine stem. These spines were preferentially distributed in distal regions of the dendritic tree and were usually involved in synaptic glomeruli. While the morphology of the appendages in the complex spines varied, they tended to exhibit a bilobed or multilobulated appearance. The presence of complex spines was previously noted at the light microscopic level in iV-Cul and in PaV nuclei (see Chapter Two). The presence of these complex spines appears to represent an important component in the neural processing substrate in iV-Cul as reflected in their involvement in synaptic glomeruli. Similar distinctions in spine morphology have not yet been reported in neighboring somatosensory medullary nuclei.

The most intriguing aspect of the ultrastructural organization of iV-Cul neuropil was the conspicuous presence of an unusually large amount of astrocytic glial processes. These glial processes surrounded each tissue element and often formed several lamellae around dendritic or somatic profiles as well as synaptic complexes including simple synaptic glomeruli. These encapsulations often appeared to isolate these structures from neighboring tissue elements. These

"isolated" elements were quite obvious even at low power magnification throughout the neuropil. The presence of these extensively isolated structures is not peculiar to iV-Cul however, since similar structures have been reported in other medullary somatosensory nuclei, especially those located near the brain surface, such as the PaV (Chan-Palay, '78a) and Cul (Rosenstein, Page and Leure-duPree, '77) nuclei. In these latter nuclei, these unique glial encapsulations have been reported to be preferentially distributed along blood vessels. However, they did not exhibit any preferential orientation within iV-Cul neuropil. Although the precise function of these glial encapsulations in the CNS is not known, several theories have been proposed to explain their presence. It has been postulated that these structures may function in the segregation of receptor surfaces through the isolation of neighboring synaptic complexes (Peters and Palay, '66; Pappas, Cohen and Purpura, '66). It has also been suggested that these structures may act as exclusion barriers for potassium ions (Pinching and Powell, '71; Spacek and Lieberman, '74) and extracellular fluids (Szentagothai, '70). Finally, it has been proposed that such structures may serve as the morphological basis for multiple repetitive discharge (Spacek and Lieberman, '74), a phenomenon which has been demonstrated to exist in Cul (Cooke, Larson, Oscarsson and Sjolund, '71; Rosen and Sjolund, '73a,b; and Campbell, Parker and Welker, '74). The ultrastructural analysis conducted in the present study provides no information regarding the function of these glial encapsulations in iV-Cul.

Synaptology

The present study reveals that the synaptic population of iV-Cul consists of a morphologically heterogeneous group of axon boutons. The morphological variety of axon terminals in iV-Cul suggests that the neuronal activity of the precerebellar neurons in iV-Cul are modulated by a number of different neuron populations. Similar heterogeneity of axonal endings have also been reported in Cul (Rosenstein and Leure-duPree, '77; and O'Neal and Westrum, '73), LR (Mizuno, Konishi, and

Nakamura, '75; Andrezik and King, '77; and Hrycyshyn and Flumerfelt, '81), SG (Gobel et al., '80; Gobel, '74; and Ruda and Gobel, '80), PaV (Chan-Palay, '78a,b) and Vi (Westrum and Black, '71; and Ide and Killackey, '85). However, the specific types of axonal endings and their inter-relations with iV-Cul neurons does not entirely conform to any of the patterns previously reported in these neighboring somatosensory nuclei.

The heterogeneous population of axonal endings described in the present study formed axodendritic, axospinous and axosomatic contacts with iV-Cul neurons. The largest number of synaptic contacts consisted of axodendritic and axospinous synapses with the greatest number of these located on peripheral portions of the dendritic tree. In contrast, the somata and proximal dendrites of iV-Cul neurons were relatively free of synaptic contacts suggesting that the vast majority of synaptic integration occurs on the peripheral dendritic arbors of iV-Cul neurons. The distribution of synaptic contacts on Cul and LR neurons is generally similar to that observed in iV-Cul in which the distal dendrites have a greater role in synaptic integration than the proximal dendrites or somata (Rosenstein and Leure-duPree, '77; Mizuno et al., '75; Andrezik and King, '77; and Hrycyshyn and Flumerfelt, '81). However, the number of axosomatic contacts was relatively small in iV-Cul in comparison to the number of such contacts in Cul and LR. On the other hand, axosomatic contacts have been reported to be a prominent feature of PaV (Chan-Palay, '78a,b) and Vi (Ide and Killackey, '85) neuropil.

One of the most striking aspects of the ultrastructural organization of iV-Cul was the absence of any distinguishable axo-axonic synapse. The unusually large amount of astrocytic glial processes present in iV-Cul may partially contribute to this situation since their presence necessarily prevents close apposition of axonal endings. Serial axo-axonic synapses form the morphological basis for presynaptic inhibition or facilitation in the CNS. The absence of such synapses in iV-Cul

indicates that presynaptic modulation of afferent impulses does not exist in iV-Cul. The absence of axo-axonic synapses is a feature which iV-Cul shares with other medullary nuclei including LR (Mizuno and Nakamura, '73). However, the absence of axo-axonic contacts in these two nuclei contrasts sharply with the fairly common appearance of such synaptic contacts in SG (Gobel, '74), PaV (Chan-Palay, '78a,b), Cul (Rosenstein and Leure-duPree, '77) and Vi (Ide and Killackey, '85). This difference is one of the most notable between iV-Cul and neighboring nuclei and provides strong support for the recognition of this medullary region as a distinct nucleus rather than a simple extension of neighboring structures.

The results of the present study indicate the presence of eight morphologically distinct types of terminals within iV-Cul. These different types of terminals are distinguished primarily by the morphology of their synaptic vesicle content, the type of associated junctional complex, and their distribution along the soma-dendritic tree. In general they can be grouped into three classes depending upon whether they contain predominantly spherical-shaped agranular synaptic vesicles (Types 1 through 4); predominantly flattened or pleomorphic-shaped agranular synaptic vesicles (Types 5 through 7); or a heterogeneous population of large dense-core vesicles (Type 8). Five of these terminal (Types 1 through 4 and Type 8) were associated with asymmetrical synaptic junctions, while three types of boutons (Types 5 through 7) were associated with symmetrical synaptic junctions. Each of these eight types of bouton terminals exhibited distinct distribution patterns along the soma-dendritic tree as summarized in Table I.

The majority of the axonal endings present in iV-Cul possessed primarily spherical-shaped agranular synaptic vesicles. Variations in the size of these spherical-shaped synaptic vesicles contributed to the distinction of the different types of terminals in this category. In particular, Types 1 through 3 contained large (40-60 nm) synaptic vesicles while Type 4 contained smaller (35-55 nm) synaptic

vesicles. Similar variations in the size of spherical-shaped agranular synaptic vesicles have been reported in Cul (Rosenstein and Leure-duPree, '77). In iV-Cul, these spherical-shaped agranular synaptic vesicle containing terminals appear to be preferentially distributed to distal portions of the dendritic tree, a pattern which appears to be common in medullary somatosensory nuclei (Rosenstein and Leure-duPree, '77; Ide and Killackey, '85; and Mizuno et al., '75).

Axonal endings exhibiting flattened or pleomorphic-shaped agranular synaptic vesicles (Types 5 through 7) constituted only a minority of the total number of synaptic endings in iV-Cul. However, these terminals had a more generalized distribution along the soma-dendritic tree than those terminals containing spherical-shaped agranular synaptic vesicles. It has been reported that the presence of flattened and pleomorphic-shaped synaptic vesicles is affected by the type of fixative used in the processing of the tissue for electron microscopy (Walberg, '66; Bodian, '70; and Valdivia, '71). Unfortunately, the fixatives used in other electron microscopic examinations of medullary somatosensory nuclei did not always produce such changes in the morphology of synaptic vesicles and so direct comparisons between the types of flattened and pleomorphic-shaped synaptic vesicle containing terminals identified here and those other medullary nuclei is not possible at this time.

It has long been suggested that those axonal endings which contain spherical-shaped agranular synaptic vesicles and establish asymmetrical synaptic contacts may be associated with an excitatory function, while those axonal endings which contain flattened or pleomorphic-shaped agranular synaptic vesicles and establish symmetrical synaptic contacts may be associated with an inhibitory function (Uchizuno, '65, '67). The extension of this association of structure and function as a general rule throughout the CNS has not proven to be valid (Angaut and Sotelo, '73). The application of these generalities to a particular nucleus in the absence of

corroborating electrophysiological data should, therefore, always be done cautiously. Nevertheless, some speculation regarding the implications of such generalities within iV-Cul are warranted at this time since it may allow some insight into the function of this relatively uninvestigated nucleus.

The fact that the majority of the synaptic contacts observed throughout iV-Cul contained primarily spherical-shaped agranular synaptic vesicles and established asymmetrical synaptic contacts may indicate a preponderance of excitatory synaptic inputs impinging on iV-Cul neurons. Although those axonal endings which possessed predominantly flattened or pleomorphic-shaped synaptic vesicles and established symmetrical synaptic contacts were fewer in number, they were interestingly the sole source of axosomatic inputs to iV-Cul neurons and may therefore provide a relatively strong inhibitory influence over the activity of these neurons. In addition, these "presumptive"inhibitory endings were also conspicuously placed in strategic positions proximal to glomerular complexes, at the base of proximal dendrites, and at dendritic branch points. In the absence of axo-axonal synaptic relationships in iV-Cul, the strategic placement of these "presumptive" inhibitory synapses at these positions along the soma-dendritic tree may allow for the effective modulation of excitatory transmission through this nucleus. The higher percentage of the presumed excitatory versus inhibitory inputs to iV-Cul is a pattern generally consistent with that found in other medullary somatosensory nuclei.

A small percentage of the total population of synaptic vesicles in iV-Cul were dense-core vesicles. In fact, only one of the eight types of boutons (Type 8) contained predominantly dense-core vesicles. The presence of dense-core synaptic vesicles have long been associated with monoaminergic fibers within the CNS. The paucity of dense-core vesicle containing terminals in iV-Cul may therefore suggest that monoaminergic inputs to this region do not play a significant role in the overall functioning of this nucleus. In many nuclei monoaminergic inputs are not involved

in synaptic transmission directly since they do not form synaptic contacts, but are rather involved in the non-synaptic release of neuromodulators (for a complete review see Chan-Palay, '77b). The dense-core vesicle containing terminal in the present study clearly established asymmetrical synaptic junctions with dendritic profiles. However, the results of the present study provide no information on whether or not every Type 8 terminal establishes synaptic contacts in iV-Cul. It has also been reported that some monoaminergic terminals in the brainstem contain predominantly spherical-shaped synaptic vesicles (Chan-Palay, '78; and Ruda and Gobel, '80). It is possible that some of these types of axonal endings in iV-Cul may represent a monoaminergic inputs to this nucleus. However, immunocytochemical studies of the distribution of monoaminergic fibers do not indicate that this region of the lateral medulla receives a significant monoaminergic input (Hokfelt, Martensson, Bjorklund, Kleinau and goldstein, '84). A dense-core vesicle containing terminal, such as that described here, has also been reported to represent the least common terminal type in Cul (Rosenstein and Leure-duPree, '77). In contrast however, dense-core vesicle containing terminals represent the predominant type of axonal endings in PaV (Chan-Palay, '78a,b). They are also fairly common throughout SG (Ruda and Gobel, '80; and Gobel, '74). These differences indicate another major difference in the functional organization of iV-Cul and neighboring medullary nuclei.

A distinctive feature of iV-Cul neuropil is the presence of synaptic glomerular complexes. These synaptic glomeruli form the primary site for somatosensory integration in the CNS. The synaptic glomeruli in iV-Cul were readily apparent throughout the nucleus and were relatively simple in nature. They were composed of a few peripherally distributed dendritic shafts and dendritic spines surrounding a single large central bouton which formed asymmetrical synaptic contacts with these peripheral elements. In some instances a second axonal

ending was present as a peripheral bouton which synaptically contacted the parent dendritic shaft. The entire glomerulus was characteristically encapsulated by several astrocytic glial processes. This simplicity in the organization of the synaptic glomeruli in iV-Cul contrasts sharply with the relative complexity of synaptic glomeruli in other somatosensory nuclei (Rosenstein and Leure-duPree, '77; Ide and Killackey, '85; Chan-Palay, '78a,b; Gobel, '74). The glomeruli in these latter nuclei usually possess numerous peripheral components distributed around the central bouton. In addition, they commonly contain peripheral boutons which represent presynaptic axonal endings forming axo-axonic contacts with the central bouton. Dendro-axonic and dendro-dendritic interactions are also sometimes an integral component of these glomeruli, as is the case in SG (Gobel, '74). The differences in glomerular organization in iV-Cul and neighboring somatosensory nuclei represent still another significant morphological feature underlying basic differences in the processing of somatosensory information in these medullary nuclei.

Sources of Input

A prominent afferent input to iV-Cul, arising from the cervical spinal cord, has previously been anatomically demonstrated at the light microscopic level (Phelan and Falls, '84b; see also Chapter Four). This spinal input was electron microscopically examined in the present study using the anterograde labeling of these fibers following HRP injections into the upper cervical spinal cord. The results illustrate that the spinal afferents to iV-Cul end as Type I terminals. The diagram in Figure 24 schematically summarizes the spatial relationship of identified spinal afferent terminals with other synaptic profiles in iV-Cul. The HRP-identified spinal afferent endings synaptically contacted dendritic shafts as well as complex and simple dendritic spines. They were primarily involved in synaptic glomeruli. The absence of any axonal boutons at locations presynaptic to these spinal afferent terminals suggests that no presynaptic inhibition or facilitation of these "presumed"

excitatory afferent inputs exists within the glomerulus of iV-Cul. However, the common appearance of flattened synaptic vesicle containing terminals, representing presumptive inhibitory synapses, at locations immediately proximal to these excitatory inputs suggests that postsynaptic modulation of spinal afferent information is nevertheless an integral component of somatosensory processing in iV-Cul.

A spinal afferent projection to the neighboring interstitial PaV nucleus has not yet been reported in any species. However, spinal afferents have anatomically been demonstrated in Cul (Rustioni and Marchi, '68; and Basbaum and Hand, '73), LR (Kunzle, '73; Mizuno et al., '75; Mizuno and Nakamura, '77), and Vi (Phelan and Falls, 84b; see also Chapter Four). The electron microscopic examination of identified primary spinal afferent fibers in Cul (Rosenstein, Page and Leure-duPree, '77) and LR (Westman, Danckwardt-Lilliestrom, Dietrichs, Svensson and Walberg, '86) revealed that these inputs also represent central glomerular endings. The morphology of the HRP-identified Type I spinal afferent fibers in iV-Cul was particularly similar to that of the primary spinal afferents in Cul.

Since no other source of afferent input to iV-Cul has yet been anatomically determined, the origin of the remaining types of axonal endings revealed in the present study remain unknown. A potential source of some of these endings may possibly be iV-Cul neurons themselves. One way this could be achieved is through the presence of recurrent axon collaterals on iV-Cul neurons. Although previous examination of Golgi impregnated iV-Cul neurons failed to reveal the presence of any intrinsic recurrent axon collaterals (see Chapter Two), final resolution of this question must await the application of more reliable labeling techniques such as the intracellular injection of HRP. An alternative way that iV-Cul neurons could themselves contribute to the population of terminal boutons within the neuropil is through dendro-dendritic interactions by way of direct dendritic shaft apposition or

through presynaptic dendritic spines. The present study did not reveal the presence of any presynaptic dendrites within iV-Cul. Although some dendritic profiles often contained a rare dense-core vesicle, no accumulation of vesicles or presynaptic membrane specialization were ever observed. Furthermore, close apposition of dendritic surfaces was rarely seen because of the large amount of astrocytic glial processes which enveloped most neural elements in the nucleus. In addition, the present study found no evidence for any presynaptic dendritic spines. It must be noted however that serial reconstruction of the larger spines and spine-like appendages was not attempted in the present study because of the tortuous course that these structures often followed in the neuropil. The possibility therefore remains that some of the axonal endings observed in iV-Cul may actually represent presynaptic dendritic spines. The existence of presynaptic dendrites and dendritic spines has been reported in neighboring somatosensory nuclei, especially in SG where they form an integral component of the morphological integrative processing substrate (Gobel, '76).

Functional Considerations

The electrophysiological and pharmacological nature of iV-Cul neurons remains relatively obscure at this time. Since mossy fiber inputs to the cerebellum are primarily excitatory in nature, the iV-Cul projection to the cerebellum may also likely be excitatory. Furthermore, the afferent spinal input to iV-Cul may be, based on its central position in synaptic glomeruli and the associated asymmetrical junctional complex, providing an excitatory input to iV-Cul neurons. In this regard, inhibitory synaptic boutons in central positions of glomeruli have not been reported in any medullary somatosensory nuclei. Therefore, the iV-Cul nucleus may represent a brainstem relay site for a disynaptic excitatory pathway to the cerebellum from the spinal cord. Whether the spinal input to iV-Cul represents a direct monosynaptic primary input or rather a polysynaptic input via secondary

spinal neurons is not yet known (see Chapter Four). However, the general morphology of spinal afferents in iV-Cul closely parallels that of known primary spinobulbar inputs (Rosenstein et al., '77). This strongly suggests that the HRP-identified spinal afferents to iV-Cul may also represent a primary spinal input. Light microscopic examination of the distribution of the afferent spinal input to iV-Cul indicates that these fibers are densely distributed throughout the entire extent of the nucleus (see Chapter Four). Unfortunately, the results of the present study do not indicate whether or not every iV-Cul neuron lies postsynaptic to the spinal input from the cervical spinal cord. In addition, the functional information conveyed by these spinal afferent fibers has yet to be determined. Nevertheless, based on the origin of the spinal fibers in the upper cervical cord and the projection of iV-Cul neurons to cerebellar target sites similar to those of Cul neurons (Somana and Walberg, '79), the iV-Cul nucleus appears to be involved in the relay of somatosensory information from neck and/or forelimb regions of the body. Further anatomical determinations of the origin of other afferent inputs to iV-Cul is certainly an essential step in gaining some knowledge of the precise role of iV-Cul in the integrative processing of somatosensory information in the lateral medulla. If the nucleus receives primary trigeminal inputs, for example, then perhaps the nucleus represents an accessory spinocerebellar pathway for regions of the head and neck which receive convergent inputs from spinal and trigeminal fibers.

The iV-Cul nucleus can be histochemically distinguished from adjoining areas by its intense staining for acetylcholinesterase (AchE) (Paxinos and Watson, '82; and Butcher and Woolf, '84). The absence of immunocytochemical staining of neurons in this region, using antibodies to the more specific cholinergic marker choline acetyltransferase (Kimura, McGeer and Peng, '84), suggests that iV-Cul receives an extrinsic cholinergic input. It has previously been demonstrated that cholinergic neurons are present in the spinal cord (Kimura et al., '84). It is possible

therefore that the spinal input to iV-Cul may represent a source of acetylcholine to this nucleus.

The putative neurotransmitter content of iV-Cul neurons is not known since the nucleus has only recently been recognized as a distinct nucleus and many of the immunocytochemical studies to date have not specifically reported the distribution of identified neurotransmitter containing neurons in this region of the lateral medulla. However, in a recent immunocytochemical study describing the distribution of 4-aminobutyrate:2-oxoglutarate transaminase (GABA-T) intensive neurons in the rat hindbrain (Nagai, Maeda, Imai, McGeer and McGeer, '85), GABA-T intensive neurons were schematically illustrated in a region which may correspond to iV-Cul. In another study, glutamic acid decarboxylase (GAD) positive cell bodies were also illustrated in a similar region of the lateral medulla (Mugnaini and Oertel, '85). The presence of GABA-T (the enzyme which catabolizes the inhibitory transmitter gamma-aminobutyric acid, i.e. GABA) and GAD (the enzyme responsible for the synthesis of GABA through the decarboxylation of glutamic acid) have proven to be reliable endogenous markers for GABAergic neurons in the CNS. The immunocytochemical detection of these two enzymes in neurons in or near iV-Cul raises the possibility that some of the neurons in this nucleus may represent GABAergic medullary neurons. The presence and extent of GABAergic neurons in iV-Cul is an important point worthy of future study since it would suggest that some part of the iV-Cul projection to the cerebellum may have a GABA mediated "inhibitory" influence over the activity of cerebellar neurons.

In an earlier investigation of the distribution of immunocytochemically identified substance P (SP) containing neurons in interstitial parts of the SVT, Chan-Palay ('78b) reported that up to 30% of the interstitial SVT neurons contained SP. In that study, Chan-Palay did not distinguish between iV-Cul and PaV nuclei such that it was not clear whether neurons in iV-Cul may represent SP containing

cells. However, in a subsequent study of the distribution of SP in rat medulla (Yamazoe et al., '84), a moderate density of SP fibers were illustrated within the region occupied by iV-Cul, but no SP immunoreactive cell bodies were detected in the same region. In addition, this latter study detected a small amount of enkephalinergic fibers in this region. The presence of SP and enkephalin fibers in iV-Cul might indicate the involvement of this nucleus in medullary nociceptive pathways since these putative neurotransmitters have long been associated with pain processing pathways in the brainstem.

The cytology and synaptic organization of iV-Cul as revealed in the present study is distinctly different enough from that reported for any of the neighboring somatosensory nuclei. In particular, the absence of axo-axonic synapses, the relative paucity of dense-core vesicle containing terminals, the relatively simple organization of the synaptic glomeruli, and the heterogeneous axonal endings in iV-Cul are all features which serve to distinguish this nucleus from any of the surrounding structures with which it has long been associated. In other words, despite some rather striking similarities in the ultrastructural organization of iV-Cul and neighboring precerebellar medullary nuclei, the results of the present study provides overwhelming evidence supporting the recent proposal that this nucleus represents a morphologically and functionally distinct precerebellar medullary nucleus. Further investigations of the electrophysiological and pharmacological properties of this nucleus may prove useful in providing insights into information processing in a relatively simple model of the relay of spinal information to the cerebellum through the medulla.

SUMMARY AND CONCLUSIONS

The overall intent of this Dissertation was to provide a basic foundation of detailed anatomical information regarding the structural and functional organization of Vi and adjacent regions including InSy-SVT in the rat. Five main phases of research encompassing several different experiments were conducted in order to achieve this goal.

The combined results of the various phases of this Dissertation, in conjunction with previous studies, provide new insights into the structural and functional organization of Vi and adjacent regions of the medulla including InSy-SVT. In particular, the results in Chapter One, in conjunction with those in Chapters Three and Four, indicate that Vi is a non-homogeneous nucleus consisting of several morphologically and functionally discrete regions which differ in their cytoarchitecture, myeloarchitecture and connectivity within the neuraxis. These studies also reveal the presence of a significant spinal input to Vi which may be relayed through different regions of Vi to the thalamus or the cerebellum. The results of these experiments also reveals a unique pattern of reciprocal relationships between Vi and the upper cervical spinal cord. In addition, the present study identifies an extensive secondary projection from cells in Vi to the thalamus, cerebellum and spinal cord. The complex distribution and morphology of these efferent projections supports the presence of functionally distinct regions in Vi. These results together implicate Vi in a variety of functions including an intimate involvement in the integration of trigeminal-neck related reflexes.

The combined results of Chapters Two, Four and Five document the existence of a structural and functional heterogeneity within InSY-SVT in the rat. In addition, these studies reveal a preferential distribution of spinal afferents to one of the five components in this system. Finally, one of the components is identified as a previously unrecognized precerebellar medullary relay nucleus which relays spinal afferent information to the cerebellum.

Despite the wealth of anatomical information provided in the various studies which form the body of this Dissertation, there are many questions which remain unanswered. For instance, How do the different regions in Vi differ with respect to their electrophysiological and phramacological characteristics? What is the precise origin of the spinotrigeminal pathway? Are there distinct primary and secondary components? What is the precise locus of termination of the trigeminospinal neurons projecting to the upper cervical spinal cord? What are the precise functions of the various regions identified in InSy-SVT? What is the source of the various synaptic terminals identified in iV-Cul? Do the thalamic projection neurons in caudal portions of Vi transmit more specific vibrissae information to the thalamus? What is the extent of collateralization throughout Vi?

BIBLIOGRAPHY

BIBLIOGRAPHY

Abrahams, V.C., and F.J.R. Richmond (1977) Motor role of the spinal projections of the trigeminal system. In D.J. Anderson and B. Matthews (eds.): Pain in the Trigeminal Region. Elsevier/North Holland Biomedical Press, Amsterdam, pp.405-411.

Abrahams, V.C., G. Anstee, F.J.R. Richmond, and P.K. Rose (1979) Neck muscle and trigeminal input to the upper cervical and lower medulla of the cat. Canad. J. Physiol. Pharmacol. 57:642-651.

Albe-Fessard, D., J. Boivie, G. Grant, and A. LeVante (1975) Labelling of cells in the medulla oblongata and the spinal cord of the monkey after injections of horseradish peroxidase in the thalamus. Neurosci. Lett. 1:75-80.

Altman, J., and S.A. Bayer (1980) Development of the brain stem in the rat. I. Thymidine-radiographic study of the time of origin of neurons of the lower medulla. J. Comp. Neurol. 194:1-35.

Andrezik, J.A. and J. King (1977) The lateral nucleus of the opossum (*Didelphis virginiana*). I. Conformation, cytology and synaptology. J. Comp. Neurol. 174:119-149.

Angaut, P., and C. Sotelo (1973) The fine structure of the cerebellar central nuclei in the cat. II. Synaptic organization. Exp. Brain Res. 16: 431-454.

Arvidsson, J. (1982) Somatotopic organization of vibrissae afferents in the trigeminal sensory nuclei of the rat studied by transganglionic transport of HRP. J. Comp. Neurol. 211:84-92.

Arvidsson, J., and L. Thomander (1984) An HRP study of the central course of sensory intermediate and vagal fibers in peripheral facial nerve branches in the cat. J. Comp. Neurol. 223:35-45.

Arvidsson, J., and S. Gobel (1981) An HRP study of the central projections of primary trigeminal neurons which innervate tooth pulps in the cat. Brain Res. 210:1-16.

Astrom, K. (1953) On the central course of afferent fibers in the trigeminal, facial, glossopharyngeal, and vagal nerves and their nuclei in the mouse. Acta Physiol. Scand. 29:209-320.

Atweh, S.F., B.M. Dajani, N.E. Saade, and S.J. Jabbur (1985) Supraspinal inhibition of trigeminal input into subnucleus caudalis by dorsal column stimulation. Brain Res. 348:401-404.

Azerad, J., A. Woda, and D. Albe-Fessard (1982) Physiological properties of neurons in different parts of the cat trigeminal sensory complex. Brain Res. 246:7-21.

Basbaum, A. and P.S. Hand (1973) Projections of cervicothoracic dorsal roots to the cuneate nucleus of the rat, with observations on cellular "baskets". J. Comp. Neurol. 148:347-360.

Bates, C.A., and H.P. Killackey (1985) The organization of the neonatal rat's brainstem trigeminal complex and its role in the formation of central trigeminal patterns. J. Comp. Neurol. 240:265-287.

Beck, C.H.M. (1976) Dual dorsal columns: A review. Can. J. Neurol. Sciences. 3:1-7.

Beckstead, R.M., and R. Norgren (1979) An autoradiographic examination of the central distribution of the trigeminal, facial, glossopharyngeal, and vagal nerves in the monkey. J. Comp. Neurol, 184:455-472.

Belford, G.R., and H.P. Killackey (1979) Vibrissae representation in subcortical trigeminal centers of the neonatal rat. J. Comp. Neurol. 183:305-322.

Berkley, K.J., A. Blomqvist, A. Pelt, and R. Flink (1980) Differences in the collateralization of neuronal projections from the dorsal column nuclei and lateral cervical nucleus to the thalamus and tectum in the cat: An anatomical study using two different double-labeling techniques. Brain Res. 202:273-290.

Berkley, K.J., and P.J. Hand (1978) Projections to the inferior olive of the cat. II. Comparisons of input from the gracile, cuneate and the spinal trigeminal nuclei. J. Comp. Neurol, 180:253-264.

Biendenbach, M.A. (1977) Response to trigeminal neurons in pars interpolaris to non-noxious and noxious stimulation. In D. Anderson and B.J. Matthews (eds.): Pain in the Trigeminal Region. Elsevier/North Holland, Biomedical Press. pp.233-242.

Bodian, D. (1970) An electron microscopic characterization of classes of synaptic vesicles by means of controlled aldehyde fixation. J. Cell. Biol, 44:115-124.

Bowsher, D., A. Brodal, and F. Walberg (1960) The relative values of the Marchi method and some silver impregnation techniques. A critical survey. Brain 83:150-160.

Breazile, J.E. (1967) The cytoarchitecture of the brain stem of the domestic pig. J. Comp. Neurol, 129:169-188.

Breazile, J.E., and R.L. Kitchell (1968) Ventrolateral spinal cord afferents to the brain stem in the domestic pig. J. Comp. Neurol. 133:363-372.

Brodal, A. (1941) Die Verbindungen des Nucleus cuneatus externus mit dem Kleinhirn beim Kaninchen und bei der Katze. Experimentelle Untersuchungen. Ztschr. f. d. ges. Neurol. u. Psychiat. 171:167-199.

Brodal, A. (1981) Neurological anatomy in relation to clinical medicine. New York, Oxford, Oxford University Press.

Brodal, A., T. Szabo, and A. Torvik (1956) Corticofugal fibers to sensory trigeminal nuclei and nucleus of the solitary tract. An experimental study in the cat. J. Comp. Neurol, 106:527-556.

Brown, J.W. (1858b) The nucleus of the spinal tract of the trigeminal nerve in the gibbon (*Hylobates lar*). Anat. Rec. 130:278.

Brown, J.W. (1956) The development of the nucleus of the spinal tract of V in human fetuses of 14 to 21 weeks of menstrual age. J. Comp. Neurol, 106:393-423.

Brown, J.W. (1958a) The development of subnucleus caudalis of the nucleus of the spinal tract of V. J. Comp. Neurol, 110:105-134.

Brown, J.W. (1962) Differentiation of the human subnucleus interpolaris and subnucleus rostralis of the nucleus of the spinal tract of the trigeminal nerve. J. Comp. Neurol, 119:55-75.

Brown, J.T., V. Chan-Palay, and S.L. Palay (1977) A study of afferent input to the inferior olivary complex in the rat by retrograde axonal transport of horseradish peroxidase. J. Comp. Neurol. 176:1-22.

Bruce, L.L., J.G. McHaffie, and B.E. Stein (1984) Organization of the hamster trigeminal complex: Projections to superior colliculus, thalamus, and spinal cord. Soc. Neurosci. Abstr. 10:483.

Burton, H., A.D. Craig, Jr., D.A. Poulos, and J.T. Molt (1979) Efferent projection from temperature sensitive recording loci within the marginal zone of the nucleus caudalis of the spinal trigeminal complex in the cat. J. Comp. Neurol. 183:753-778.

Burton, H., and A.D. Craig, Jr. (1979) Distribution of trigeminothalamic projection cells in cat and monkey. Brain Res. 161:515-521.

Burton, H., and A.D. Loewy (1976) Descending projections from the marginal cell layer and other regions of the monkey spinal cord. Brain Res. 116:485-491.

Burton, H., and A.D. Loewy (1977) Projections to the spinal cord from medullary somatosensory relay nuclei. J. Comp. Neurol. 173:773-792.

Butcher, L.L. and N.J. Woolf (1984) Histochemical distribution of acetylcholinesterase in the central nervous system: Clues to the localization of cholinergic neurons. In A. Bjorklund, T. Hokfelt, and M.J. Kuhar (eds.): Handbook of Chemical Neuroanatomy, Volume 3:Classical transmitters and transmitter receptors in the CNS, Part II. Elsevier, New York, pp. 1-50.

Cabana, T., and G.F. Martin (1984) Developmental sequence in the origin of descending spinal pathways. Studies using retrograde transport techniques in the North American Opossum (*Didelphis virginiana*). Dev. Brain Res. 15:247-263.

Cadden, S.W., L. Villanueva, D. Chitour, and D. Le Bars (1983) Depression of activities of dorsal horn convergent neurones by propriospinal mechanisms triggered by noxious inputs: Comparison with diffuse noxious inhibitory controls (DNIC). Brain Res. 275:1-11.

Campbell, S.K., T.D. Parker, and W. Welker (1974) Somatotopic organization of the external cuneate nucleus in albino rats. Brain Res. 77:1-23.

Cechetto, D.F., D.G. Standaert, and C.B. Saper (1985) Spinal and trigeminal dorsal horn projections to the parabrachial nucleus in the rat. J. Comp. Neurol. 240:153-160.

Cervero, F., and J.H. Wolstencroft (1984) A positive feedback loop between spinal cord nociceptive pathways and antinociceptive areas of the cat's brain stem. Pain 20:125-138.

Chan-Palay, V. (1977a) Indoleamine neurons and their processes in the normal rat brain and in chronic diet-induced thiamine deficiency demonstrated by uptake of 3H-Serotonin. J. Comp. Neurol. 176:467-494.

Chan-Palay, V. (1977b) Cerebellar Dentate Nucleus, Organization, Cytology, and Transmitters. Berlin, Heidelberg, New York: Springer-Verlag.

Chan-Palay, V. (1978a) The paratrigeminal nucleus. I. Neurons and synaptic organization. J. Neurocytol. 7:405-418.

Chan-Palay, V. (1978b) The paratrigeminal nucleus. II. Identification and inter-relations of catecholamine axons, indoleamine axons, and Substance P immunoreactive cells in the neuropil. J. Neurocytol. 7:419-442.

Cheek, M.D., A. Rustioni, and D.L. Trevino (1975) Dorsal column nuclei projections to the cerebellar cortex in cats as revealed by the use of the retrograde transport of horseradish peroxidase. J. Comp. Neurol. 164:31-46.

Ciriello, J., A.W. Hrycyshyn, and F.R. Calaresu (1981a) Horseradish peroxidase study of brain stem projections of carotid sinus and aortic depressor nerves in the cat. J. Auton. Nerv. Sys. 4:43-61.

Ciriello, J., A.W. Hrycyshyn, and F.R. Calaresu (1981b) Glossopharyngeal and vagal afferent projections to the brain stem of the cat: A horseradish peroxidase study. J. Auton. Nerv. Sys. 4:63-79.

Contreras, R.J., R.M. Beckstead, and R. Norgren (1982) The central projections of the trigeminal, facial, glossopharyngeal and vagus nerves: an autoradiographic study in the rat. J. Auton. Nerv. Sys. 6:303-322.

Cooke, J.D., B. Larson, O. Oscarsson and B. Sjolund (1971a) Origin and termination of cuneocerebellar tract. Exp. Brain Res. 13:339-358.

Craig, A.D., Jr. (1978) Spinal and medullary input to the lateral cervical nucleus. J. Comp. Neurol. 181:729-744.

Craig, A.D., Jr., and H. Burton (1981) Spinal and medullary lamina I projection to nucleus submedius in medial thalamus: a possible pain center. J. Neurophysiol. 45:443-466.

Crosby, E.C., and R.E. Yoss (1954) The phylogenetic continuity of neural mechanisms as illustrated by the spinal tract of V and its nucleus. Res. Publ. Ass. Nerv. Ment. Dis. 33:174-208.

Crosby, E.C., T. Humphrey, and E.W. Lauer (1962) Correlative Anatomy of the Nervous System. The Macmillan Co., New York.

Crutcher, K.A., A.O. Humbertson, Jr., and G.F. Martin (1978) The origin of brainstem-spinal pathways in the North American Opossum (*Didelphis virginiana*). Studies using the horseradish peroxidase method. J. Comp. Neurol. 179:169-194.

Culberson, J.L., and D.L. Kimmel (1972) Central distribution of primary afferent fibers of the glossopharyngeal and vagal nerves in the opossum, *Didelphis virginiana*. Brain Res. 44:325-335.

Darian-Smith, I. (1966) Neural mechanisms of facial sensation. Int. Rev. Neurobiol. 9:301-395.

Darian-Smith, I. (1973) The trigeminal system. In: A. Iggo (ed.): Handbook of Sensory Physiology, Vol. II, Somatosensory System. Springer-Verlag, Berlin, pp. 271-314.

Darian-Smith, I., R. Proctor, and R.D. Ryan (1963) A single-neurone investigation of somatotopic organization within the cat's trigeminal brain-stem nuclei. J. Physiol. 168:147-157.

Darian-Smith, I., and T. Yokota (1966) Cortically evoked depolarization of trigeminal cutaneous afferent fibers in the cat. J. Neurophysiol. 29:185-206.

Dawson, N.J., R.F. Hellon, and J.I. Hubbard (1980) Cell responses evoked by tooth pulp stimulation above the marginal layer of the cat's trigeminal nucleus caudalis. J. Comp. Neurol. 193:983-994.

de Pommery, J., F. Roudier, and D. Menetrey (1984) Postsynaptic fibers reaching the dorsal column nuclei in the rat. Neurosci. Lett. 50:319-323.

Del Fiacco, M., M.L. Dessi and M.C. Levanti (1984) Topographical localization of substance P in the human post-mortem brainstem. An immunohistochemical study in the newborn and adult tissue. Neuroscience 12:591-611.

Dostrovsky, J.O., and R.F. Hellon (1978) The representation of facial temperature in the caudal trigeminal nucleus of the cat. J. Physiol. 277:29-47.

Drew, J.P., Westrum, L.E. and R.H.Ho (1986) Mapping of the normal distribution of substance P-like immunoreactivity in the spinal trigeminal nucleus of the cat. Exp.Neurol, 93:168-179.

Dubbeldam, J.L., and H.J. Karten (1978) The trigeminal system in the pigeon (*Columba livia*). I. Projections of the gasserian ganglion. J. Comp. Neurol, 180:661-678.

Dubner, R., and G.J. Bennett (1983) Spinal and trigeminal mechanisms of nociception. Ann. Rev. Neurosci, 6:381-418.

Dubner, R., and B.J. Sessle (1971) Presynaptic excitability changes of primary afferent and corticofugal fibers projecting to trigeminal brain stem nuclei. Exp. Neurol, 30:223-238.

Dubner, R. B.J. Sessle, and A.T. Storey (1978) The Neural Basis of Oral and Facial Function, New York, Plenum.

Dunn, R.C., Jr., and D.L. Tolbert (1982) The corticotrigeminal projection in the cat. A study of the organization of cortical projections to the spinal trigeminal nucleus. Brain Res, 240:13-25.

Durham, D., and T.A. Woolsey (1984) Effects of neonatal whisker lesions on mouse central trigeminal pathways. J. Comp. Neurol, 223:424-447.

Edwards S.B., C.L. Ginsburgh, C.K. Henkel, and B.E. Stein (1979) Sources of subcortical projections to the superior colliculus in the cat. J. Comp. Neurol, 184:309-330.

Eisenmann, J., S. Landgren, and D. Novin (1963) Functional organization in the main sensory trigeminal nucleus and in the rostral subdivision of the nucleus of the spinal trigeminal tract in the cat. Acta Physiol. Scand, 59 (214):1-44.

Eller, T. and V. Chan-Palay (1976) Afferents to the cerebellar lateral nucleus: Evidence from retrograde transport of horseradish peroxidase after pressure injections through micropipettes. J. Comp. Neurol, 166:285-302.

Erzurumlu, R.S., C.A. Bates, and H.P. Killackey (1980) Differential organization of thalamic projection cells in the brain stem trigeminal complex of the rat. Brain Res, 198:427-433.

Erzurumlu, R.S., and H.P. Killackey (1979) Efferent connections of the brainstem trigeminal complex with the facial nucleus of the rat. J. Comp. Neurol, 188:75-86.

Erzurumlu, R.S., and H.P. Killackey (1980) Diencephalic projections of the subnucleus interpolaris of the brainstem trigeminal complex in the rat. Neurosci, 5:1891-1901.

Fallon, J.H. and F.M. Leslie (1986) Distribution of dynorphin and enkephalin peptides in the rat brain. J. Comp. Neurol, 249:293-336.

Falls, W.M. (1983) A golgi type II neuron in trigeminal nucleus oralis: A golgi study in the rat. Neurosci. Lett, 41:1-7.

Falls, W.M. (1984a) Axonal endings terminating on dendrites of identified large trigeminospinal projection neurons in rat trigeminal nucleus oralis. Brain Res, 324:335-341.

Falls, W.M. (1984b) Termination in trigeminal nucleus oralis of ascending intratrigeminal axons originating from neurons in the medullary dorsal horn: an HRP study in the rat employing light and electron microscopy. Brain Res, 290:136-140.

Falls, W.M. (1984c) The morphology of neurons in trigeminal nucleus oralis projecting to the medullary dorsal horn (trigeminal nucleus caudalis): A retrograde horseradish peroxidase and golgi study. Neuroscience 13:1279-1298.

Falls, W.M. and J. King (1980) Golgi studies of interneurons and internuclear projection neurons in the ventrolateral subdivisions of trigeminal nucleus oralis. Soc. Neurosci. Abstr. 6:65.

Falls, W.M., and K.D. Phelan (1984) The interstitial nucleus of the spinal V tract: Anatomical organization and patterns of connectivity. Soc. Neurosci. Abstr. 10:482.

Falls, W.M., R.E. Rice, and J.P. VanWagner (1985) The dorsomedial portion of trigeminal nucleus oralis (Vo) in the rat: Cytology and projections to the cerebellum. Somatosens. Res. 3:89-118.

Faull, R.L.M. (1977) A comparative study of the cells of origin of cerebellar afferents in the rat, cat, and monkey studied with the horseradish peroxidase technique: I. The nonvestibular brainstem afferents. Anat. Rec. 187:577.

Feldman, S.G., and L. Kruger (1980) An axonal transport study of the ascending projection of medial lemniscal neurons in the rat. J. Comp. Neurol. 192:427-454.

Finley, J.C.W., J.L. Maderdrut, L.J. Roger, and P. Petrusz (1981) The immunocytochemical localization of somatostatin-containing neurons in the rat central nervous system. Neuroscience 7:2173-2192.

Friede, R.L. (1959) Histochemical investigations on succinic dehydrogenase in the central nervous system-II. Atlas of the medulla oblongata of the guinea pig. J. Neurochem. 4:111-123.

Fukishima, T., and F.W.L. Kerr (1979) Organization of trigeminothalamic tracts and other thalamic afferent systems of the brainstem in the rat: Presence of gelatinosa neurons with thalamic connections. J. Comp. Neurol. 183:169-184.

Fuse, G. (1919) Beitrage zur normalen Anatomie des der spinalen Trigeminuswurzel angehoren Graues, vor allem der Substantia gelatinosa Rolando beim Menschen. Arb. a. d. Anat. Inst. D. Kaiserlich-Japanischen Univ. Zu Sendai 2:87-189.

Gerhardt, L., and J. Olszewski (1969) Medulla oblongata and pons. Primatolog. 2(3):1-234.

Giesler, G.J., Jr., R.L. Nahin, and A.M. Madsen (1984) Postsynaptic dorsal column pathway in the rat. I. Anatomical studies. J. Neurophysiol. 51:260-275.

Glees, P. (1946) Terminal degeneration within the central nervous system as studies by a new silver method. J. Neuropath. Exp.Neurol. 5:54-59.

Gobel, S. (1971a) Recent observations on the structural organization of the spinal V nucleus in the cat: The deep bundles. Soc. Neurosci. Abstr. 1:110.

Gobel, S. (1971b) Structural organization in the main sensory trigeminal nucleus. In R. Dubner and Y. Kawamura (eds.): Oral-Facial Sensory and Motor Mechanisms, Appleton-Century-Crofts, New York, pp. 183-204.

Gobel, S. (1974) Synaptic organization of the substantia gelatinosa in the spinal trigeminal nucleus of the adult cat. J. Neurocytol. 3:219-243.

Gobel, S. (1975a) Golgi studies of the substantia gelatinosa neurons in the spinal trigeminal nucleus. J. Comp. Neurol. 162: 397-415.

Gobel, S. (1975b) Neurons with two axons in the substantia gelatinosa layer of the spinal trigeminal nucleus of the adult cat. Brain Res. 88:333-338.

Gobel, S. (1976a) Principles of organization in the substantia gelatinosa layer of the spinal trigeminal nucleus. Adv. Pain Res. and Ther. 1:165-170.

Gobel, S. (1976b) Dendro-axonic synapses in the substantia gelatinos of the spinal trigeminal nucleus of the cat. J. Comp. Neurol. 125-176.

Gobel, S. (1978a) Golgi studies of the neurons in layer I of the dorsal horn of the medulla (trigeminal nucleus caudalis). J. Comp. Neurol. 180:375-394.

Gobel, S. (1978b) Golgi studies of the neurons in layer II of the dorsal horn of the medulla (trigeminal nucleus caudalis). J. Comp. Neurol. 180:395-414.

Gobel, S., G.J. Bennet, B. Allen, E. Humphrey, Z.Seltzer, M. Abdelmoumene, H. Hayashi, and M.J. Hoffert (1982) Synaptic connectivity of substantia gelatinosa neurons with reference to potential termination sites of descending axons. In B. Sjolund and A. Bjorklund (eds.): Brain Stem Control of Spinal Mechanisms. Elsevier/North-Holland Biomedical Press, Amsterdam, pp. 135-158.

Gobel, S., W.M. Falls, and S. Hockfield (1977) The division of the dorsal and ventral horns of the mammalian caudal medulla into eight layers using anatomical criteria. In D.J. Anderson and B. Matthews (eds.): Pain in the Trigeminal Region, Elsevier/North-Holland Biomedical Press, Amsterdam, pp. 443-453.

Gobel, S., and S. Hockfield (1977) An anatomical analysis of the synaptic circuitry of layers I, II and III of trigeminal nucleus caudalis in the cat. In D.J. Anderson and B. Matthews (eds.): Pain in the Trigeminal Region. Elsevier/North-Holland Biomedical Press, Amsterdam, pp. 203-211.

Gobel, S., and M.B. Purvis (1972) Anatomical studies of the organization of the spinal V nucleus: the deep bundles and the spinal V tract. Brain Res. 48:27-44.

Gobel, S., W.M. Falls, G.J. Bennet, M. Abdelmoumene, H. Hayashi, and E. Humphrey (1980) An EM analysis of the synaptic connections of horseradish peroxidase-filled stalked cells and islet cells in the substantia gelatinosa of adult cat spinal cord. J. Comp. Neurol. 194:781-807.

Gordon, G., and G. Grant (1972) Afferents to the dorsal column nuclei from dorsolateral funiculus of the spinal cord. Acta Physiol. Scand. 84:30A.

Gordon, G., S. Landgren, and W.A. Seed (1961) The functional charateristics of single cells in the caudal part of the spinal nucleus of the trigeminal nerve of the cat. J. Physiol. 158:544-559.

Gould, B.B. (1980) Organization of afferents from the brain stem nuclei to the cerebellar cortex in the cat. Adv. Anat. Embryol. Cell Biol. 62:1-90.

Granum, S.L. (1986) The spinothalamic system of the rat. I. Locations of cells of origin. J. Comp. Neurol. 247:159-180.

Greenwood, L.F. and B.J. Sessle (1976) Inputs to trigeminal brain stem neurones from facial, oral, tooth pulp and pharyngolaryngeal tissues. II. Role of trigeminal nucleus caudalis in modulating responses to innocuous and noxious stimuli. Brain Res. 117:227-238.

Gruberg, E.R., E.A. Newman, and P.H. Hartline (1984) 2-Deoxyglucose labeling of the infrared sensory system in the rattlesnake, *Crotalus viridus*. J. Comp. Neurol. 229:321-328.

Gwyn, D.G., G.P. Nicholson and B.A. Flumerfelt (1977) The inferior olivary nucleus of the rat: A light and electron microscopic study. J. Comp. Neurol. 174:489-520.

Hamilton, R.B., H. Ellenberger, D. Liskosky, and N. Schneiderman (1981) Parabrachial area as mediator of bradycardia in rabbits. J. Auton. Nerv. Sys. 4:261-281.

Hand, P.J. (1966) Lumbosacral dorsal root terminations in the nucleus gracilis of the cat. Some observations on terminal degeneration in other medullary sensory nuclei. J. Comp. Neurol. 126:137-156.

Hayashi, H. (1980) Distribution of vibrissae afferent fiber collaterals in the trigeminal nuclei as revealed by intra-axonal injection of horseradish peroxidase. Brain Res. 183:442-446.

Hayashi, H. (1982) Differential terminal distribution of single large cutaneous afferent fibers in the spinal trigeminal nucleus and in the cervical spinal dorsal horn. Brain Res. 244:173-177.

Hayashi, H. (1985a) Morphology of central terminations of intra-axonally stained, large, myelinated primary afferent fibers from facial skin in the rat. J. Comp. Neurol. 237:195-215.

Hayashi, H. (1985b) Morphology of terminations of small and large myelinated trigeminal primary afferents fibers in the rat. J. Comp. Neurol. 240:71-89.

Hayashi, H., R. Sumino, and B.J. Sessle (1984) Functional organization of trigeminal subnucleus interpolaris: Nociceptive and innocuous afferent inputs, projections to thalamus, cerebellum, and spinal cord, and descending modulation from periaqueductal gray. J. Neurophysiol. 51:890-905.

Heimer, L, (1967) Silver impregnation of terminal degeneration in some forebrain fiber systems: A comparative evaluation of current methods. Brain Res. 5:86-108.

Helke, C.J., C.W. Shults, T.N. Chase, and T.L. O'Donohue (1984) Autoradiographic localization of substance P receptors in rat medulla: Effect of vagotomy and nodose gangliectomy. Neuroscience 12:215-223.

Hinrichsen, C.F.L., and C.D. Watson (1983) Brain stem projections to the facial nucleus of the rat. Brain Behav. Evol. 22:153-163.

Hockfield, S., and S. Gobel (1978) Neurons in and near nucleus caudalis with long ascending projection axons demonstrated by retrograde labeling with horseradish peroxidase. Brain Res. 139:333-339.

Hockfield, S., and S. Gobel (1982) An anatomical demonstration of projections to the medullary dorsal horn (trigeminal nucleus caudalis) from rostral trigeminal nuclei and the contralateral caudal medulla. Brain Res. 252:203-211.

Hokfelt, T., R. Martensson, A. Bjorklund, S. Kleinau, and M. Goldstein (1984) Distribution maps of tyrosine-hydroxylase-immunoreactive neurons in the rat brain. In A. Bjorklund, and T. Hokfelt (eds.) Handbook of Chemical Neuroanatomy. Volume 2:Classical transmitters and transmitter receptors in the CNS. Part I. Elsevier, New York, pp. 277-379.

Hollander, H., and J.L. Vaaland (1968) A reliable staining method for semithin sections in experimental neuroanatomy. Brain Res. 10:120-126.

Hrycyshyn, A.W. and B.A. Flumerfelt (1981) Cytology and synaptology of the lateral reticular nucleus of the cat. J. Comp. Neurol. 197:447-475.

Hu, J.W., and B.J. Sessle (1984) Comparisons of responses of cutaneous nociceptive and non-nociceptive brain stem neurons in trigeminal nucleus caudalis (medullary dorsal horn) and subnucleus oralis to natural and electrical stimulation of tooth pulp. J. Neurophysiol. 52:39-53.

Hu, J.W., J.O. Dostrovsky, and B.J. Sessle (1981) Functional properties of neurons in cat trigeminal subnucleus caudalis (medullary dorsal horn). I. Responses to oral-facial noxious and nonnoxious stimuli and projections to thalamus and subnucleus oralis. J. Neurophysiol, 45:173-192.

Hubbard, J.I., and R.F. Hellon (1980) Excitation and inhibition of marginal layer and interstitial interneurons in cat nucleus caudalis by mechanical stimuli. J. Comp. Neurol, 193: 995-1007.

Huerta, M.F., A. Frankfurter, and J.K. Harting (1983) Studies of the principal sensory and spinal trigeminal nuclei of the rat: projections to the superior colliculus, inferior olive, and cerebellum. J. Comp. Neurol, 220:147-167.

Huerta, M.F., T. Hashikawa, M.J. Gayoso, and J.K. Harting (1985) The trigemino-olivary projection in the cat: contribution of individual subnuclei. J. Comp. Neurol. 241:180-190.

Humphrey, T., and D. Hooker (1959) Double simultaneous stimulation of human fetuses and the anatomical patterns underlying the reflexes elicited. J. Comp. Neurol, 112:75-102.

Ide, L.S., and H.P. Killackey (1985) Fine structural survey of the rat's brainstem sensory trigeminal complex. J. Comp. Neurol, 235:145-168.

Ikeda, M. (1979) Projections from the spinal and the principal sensory nuclei of the trigeminal nerve to the cerebellar cortex in the cat, as studied by retrograde transport of horseradish peroxidase. J. Comp. Neurol, 184:567-586.

Ikeda, M., M. Matsushita, and T. Tanami (1982) Termination and cells of origin of the ascending intranuclear fibers in the spinal trigeminal nucleus of the cat. A study with the horseradish peroxidase technique. Neurosci. Lett, 31:215-220.

Ikeda, M., T. Tanami, and M. Matsushita (1984) Ascending and descending internuclear connections of the trigeminal sensory nuclei in the cat. A study with the retrograde and anterograde horseradish peroxidase technique. Neuroscience 12:1243-1260.

Imai, H., D.A. Steindler, and S.T. Kitai (1983) A rapid and simple method for the determination of delivery after iontophoretic and pressure injections of radioactive tracer substances. J. Neurosci. Meth, 7:389-396.

Imai, Y., and T. Kusama (1969) Distribution of the dorsal root fibers in the cat. An experimental study with the Nauta method. Brain Res, 13: 338-359.

Ishidori, H., T. Nishimori, Y. Shigenaga, S. Suemune, Y. Dateoka, M. Sera and N. Nagasaka (1986) Representation of upper and lower primary teeth in the trigeminal sensory nuclear complex in the young dog. Brain Res, 370:153-158.

Itoh, K., A. Konishi, S. Nomura, N. Mizuno, Y.Nakamura, and T. Sugimoto (1975) Application of the coupled oxidative reaction to electron microscopic demonstration of labeled processes: cobalt-glucose oxidase method. Brain Res, 175:341-346.

Jacquin, M.F., R.D. Mooney, and R.W. Rhoades (1986) Morphology, response properties, and collateral projections of trigeminothalamic neurons in brainstem subnucleus interpolaris of rat. Exp. Brain Res, 61:457-468.

Jacquin, M.F., W.E. Renehan, R.D. Mooney, and R.W. Rhoades (1986) Structure-function relationships in rat medullary and cervical dorsal horns. I. Trigeminal primary afferent. J. Neurophys, 55:1153-1186.

Jacquin, M.F., and R.W. Rhoades (1983) Central projections of the normal and 'regenerate' infraorbital nerve in adult rats subjected to neonatal unilateral infraorbital lesions: a transganglionic horseradish peroxidase study. Brain Res. 269:137-144.

Jacquin, M.F., D. Woerner, A.M. Szczepanik, V. Riecker, R.D. Mooney, and R.W. Rhoades (1986) Structure-function relationships in rat brainstem subnucleus interpolaris. I. Vibrissa primary afferents. J. Comp. Neurol. 243:266-279.

Jancso, G., and E. Kiraly (1980) Distribution of chemosensitive primary sensory afferents in the central nervous system of the rat. J. Comp. Neurol. 190:781-792.

Jane, J.A., and D.M. Schroeder (1971) A comparison of dorsal column nuclei and spinal afferents in the european hedgehog (*Erinaceus europaeus*). Exp. Neurol. 30:1-17.

Johnson, F.H. (1954) Experimental study of spino-reticular connections in the cat. Anat. Rec. 118:316.

Johnson, L.R., L.E. Westrum, and L.M. O'Neill (1984) Golgi-EM studies of dental relay sites in spinal trigeminal nucleus. Soc. Neurosci. Abstr. 10:482.

Joseph, J.W., G.M. Shambes, J.M. Gibson, and W. Welker (1978) Tactile projections to granule cells in caudal vermis of the rat's cerebellum. Brain Behav. Evol. 15:141-149.

Kageyama, G.H. and M.T.T. Wong-Riley (1982) Histochemical localization of cytochrome oxidase in the hippocampus: Correlation with specific neuronal types and afferent pathways. Neuroscience 7:2337-2361.

Karamanlidis, A.N. (1968) Trigemino-cerebellar fiber connections in the goat studied by means of the retrograde cell degeneration method. J. Comp. Neurol. 133:71-88.

Karamanlidis, A.N. (1975) Trigeminothalamic fibre connections in the donkey (*Equus asinus*) studied by means of the retrograde cell degeneration method. Acta. Anat. 93:126-134.

Karamanlidis, A.N., H. Michaloudi, O. Mangana, and R.P. Saigal (1978) Trigeminal ascending projections in the rabbit, studied with horseradish peroxidase. Brain Res. 156:110-116.

Kawana, E., and T. Kusama (1964) Projections of the sensory motor cortex to the thalamus, the dorsal column nuclei, the trigeminal nucleus and the spinal cord in the cat. Folia. Psychiat. Neurol. Jap. 18:337-380.

Keller, J.H., and P.J. Hand (1970) Dorsal root projections to nucleus cuneatus of the cat. Brain Res. 20:1-17.

Kemplay, S.K., and K.E. Webster (1986) A qualitative and quantitative analysis of the distributions of cells in the spinal cord and spinomedullary junction projecting to the thalamus of the rat. Neuroscience 17:768-789.

Kerr, F.W.L. (1962) Facial, vagal and glossopharyngeal nerves in the cat. Arch. Neurol. 6:264-281.

Kerr, F.W.L. (1966a) On the question of ascending fibers in the pyramidal tract: with observations on spinotrigeminal and spinopontine fibers. Exp. Neurol. 14:77-85.

Kerr, F.W.L. (1966b) The ultrastructure of the spinal tract of the trigeminal nerve and the substantia gelatinosa Exp. Neurol. 16:359-376.

Kerr, F.W.L. (1970a) Peripheral versus central factors in trigeminal neuralgia. In R. Hassler and A.E. Walker (eds.): Trigeminal Neuralgia, Pathogenesis and Pathophysiology. George Thiem Verlag, Stuttgart, pp. 180-190.

Kerr, F.W.L. (1970b) The fine structure of the subnucleus caudalis of the trigeminal nerve. Brain Res. 23:129-145.

Kerr, F.W.L. (1971) Electron microscopic observations on primary deafferentation of the subnucleus caudalis of the trigeminal nerve. In R. Dubner and Y. Kawamura (eds.): Oral-Facial Sensory and Motor Mechanisms. Appleton-Century-Crofts, New York, pp. 159-182.

Kerr, F.W.L. (1972a) The potential of cervical primary afferents to sprout in the spinal nucleus of V following long term trigeminal denervation. Brain Res. 43:547-560.

Kerr, F.W.L. (1972b) Central relationships of trigeminal and cervical primary afferents in the spinal cord and medulla. Brain Res. 43:561-572.

Kerr, F.W.L. (1975) The ventral spinothalamic tract and other ascending systems of the ventral funiculus of the spinal cord. J. Comp. Neurol. 159:335-356.

Kerr, F.W.L. (1979) Craniofacial neuralgias. Adv. Pain Res. and Ther. 3:283-295.

Kerr, F.W.L., L. Kruger, H.O. Schwassman, and R. Stern (1968) Somatotopic organization of mechanoreceptor units in the trigeminal nuclear complex of the Macaque. J. Comp. Neurol. 134:127-144.

Kilduff, T.S., F.R. Sharp, and H.C. Heller (1982) [^{14}C]2-deoxyglucose uptake in ground squirrel brain during hibernation. J. Neurosci. 2:143-157.

Kilduff, T.S., F.R. Sharp, and H.C. Heller (1983) Relative 2-deoxyglucose uptake of the paratrigeminal nucleus increases during hibernation. Brain Res. 262:117-123.

Kilduff, T.S., H.C. Heller, and F. Sharp (1984) Paratrigeminal nucleus: A previously unrecognized thermal relay? In J.R.S. Hales (ed.): Thermal Physiology New York, Raven Press. pp.101-104.

Killackey, H.P., and G.R. Belford (1979) The formation of afferent patterns in the somatosensory cortex of the neonatal rat. J. Comp. Neurol. 183:285-304.

Killackey, H.P., and R.S. Erzurumlu (1981) Trigeminal projections to the superior colliculus of the rat. J. Comp. Neurol. 201:221-242.

Kimura, H., P.L. McGeer, and J.-H. Peng (1984) Choline acetylcholinesterase-containing neurons in the rat brain. In A. Bjorklund, T. Hokfelt, and M.J. Kuhar (eds.): Handbook of Chemical Neuroanatomy, Volume 3:Classical transmitters and transmitter receptors in the CNS, Part II. Elsevier, New York, pp. 51-67.

King, G.W. (1980) Topology of ascending brainstem projections to nucleus parabrachialis in the cat. J. Comp. Neurol. 191:615-638.

Kluver, H., and E. Barrera (1953) A method for the combined staining of cells and fibers in the nervous system. J. Neuropathol. Exp. Neurol. 12:400-403.

Krieg, W.J.S. (1942) Functional Neuroanatomy The Blankiston Co., Philadelphia-Toronto.

Krieg, W.J.S. (1950) Subdivisions of nuclei of spinal trigeminal tract in the rat. Anat. Rec. 106:279.

Kruger, L. (1971) A critical review of theories concerning the organization of the sensory trigeminal nuclear complex of the rat brain stem. In R. Dubner and Y. Kawamura (eds.): Oral-Facial Sensory and Motor Mechanisms. Appleton-Century-Crofts, New York, pp. 135-138.

Kruger, L. (1979) Functional subdivisions of the brainstem sensory trigeminal nuclear complex. Adv. Pain Res. and Ther, 3:197-209.

Kruger, L., and F. Michel (1962a) A morphological and somatotopic analysis of single unit activity in the trigeminal sensory complex of the cat. Exp. Neurol. 5:139-156.

Kruger, L., and F. Michel (1962b) Reinterpretation of the representation of pain based on physiological excitation of single neurons in the trigeminal sensory complex. Exp. Neurol. 5:157-178.

Kruger, L., and R.F. Young (1981) Specialized features of the trigeminal nerve and its central connections. In M. Samii and P.J. Janetta (eds.): The Cranial Nerves. Anatomy-Pathology-Pathophysiology-Diagnosis-Treatment, Springer-Verlag, New York, pp. 273-301.

Kruger, L., R. Siminoff, and P. Witkovsky (1961) Single neuron analysis of dorsal column nuclei and spinal nucleus of trigeminal in cat. J. Neurophysiol. 24:333-349.

Kruger, L., S. Saporta, and S.G. Feldman (1977) Axonal transport studies of the sensory trigeminal complex. In D.J. Anderson and B. Matthews (eds.): Pain in the Trigeminal Region. Elsevier/North Holland Biomedical Press, Amsterdam, pp. 191-201.

Kunc, Z. (1970) Significant factors pertaining to the results of trigeminal tractotomy. In R. Hassler and A.E. Walker (eds.): Trigeminal neuralgia, Stuttgart, Georg Thieme Verlag.

Kunzle, H. (1973) The topographical organization of spinal afferents to the lateral reticular nucleus of the cat. J. Comp. Neurol, 149:107-110.

Kusama, T., K. Otani, and E. Kawana (1966) Projections of the motor, somatic sensory, auditory and visual cortices in cats. Progr. Brain Res. 21A:292-322.

Kuypers, H.G.J.M., and V.A. Maisky (1975) Retrograde axonal transport of horseradish peroxidase from spinal cord to brain stem cell groups in the cat. Neurosci. Lett. 1:9-14.

Kuypers, H.G.J.M., and J.D. Tuerk (1964) The distribution of the cortical fibres within the nuclei cuneatus and gracilis in the cat. J. Anat. 98:143-162.

Leong, S.K., J.Y. Shieh, and W.C. Wong (1984a) Localizing spinal-cord-projecting neurons in adult albino rats. J. Comp. Neurol, 228:1-17.

Leong, S.K., J.Y. Shieh, and W.C. Wong (1984b) Localizing spinal-cord-projecting neurons in neonatal and immature albino rats. J. Comp. Neurol, 228:18-23.

Ljungdahl, A., T. Hokfelt, and G. Nilsson (1978) Distribution of substance P-like immunoreactivity in the central nervous system of the rat. I. Cell bodies and nerve terminals. Neurosci. 3:861-943.

Loewy, A.D., and C.B. Saper (1978) Edinger-Westphal nucleus: projections to the brain stem and spinal cord in the cat. Brain Res., 150:1-27.

Lovick, T.A., and J.H. Wolstencroft (1983) Projections from brain stem nuclei to the spinal trigeminal nucleus in the cat. Neurosci. 9:411-420.

Lu, G.-W., G.J. Bennet, N. Nishikawa, and R. Dubner (1985) Spinal neurons with branched axons traveling in both the dorsal and dorsolateral funiculi Exp. Neurol, 87:571-577.

Ma, P.M., and T.A. Woolsey (1984) Cytoarchitectonic correlates of the vibrissae in the medullary trigeminal complex of the mouse. Brain Res. 306:374-379.

Magnusson, K.R., J.R. Clements, A.A. Larson, J.E. Madl, and A J. Beitz (1987) Localization of glutamate in trigeminothalamic projection neurons: A combined retrograde transport-immunohistochemical study. Somatosens. Res. 4:177-190.

Mann, C., J.L. Oliveras, F. Sierralta, and J.M. Besson (1982) Effects of morphine on various nociceptive reactions induced by trigeminal stimulation (tooth pulp, tract and nucleus oralis-interpolaris of the spinal trigeminal nucleus) in the freely moving rat. In B. Matthews and R.G. Hill (eds.): Anatomical, Physiological and Pharmacological Aspects of Trigeminal Pain. Excerpta Medica, Amsterdam, pp. 261-262.

Manni, E., G. Palmieri, R. Marini, and V.E. Petterossi (1975) Trigeminal influences on extensor muscles of the neck. Exp. Neurol. 47:330-342.

Mantle-St. John, L.A. and D.J. Tracey (1987) Somatosensory nuclei in the brainstem of the rat: Independent projections to the thalamus and cerebellum. J. Comp. Neurol. 255:259-271.

Marfurt, C.F. (1981) The central projections of trigeminal primary afferent neurons in the cat as determined by the transganglionic transport of horseradish peroxidase. J. Comp. Neurol. 203:785-798.

Marfurt, C.F., and D.F. Turner (1984) The central projections of tooth pulp afferent neurons in the rat as determined by the transganglionic transport of horseradish peroxidase. J. Comp. Neurol. 223:535-547.

Massopust, L.C., D.H. Hauge, J.C. Ferneding, W.G. Doubek, and J.J. Taylor (1985) Projection systems and terminal localization of dorsal column afferents: An autoradiographic and horseradish peroxidase study in the rat. J. Comp. Neurol. 237:533-544.

Matsushita, M., M. Ikeda, and N. Okado (1982) The cells of origin of the trigeminothalamic, trigeminospinal and trigeminocerebellar projections in the cat. Neurosci. 7:1439-1454.

Matsushita, M., N. Okada, M. Ikeda, and Y. Hosoya (1980) Identification of spinal projecting neurons in the cat trigeminal spinal and mesencephalic nuclei using the retrograde horseradish peroxidase technique. In M. Ito, N. Tsukahara, K Kubota and K. Yagi (eds.): Integrative Control Functions of the Brain, Vol. III, Elsevier/North Holland Biomedical Press, Amsterdam, pp. 161-163.

Matsushita, M., N. Okado, M. Ikeda, and Y. Hosoya (1981) Descending projections from the spinal and mesencephalic nuclei of the trigeminal nerve to the spinal cord in the cat. A study with the horseradish peroxidase technique. J. Comp. Neurol. 196:173-187.

McHaffie, J.G., L.L. Bruce, and B.E. Stein (1984) Trigeminotectal projections: Comparisons among several mammals. Soc. Neurosci. Abstr. 10:483.

Meessen, H., and J. Olszewski (1949) A Cytoarchitectonic Atlas of the Rhombencephalon of the Rabbit. S. Karger, Basel-New York.

Menetrey, D., J. Leah, and J. dePommery (1987) Efferent projections of the paratrigeminal nucleus in the rat. Neurosci. Lett. 73:48-52.

Mesulam, M.-M. (1978) Tetramethylbenzidine for horseradish peroxidase neurohistochemistry: A non-carcinogenic blue reaction product with superior sensitivity for visualizing neural afferents and efferents. J. Histochem. Cytochem. 26:106-117.

Mizuno, N., A. Konishi, and Y. Nakamura (1975) An electron microscope study of synaptic organization in the lateral reticular nucleus of the medulla oblongata in the cat. Brain Res. 94:369-381.

Mizuno, N. and Y. Nakamura (1975) An electron microscopic study of spinal afferents to the lateral reticular nucleus of the medulla oblongata in the cat. Brain Res. 53:187-191.

Mizuno, N., S. Nomura, and Y. Takeuchi (1980) The parabrachial nucleus as an intermediate relay station of the visceral afferent pathways in the cat. In M. Ito, N. Tsukahara, K Kubota and K. Yagi (eds.): Integrative Control Functions of the Brain, Vol. III, Elsevier/North Holland Biomedical Press, Amsterdam, pp. 51-64.

Molenaar, G.J. (1974) An additional trigeminal system in certain snakes possessing infrared receptors. Neth. J. Zool. 27:133-180.

Molenaar, G.J. (1977) The rhombencephalon of *Python reticulatus*, a snake possessing infrared receptors. Neth. J. Zool. 27:133-180.

Molenaar, G.J. (1978a) The sensory trigeminal system of a snake in the possession of infrared receptors. I. The sensory trigeminal nuclei. J. Comp. Neurol. 179:123-136.

Molenaar, G.J. (1978b) The sensory trigeminal system of a snake in the possession of infrared receptors. II. The central projections of the trigeminal nerve. J. Comp. Neurol. 179:137-152.

Mugnaini, E. and W.H. Oertel (1985) An atlas of the distribution of GABAergic neurons and terminals in the rat CNS as revealed by GAD immunohistochemistry. In A. Bjorklund and T. Hokfelt (eds.): Handbook of Chemical Neuroanatomy, Vol. 4:GABA and Neuropeptides in the CNS, Part I, Elsevier, New York, pp. 435-595.

Nagai, T., T. Maeda, H. Imai, P. L. McGeer, and E.G. McGeer (1985) Distribution of GABAT-containing neurons in the rat hindbrain. J. Comp. Neurol. 231:260-269.

Nauta, W.J.H. (1957) Silver impregnation of degenerating axons. In W.F. Winle (ed.): New Research Techniques in Neuroanatomy, C.C. Thomas, Springfield, Illinois, pp. 17-26.

Nauta, W.J.H., and H.G.J.M. Kuypers (1958) Some ascending pathways in the brain stem reticular formation. In L.D. Proctor (ed.): Reticular Formation of the Brain, Henry Ford Hospital International Symposium, Little Brown and Co., Boston, pp. 3-30.

Noback, C.R. (1959) Brain of a gorilla. II. Brain stem nuclei. J. Comp. Neurol. 111:345-385.

Noback, C.R., and L. Goss (1959) Brain of a gorilla. I: Surface anatomy and cranial nerve nuclei. J. Comp. Neurol. 111:321-344.

Nomura, S., and N. Mizuno (1982) Central distribution of afferent and efferent components of the glossopharyngeal nerve: an HRP study in the cat. Brain Res. 236:1-13.

Nomura, S., and N. Mizuno (1986) Histochemical demonstrations of vibrissae-representing patchy patterns of cytochrome oxidase activity within the trigeminal sensory nuclei in the cat. Brain Res. 380:167-171.

Nomura, S., K. Itoh, T. Sugimoto, Y. Yasui, H. Kamiya and N. Mizuno. (1986) Mystacial vibrissae representation within the trigeminal sensory nuclei of the cat. J. Comp. Neurol. 253:121-133.

Nord, S.G. (1967) Somatotopic organization in the spinal trigeminal nucleus, the dorsal column nuclei and related structures in the rat. J. Comp. Neurol. 130:343-356.

Nord, S.G. (1968) Receptor field characteristics of single cells in the rat spinal trigeminal complex. Exp. Neurol. 21:236-243.

O'Neal, J.T. and L.L. Westrum (1973) The fine structural synaptic organization of the cat lateral cuneate nucleus. A study of sequential alterations in degeneration. Brain Res. 51:97-124.

Olschowska, J.A., T.L. O'Donohue, G.P. Mueller, and D.M. Jacobowitz (1982) The distribution of corticotropin releasing factor-like immunoreactive neurons in rat brain. Peptides 3:995-1015.

Olszewski, J. (1950) On the anatomical and functional organization of the spinal trigeminal nucleus. J. Comp. Neurol. 92:401-413.

Olszewski, J., and D. Baxter (1954) Cytoarchitecture of the Human Brain Stem. S. Karger, New York-Basel.

Oswaldo-Cruz, E., and C.E. Rocha-Miranda (1968) The Brain of the Opossum (Didelphis Marsupialis). A cytoarchitectonic atlas in stereotaxic coordinates. Instituto de Biofisica, Brasil.

Palkovits, M., and D.M. Jocobowitz (1974) Topographic atlas of catecholamine and acetylcholinesterase-containing neurons in the rat brain. II. Hindbrain (mesencephalon, rhombencephalon). J. Comp. Neurol. 157:29-42.

Panneton, W.M., and H. Burton (1981) Corneal and periocular representation within the trigeminal sensory complex in the cat studied with transganglionic transport of horseradish peroxidase. J. Comp. Neurol. 199:327-344.

Panneton, W.M., and H. Burton (1982) Origin of ascending intratrigeminal pathways in the cat. Brain Res. 236:463-470.

Panneton, W.M., and H. Burton (1985) Projections from the paratrigeminal nucleus and the medullary and spinal dorsal horns to the peribrachial area in the cat. Neuroscience 15:779-797.

Panneton, W.M., and A.D. Loewy (1980) Projections of the carotid sinus nerve to the nucleus of the solitary tract in the cat. Brain Res. 191:239-244.

Panneton, W.M., and G.F. Martin (1983) Brainstem projections to the facial nucleus of the opossum. A study using axonal transport techniques. Brain Res. 267:19-33.

Pappas, G. D., E. B. Cohen, and D. P. Purpura (1966) Fine structure of synaptic and non-synaptic neuronal relations in the thalamus of the cat. In D.P. Purpura and M.D. Yahr (eds.): The Thalamus, Columbia University Press, New York, pp.47-75.

Patrick, G.W., and D.E. Haines (1982) Cerebellar afferents to paramedian lobule from trigeminal complex in Tupaia glis: A horseradish peroxidase (HRP) study. J. Morphol. 172:209-222

Patrick, G.W. and M.A. Robinson (1984) Connections of the trigeminal nuclei with cerebellar cortex and thalamus using double-labelling methods in the rat. Anat. Rec. 134A.

Paxinos, G., and C. Watson (1985) The Rat Brain in Stereotaxic Coordinates. Academic Press, New York.

Peacock, M.J., and J.H. Wolstencroft (1976) Projections of reticular neurones to dorsal regions of the spinal cord in the cat. Neurosci. Lett. 2:7-11.

Pearson, J.C., and D.A. Garfunkel (1983) Evidence for thalamic projections from external cuneate nucleus, cell groups Z and X, and the mesencephalic nucleus of the trigeminal nerve in squirrel monkey. Neurosci. Lett. 41:41-47.

Peschanski, M. (1984) Trigeminal afferents to the diencephalon in the rat. Neuroscience 12:465-487.

Peters, A., and S.L. Palay (1966) The morphololgy of laminae A and A1 of the dorsal nucleus of the lateral geniculate body of the cat. J. Anat. (London) 100:451-468.

Phelan, K.D., and W.M. Falls (1983) A golgi analysis of trigeminal nucleus interpolaris in the adult rat. Soc. Neurosci. Abstr. 9:246.

Phelan, K.D., and W.M. Falls (1984a) Observations on the cyto- and myeloarchitectural organization of trigeminal nucleus interpolaris in the adult rat. Anat. Rec. 208:138a.

Phelan, K.D., and W.M. Falls (1984b) The distribution of spinal afferents and trigeminospinal efferents within trigeminal nucleus interpolaris and oralis. Soc. Neurosci. Abstr. 10:796.

Phelan, K.D., and W.M. Falls (1985) A comparison of the distribution and morphology of thalamic, cerebellar and spinal projecting neurons within trigeminal nucleus interpolaris of the rat. Soc. Neurosci. Abstr. 11:560.

Phelan, K.D., and W.M. Falls (1986) A survey of the synaptic organization in the insular trigeminal-cuneatus lateralis nucleus of the rat. Soc. Neurosci. Abstr. 12:326.

Phelps, P.E., R.P. Barber, C.R. Houser, G.D. Crawford, P.M. Salvaterra, and J.E. Vaughn (1984) Postnatal development of neurons containing choline acetyltransferase in rat spinal cord: an immunocytochemical study. J. Comp. Neurol. 229:347-361.

Pinching, A.J., and T.P.S. Powell (1971a) The neuron types of the glomerular layer of the olfactory bulb. J.Cell. Sci. 9:305-345.

Poulos, D.A., and J.T. Molt (1977) Thermosensory mechanisms in the spinal trigeminal nucleus of cats. In D.J. Anderson and B. Matthews (eds.): Pain in the trigeminal region. Elsevier/North-Holland Biomedical Press, Amsterdam, pp. 213-224.

Price, D.D., R. Dubner, and J.W. Hu (1976) Trigeminothalamic neurons in nucleus caudalis responsive to tactile, thermal, and nociceptive stimulation of monkey's face. J. Neurophysiol. 39:936-953.

Race, D.L., and W.M. Falls (1986) Morphology and distribution of neurons in rat trigeminal nucleus interpolaris projecting to orofacial tactile areas of the cerebellar hemispheres Anat. Rec.

Ramon y Cajal, S. (1909) Histologie du Systeme Nerveux de l'Homme et des Vertebres. Institute Ramon y Cajal, Madrid (1952 reprint).

Rhoton, A.L., Jr. (1968) Afferent connections of the facial nerve. J. Comp. Neurol. 133:89-100.

Rhoton, A.L., Jr., J.L. O'Leary, and J.P Ferguson (1966) The trigeminal, facial, vagal, and glossopharyngeal nerves in the monkey. Arch. Neurol. 14:530-540.

Riley, H.A. (1960) An Atlas of the Basal Ganglia, Brain Stem and Spinal Cord, Based on Myelin-stained Material. Hafner Publishing Co., New York.

Ring, G., and D. Ganchrow (1983) Projections of nucleus caudalis and spinal cord to brainstem and diencephalon in the hedgehog (*Erinaceus europaeus and Paraechinus aethiopicus*): a degeneration study. J. Comp. Neurol. 216:132-151.

Roger, M., and J. Cadusseau (1985) Afferents to the zone incerta in the rat: A combined retrograde and anterograde study. J. Comp. Neurol. 241:480-492.

Roney, K.J., A.B. Scheibel, and G.L. Shaw (1979) Dendritic bundles: Survey of anatomical experiments and physiological theories. Brain Res. Rev. 1:225-271.

Rose, P.K., and N. Sprott (1979) Proprioceptive and somatosensory influences on neck muscle motoneurons. Progr. Brain Res. 50:255-279.

Rosen, I., and B. Sjolund (1973) Organization of group I activated cells in the main and external cuneate nuclei of the cat: Convergence patterns demonstrated by natural stimulation. Exp. Brain Res. 16: 238-246.

Rosenstein, J.M. and A.E. Leure duPree (1971) Synaptic organization of the external cuneate nucleus in the rat. J. Comp. Neurol. 175:159-180.

Rosenstein, J.M., R.B. Page, and A.E. Leure-duPree (1977) Patterns of degeneration in the external cuneate nucleus after multiple dorsal rhizotomies. J. Comp. Neurol. 175:181-206.

Ross, C., D.A. Ruggiero, and D.J. Reis (1985) Projections from the nucleus tractus solitarii to the rostral ventrolateral medulla. J. Comp. Neurol. 242:511-534.

Rossi, G.F., and A. Brodal (1956) Spinal afferents to the trigeminal sensory nuclei and the nucleus of the solitary tract. Confin. Neurol. 16:321-332.

Ruda, M.A. and S. Gobel (1980) Ultrastructural characterization of axonal endings in the substantia gelatinosa which take up [^{3} H] serotonin. Brain Res. 184:57-83.

Ruggiero, D.A., C.A. Ross, and D.J. Reis (1981) Projections from the spinal trigeminal nucleus to the entire length of the spinal cord in the rat. Brain Res. 225:225-233.

Rustioni, A. (1973) Non-primary afferents to the nucleus gracilis from the lumber cord of the cat. Brain Res. 51:81-95.

Rustioni, A. (1974) Non-primary afferents to the cuneate nucleus in the brachial dorsal funiculus of the cat. Brain Res. 75:247-259.

Rustioni, A. (1977) Spinal neurons project to the dorsal column nuclei of Rhesus monkeys. Science 196:656-658.

Rustioni, A., N.L. Hayes, and S. O'Neill (1979) Dorsal column nuclei and ascending spinal afferents in macaques. Brain 102:95-125.

Rustioni, A., and G. Macchi (1968) Distribution of dorsal root fibers in the medulla oblongata of the cat. J. Comp. Neurol. 134:113-126.

Rustioni, A., and I. Molenaar (1975) Dorsal column nuclei afferents in the lateral funiculus of the cat: distribution pattern and absence of sprouting after chronic deafferentation. Exp. Brain Res. 23:1-12.

Rustioni, A., S. Sanyal, and H.G.J.M Kuypers (1971) A histochemical study of the distribution of the trigeminal divisions in the substantia gelatinosa of the rat. Brain Res. 32:45-52.

Rustioni, A., D.E. Schmechel, S. Cheema, and D. Fitzpatrick (1984) Glutamic acid decarboxylase-containing neurons in the dorsal column nuclei of the cat. Somatosens. Res. 1:329-357.

Saigal, R.P., A.N. Karamanlidis, J. Voogd, H. Michaloudi, and O. Mangana (1982) Cerebellar cortical afferents from the dorsal column nuclei in sheep, demonstrated with retrograde transport of horseradish peroxidase. Neurosci. Lett. 29:7-12.

Saigal, R.P., A.N. Karamanlidis, J. Voogd, O. Mangana, and H. Michaloudi (1980) Secondary trigeminocerebellar projections in sheep studied with the horseradish peroxidase tracing method. J. Comp. Neurol. 189:537-553.

Sakanaka, M., S. Inagaki, S. Shiosaka, E. Senba, H. Takagi, K. Takatsuki, Y. Kawai, H. Iida, Y. Hara, and M. Tohyama (1982) Ontogeny of substance P-containing neuron systems of the rat: immunohistochemical analysis. II. Lower brain stem. Neuroscience 7:1097-1126.

Salt, T.E., R. Morris, and R.G. Hill (1983) Distribution of substance P-responsive and nociceptive neurones in relation to substance P-immunoreactivity within the caudal trigeminal nucleus of the rat. Brain Res. 273:217-228.

Saper, C.B., and A.D. Loewy (1980) Efferent connections of the parabrachial nucleus in the rat. Brain Res. 197:291-317.

Satoh, K. (1979) The origin of reticulospinal fibers in the rat: A HRP study. J. Hirnforsch. 20:313-332.

Satoh, K., D.M. Armstrong, and H.C. Fibiger (1983) A comparison of the distribution of central cholinergic neurons as demonstrated by acetylcholinesterase pharmacohistochemistry and choline acetyltransferase immunohistochemistry. Brain Res. Bull. 11:693-720.

Schroeder, D.M., and M.S. Loop (1976) Trigeminal projections in snakes possessing infrared sensitivity. J. Comp. Neurol. 169:1-14.

Schults, C.W., R. Quiron, B. Chronwall, T.N. Chase, and T.L. O'Donohue (1984) A comparison of the anatomical distribution of Substance P and Substance P receptors in the rat central nervous system. Peptides 5:1097-1128.

Senba, E., and M. Tohyama (1983) Reticulo-facial enkephalinergic pathway in the rat: an experimental immunohistochemical study. Neuroscience 10:831-839.

Sessle, B.J., and L.F. Greenwood (1976a) Inputs to trigeminal brain stem neurones from facial, oral, tooth pulp and pharyngolaryngeal tissues: I. Responses to innocuous and noxious stimuli. Brain Res. 117:211-226.

Sessle, B.J., and L.F. Greenwood (1976b) Role of trigeminal nucleus caudalis in the modulation of trigeminal sensory and motor neuronal activities. Adv. Pain Res. and Ther. 1:185-189.

Shambes, G.M., J.M. Gibson, and W. Welker (1978) Fractured somatotopy in granule cell tactile areas of rat cerebellar hemispheres revealed by micromapping. Brain Behav. Evol. 15:94-140.

Shammah-Lagnado, S.J., N. Negrao, and J.A. Ricardo (1985) Afferent connections of the zona incerta:A horseradish peroxidase study in the rat. Neuroscience 15:109-134.

Shammah-Lagnado, S.J., J.A. Ricardo, N.T.M.N. Sakamoto, and N. Negrao (1983) Afferent connections of the mesencephalic reticular formation: a horseradish peroxidase study in the rat. Neuroscience 9:391-409.

Shigenaga, Y., I.C. Chen, S. Suemune, T. Nishimori, I.D. Nasution, A. Yoshida, H. Sato, T. Okamoto, M. Sera and M. Hosoi (1986) Oral and facial representation within the medullary and upper cervical dorsal horns in the cat. J. Comp. Neurol. 242:388-408.

Shigenaga, Y., and J. Nakatani (1982) Distribution of trigeminothalamic projection cells in the caudal medulla of the cat. In B. Matthews and R.G. Hill (eds.): Anatomical, Physiological and Pharmacological Aspects of Trigeminal Pain, Excerpta Medica, Amsterdam, pp.163-174.

Shigenaga, Y., Z, Nakatani, T. Nishimori, S. Suemune, R. Kuroda, and S. Matano (1983) The cells of origin of cat trigeminothalamic projections:especially in the caudal medulla. Brain Res, 277:201-222.

Shigenaga, Y., T. Okamoto, T. Nishimori, S. Suemune, I.D. Nasution, I.C. Chen, K. Tsuru, A. Yoshida, K. Tabuchi, M. Hosoi, and H. Tsuru (1986) Oral and facial representation in the trigeminal principal and rostral spinal nuclei of the cat. J. Comp. Neurol, 244:1-18.

Shimamura, M., and R.B. Livingston (1963) Longitudinal conduction systems serving spinal and brain stem coordination. J. Neurophysiol, 26:258-272.

Shokunbi, M.T., A.W. Hrycyshyn, and B.A. Flumerfelt (1985) Spinal projections to the lateral reticular nucleus in the rat: A retrograde labelling study using horseradish peroxidase. J. Comp. Neurol, 239:216-226.

Shriver, J.E., B.M. Stein, and M.B. Carpenter (1968) Central projections of spinal dorsal roots in the monkey. I. Cervical and upper thoracic dorsal roots. Am. J. Anat, 123:27-74.

Shults, R.C., A.R. Light, and S. Donaghy (1985) Interstitial nucleus of the spinal trigeminal tract: A specific nociceptive relay for oral and peri-oral structures? Soc. Neurosci. Abstr, 11:578.

Silverman, J.D., and L. Kruger (1983) Bifurcating projections of the rat sensory trigeminal complex revealed by flourescent dye retrograde transport. Anat. Rec, 205:184A-185A.

Silverman, J.D., and L. Kruger (1985) Projections of the rat trigeminal sensory nuclear complex demonstrated by multiple flourescent dye retrograde transport. Brain Res, 361:383-389.

Sjolund, B.H. and Eriksson, M.B.E. (1980) Stimulation techniques in the management of pain. In H.W. Kosterlitz and L.Y. Terenius (Eds.), Pain and Society, Verlag Chemie GmbH, Weinheim, pp. 415-430.

Sjoqvist, O. (1938) Studies on the pain conduction in the trigeminal nerve. Acta. Psychiat. Scand. Suppl, 17:1-139.

Skofitsch, G., D.M., Jacobowitz, R.L. Eskay, and N. Zamir (1985) Distribution of atrial natriuretic factor-like immunoreactive neurons in the rat brain. Neuroscience 16:917-948.

Smith, A.O. and J.L. deVito (1984) Central neural integration for the control of autonomic responses associated with emotion. Ann. Rev. Neurosci. 7:43-65.

Smith, R.L. (1973) The ascending fiber projections from the principal sensory trigeminal nucleus in the rat. J. Comp. Neurol. 148:423-446.

Sobusiak, T., R. Zimny, and J. Zabel (1972) Comparative pattern of the primary afferent projections from the VIIIth, IXth, and Xth cranial nerves to the accessory cuneate nucleus. Anat. Anz, 131:248-258.

Somana, R., and F. Walberg (1979) The cerebellar projection from the paratrigeminal nucleus in the cat. Neurosci. Lett, 15:49-54.

Somana, R., N. Kotchabhaki, and F. Walberg (1980) Cerebellar afferents from the trigeminal sensory nuclei in the cat. Exp. Brain Res, 38:57-64.

Somers, D., and W.M. Panneton (1984) Heterogeneity of neurons in the subnucleus interpolaris of the cat. Brain Res, 309:335-340.

Spacek, J., and A.R. Lieberman (1974) Ultrastructural and three- dimensional organization of synaptic glomeruli in rat somatosensory thalamus. J. Anat. (London) 117:487-516.

Steindler, D.A. (1977) Trigemino-cerebellar projections in normal and reeler mutant mice. Neurosci. Lett. 6:293-300.

Steindler, D.A. (1985) Trigeminocerebellar, trigeminotectal, and trigeminothalamic projections: A double retrograde axonal tracing study in the mouse. J. Comp. Neurol. 237:155-175.

Stewart, W.A., and R.B. King (1963) Fiber projections from the nucleus caudalis of the spinal trigeminal nucleus. J. Comp. Neurol. 121:271-286.

Stritzel, M., M.J. Robards, and R.T. Robertson (1980) Comparison of thalamic- and midbrain-projecting cells in the trigeminal complex. Anat. Rec. 183A.

Sumino, R., and S. Nozaki (1977) Trigemino-neck reflex: its peripheral and central organization. In D.J. Anderson and B. Matthews (eds.): Pain in the Trigeminal Region. Elsevier/North-Holland Biomedical Press, pp. 365-374.

Swenson, R.S., R.J. Kosinski, and A.J. Castro (1984) Topography of spinal, dorsal column nuclear, and spinal trigeminal projections to the pontine gray in rats. J. Comp. Neurol. 222:301-311.

Szentagothai, J. (1970) Glomerular synapses, complex synaptic arrangements and their operational significance. In F.O. Schmitt (ed.): The Neurosciences, Second Study Program. Rockefeller University Press, New York. pp.427-443.

Taber, E. (1961) The cytoarchitecture of the brain stem of the cat. I. Brain stem nuclei of cat. J. Comp. Neurol. 116:27-70.

Takeuchi, Y., M. Uemura, K. Matsuda, R. Matsushita, and N. Mizuno (1980) Parabrachial nucleus neurons projecting to the lower brain stem and the spinal cord. A study in the cat by the Fink-Heimer and the horseradish peroxidase methods. Exp. Neurol. 70:403-413.

Tohyama, M., K. Sakai, M. Touret, D. Salvert, and M. Jouvet (1979) Spinal projections from the lower brain stem in the cat as demonstrated by the horseradish peroxidase technique. II. Projections from the dorsolateral pontine tegmentum and raphe nuclei. Brain Res. 176: 215-231.

Tolbert, D.L., R.C. Dunn, Jr., and G.A. Vogler (1984) The postnatal development of corticotrigeminal projections in the cat. J. Comp. Neurol. 228:478-490.

Torvik, A. (1956) Afferent connections to the sensory trigeminal nuclei, the nucleus of the solitary tract and adjacent structures. An experimental study in the rat. J. Comp. Neurol. 106:51-142.

Uchizono, K. (1965) Characteristics of excitatory and inhibitory synapses in the central nervous system of the cat. Nature (London) 207:642-643.

Uchizono, K. (1967) Synaptic organization of the Purkinje cell in the cerebellum of the cat. Exp. Brain Res. 4:97-114.

Valdivia, O. (1971) Methods of fixation and the morphology of synaptic vesicles. J. Comp. Neurol. 142:257-273.

Valverde, F. (1961) Reticular formation of the pons and medulla oblongata. A golgi study. J. Comp. Neurol. 116:71-99.

Valverde, F. (1962) Reticular formation of the albino rat's brain stem. Cytoarchitecture and corticofugal connections. J. Comp. Neurol. 119:25-53.

Villanueva, L., M. Peschanski, B. Calvino, and D. Le Bars (1986) Ascending pathways in the spinal cord involved in triggering of diffuse noxious inhibitory controls in the rat. J. Neurophys. 55:34-55.

Voris, H.C., and N.L. Hoerr (1932) The hindbrain of the opossum, *Didelphis virginiana*. J. Comp. Neurol. 54:277-355.

Walberg, F. (1966) Elongated vesicles in terminal boutons of the central nervous system, a result of aldehyde fixation. Acta. Anat. 65:224-235.

Walberg, F. (1982) The trigemino-olivary projection in the cat as studied with retrograde transport of horseradish peroxidase. Exp. Brain Res. 45:101-107.

Watson, C.R.R., and R.C. Switzer, III (1978) Trigeminal projections to cerebellar tactile areas in the rat-origin mainly from n. interpolaris and n. principalis. Neurosci. Lett. 10:77-82.

Weisberg, J.A., and A. Rustioni (1979) Differential projections of cortical sensorimotor areas upon the dorsal column nuclei of cats. J. Comp. Neurol. 184:401-422.

Westman, J., N. Danckwardt-Lilliestrom, E. Dietrichs, B.A. Svensson, and F. Walberg (1986) Ultrastructure of spinal efferents to the lateral reticular nucleus: An EM study using anterograde transport of WGA-HRP complex. J. Comp. Neurol. 246:301-311.

Westrum, L.E., and R.C. Canfield (1977) Light and electron microscopy of degeneration in the brain stem spinal trigeminal nucleus following tooth pulp removal in adult cats. In D.J. Anderson and B. Matthews (eds.): Pain in the Trigeminal Region. Elsevier/North-Holland Biomedical Press, Amsterdam, pp. 171-179.

Westrum, L.E., R.C. Canfield, and R.G. Black (1976a) Transganglionic degeneration in the spinal trigeminal nucleus following removal of tooth pulps in adult cats. Brain Res. 101:137-140.

Westrum, L.E., R.C. Canfield, and R.G. Black (1976b) Axonal degeneration patterns in the cat brainstem spinal trigeminal nucleus after tooth pulp removal. Adv. Pain Res. and Ther. 1:161-164.

Westrum, L.E., R.C. Canfield, and T.A. O'Connor (1980) Projections from dental structures to the brain stem trigeminal complex as shown by transganglionic transport of horseradish peroxidase. Neurosci. Lett. 20:31-36.

Westrum, L.E., R.C. Canfield, and T.A. O'Connor (1981) Each canine tooth projects to all brain stem trigeminal nuclei in cat. Exp. Neurol. 74:787-799.

Wold, J.E., and A. Brodal (1973) The projection of cortical sensorimotor regions onto the trigeminal nucleus in the cat. An experimental anatomical study. Neurobiol. 3:353-375.

Wold, J.G., and A. Brodal (1974) The cortical projection of the orbital and proreate gyri to the sensory trigeminal nuclei in the cat. An experimental anatomical study. Brain Res. 65:381-395.

Wong-Riley, M. (1979) Changes in the visual system of monocularly sutured or enucleated cats demonstrable with cytochrome oxidase histochemistry. Brain Res. 171:11-28.

Wong-Riley, M.T.T., and E.W. Carroll (1984) Quantitative light and electron microscopic analysis of cytochrome oxidase-rich zones in V II prestriate cortex of the squirrel monkey. J. Comp. Neurol. 222:18-37.

Wong-Riley, M.T.T. and G.H. Kageyama (1986) Localization of cytochrome oxidase in the mammalian spinal cord and dorsal root ganglia, with quantitative analysis of ventral horn cells in monkeys. J. Comp. Neurol. 245:41-61.

Wong-Riley, M.T.T., M.M. Merzenich, and P.A. Leake (1978) Changes in endogenous enzymatic reactivity to DAB induced by neuronal inactivity. Brain Res. 141:185-192.

Wong-Riley, M.T.T. and D.A. Riley (1983) The effect of impulse blockage on cytochrome oxidase activity in the cat visual system. Brain Res. 261:185-193.

Wong-Riley, M.T.T., S.M. Walsh, P.A. Leake-Jones and M.M. Merzenich (1981) Maintenance of neuronal activity by electrical stimulation of unilaterally deafferented cats demonstrable with the cytochrome oxidase technique. Ann. Otol. 82:30-32.

Wong-Riley, M.T.T., and C. Welt (1980) Histochemical changes in cytochrome oxidase of cortical barrels after vibrissal removal in neonatal and adult mice. Proc. Natl. Acad. Sci. 77:2333-2337.

Woolston, D.C., J. Kassel, and J.M Gibson (1981) Trigeminocerebellar mossy fiber branching to granule cell layer patches in the rat cerebellum. Brain Res. 209:255-269.

Woolston, D.C., J.R. LaLonde, and J.M. Gibson (1982) Comparison of response properties of cerebellar- and thalamic-projecting interpolaris neurons. J. Neurophysiol. 48:160-173.

Wunscher, W., W. Schober, and L. Werner (1965) Architektonischer Atlas vom Hirnstamm der Ratte. S. Hirzel Verlag, Leipzig.

Yamazoe, M., S. Shiosaka, T. Shibasaki, N. Ling, K. Tateishi, E. Hashimura, T. Hamaoka, J.R. Kimmel, J. Matsuo, and M. Tohyama (1984) Distribution of six neuropeptides in the nucleus tractus solitarii of the rat: an immunohistochemical analysis. Neuroscience 13:1243-1266.

Yokota, T., and N. Koyama (1982) Responses evoked in the caudal medulla by stimulation of neck muscle afferents. In B. Matthews and R.G. Hill (eds.): Anatomical, Physiological and Pharmacological Aspects of Trigeminal Pain. Excerpta Medica, Amsterdam, pp. 103-118.

Yokota, T., and N. Nishikawa (1977) Somatotopic organization of trigeminal neurons within caudal medulla oblongata. In D.J. Anderson and B. Matthews (eds.): Pain in the Trigeminal Region. Elsevier/North-Holland Biomedical Press, Amsterdam, pp.243-257.

Zeman, W., and J.R.M. Innes (1925) Craigies Neuroanatomy of the Rat. Academic Press, New York.

Zemlan, F.P., C.M. Leonard, L.-M. Kow, and D.W. Pfaff (1978) Ascending tracts of the lateral columns of the rat spinal cord: A study using silver impregnation and horseradish peroxidase techniques. Exp. Neurol. 62:298-334.

Ziehen, Th. (1913) Anatomie des Centralnervensystems. Handb. d. Anat. d. Menschen 4:2 (quoted by Astrom, '53).